

Georgia State University

ScholarWorks @ Georgia State University

Chemistry Dissertations

Department of Chemistry

12-14-2017

New Chemical Strategies for prodrug preparations: from sulfide to doxorubicin

Yueqin Zheng

Georgia State University

Follow this and additional works at: https://scholarworks.gsu.edu/chemistry_diss

Recommended Citation

Zheng, Yueqin, "New Chemical Strategies for prodrug preparations: from sulfide to doxorubicin." Dissertation, Georgia State University, 2017.
https://scholarworks.gsu.edu/chemistry_diss/139

This Dissertation is brought to you for free and open access by the Department of Chemistry at ScholarWorks @ Georgia State University. It has been accepted for inclusion in Chemistry Dissertations by an authorized administrator of ScholarWorks @ Georgia State University. For more information, please contact scholarworks@gsu.edu.

NEW CHEMICAL STRATEGIES FOR PRODRUG PREPARATIONS: FROM SULFIDE TO
DOXORUBICIN

by

YUEQIN ZHENG

Under the Direction of Binghe Wang, PhD

ABSTRACT

Prodrug is an often-used approach to facilitate the delivery of an active drug to an appropriate site with targeted release whenever possible. Proper prodrug design often relies on a few essential requirements: prodrug stability, triggered release, and selectivity. In the last few decades, there have been impressive progress in prodrug development. However, the delivery of gasotransmitters and ensuring linker stability while allowing drug release at the desired site of action are among remaining challenges. The dissertation work focuses on developing new chemical strategies to address these two issues using hydrogen sulfide (H_2S) as a model for gasotransmitters and doxorubicin as a model for anticancer compounds. In the gasotransmitter part of the project, we developed a “trimethyl lock”-lactonization based approach to deliver pure H_2S , an esterase-sensitive acetal approach to deliver persulfide, and an enrichment-triggered release method to deliver doxorubicin. The therapeutic effects of these prodrugs were evaluated in a combination of in vitro and in vivo models. The concepts described should be generally applicable and should be very useful to those interested in prodrug design.

INDEX WORDS: Hydrogen sulfide, Persulfide prodrugs, Prodrug activation, Drug delivery,

Click and release, Enrichment to release, Kinetic control drug release.

NEW CHEMICAL STRATEGIES FOR PRODRUG PREPARATIONS: FROM SULFIDE TO
DOXORUBICIN

by

YUEQIN ZHENG

A Dissertation Submitted in Partial Fulfillment of the Requirements for the Degree of
Doctor of Philosophy
in the College of Arts and Sciences
Georgia State University

2017

Copyright by
Yueqin Zheng
2017

NEW CHEMICAL STRATEGIES FOR PRODRUG PREPARATIONS: FROM SULFIDE TO
DOXORUBICIN

by

YUEQIN ZHENG

Committee Chair: Binghe Wang

Committee: Jun Yin

Donald Hamelberg

Electronic Version Approved:

Office of Graduate Studies

College of Arts and Sciences

Georgia State University

December 2017

DEDICATION

I would like to dedicate this dissertation to my parents (Lisheng Zheng and Zhaolan Zeng) and my wife (Weiwei Guo). Without you, I would not be where I am today. You gave me spiritual as well as material support in my pursuit of knowledge. Your love, kindness, encouragement and care cannot be compared by anything in the world.

I also dedicate my work to my daughter (Liya Zheng). Welcome to this world and you give me endless happiness and infinite power.

ACKNOWLEDGEMENTS

I owe my deepest gratitude to my advisor, Dr. Binghe Wang, whose encouragement, guidance and support enable me to be an independent chemist and scientist. His personality and ways of doing things not only influence my research but most importantly teach me how to be a successful person. I would also like to thank Dr. Donald Hamelberg, Dr. Jun Yin, Dr. Alfons Leopold Baumstark, Dr. Stuart Anthony Allison, Dr. Hao Xu, and Dr. Ning Fang. Their advices guide me throughout my PhD pursuing time. I want to show my great gratitude to all other faculty members and staffs for their help.

I am indebted to many of my colleges for their sensational supports and fruitful advices. Especially, I am grateful to Dr. Weixuan Chen and Dr. Chaofeng Dai for their mentoring and assistance in many ways, to Bingchen Yu, Zhixiang Pan, Manjusha Roy Choudhury, Zhengnan Yuan, Vayou Chittavong for their generous help, to Dr. Kaili Ji for all biological work, to Dr. Siming Wang and Lifang Wang for mass spectrometry work, to Mengyuann Zhu for computational modeling, and to Dr. Jianmei Cui, Dr. Danzhu Wang, Dr. Bowen Ke, Dr. Yunfeng Cheng, Dr. Xingyue Ji, Dr. Krishna Damera, Dr. Hanjing Peng, Dr. Sarah Burroughs, Dr. Alexander Draganov, Dr. Ke Wang, Dr. Jalisa Nicole Holmes, Dr. Xiaoxiao Yang, Abiodun Anifowose, Jun Zhang, Ladie Kimberly Caya De La Cruz, Wenyi Wang and all other group members for their discussions and helps in research. I am also grateful for the financial support from the National Institutes of Health and the Department of Chemistry at Georgia State University.

TABLE OF CONTENTS

ACKNOWLEDGEMENTS	1
LIST OF TABLES	5
LIST OF FIGURES	6
LIST OF SCHEMES	8
1 DEVELOPMENT OF ESTERASE-SENSITIVE PRODRUGS WITH TUNABLE RELEASE RATES AND DIRECT GENERATION OF HYDROGEN SULFIDE ...	9
1.1 INTRODUCTION.....	9
<i>1.1.1 The homeostasis of hydrogen sulfide and its pharmacological effect</i>	<i>10</i>
<i>1.1.2 Current Challenges.....</i>	<i>15</i>
<i>1.1.3 Current H₂S donors</i>	<i>21</i>
1.2 Results and Discussions	24
1.3 Conclusion.....	32
1.4 Experimental part	32
<i>1.4.1 Synthesis of HPs.....</i>	<i>33</i>
<i>1.4.2 H₂S release from HPs</i>	<i>49</i>
<i>1.4.3 Kinetic studies of esterase trigger lactone formation</i>	<i>51</i>
<i>1.4.4 Stability Studies of the thioacid group</i>	<i>53</i>
<i>1.4.5 Cell culture</i>	<i>55</i>
1.5 Acknowledgement	57

2	DEVEPMENT OF A NOVEL ESTERASE-SENSITIVE PRODRUG APPROACH FOR CONTROLLABLE DELIVERY OF PERSULFIDE SPECIES.....	58
2.1	Introduction	58
2.2	Results and Discussions	60
2.3	Conclusions	70
2.4	Experimental part	70
2.4.1	<i>Synthesis</i>	71
2.4.2	<i>Kinetic studies of P1-6 (Ps) in the presence of esterase.</i>	79
2.4.3	<i>Mechanism study of H₂S release from “acetal” based H₂S prodrugs using HPLC.</i>	82
2.4.4	<i>Cell culture</i>	83
2.4.5	<i>LC-MS studies of persulfide reactivity with S-methyl methanethiosulfonate (MMTS).</i>	87
2.4.7	<i>Myocardial Ischemia-Reperfusion Protocol.</i>	91
2.4.8	<i>Sulfane Sulfur Measurement Protocol</i>	93
2.5	Acknowledgement	94
3	AN ENRICHMENT-TRIGGERED PRODRUG ACTIVATION STRATEGY DEMONSTRATED USING A CLICK, CYCLIZE, AND RELEASE SYSTEM FOR DELIVERY OF DOXORUBICIN IN MITOCHONDRIA	95
3.1	Introduction	95
3.2	Results and Discussions	97
3.3	Conclusion.....	106

3.4 Experiment part	107
3.4.1 <i>Synthesis</i>.....	107
3.4.2 <i>Kinetic studies of the CCR system</i>	122
3.4.3 <i>Cell culture</i>	129
3.4.4 <i>Computational studies</i>.....	131
3.5 Acknowledgement	137
4 CONCLUSIONS	138
REFERENCES.....	140
APPENDICS.....	154
Appendix A. ^1H and ^{13}C Spectra of compounds in chapter 1	154
Appendix B. ^1H and ^{13}C Spectra of compounds in chapter 2	177
Appendix C. ^1H and ^{13}C Spectra of compounds in chapter 3	186
Appendix D. Mass spectrum of new compounds.	208

LIST OF TABLES

Table 1.1 The half-lives of various prodrugs. 200 μ M prodrugs in PBS with esterase 1 unit/mL at 37 °C, p=0.95, n=3.....	29
Table 1.2 HPLC monitored esterase triggering lactone formation of HPs. (n= 3, p= 0.95).....	53
Table 2.1 Total percentage of aldehyde formation (A%) and 50% aldehyde formation time ($t_{1/2}$)	63
Table 2.2 Persulfide released from precursors and trapped by DNFB	65
Table 2.3. Retention times table with Method A.....	81
Table 2.4 Reaction conditions.....	81
Table 2.5 HRMS of sulfide compounds	88
Table 3.1 Evaluation of the reaction kinetics of the CCR system.All reactions were conducted in PBS containing 10% DMSO. *not detectable because of the slow second order reaction and fast lactonization reaction. No intermediates were observed. Δ: not detectable because of Dox decomposition in PBS. (n = 3, p= 0.95).....	99
Table 3.2 IC ₅₀ in Hela cell line. (n = 3, p = 0.95)	104
Table 3.3 Retention time from the kinetic studies	124
Table 3.4 K _{obs} table from the kinetic studies.	125
Table 3.5 Lactonization rate constants.....	128
Table 3.6 Stability studies of prodrugs 55 and 56 in PBS. (5% DMSO, n = 4, p = 0.95).	128
Table 3.7 Calculated energies.	136

LIST OF FIGURES

Figure 1.1 Enzymatic pathways of H ₂ S production in mammalian cells	12
Figure 1.2 H ₂ S metabolism in the mitochondrion.	13
Figure 1.3 Ideal characteristics of H ₂ S prodrugs	21
Figure 1.4. H ₂ S generation from BW-HP-101. 200 μ M the prodrug in PBS (1% DMSO) at 37 ° C with 1 unit/mL of PLE. (p=0.95, n=3.)	26
Figure 1.5. Qualitatively detection of hydrogen sulfide releasing from BW-HP-101 by WSP-5..	
.....	26
Figure 1.6. H ₂ S generation curves.200 μ M prodrugs in PBS (1% DMSO) with 1 unit/mL esterase at 37 ° C. (p=0.95, n=3.)	28
Figure 1.7. 200 μ M HP-105 in PBS with PLE 20unit/mL. (37 ° C, 1% DMSO, p=0.95, n=3)	
.....	30
Figure 1.8. TNF- α concentrations of RAW 264.7cell culture media after 1-hour co-treatment with H ₂ S prodrugs and LPS.	31
Figure 1.9. H ₂ S release from HP-101(200 μ M) in cell culture media with or without FBS as detected using an electrode probe. (n= 3, p= 0.95)	50
Figure 1.10. H ₂ S release from HP-105 (200 μ M) in PBS at 37 ° C with 20 unit/ mL PLE. (n= 3, p= 0.95)	51
Figure 1.11. Esterase-triggered lactone formation from HP-101 as monitored with LC-MS/MS. (n= 3, p= 0.95)	52
Figure 1.12. 1H NMR spectra of reaction mixture at the 0- and 48-hour time points.....	54
Figure 1.13. Cytotoxicity of HPs. (n= 4, p=0.95)	56
Figure 2.1. P1 hydrolysis at 37 ° C in PBS (2% DMSO).....	63
Figure 2.2. HPLC chromatography. a) HPLC trace of BnSSBn reacting with Na ₂ S and MMTS.	
b) HPLC trace of esterase mediate P5 hydrolysis and persulfide trapping by MMTS. ...	67

Figure 2.3. a) Representative photomicrographs of a mid-ventricular slice after MI/R and stained with Evan's blue and 2,3,5-triphenyltetrazolium chloride for both vehicle- and prodrug- (P2) treated hearts. b) AAR/LV and INF/AAR for P2 treated or Vehicle treated mice. c) Circulating troponin I level for P2 treated, or Vehicle treated mice. d) Plasma sulfane sulfur levels at 5 minutes post intracardiac injection.....	69
Figure 2.4.Persulfide release mechanism study.....	83
Figure 2.5. Cytotoxicity of various perthiol prodrugs. H9C2 cells were treated with perthiol prodrugs with various concentrations for 24h.	85
Figure 2.6. Cytotoxicity of various perthiol prodrugs.H9C2 cells were treated with perthiol prodrugs with various concentrations for 24h.	86
Figure 2.7. Fluorescence images of P5 in cultured cells.....	87
Figure 2.8.H ₂ S release from 100 μM P1 to P6	91
Figure 3.1.General approach for drug release based on reaction kinetics, leading to enrichment triggered release (ETR).....	98
Figure 3.2. Cytotoxicity evaluation of various prodrugs(n = 4, p = 0.95).....	106
Figure 3.3.Studies of cytotoxicity (n = 4).....	130

LIST OF SCHEMES

Scheme 1.1 Current H ₂ S donors (Before 2016).....	22
Scheme 1.2. The general concept of cyclization driven prodrugs of hydrogen sulfide.....	24
Scheme 1.3. Synthesis of “trimethyl lock”-based H ₂ S prodrug HP-101 and the mechanism of esterase triggered H ₂ S release.....	24
Scheme 1.4. Relative rate constants for lactonization of various hydroxydihydrocinnamic acids. 110-113	27
Scheme 1.5 Synthesis of “trimethyl lock”-based H ₂ S prodrug HP-101	33
Scheme 1.6 Systhesis of HP-102	34
Scheme 1.7 Synthesis of HP-103.....	37
Scheme 1.8 Synthesis of HP-104.....	41
Scheme 1.9 Synthesis of HP-105.....	45
Scheme 2.1. General design of persulfide prodrugs, and their release mechanism.....	60
Scheme 2.2. Structures of persulfide prodrugs.	61
Scheme 2.3. Benzyl persulfide was release from P1 and trapped by 33	62
Scheme 2.4. Persulfide released from precursors and trapped by DNFB.....	65
Scheme 2.5. Persulfides react with MMTS	66
Scheme 3.1.General concept of the CCR system.	96
Scheme 3.2. Schematic representations of the reaction between tetrazine 60 and alkyne 52 (kcal·mol ⁻¹)	101
Scheme 3.3 Synthesis of 59	107
Scheme 3.4 Synthesis of Dansylamine prodrugs.....	113
Scheme 3.5 Synthesis of TPP-Alkyne.	115
Scheme 3.6 Synthesis of Alkyne 52	119
Scheme 3.7. Unique imaginary frequencies.	136

1 DEVELOPMENT OF ESTERASE-SENSITIVE PRODRUGS WITH TUNABLE RELEASE RATES AND DIRECT GENERATION OF HYDROGEN SULFIDE

Abstract: This chapter is mainly based on my publications: *Angew. Chem. Int. Ed.* in 2016 from page 4514-4518, *Med. Res. Rev.* in 2017, DOI: 10.1002/med.21433. Hydrogen sulfide (H_2S) is an endogenously produced signaling molecule in mammals and is critical to human health and disease. Prodrugs that release hydrogen sulfide upon esterase-mediated cleavage of an ester group followed by lactonization are described herein. By modifying the ester group and thus its susceptibility to esterase, and structural features critical to the lactonization rate, H_2S release rates can be tuned. Such prodrugs directly release hydrogen sulfide without the involvement of perthiol species, which are commonly encountered with existing H_2S donors. Additionally, such prodrugs can easily be conjugated to another non-steroidal anti-inflammatory agent, leading to easy synthesis of hybrid prodrugs. As a biological validation of the H_2S prodrugs, the anti-inflammatory effects of one such prodrug were examined by studying its ability to inhibit LPS-induced TNF- α production in RAW 264.7 cells. This type of H_2S prodrugs shows great potential as both research tools and therapeutic agents.

1.1 INTRODUCTION

Hydrogen sulfide (H_2S) is most widely known as a poisonous gas with the smell of rotten eggs. However, research in recent years has convincingly demonstrated the role of H_2S as an endogenous gasotransmitter with importance on par with that of nitric oxide (NO) and carbon monoxide (CO).¹⁻² H_2S has been shown to have anti-inflammation,³⁻⁷ anti-tumor,⁸⁻¹² ion channel regulation,¹³⁻¹⁶ cardiovascular protection^{4, 17-20} and anti-oxidation effects.²¹⁻²² Along with these physiological roles, H_2S is emerging as a potential therapeutic agent much the same way as NO²³²⁴ and CO.²⁵

There have been numerous research publications demonstrating the tremendous therapeutic potential of H₂S.^{3, 26-32} With the demonstrated therapeutic effect, the development of H₂S-based therapeutics relies on the ability to deliver hydrogen sulfide to the desired location(s), at the appropriate concentrations, and with the appropriate pharmacokinetics. Because H₂S is an endogenous gaseous signaling molecule, it is recognized that low levels of H₂S (nanomolar) may be tolerated indefinitely.³³ On the other hand, it is commonly accepted that H₂S dose-response curves are generally bell shaped with a very narrow therapeutic window.³⁴ Thus delivery of precisely controlled-doses is a critical issue in the development of H₂S-based therapeutics. Direct inhalation obviously would not be an acceptable approach for many reasons including smell, irritation, enhanced local concentrations at the first point of administration (lung), difficulties in controlling dosage, and dependence on patient's lung functions and physical states. Some of the same issues are true with simple administration of fast-releasing H₂S donors such as NaHS and Na₂S. In addition, H₂S has many unique properties, which present a special set of challenges in the development of therapeutics.

1.1.1 The homeostasis of hydrogen sulfide and its pharmacological effect

To appropriately discuss delivery and developability issues, it is important to understand the fundamentals of hydrogen sulfide homeostasis in normal physiology. Very different from most other signaling molecules is the chemical properties of H₂S, which contribute to its biological activities and homeostasis. For example, most signaling molecules that act on receptors and/or enzymes do so by simple binding without chemical reactions. However, for H₂S, its chemical reactivity is an important part of its biological functions and fate. Thus any analysis of H₂S-based therapeutics needs to take into consideration its unique properties and reactivity. H₂S is a small

molecule, slightly larger than water with the following properties: (1) acidity, (2) reducing ability, (3) high affinity to iron-containing molecules such as heme, (4) easy convertibility among species of different oxidation states, (5) polymerizability and existence in various oligomeric states, (6) volatility, and (7) high water solubility (up to 80 mM at 37 °C³⁵). Specifically, H₂S is a weak acid with pK_a values (37 °C) for the first and second dissociation steps being around 6.88 and 19 respectively.³⁶ Thus under physiological conditions (pH = 7.4), H₂S largely exists in two forms: the neutral molecular form (H₂S) and the mono-ionized form (HS⁻). Sulfide (S²⁻) is a very minor component simply because of the second pKa being very high. Further complicating the picture is the fact that hydrogen sulfide, and its oxidized forms such as SO₂³⁷⁻³⁸ and persulfide³⁹⁻⁴² may all have their own biological activities. Thus detailed mechanistic understanding will depend on the ability to deliver a “clean” species with well-defined concentration and delivery rates.

1.1.1.1 H₂S redox in biology: production, metabolism and signaling pathways

In mammals, enzyme-catalyzed endogenous H₂S production is well understood.⁴³⁻⁴⁶ Basically, these processes are part of cysteine metabolism, with cystathionine β-synthase (CBS), cystathionine γ-lyase (CSE), and 3-mercaptopropyruvate sulfurtransferase(3MST) (Figure 1.1) being the key enzymes involved. CBS catalyzes a β substitution reaction of serine to form cystathionine, and then CSE catalyzes the elimination of cystathionine to form cysteine, α-ketobutyrate and NH₃. CBS and CSE also directly catalyze H₂S release from cysteine or homocysteine. Cysteine aminotransferase (CAT) transfers the amino group from cysteine to a keto acid, typically α-ketoglutarate, forming 3-mercaptopropyruvate (3MP). Then 3MST produces H₂S from 3MP. The expression of these enzymes is tissue specific, with CBS being found predominantly in the nervous

system and liver, and CSE activity being higher than CBS activity in the aorta, portal vein and other vascular tissues.⁴⁷ 3MST is expressed in the central nervous system, mostly in glial cells, hippocampal pyramidal neurons, cerebellar Purkinje cells, and mitral cells in the olfactory bulb. In addition to the expression and distribution of these enzymes, endogenous production of H₂S also depends on availability of substrates and enzyme activity, which might be affected by many properties of the intracellular environment such as the redox state.

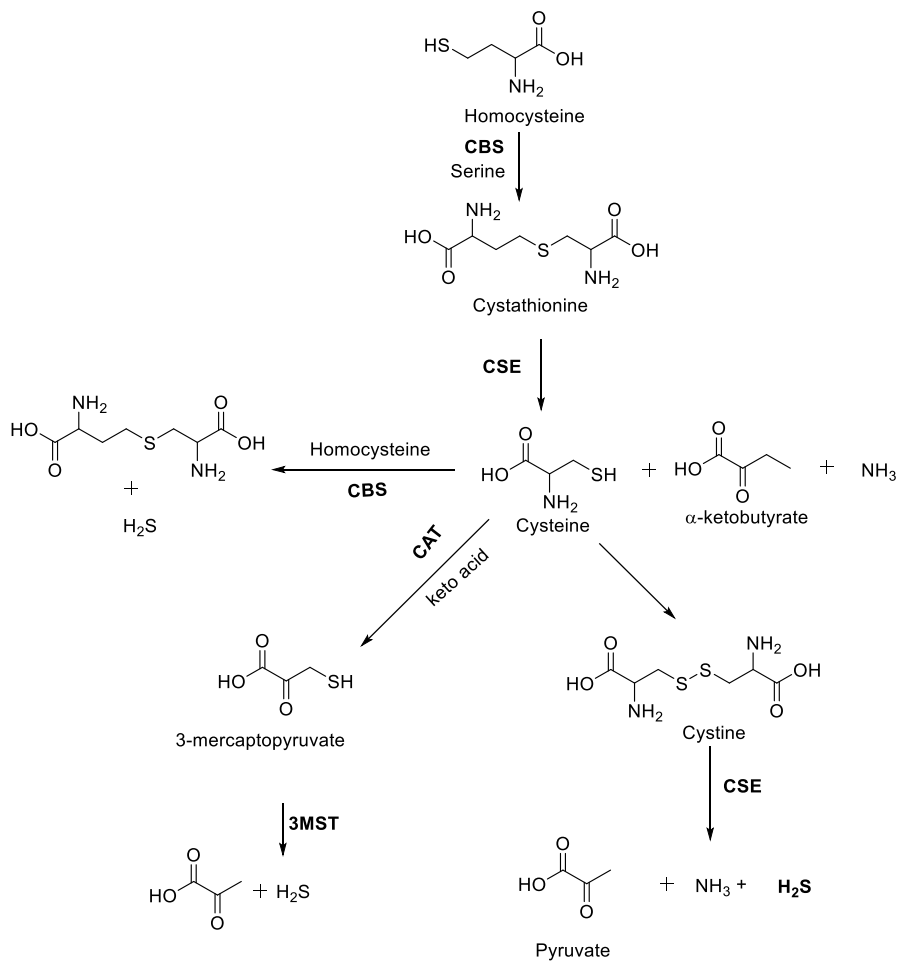


Figure 1.1 Enzymatic pathways of H₂S production in mammalian cells

H₂S is metabolized via the sulfide oxidation pathway in the mitochondria.⁴⁸⁻⁵⁰ Basically, a membrane-bound sulfide:quinone oxidoreductase (SQR) oxidizes H₂S to a SQR persulfide

intermediate. In the presence of O_2 and water, sulfur dioxygenase (SDO) oxidizes the persulfide intermediate to sulfite.⁵¹⁻⁵³ Then Rhodanese transfers a sulfane sulfur (SQR persulfide) to sulfite to form thiosulfate ($S_2O_3^{2-}$)⁵⁴ (Figure 1.2), which reacts with glutathione (GSH) via catalysis by thiosulfate sulfurtransferase (TST) to produce GSSH. Subsequently, GSSH is used as a substrate by SDO to generate sulfite, which is further metabolized to sulfate by sulfite oxidase (SO). In addition, H_2S can be converted to dimethylsulfide by cytosolic methylation. Another possible pathway for H_2S removal is related to the interaction of H_2S with myoglobin (Mb) and hemoglobin (Hb) to form the sulfheme complex.⁵⁵⁻⁵⁷ One cannot help but wonder whether the various intermediates have their own regulatory roles, which would be a good reason for nature to use such a complex transformation process.

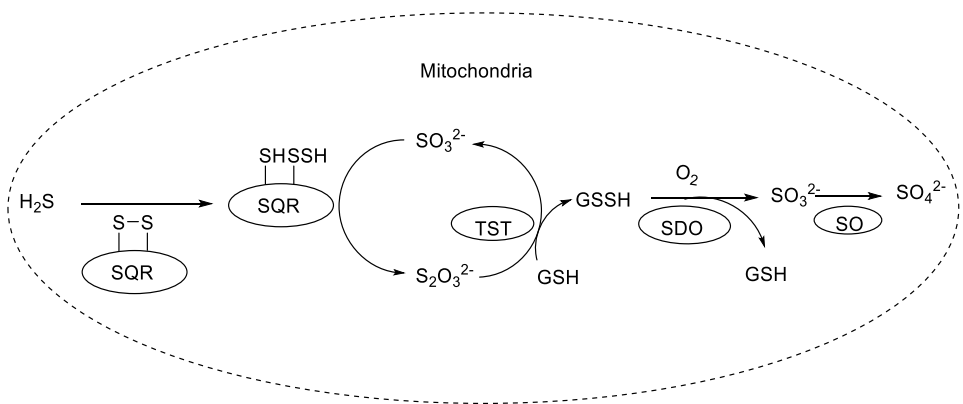


Figure 1.2 H_2S metabolism in the mitochondrion.

Besides the enzymatic regulation of H_2S production and metabolism, H_2S could also be stored in proteins by forming persulfide through persulfidation (S-sulphydratation).⁵⁸⁻⁶⁰ Most, if not all, S-sulphydratation occurs at reactive cysteine residues in proteins and results in the conversion of the thiol (-SH) group of a cysteine to a persulfide group (-SSH), which is also the major pathway of sulfide signaling.^{58-59, 61-63} The formation of persulfide in cysteine residues of a protein can cause structural changes, which alter protein activity and lead to a cellular and physiological responses

to H₂S. For instance, in 2011, Mustafa *et al.* observed that S-sulphydratation of Cys-43 in the Kir 6.1 subunit of the ATP-sensitive potassium channels (K_{ATP}) reduces ATP binding and enhances phosphatidylinositol 4,5-bisphosphate (PIP₂) binding, which leads to K_{ATP} channel activation.⁶⁴ S-sulphydratation of the calcium-dependent intermediate conductance potassium channel (IKCa) contributes to H₂S-dependent hyperpolarization of endothelial cells. All these findings indicate that H₂S is an important Endothelial Derived Hyperpolarizing Factor (EDHF) and dysregulation of the pathway may be a critical factor in the development of vascular diseases such as hypertension. As an additional example, in 2013 Yang and co-workers⁶⁵ demonstrated that S-sulphydratation of Kelch-like ECH-associated protein 1 (Keap1) at Cys-151 enhances nuclear translocation of Nuclear Factor (erythroid-derived 2)-like 2 (Nrf2), antioxidant gene transcription, and GSH production; and thus protects cells from oxidative stress and premature senescence. These findings point to an important function of H₂S against cellular aging via the post-translational modification of the Keap1/Nrf2 axis and associated oxidative stress. All these studies show that persulfide formation is a posttranslational modification of the cysteine residue. However, it needs to be noted that the sulfur atom of H₂S as well as thiols (R-SH) possesses the same oxidation state (-2); thus direct persulfide formation via H₂S is not possible. There are two proposed persulfide formation mechanisms. One is the addition of SH⁻ to a sulfenic (S-OH) group in proteins to form persulfide. Since protein thiolate (R-S⁻) is a strong nucleophile, it readily reacts with H₂O₂ to yield the corresponding sulfenic group, which, in turn, reacts with SH⁻ to yield the corresponding persulfide.⁶⁶⁻⁶⁷ The other mechanism relies on polysulfides. Some recent studies showed that polysulfides can be synthesized endogenously by 3MST,⁶⁸⁻⁷⁰ and are much more potent in inducing persulfide formation.

Sulfide-hemeprotein interactions are also involved in sulfide signaling. Sulfide has strong affinity for heme proteins such as cytochrome c oxidase (CcO), Mb, and Hb, and can convert the high spin ferric center of heme protein to a low spin ferric-sulfide complex, reducing the central metal from the ferric to ferrous state, or forming ferrous-sulfide complexes. The effects of sulfide on heme proteins are concentration-dependent. For example, at high concentrations, H₂S binds directly to the ferric heme α3 center and completely inhibits CcO activity, leading to inhibition of the mitochondrial respiration and subsequent toxicity; however at low concentrations (nearly stoichiometric), H₂S stimulates O₂ consumption without having an inhibitory effect.⁷¹ There have been studies⁷² showing that the interaction of H₂S with heme proteins would decrease cellular ATP concentration and activate K_{ATP} channels. These interactions can also regulate the function of heme proteins, produce bioactive sulfide metabolites and protect against heme-induced oxidative stress, which plays an important role in sulfide signaling.

All indications are that the redox chemistry of H₂S and its affinity to iron are the key characteristics that contribute to its biology.

1.1.2 Current Challenges.

It is clear that there is growing understanding of sulfide signaling pathways and its various biological effects including the relaxation of blood vessels, cytoprotection against oxidative stress, and anti-inflammatory actions that would warrant significant efforts in translating the known pharmacological effects of H₂S to the development of H₂S-based therapeutics. A major issue is the development of H₂S donors or prodrugs as potential therapeutics. This is because there are obvious concerns with using H₂S or its salt forms. For example, the volatile nature and stench odor make H₂S or its salts very unlikely delivery forms for pharmaceutical uses. Beyond the

superficial, there are also mechanistic reasons for the development of donors and prodrugs that can afford sustained release of H₂S. First, as discussed above, the dose-response curves in almost all known pharmacological experiments for H₂S are bell-shaped with a narrow therapeutic window. Thus there is a need to deliver precise amounts of H₂S. However, there are complex processes of maintaining H₂S homeostasis in living system and H₂S is volatile. Thus bolus administration of H₂S would only lead to a spike of H₂S concentration. Although there have been no systematic studies of the effect of duration of H₂S treatment, one can assume that a sustained and constant level of H₂S for certain duration would be far more desirable than a quick spike for therapeutic applications. Second, much of hydrogen sulfide's effect resides with its redox chemistry. A quick bolus administration of H₂S is likely to change the cellular redox states and the effect may go well beyond H₂S-specific functions. Third, at high H₂S concentrations after bolus administrations, the distribution of various sulfur species may be very different from that of the physiologic state. It is well known that persulfide species may have activities of their own.^{69, 73} Some studies already showed that polysulfides formed in solutions of H₂S mediate protein thiol oxidation, which converts cysteinyl thiolates (Cys-S⁻) to persulfides (Cys-S-S⁻).⁶⁹ There are suggestions that polysulfides/thiosulfates rather than H₂S itself are the actual active molecules responsible for persulfide formation, and thus mediate sulfide signaling.⁶⁹ Depending on the release rates and their own oxidation states, using different H₂S donors at the same concentration might lead to the generation of different concentrations of various sulfur species. Thus this change in distribution could make mechanistic studies very hard, or even physiologically irrelevant. Meanwhile, “pure” polysulfide donors are highly desired in this field, but it is still quite a challenge for synthetic chemists to make such molecules at high purity. Another difficulty in H₂S research is the lack of understanding of the ideal concentration of H₂S in physiology and in therapy, including the

question of the normal endogenous H₂S concentration range in circulation. This is largely due to the lack of sensitive methods for the detection of H₂S and the lack of H₂S donors with well-defined release rates that would allow a detailed examination of the H₂S concentration-effect relationship issue. Although there are many methods for detecting H₂S including the colorimetric methylene blue method, ion-selective or polarographic electrodes, gas chromatography with flame photometry, the monobromobimane assay, and assays using various fluorescent probes,⁷⁴⁻⁷⁵ none quite comes to the needed sensitivity and response time for the near real time detection of H₂S at physiological concentrations. A wide physiological concentration range has been reported: from 0.1 μM to more than 300 μM.³ As a conservative estimate, plasma H₂S levels in healthy humans or animals might be in the high nanomolar to low micromolar range.³ The lack of methods for accurately monitoring H₂S levels in circulation or in the targeted organs and systems makes it hard to estimate the therapeutic dosages. Thus prodrugs, which directly release H₂S without involving redox chemistry, will be important research tools for dissecting many of the remaining issues.

Even in developing H₂S prodrugs, there are unique challenges as compared to prodrugs of other small molecules. Much of these challenges are associated with H₂S's volatility and rapid metabolism. For example, for a prodrug of a small molecule drug with a half-life in hours, the dosage of the prodrug can be easily translated into a stoichiometric concentration because the drug released would persist within the circulation for a reasonable period of time. However, for a gasotransmitter, this is very different. Because of its volatility and thus its constant evaporation/exhalation, H₂S concentration is a balance between exhalation and production. If one takes into consideration the cellular metabolism of H₂S, then it becomes easy to understand why the concentration of the administered prodrug may not have a linear relationship with H₂S concentration. In one study, it was found that for a series of H₂S prodrugs with different release

rates at 200 μM , the highest peak H_2S concentration achieved was only 50% of the prodrug concentration in a solution experiment when the release half life is short (13 min).⁷⁶ Then the concentration quickly drops. On the other hand, another prodrug in the same series with a slower release rate ($t_{1/2}$, 100 min) provided a sustained concentration of H_2S at 5% of its prodrug concentration for over 1 h. Therefore, one can see that H_2S prodrug release rate plays a very important role in determining the concentration of the drug. In addition, to address the biological effect of H_2S prodrugs, well-defined control compounds are also necessary. With polysulfide compounds, this is hard to achieve.

1.1.2.1 Developability issues related to H_2S donors or prodrugs

In drug discovery and development, assessing developability is a critical step.⁷⁷⁻⁷⁹ Prodrugs are no exceptions,⁸⁰ however, with unique features, which are discussed in later sections. Drug developability is a complex issue; it is well known that there are many examples of drugs in the market that do not fit the model of modern day criteria. Nevertheless, literature developability criteria are very important reference points. When judgment calls are made, there is a need to have a clear understanding of why one needs to deviate from the “standard” developability criteria.

In assessing drug developability, one typically needs to consider pharmacokinetics, metabolism, permeability, protein binding, toxicity, efficacy, chemical tractability, and drug-drug interactions, among other important factors.⁷⁷⁻⁷⁸ When it comes to criteria that can guide the design of new chemical entities (NCE), there are many specific factors to consider. The most well-known is the Lipinski’s “Rule of Five.” When it comes to specific molecular properties to assess, experiments commonly include determinations of solubility, stability, membrane permeability,

p450/microsomal metabolism, cytotoxicity, mutagenicity, hERG inhibition (cardiotoxicity), p450 inhibition and induction, and protein binding.

In applying drug developability assessment to a prodrug project, there are unique issues to consider. This is especially true for prodrugs of a gasotransmitter. First, the potency and efficacy issues are no longer the same as in a typical small molecule drug discovery project. This is because the active drug itself is already fixed. In the case of hydrogen sulfide, its potency and efficacy are defined by the parent drug already. Second, for a gasotransmitter prodrug such as H₂S, the drug permeability issue is very different from that of a typical small molecule drug. The prodrug itself actually does not necessarily need to penetrate any barrier as long as the parent drug can reach the site of action. With a gasotransmitter, the parent drug itself is very permeable across cellular barriers. Thus the prodrug does not even need to get into the intracellular space in order to be effective. In a way, sometimes it might be preferred that the prodrug not get into the cell in order to minimize side effect and toxicity issues. This aspect is very different from that of a traditional small molecule drug discovery project. Another unique issue for a prodrug of a gasotransmitter is the dose-response issue. As discussed above, the relationship between the drug effective dose and the prodrug dose is not necessarily a linear relationship because of the volatility and rapid metabolism of H₂S. The relationship among release rates, volatility, and rate of metabolism defines the “steady state” concentration, if any. Thus having well-defined release rates is very important for the future development of H₂S prodrugs. Additional developability issues unique to hydrogen sulfide include odor and ready inter-conversions of various species. The first would be expected to significantly affect patient compliance, dispensing, and storage; and the second would be expected to affect chemical tractability in process chemistry, quality control, dosage determination, and the overall approval process by the US Food and Drug Administration (FDA).

Thus developing prodrug forms that can overcome these issues are also very critical to the future of H₂S-based therapeutics.

1.1.2.2 Ideal Hydrogen sulfide prodrugs

With the above discussions of developability issues and associated challenges, we layout some ideal characteristics of H₂S donors or prodrugs for therapeutic applications (Figure 1.3), which could serve as reference points in evaluating existing donors and in guiding future efforts. First of all, tunable and controllable H₂S release rates are essential properties. The release rate of H₂S prodrugs directly affects the effective concentration of the parent drug and thus their functions. Therefore, designing H₂S prodrugs with a range of controllable release rates is highly desired. Along this line, the use of well-defined triggering mechanisms for release will be very much desired for certain applications. Second, stability during storage, drug preparation, or formulation is required. Third, water solubility is essential for the eventual drug delivery and absorption. It is well known that drugs need to have certain water solubility in order to be absorbed and to be effective.⁷⁹ Water solubility is also an important factor that could affect formulability and pharmacokinetic issues. Fourth, chemical tractability is critical to all small molecule drugs. The ability to prepare and characterize the prodrug with sufficient purity and well-defined distribution of various species is critical to the viability of a drug discovery and development project. Fifth, the presence of aversive odor and taste is a developability issue for all drugs. This issue is especially prominent with H₂S prodrugs because of its known unpleasant odor, which is expected to not only affect patient compliance, but also storage and delivery. Thus finding ways to ameliorate the undesirable odor will be important. Lastly, unique to prodrug development is the

issue of tractability of the side product(s) after drug release from the prodrug. This issue is important at the research stage so that there is a proper control compound. More importantly, at the clinical development stage there needs to be a good understanding of the chemical species introduced into the human body and a reasonable level of assurance that the “side product(s)” does not have undesirable effects.

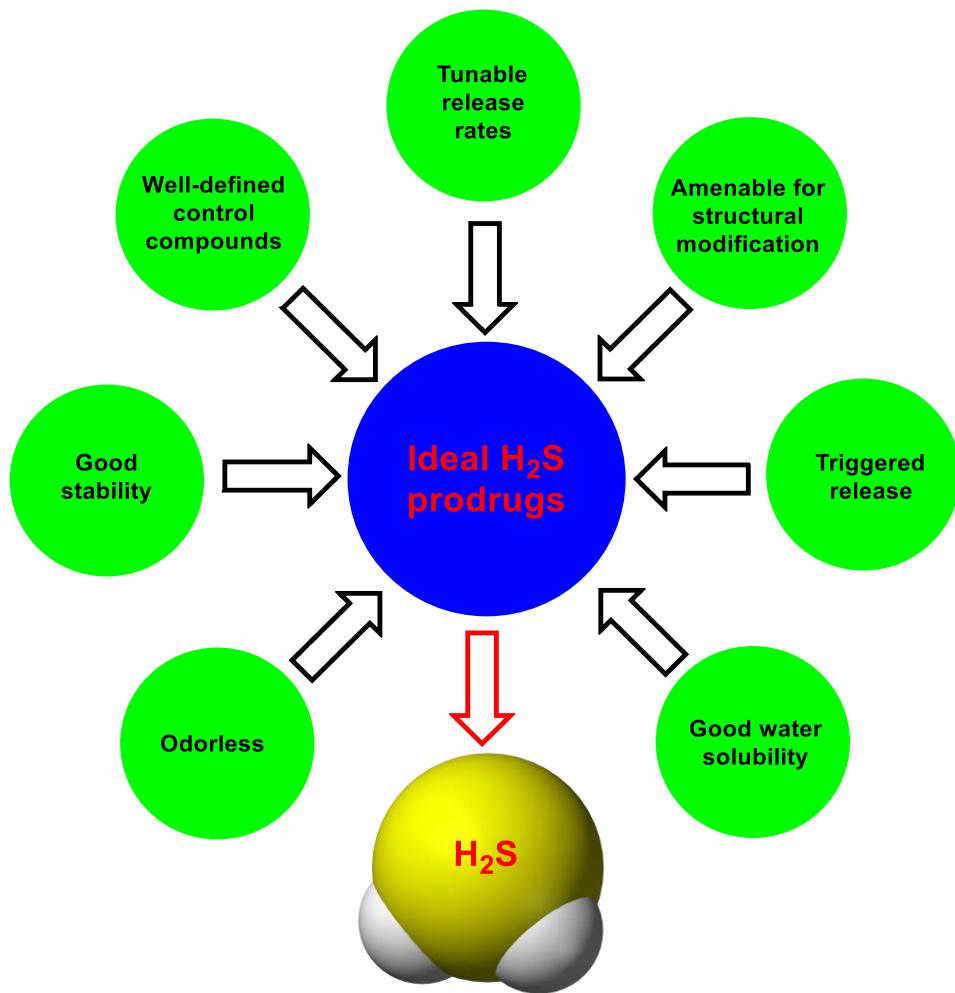
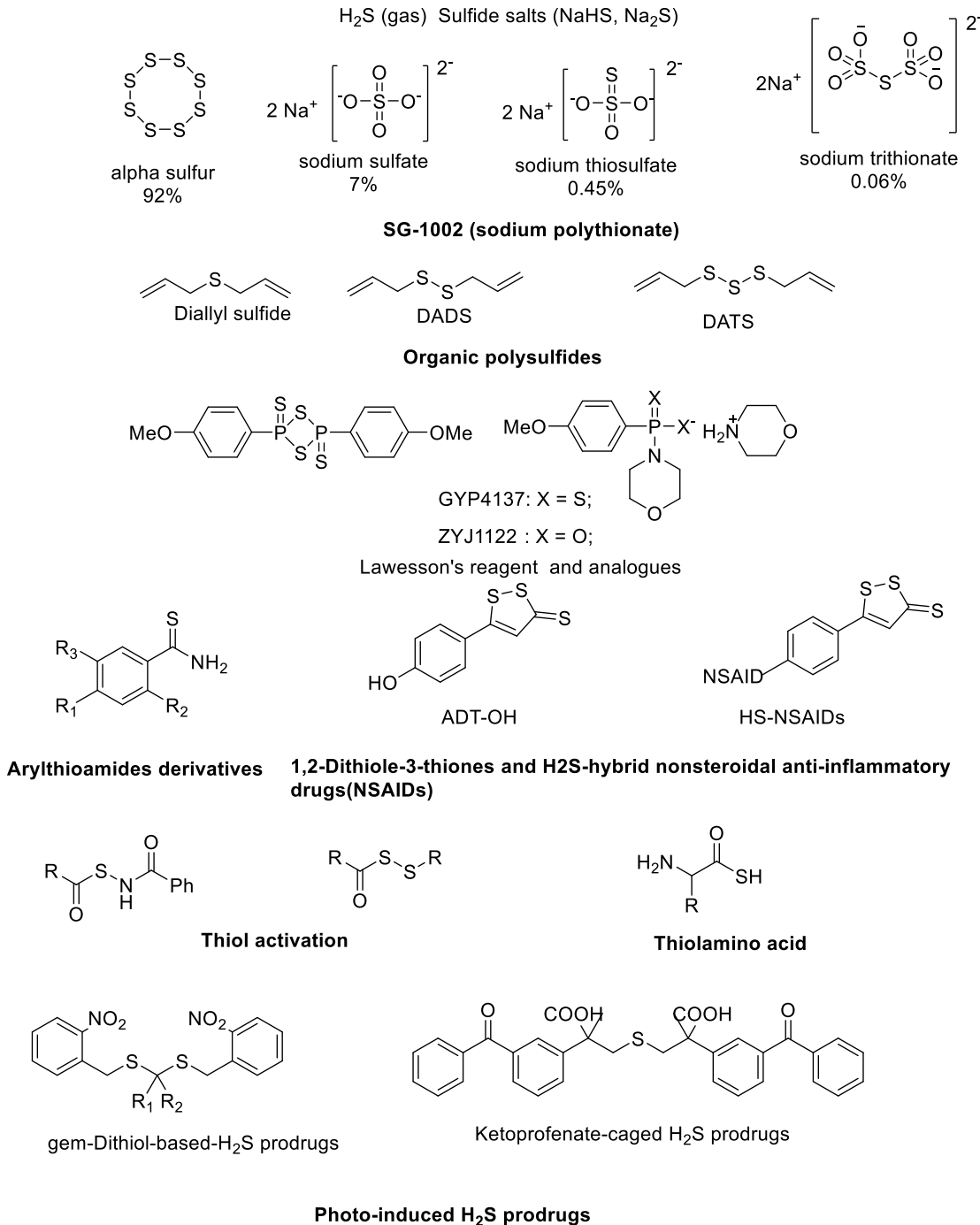


Figure 1.3 Ideal characteristics of H_2S prodrugs

1.1.3 Current H_2S donors

In the past several years, many series H_2S prodrugs have been developed. We summarize the prodrugs which was discovered before 2016.(Scheme 1.1)



Scheme 1.1 Current H₂S donors (Before 2016)

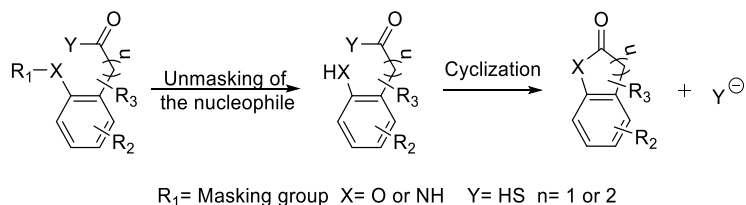
In studying the physiological and pathological properties of H₂S, H₂S gas or inorganic sulfide salts such as Na₂S and NaHS have been widely used. However, the uncontrollable release of H₂S from sulfide salts and the toxic effects of excessive H₂S limit their potential as possible therapeutic agents.⁸¹⁻⁸² Moreover, inorganic sulfide salts could not mimic the slow and continuous

H₂S production in the biological system, which further limits their usage. Therefore, new H₂S releasing agents (H₂S donors) are of great clinical and research interests.^{26, 81-83} Currently, there are seven types of H₂S donors that have been reported:⁸⁴ 1) garlic and related sulfur compounds;⁸⁵ 2) Lawensson's reagent and analogs (GYY4137);⁴ 3) 1,2-dithiole-3-thiones (DTTs) and hybrids of H₂S and non-steroidal anti-inflammatory drugs;⁸⁶⁻⁸⁸ 4) thiol-activated H₂S donors;⁸⁹⁻⁹¹ 5) photo-induced H₂S donors;⁹²⁻⁹³ and 6) thiol amino acid;⁹⁴ and 7) polysulfide (SG-1002).⁹⁵ There are some obvious limitations among these H₂S donors. First of all, the release rates of H₂S from most donors such as GYY4137 and DTTs are hard to control, and the effect of their byproducts associated with H₂S release is unclear. Furthermore, existing H₂S donor systems lack well defined negative controls. Some H₂S donors, such as thiol-activated H₂S donors would generate the perthiol intermediates, which may also have certain physiological effect, making it hard to deconvolute the experimental results. Almost all existing donors release precursors of H₂S. Thus the correlation of H₂S release and the amount of donor added is difficult. H₂S donors that can mimic endogenous H₂S production through a single enzymatic step are currently not available. Recently, Moore *et al*⁹⁶ tested the effect of GYY4137 on the release of pro- and anti-inflammatory mediators in lipopolysaccharide (LPS)-treated murine RAW264.7 macrophages, and found that the effects of H₂S on inflammatory processes are complex and dependent not only on H₂S donor concentration but also on the rate of H₂S generation. Therefore, there is a need for new H₂S prodrugs, which directly generate H₂S with well-defined and tunable release rates that are not directly affected by the redox balance of the cellular environment and the presence of other thiol species. Such H₂S donors/prodrugs will be very important research tools in delineating the functions of H₂S and lay a foundation for the future development of H₂S-based therapeutics.

1.2 Results and Discussions

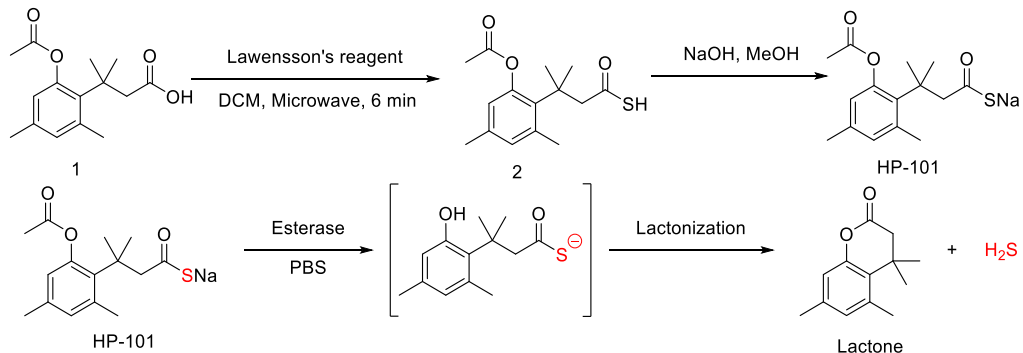
Our lab has long-standing interests in prodrugs based on intramolecular cyclizations.⁹⁷⁻⁹⁹

We took advantage of one such lactonization prodrug systems (Scheme 1.2), and designed esterase-sensitive prodrugs of H₂S. Specifically, the nucleophilic hydroxyl or amino group can be masked as an ester or amide, and the drug, H₂S, can be conjugated to the carbonyl carbon in the form of a thioacid. After hydrolysis of the masking group, the nucleophile can attack the carbonyl group and undergo a lactonization reaction, and thus release hydrogen sulfide.



Scheme 1.2. The general concept of cyclization driven prodrugs of hydrogen sulfide

To test the idea, we first synthesized prodrug BW-HP-101, which uses a “trimethyl lock” and thus stereochemical control to facilitate lactonization.^{97, 100-104} The synthesis of BW-HP-101 was accomplished by treating compound **1**,¹⁰⁵ with Lawesson's reagent under microwave conditions,¹⁰⁶ followed by reaction with one equivalent of sodium hydroxide (Scheme 1.3).



Scheme 1.3. Synthesis of “trimethyl lock” -based H₂S prodrug HP-101 and the mechanism of esterase triggered H₂S release

The novel BW-HP-101 is a very stable white and odorless solid, and has very good water solubility, allowing 10 mM stock solutions to be prepared in aqueous buffer. The prodrug showed no obvious decomposition during storage at room temperature for 3 days and at -20 °C for 3 month.

To examine the feasibility of concept described in Schemes 1 and 2, we studied whether esterase can catalyze H₂S release from BW-HP-101 by using a H₂S-selective microelectrode, and found time-dependent H₂S release in the presence of porcine liver esterase (PLE) (Figure 1.4) with a peak concentration at about 15 min. H₂S release was further confirmed by using a well-known hydrogen sulfide fluorescent probe WSP-5¹⁰⁷ (Figure 1.5). Strong fluorescence was detected when WSP-5 was incubated with the prodrug in the presence of PLE in phosphate buffer saline (PBS) or cell culture media containing fetal bovine serum (FBS). Such results indicate that BW-HP-101 indeed releases H₂S in PBS with esterase catalysis, or cell culture media containing FBS. In contrast, incubation in PBS alone did not lead to H₂S formation, indicating the chemical stability of the prodrug. Lactone formation was also confirmed by NMR (SI). As another piece of evidence on the stability of the thioacid group, thioactic acid was incubated in aqueous solution; no decomposition was observed within 48 h.

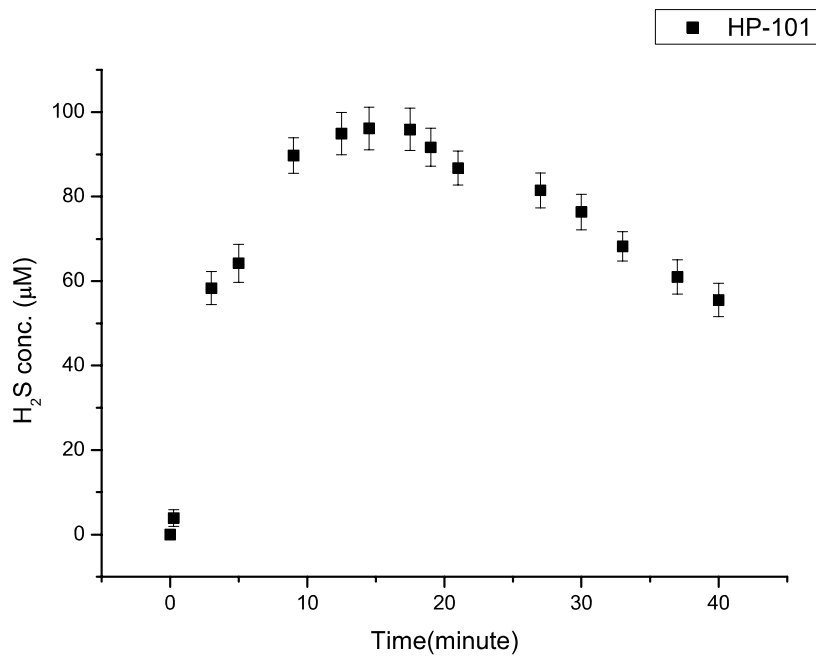


Figure 1.4. H_2S generation from BW-HP-101. 200 μM the prodrug in PBS (1% DMSO) at 37 $^{\circ}C$ with 1 unit/mL of PLE. ($p=0.95$, $n=3$.)

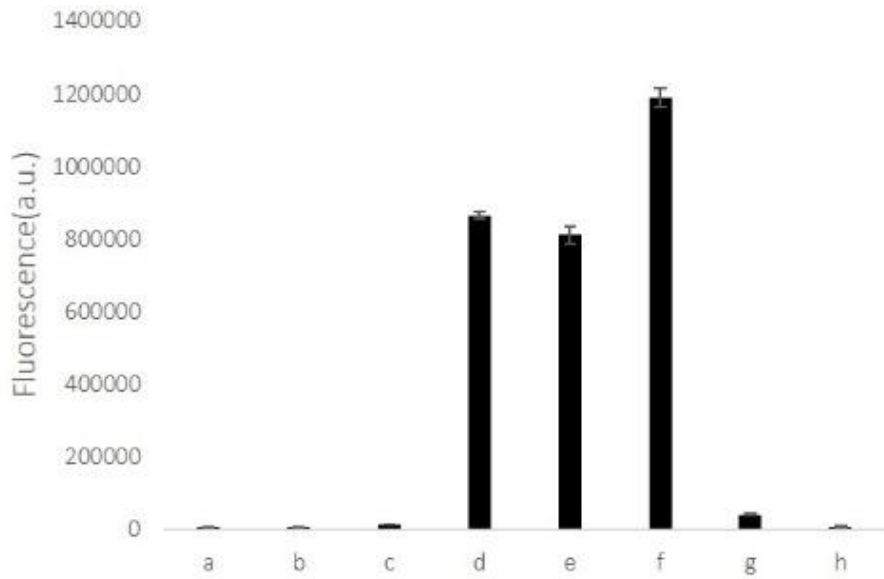
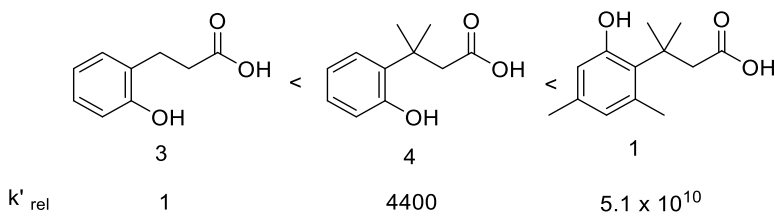


Figure 1.5. Qualitatively detection of hydrogen sulfide releasing from BW-HP-101 by WSP-5. The concentration of WSP-5 is 50 μM , and the intensities of fluorescence were recorded after 5 min of incubation of WSP-5 with different substrates at room temperature. a: WSP-5 only in PBS; b: WSP-5+ 200 μM prodrug in PBS; c: WSP-5+ 200 μM prodrug in DMEM (No FBS), no cells; d: WSP-5+ 200 μM prodrug in DMEM (with FBS)+ cells e: WSP-5+ 200 μM prodrug

in DMEM (with FBS), no cells; f: WSP-5+ 200 μM prodrug + 1 unit/mL of esterase; g: WSP-5+200 μM GYY1437; h: WSP-5+1unit/mL esterase.

All these studies demonstrate the expected enzyme-catalyzed release of hydrogen sulfide from the prodrug system. We then further studied the tunability of the release rates by varying the ester group and factors controlling the lactonization step. Variations of the ester group allows for tuning the rate of the unmasking step. For ester hydrolysis, it has been shown that increasing the size of the acyl moiety results in decreased catalytic hydrolysis rate.¹⁰⁸⁻¹⁰⁹ Thus we reasoned that modifying the acyl moiety should help tune the hydrolysis rates. The second direction in tuning H₂S releasing rates is based on controlling the lactonization rate by varying the number of methyl groups in the system. It is well known that the lactonization of compound **1** is much faster than that of o-hydroxydihydrocinnamic acids **3** and **4**, which lack pendant methyl groups (Scheme 1.4) and thus has decreased entropic control of the conformation favorable for lactonization.¹⁰¹ Therefore, BW-HP-102, -103, and -104 were synthesized to tune the release rates. BW-HP-102 and BW-HP-104 contain a large acyl moiety cyclopropanecarbonyl ester and BW-HP-103 and BW-HP-104 lack two methyl groups on phenyl ring.



Scheme 1.4. Relative rate constants for lactonization of various hydroxydihydrocinnamic acids.
110-113

H₂S release from these prodrugs was studied (Figure 1.6). As designed, these prodrugs show very different H₂S release rates. For 200 μM of the prodrug in PBS at 37 °C with 1unit/mL

PLE, the peak H₂S concentration for the fastest one, BW-HP-101, was about 95 μM at 15 min; and for the slowest one, BW-HP-104, it was about 13 μM at 43 min. Such results bring out an important issue, i.e. the same concentration of the prodrug may mean very different effective H₂S concentrations, depending on the release rates. This issue is especially important in delivering a gaseous molecule because of its volatility nature and the lack of “accumulation,” which is in direct contrast to the delivery of non-volatile drugs. In the latter case, a slower release may only affect the onset time, but not the final concentration. With a gaseous molecule, release rates affect the onset time, the peak concentration, and the eventual concentration significantly. Thus when comparing the results using various H₂S prodrugs/donors, particular attention needs to be paid to the release rate and effective concentration issue.

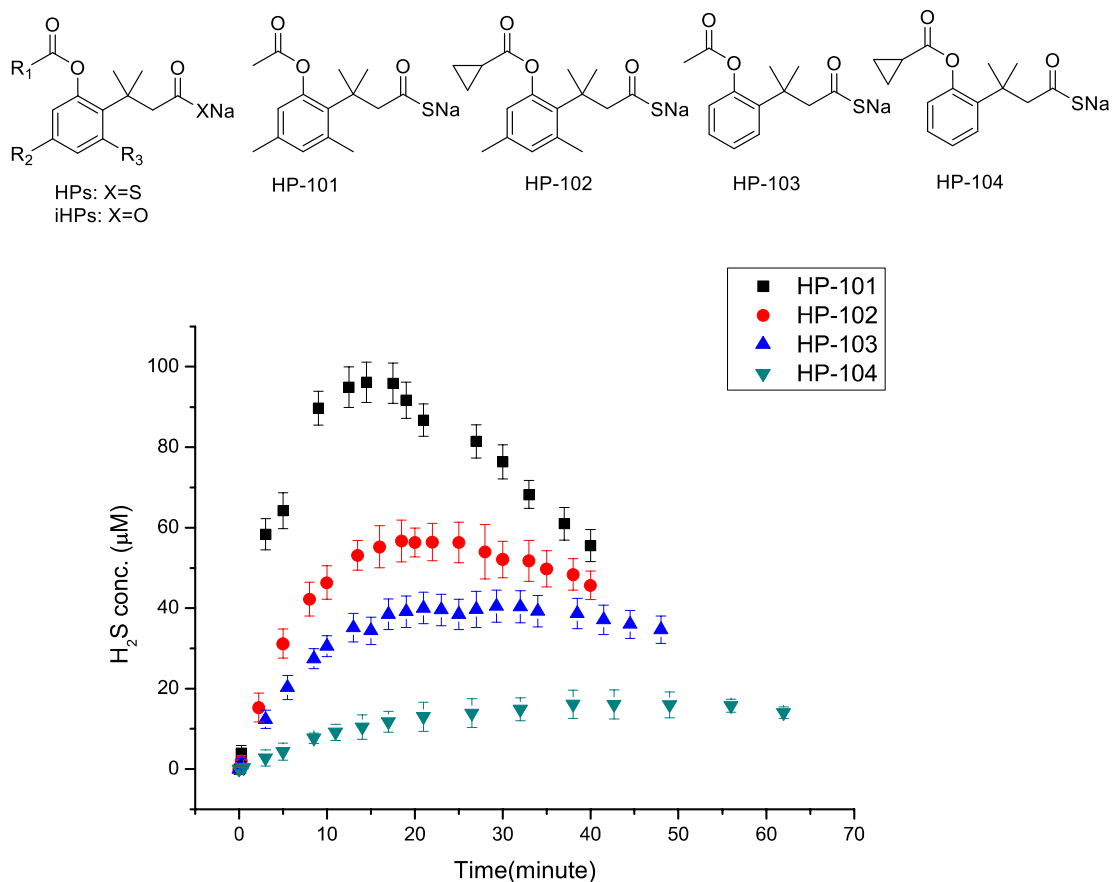


Figure 1.6. H₂S generation curves. 200 μM prodrugs in PBS (1% DMSO) with 1 unit/mL esterase at 37 °C. (p=0.95, n=3.)

We also monitored the lactone product formation by HPLC (Table 1.1), and found $t_{1/2}$ ranging from 13 to 99 min for 200 μM prodrugs in the presence of PLE. Such results further demonstrated the concept of tuning the H_2S release rates.

Table 1.1 The half-lives of various prodrugs. 200 μM prodrugs in PBS with esterase 1 unit/mL at 37 °C, $p=0.95$, $n=3$.

	BW-HP-101	BW-HP-102	BW-HP-103	BW-HP-104
$T_{1/2}$ (min)	13.0 ±2.4	28.7±1.5	44.5±2.1	99.0 ±8.9

The conjugation of two drugs with the same therapeutic indication, but different mechanisms, is attracting a great deal of attention in the hybrid drug field.¹¹⁴ Especially interesting is the idea of conjugating a non-steroidal anti-inflammatory drug (NSAID) to a H_2S donor,¹¹⁵ which has known anti-inflammatory effects. H_2S -NSAIDs have shown remarkable improvements in activity and tolerability as compared with the related parent compounds.¹¹⁴ However, few of the hydrogen sulfide prodrugs could be successfully applied to hybrid drug preparation for chemistry reasons, and existing H_2S -NSAIDs also suffer from the lack of control in H_2S release. Because most NSAIDs have a free carboxyl group, their conjugation to one of our prodrugs is not only easy, but also leads to a hybrid prodrug, which uses the same mechanism to release both drugs. This is very unique among all known H_2S hybrid drugs. Thus, we also synthesized BW-HP-105, which is formed by coupling the novel H_2S release system to naproxen (Figure 1.7). HPLC kinetic studies showed that BW-HP-105 could generate naproxen and H_2S by treatment with an esterase. Compared to other H_2S prodrugs with the same stereochemical control (BW-HP-101, 102), BW-

HP-105 showed a slower hydrolysis rate as expected because of the larger masking group (naproxen as the acyl group). The H₂S-NSAID hybrid shown here is the first example of controllable H₂S release employing the same mechanism to “activate” both drugs, and will be a very useful research tool and potential therapeutic agent.

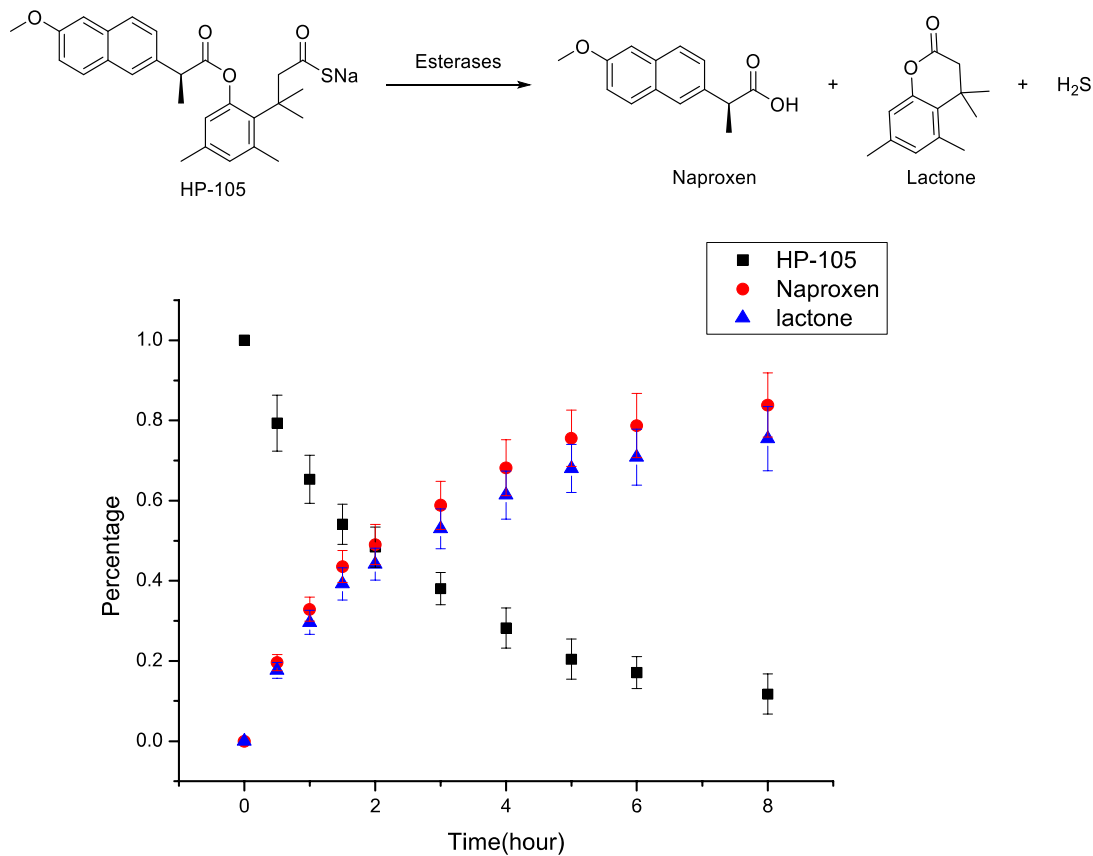
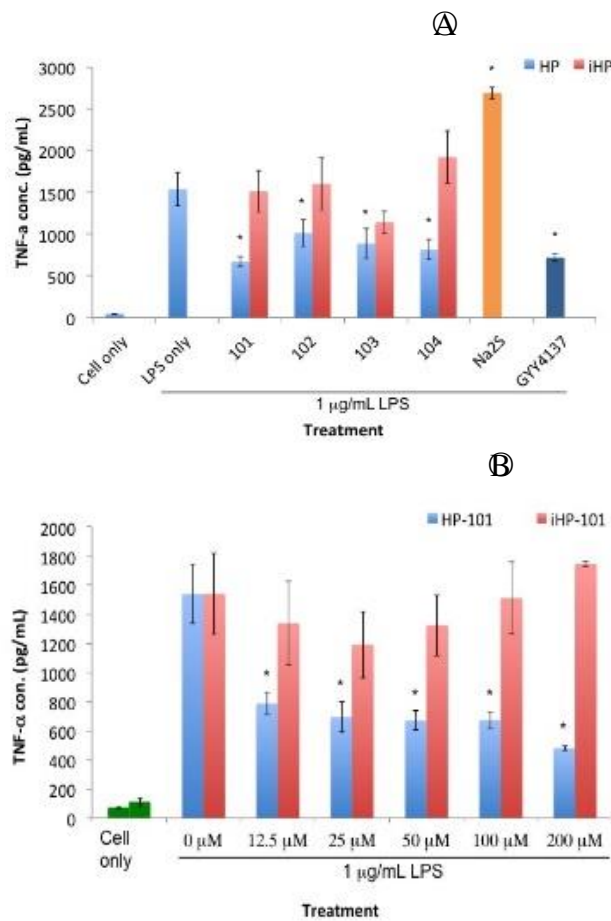


Figure 1.7. 200 μM HP-105 in PBS with PLE 20unit/mL. (37 °C, 1% DMSO, $p=0.95$, $n=3$)

We next tested whether such compounds also produced H₂S-associated biological effects *in vitro*. For such studies, negative control compounds are always important. However, there are no good control compounds for existing H₂S prodrugs. To address this issue, we used the inactive oxyacid version of the prodrugs (iHPs, Figure 1.6) as the control compounds. Compared to thioacid prodrugs, iHPs have the same chemical structural frame except replacing sulfur with oxygen.

We first tested the cytotoxicity of these prodrugs on RAW264.7 macrophages. None showed any toxicity at 200 μ M. We then examine the effect of the prodrugs on TNF- α production after co-treatment of the cell with the prodrugs and 1 μ g/mL LPS for one hour, using an ELISA kit (Figure 1.8). The results showed that only the prodrugs and GYY 4137 effectively inhibited TNF- α secretion, and Na₂S showed pro-inflammatory effect, which is similar to literature results.⁹⁶ None of the iHPs showed the same effect, which clearly demonstrated that the inhibition effect on TNF- α production came from the H₂S released from the respective prodrug.



*Figure 1.8. TNF- α concentrations of RAW 264.7 cell culture media after 1-hour co-treatment with H₂S prodrugs and LPS.(A) Treatment with 50 μ M HPs, iHPs Na₂S and GYY4137. (B) Treatment with various concentrations of BW-HP-101 and iHP-101 (n=4 *: p<0.05)*

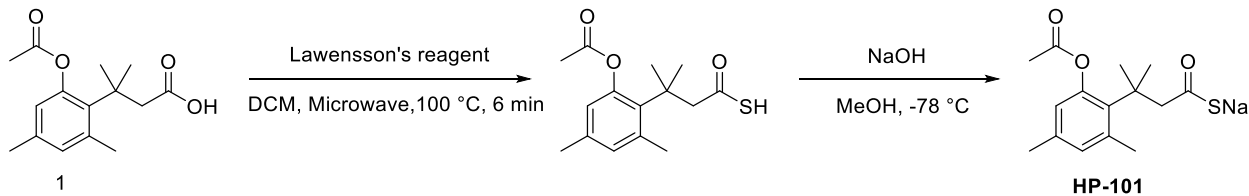
1.3 Conclusion

In conclusion, we successfully investigated a new strategy of making H₂S prodrugs by using an esterase catalyzed lactonization prodrug system. Compared to existing H₂S prodrugs/donors, the new H₂S prodrugs described show several unique features. First of all, they have controlled H₂S release rates. This aspect seems to be the most challenging and important issue in the field of H₂S donors. Secondly, the trigger is an enzyme ubiquitous in the biological system.[23] Thirdly, the prodrugs require a specific type of enzyme to trigger H₂S release, which afford the potential for controlled release at preferred sites. Fourthly, as research tools, the prodrugs described have well-defined negative controls. Fifthly, this strategy provides the first H₂S-NSAIDs hybrids with controllable release rates. We believe that these new H₂S prodrugs will be very useful research tools to others working in this field.

1.4 Experimental part

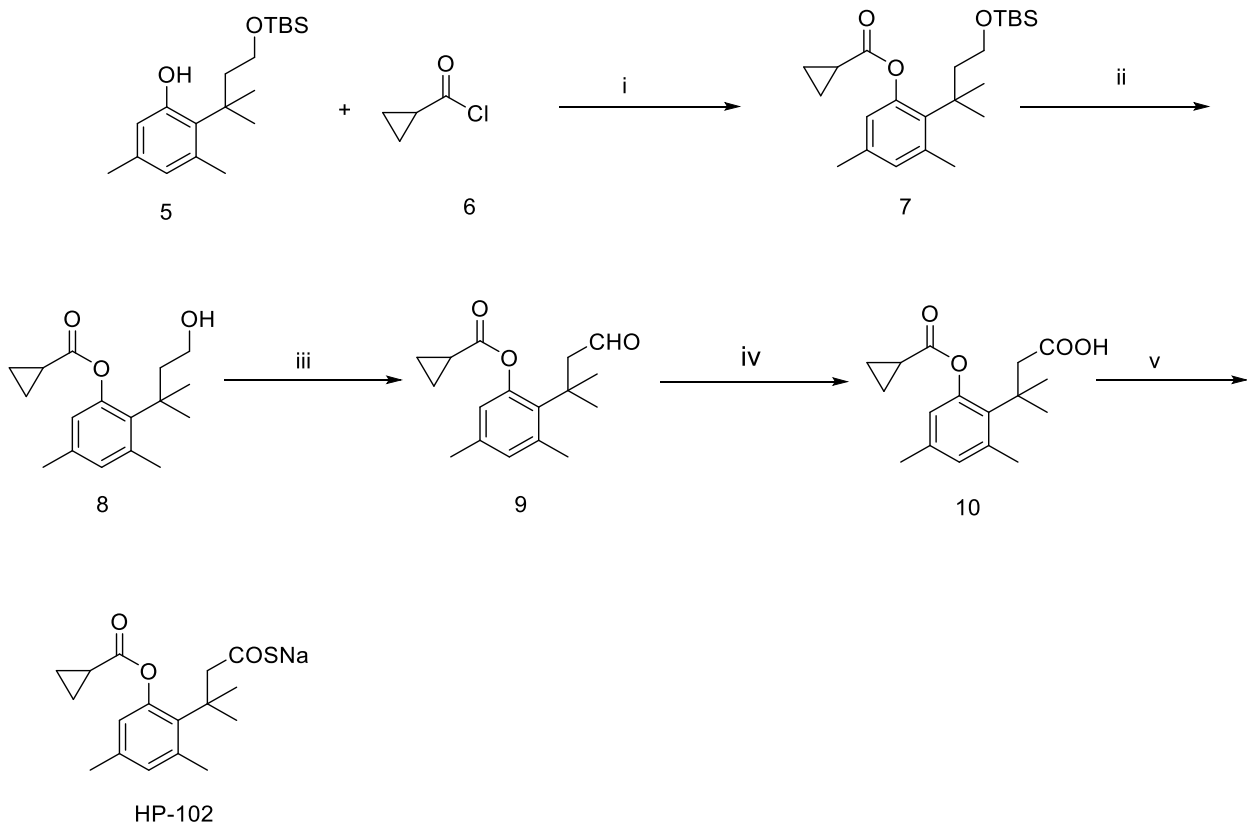
General Information: All reagents and solvents were of reagent grade and were purchased from Aldrich. ¹H-NMR (400 MHz) and ¹³C-NMR (100 MHz) spectra were recorded on a Bruker Avance 400 MHz NMR spectrometer. Mass spectral analyses were performed on an ABI API 3200 (ESI-Triple Quadruple). HPLC was performed on a Shimadzu Prominence UFC (column: Waters C18 3.5 μM, 4.6×100 mm). UV-Vis absorption spectra were recorded on a Shimadzu PharmaSpec UV-1700 UV-Visible spectrophotometer. Fluorescence spectra were recorded on a Shimadzu RF-5301PC fluorometer. 96-Well plates were read and recorded on a PerkinElmer 1420 multi-label counter. Compounds **1**,^{105,116} **5**,¹⁰⁵ **11**,¹⁰⁵ WSP-5¹⁰⁷ and GYY 4137⁴ were synthesized according to literature procedures.

1.4.1 Synthesis of HPs



Scheme 1.5 Synthesis of “trimethyl lock” -based H₂S prodrug HP-101

Synthesis of sodium 3-(2-acetoxy-4, 6-dimethylphenyl)-3-methylbutanethioate (HP-101). A solution of 3-(2-acetoxy-4,6-dimethylphenyl)-3-methylbutanoic acid (**1**, 78 mg, 0.3 mmol), Lawesson's reagent (60 mg, 0.15 mmol) and 1.5 mL CH₂Cl₂ in a sealed tube was subjected to microwave irradiation (100 °C , 6 min). After completion of reaction, the solution mixture was diluted with dichloromethane (DCM, 5 mL). The organic layer was washed by 1 N HCl and brine, and dried over anhydrous sodium sulfate. Then, after filtration, DCM was removed under vacuum. The residue was purified by flash column chromatography (hexane: ethyl acetate =10:1) to give an oily residue (59 mg). The oil product was dissolved in methanol, and a NaOH solution (8.4 mg in 2 mL methanol) was added at -78 °C. After 3 minutes, the methanol in the reaction mixture was removed by rotavapor. Diethyl ether was added into the crude product, and the final product was precipitated from diethyl ether as a white solid (57 mg, 67%). ¹H NMR (CD₃OD): δ 6.80 (s, 1H, Ph-H), 6.53 (s, 1H, Ph-H), 3.33 (s, -CH₂-CO-), 2.58 (s, 3H, Ph-CH₃), 2.32 (s, 3H, -CO-CH₃), 2.21 (s, 3H, Ph-CH₃), 1.54 (s, 6H, Ph-C(CH₃)₂-); ¹³C NMR (CD₃OD): δ 219.0, 172.4, 150.7, 139.4, 137.0, 136.4, 132.9, 123.9, 64.4, 40.6, 31.8, 25.7, 22.0, 20.2. HRMS calcd for C₁₅H₁₉O₃S [M-H]⁻ 279.1055, found: 279.1051.



Scheme 1.6 Synthesis of HP-102

[0001] *Synthesis of 2-(4-((tert-butyldimethylsilyl)oxy)-2-methylbutan-2-yl)-3,5-dimethylphenyl cyclopropanecarboxylate (7).* To a solution of 2-(4-((tert-butyldimethylsilyl)oxy)-2-methylbutan-2-yl)-3,5-dimethylphenol (**5**, 1.9 g, 5.9 mmol) and Et_3N (1.2 ml, 8.8 mmol) in DCM (150 mL) was added dropwise cyclopropanecarbonyl chloride (**6**, 0.8 ml, 8.8 mmol) at 0 °C during a period of 10 min. The mixture was allowed to warm to room temperature and was stirred for an additional 12 h. Then the reaction was quenched with the addition of H_2O (100 mL), and extracted with ethyl acetate (2×150 mL). The combined organic phase was dried over anhydrous Na_2SO_4 and evaporated under reduced pressure to give the crude product, which was purified by column

chromatography (hexane: ethyl acetate =100:1) to give a colorless oil (1.04 g, 46%). ¹H NMR (CDCl₃): δ 6.79 (s, 1H), 6.56 (s, 1H), 3.50 (t, *J* = 8.0 Hz, 2H), 2.52 (s, 3H), 2.22 (s, 3H), 2.06 (t, *J* = 8.0 Hz, 2H), 1.86-1.80 (m, 1H), 1.49 (s, 6H), 1.17-1.13 (m, 2H), 1.01-0.95 (m, 2H), 0.85 (s, 9H), -0.02 (s, 6H); ¹³C NMR (CDCl₃): 174.1, 150.1, 138.4, 136.0, 134.3, 132.3, 123.2, 61.0, 46.1, 39.3, 32.0, 26.1, 25.4, 20.3, 18.4, 13.7, 8.9, -5.2. HRMS calcd for C₂₃H₃₈O₃Si [M+H]⁺ 391.2663, found: 391.2649.

Synthesis of 2-(4-hydroxy-2-methylbutan-2-yl)-3,5-dimethylphenyl cyclopropanecarboxylate (8).

To a solution of 2-(4-((tert-butyldimethylsilyl)oxy)-2-methylbutan-2-yl)-3,5-dimethylphenyl cyclopropanecarboxylate (**7**, 1.04 g, 2.7 mmol) in tetrahydrofuran (THF, 15 mL) was added H₂O (15 mL) and AcOH (45 mL). The reaction mixture was stirred at room temperature for 4 h, quenched with H₂O (50 mL), and extracted with ethyl acetate (2 × 150 mL). The combined organic phase was dried over anhydrous Na₂SO₄, evaporated under reduced pressure, and purified by silica gel column chromatography (hexane: ethyl acetate =6:1) to give a colorless oil (680 mg, 91%). ¹H NMR (CDCl₃): δ 6.81 (s, 1H), 6.55 (s, 1H), 3.54 (t, *J* = 8.0 Hz, 2H), 2.52 (s, 3H), 2.22 (s, 3H), 2.06 (t, *J* = 8.0 Hz, 2H), 1.87-1.82 (m, 1H), 1.51 (s, 6H), 1.18-1.14 (m, 2H), 1.04-0.99 (m, 2H); ¹³C NMR (CDCl₃): 174.8, 150.0, 138.5, 136.3, 134.1, 132.5, 123.4, 60.7, 45.9, 39.3, 32.2, 25.5, 20.3, 13.7, 9.1. HRMS calcd for C₁₇H₂₄O₃ [M+H]⁺ 277.1798, found: 277.1789.

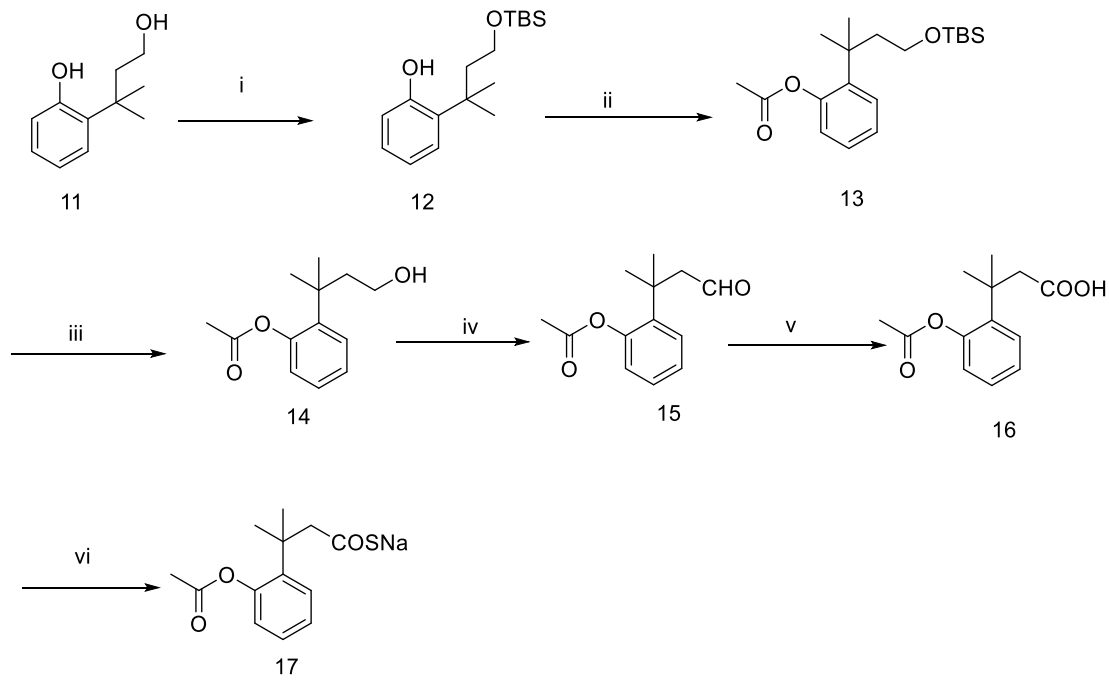
Synthesis of 3,5-dimethyl-2-(2-methyl-4-oxobutan-2-yl)phenylcyclopropanecarboxylate (9). To a solution of PCC (1.5 g, 7.0 mmol) in DCM (20 mL) was added dropwise 2-(4-hydroxy-2-methylbutan-2-yl)-3,5-dimethylphenyl cyclopropanecarboxylate (**8**, 0.96 g, 3.5 mmol) in DCM (25 mL) at room temperature. After 2 h, the mixture was directly subjected to column

chromatography (hexane: ethyl acetate =10:1) to obtain the pure product as colorless oil (0.8 g, 83%). ^1H NMR (CDCl_3): δ 9.55 (t, J = 4Hz, 1H), 6.84 (s, 1H), 6.61 (s, 1H), 2.84 (d, J = 4.0 Hz, 2H), 2.53 (s, 3H), 2.23 (s, 3H), 1.86-1.80 (m, 1H), 1.57 (s, 6H), 1.17-1.14 (m, 2H), 1.05-1.00 (m, 2H); ^{13}C NMR (CDCl_3): 203.3, 174.1, 149.7, 137.9, 136.9, 132.8, 132.7, 123.5, 56.8, 38.3, 31.7, 25.5, 20.4, 13.6, 9.1. HRMS calcd for $\text{C}_{17}\text{H}_{22}\text{O}_3$ [M+H] $^+$ 275.1642, found: 275.1632.

Synthesis of 3-(2-((cyclopropanecarbonyl)oxy)-4,6-dimethylphenyl)-3-methylbutanoic acid (10). To a solution of 3,5-dimethyl-2-(2-methyl-4-oxobutan-2-yl)phenyl cyclopropanecarboxylate (**9**, 200 mg, 0.73 mmol) in *t*-BuOH (4 mL) and 2-methylbut-2-ene (0.7 mL), NaClO_2 (98 mg, 1.08 mmol) in 0.67 M NaH_2PO_4 (0.8 mL) was added dropwise at room temperature. After 2 h, the reaction mixture was quenched with H_2O (10 mL), and extracted with ethyl acetate (2×50 ml). The combined organic phase was dried over anhydrous Na_2SO_4 and then evaporated under reduced pressure to give the crude product, which was purified by column chromatography (hexane: ethyl acetate =5:1) to yield a white solid (110 mg, 52%). ^1H NMR (CDCl_3): δ 6.80 (s, 1H), 6.59 (s, 1H), 2.86 (s, 2H), 2.53 (s, 3H), 2.22 (s, 3H), 1.89-1.83 (m, 1H), 1.58 (s, 6H), 1.18-1.14 (m, 2H), 1.03-0.98 (m, 2H); ^{13}C NMR (CDCl_3): 177.5, 174.2, 149.7, 138.1, 136.4, 133.5, 132.5, 123.2, 47.7, 38.9, 31.4, 25.4, 20.4, 13.6, 9.1. HRMS calcd for $\text{C}_{17}\text{H}_{22}\text{O}_4$ [M+H] $^+$ 291.1591, found: 291.1580.

Synthesis of Sodium 3-(2-((cyclopropanecarbonyl)oxy)-4,6-dimethylphenyl)-3-methylbutanethioate (HP-102). To a solution of 3-(2-((cyclopropanecarbonyl)oxy)-4,6-dimethylphenyl)-3-methylbutanoic acid (**10**, 110 mg, 0.38 mmol) in DCM (5 mL) was added Lawesson's reagent (77 mg, 0.19 mmol). The mixture was heated in a microwave at 100 °C for 6 min. The mixture was directly subjected to column chromatography (hexane: ethyl acetate =25:1)

to obtain the pure product as colorless oil, which was then dissolved in 5 ml methanol. Then 2.5 ml of 0.1 M NaOH methanol solution was added at -78 °C. After 5 min, the mixture was allowed to warm to room temperature and the solvent was removed by vacuum. The final product was achieved by precipitation from ether as a white solid (70 mg, 56%). ¹H NMR (400 MHz, CD₃OD): δ 6.77 (d, *J* = 0.8 Hz, 1H), 6.46 (d, *J* = 0.8 Hz, 1H), 3.35 (s, 2H), 2.56 (s, 3H), 2.18 (s, 3H), 1.99-1.98 (m, 1H), 1.53 (s, 6H), 1.09-1.04 (m, 4H); ¹³C NMR (CDCl₃): 196.1, 174.0, 149.8, 138.1, 136.7, 133.0, 132.6, 123.3, 58.5, 39.9, 31.5, 25.6, 20.4, 13.7, 9.2. HRMS calcd for C₁₇H₂₁NaO₃S [M+H]⁺329.1182, found: 329.1168.



Reagents and conditions: (i) *tert*-Butyldimethylsilyl chloride(TBDMSCl), Dimethylformamide (DMF), imidazole, 92%; (ii) acetic anhydride, 4-Dimethylaminopyridine(DMAP), 3 h, 91%; (iii) AcOH/H₂O, THF, rt, 12 h, 91%; (iv) PCC, DCM, rt, 2h, 92%; (v) NaClO₂/NaH₂PO₄, 2-methylbut-2-ene, *t*-BuOH, rt, 2 h; 79% (vi) 1) Lawesson's reagent, DCM, microwave, 6 min; 2) NaOH, methanol, -78 °C, 60% for the last two steps.

Scheme 1.7 Synthesis of HP-103.

Synthesis of 2-(4-((tert-butyldimethylsilyl)oxy)-2-methylbutan-2-yl)phenol (12). To a 20-ml vial was added 2-(4-hydroxy-2-methylbutan-2-yl)phenol (**11**, 2.5 g, 14 mmol), imidazole (2.8 g, 42 mmol), TBDMSCl (4.2 g, 28 mmol) and DMF (7 ml). The mixture was stirred for 5 min at room temperature, then quenched with the addition of H₂O (100 mL), and extracted with ethyl acetate (2×150 mL). The combined organic phase was washed by saturated NaHCO₃ (2×150 mL) and dried over anhydrous Na₂SO₄ and evaporated under reduced pressure to give the crude product, which was purified by recrystallization in methanol to give a white solid (3.8 g, 92%). ¹H NMR (400 MHz CDCl₃): δ 7.19 (d, *J* = 7.6 Hz, 1H), 7.08-7.04 (m, 1H), 6.86-6.83 (m, 1H), 6.66 (d, *J* = 7.6 Hz, 1H), 6.10 (s, 1H), 3.51 (t, *J* = 7.6 Hz, 2H), 2.17 (t, *J* = 7.6 Hz, 2H), 1.42 (s, 6H), 0.88 (s, 9H), 0.02 (s, 6H). ¹³C NMR (CDCl₃) δ 154.9, 134.1, 127.7, 127.3, 120.2, 116.9, 61.7, 43.3, 36.7, 29.0, 26.1, 18.5, -5.1. HRMS calcd for C₁₇H₃₀O₂Si [M+H]⁺295.2088, found: 295.2075.

Synthesis of 2-(1-((tert-butyldimethylsilyl)oxy)-2-methylpropan-2-yl)phenyl acetate (13). To a solution of 2-(4-((tert-butyldimethylsilyl)oxy)-2-methylbutan-2-yl)phenol (**12**, 1.53 g, 5.6 mmol) in DCM (10 mL), was added acetic anhydride (1.63 g, 3 mmol), Et₃N (1.62 g, 16 mmol) and DMAP (0.29 g, 2.4 mmol). The mixture was stirred at room temperature for 2 h. The reaction was quenched with H₂O (10 mL) and extracted with ethyl acetate (2 × 50 mL). The combined organic phase was dried over anhydrous Na₂SO₄ and evaporated under reduced pressure to give the crude product, which was then purified by column chromatography (hexane: ethyl acetate =100:1) to obtain colorless oil (1.6 g, 91%). ¹H NMR (CDCl₃): δ 7.33 (dd, *J* = 7.6 Hz, 1.2 Hz, 1H), 7.25-7.21 (m, 1H), 7.18-7.14 (m, 1H), 7.00 (dd, *J* = 7.6 Hz, 1.2 Hz, 1H), 3.41 (t, *J* = 7.6 Hz, 2H), 2.33 (s, 3H) 2.01 (t, *J* = 7.6 Hz, 2H), 1.37 (s, 6H), 0.84 (s, 9H), -0.04 (s, 6H). ¹³C NMR (CDCl₃) δ 169.5,

149.2, 139.0, 128.2, 127.2, 125.8, 124.1, 60.6, 44.5, 36.9, 29.3, 26.1, 21.8, 18.4, -5.2. HRMS cald for C₁₉H₃₂O₃Si [M+H]⁺337.2193, found: 337.2201.

Synthesis of 2-(4-hydroxy-2-methylbutan-2-yl)phenyl acetate (14). To a solution of 2-((tert-butyldimethylsilyl)oxy)-2-methylpropan-2-yl)phenyl acetate (**13**) in 3 ml THF (1.50 g, 4.46 mmol), was added H₂O (3 mL) and AcOH (9 mL). The reaction mixture was stirred at room temperature for 4 h, quenched with H₂O (10 mL), and extracted with ethyl acetate (2×50 mL). The combined organic phase was dried over anhydrous Na₂SO₄ and evaporated under reduced pressure to give the crude product, which was purified by column chromatography (hexane: ethyl acetate =2:1) to obtain colorless oil (900 mg, 91%). ¹H NMR (CDCl₃): δ 7.32 (dd, *J* = 7.6 Hz, 1.6 Hz, 1H), 7.25-7.21 (m, 1H), 7.18-7.14 (m, 1H), 6.98 (dd, *J* = 7.6 Hz, 1.6 Hz, 1H), 3.40 (t, *J* = 7.6 Hz, 2H), 2.34 (s, 3H), 1.99 (t, *J* = 7.6 Hz, 2H), 1.37 (s, 6H). ¹³C NMR (CDCl₃) δ 169.9, 149.1, 138.8, 128.1, 127.3, 126.0, 124.2, 60.1, 44.4, 36.7, 29.2, 21.8. For C₁₃H₁₈O₃ [M+H]⁺223.1329, found: 223.1333.

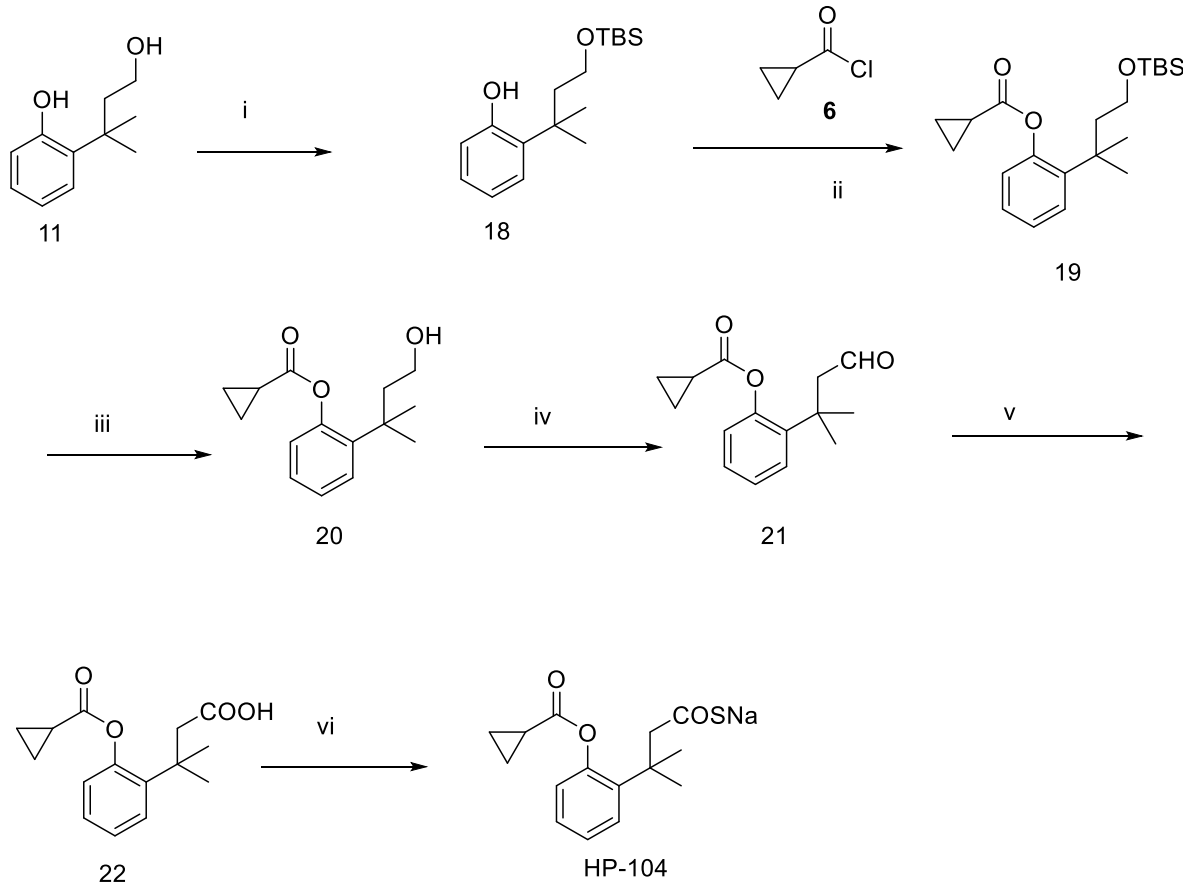
Synthesis of 2-(2-methyl-4-oxobutan-2-yl)phenyl acetate (15). To a solution of PCC (1.55 g, 7.2 mmol) in DCM (5 mL), a solution of (2-(4-hydroxy-2-methylbutan-2-yl)phenyl acetate (**14**, 710 mg, 3.20 mmol) in DCM (5 mL) was added dropwise at room temperature. After 2 h, the mixture was directly subjected to column chromatography (hexane: ethyl acetate =10:1) to obtain the pure product as colorless oil (650 mg, 92%). ¹H NMR (CDCl₃): δ 9.45 (t, *J* = 2.8 Hz, 1H), 7.38 (dd, *J* = 7.6 Hz, 1.6 Hz, 1H), 7.30-7.26 (m, 1H), 7.22-7.18 (m, 1H), 7.05 (dd, *J* = 7.6 Hz, 1.6 Hz, 1H), 2.79 (d, *J* = 2.8 Hz, 2H), 2.36 (s, 3H), 1.46 (s, 6H). ¹³C NMR (CDCl₃): δ 202.8, 169.3, 149.0,

137.5, 128.0, 127.8, 126.2, 124.5, 54.6, 36.3, 29.1, 21.8. HRMS calcd for C₁₃H₁₆O₃ [M+H]⁺ 221.1172, found: 221.1178.

*Synthesis of 3-(2-acetoxyphenyl)butanoic acid (**16**)*. To a solution of 2-(2-methyl-4-oxobutan-2-yl)phenyl acetate (**15**, 600 mg, 2.73 mmol) in *t*-BuOH (12 mL) and 2-methylbut-2-ene (2.5 mL) was added dropwise NaClO₂ (564 mg, 6.27 mmol) in 0.67M NaH₂PO₄ (2.0 mL) at room temperature. After 2 h, the reaction was quenched with H₂O (20 mL), and extracted with ethyl acetate (2×50 ml). The combined organic phase was dried over anhydrous Na₂SO₄ and evaporated under reduced pressure to afford the crude product, which was purified by column chromatography (hexane: ethyl acetate =5:1) to obtain a white solid (510 mg, 79%). ¹H NMR (CDCl₃): δ 7.38 (dd, *J* = 8.0 Hz, 1.6 Hz, 1H), 7.27-7.23 (m, 1H), 7.19-7.15 (m, 1H), 7.03 (dd, *J* = 8.0 Hz, 1.6 Hz, 1H), 2.79 (s, 2H), 2.35 (s, 3H) 1.47 (s, 6H). ¹³C NMR (CD₃OD) δ 175.2, 171.0, 150.4, 139.9, 128.9, 128.2, 126.7, 125.2, 46.6, 37.4, 29.1, 21.6. HRMS calcd for C₁₃H₁₆O₄ [M+Na]⁺ 259.0941, found: 259.0945.

*Synthesis of sodium 3-(2-acetoxyphenyl)-3-methylbutanethioate (**HP-103**)*. A solution of 3-(2-acetoxyphenyl)butanoic acid (**16**, 100 mg, 0.42 mmol) and Lawesson's reagent (85 mg, 0.21 mmol) in DCM (5 mL) in a sealed tube was subjected to microwave irradiation (100 °C, 6 min). The mixture was directly subjected to column chromatography (hexane: ethyl acetate =20:1) to obtain the pure product as colorless oil, which was then dissolved in 5 ml methanol. To this solution 3 ml of 0.1 M NaOH methanol solution was added at -78 °C. After 5 min, the mixture was allowed to warm to room temperature and the solvent was removed by vacuum. The final product was achieved by recrystallization in ether as a white solid (70 mg, 60%). ¹H NMR (CD₃OD): δ 7.39 (dd, *J* = 8.0Hz, 1.6 Hz, 1H), 7.26-7.22 (m, 1H), 7.19-7.15 (m, 1H), 7.04 (dd, *J* = 8.0Hz, 1.6

Hz, 1H), 3.18 (s, 2H), 2.36 (s, 3H) 1.44 (s, 6H). ^{13}C NMR (CDCl_3) δ 195.7, 169.3, 148.9, 137.5, 128.0, 127.8, 126.0, 124.2, 56.2, 37.5, 28.4, 21.8. HRMS calcd for $\text{C}_{13}\text{H}_{15}\text{NaO}_3\text{S}$ [M-Na] $^+$ 251.0747, found: 251.0742.



Reagents and conditions (i) TBDMSCl, imidazole, DMF, rt, 92%; (ii) Et₃N, DCM, 0 °C-rt, 12 h, 73%; (iii) AcOH/H₂O, THF, rt, 12 h, 85%; (iv) PCC, DCM, rt, 2 h 88%; (v) NaClO₂/NaH₂PO₄, 2-methylbut-2-ene, t-BuOH, rt, 2 h 65%; (vi) 1) Lawesson's reagent, DCM, microwave, 6 min; 2) NaOH, methanol, -78 °C, 65% for the last two steps .

Scheme 1.8 Synthesis of HP-104.

Synthesis of 2-((tert-butyldimethylsilyl)oxy)-2-methylbutan-2-ylphenol (18). To a 20-ml vial was added 2-(4-hydroxy-2-methylbutan-2-yl)phenol (11, 2.5 g, 14 mmol), imidazole (2.8 g, 42 mmol), TBDMSCl (4.2 g, 28 mmol) and DMF (7 ml). The mixture was stirred for 5 min at room

temperature, then quenched with the addition of H₂O (100 mL), and extracted with ethyl acetate (2×150 mL). The combined organic phase was washed by saturated NaHCO₃ (2×150 mL), dried over anhydrous Na₂SO₄, and evaporated under reduced pressure to give the crude product, which was purified by recrystallization in methanol to give a white solid (3.8 g, 92%). ¹H NMR (CDCl₃): δ 7.19 (d, *J* = 7.6 Hz, 1H), 7.08-7.04 (m, 1H), 6.86-6.83 (m, 1H), 6.66 (d, *J* = 7.6 Hz, 1H), 6.10 (s, 1H), 3.51 (t, *J* = 7.6 Hz, 2H), 2.17 (t, *J* = 7.6 Hz, 2H), 1.42 (s, 6H), 0.88 (s, 9H), 0.02 (s, 6H). ¹³C NMR (CDCl₃) δ 154.9, 134.1, 127.7, 127.3, 120.2, 116.9, 61.7, 43.3, 36.7, 29.0, 26.1, 18.5, -5.1. HRMS calcd for C₁₇H₃₀O₂Si [M+H]⁺295.2088, found: 295.2075.

Synthesis of 2-(4-((tert-butyldimethylsilyl)oxy)-2-methylbutan-2-yl)phenyl cyclopropanecarboxylate (19). To a solution of 2-(4-((tert-butyldimethylsilyl)oxy)-2-methylbutan-2-yl)phenol (**18**, 2.0 g, 6.8 mmol) and Et₃N (1.4 g, 13.6 mmol) in DCM (150 mL) was added dropwise cyclopropanecarbonyl chloride (**6**, 1.46 g, 13.6 mmol) at 0 °C. The mixture was allowed to warm to room temperature and stirred for 12 h. Then the reaction was quenched with the addition of H₂O (100 mL), and solution was extracted with ethyl acetate (2×150 mL). The combined organic phase was dried over anhydrous Na₂SO₄ and evaporated under reduced pressure to give the crude product, which was purified by column chromatography (hexane: ethyl acetate =50:1) to give a colorless oil (1.8 g, 73%). ¹H NMR (CDCl₃): δ 7.32 (dd, *J* = 7.6 Hz, 1.6 Hz, 1H), 7.23-7.19 (m, 1H), 7.16-7.12 (m, 1H), 6.98 (dd, *J* = 7.6 Hz, 1.6 Hz, 1H), 3.41 (t, *J* = 7.6 Hz, 2H), 2.03 (t, *J* = 7.6 Hz, 2H), 1.92-1.85 (m, 1H), 1.38 (s, 6H), 1.19-1.18 (m, 2H), 1.05-1.00 (m, 2H), 0.84 (s, 9H), -0.04 (s, 6H). ¹³C NMR (CDCl₃) δ 173.5, 149.4, 139.1, 128.1, 127.1, 125.6, 124.2, 60.7, 44.5, 36.9, 29.2, 26.1, 18.3, 13.5, 9.1, -5.2. HRMS calcd for C₂₁H₃₄O₃Si [M+H]⁺363.2350, found: 363.2348.

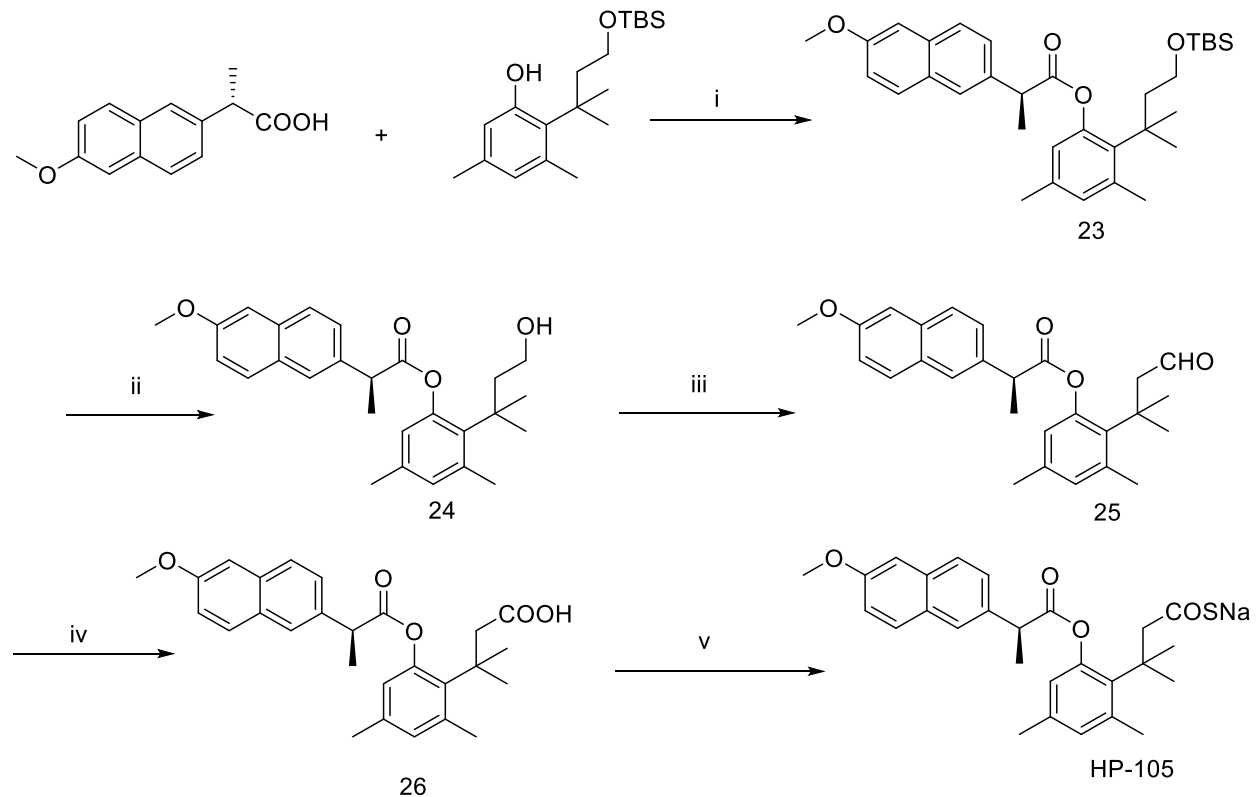
Synthesis of 2-(4-hydroxy-2-methylbutan-2-yl)phenyl cyclopropanecarboxylate (20). To a solution of 2-(4-((tert-butyldimethylsilyl)oxy)-2-methylbutan-2-yl)phenyl cyclopropanecarboxylate (**19**, 1.7 g, 4.69 mmol) in THF (20 mL) was added H₂O (20 mL) and AcOH (60 mL). The reaction mixture was stirred at room temperature for 4 h, quenched with H₂O (50 mL), and extracted with ethyl acetate (2 × 150 mL). The combined organic phase was dried over anhydrous Na₂SO₄ and evaporated under reduced pressure, and purified silica gel column chromatography (hexane: ethyl acetate = 10:1) as colorless oil (1.1 g, 95%). ¹H NMR (400 MHz CDCl₃): δ 7.32 (dd, *J* = 7.6 Hz, 1.6 Hz, 1H), 7.24-7.20 (m, 1H), 7.18-7.13 (m, 1H), 6.96 (dd, *J* = 7.6 Hz, 1.6 Hz, 1H), 3.42 (t, *J* = 7.6 Hz, 2H), 2.03 (t, *J* = 7.6 Hz, 2H), 1.93-1.87 (m, 1H), 1.39 (s, 6H), 1.21-1.17 (m, 2H), 1.07-1.02 (m, 2H). ¹³C NMR (CDCl₃) δ 174.1, 149.4, 139.0, 128.1, 127.3, 125.9, 124.3, 60.3, 44.4, 36.9, 29.2, 13.6, 9.2. For C₁₅H₂₀O₃ [M+H]⁺ 249.1485, found: 249.1485.

Synthesis of 2-(2-methyl-4-oxobutan-2-yl)phenyl cyclopropanecarboxylate (21). To a solution of PCC (2.2 g, 10.0 mmol) in DCM (20 mL) was added dropwise 2-(4-hydroxy-2-methylbutan-2-yl)phenyl cyclopropanecarboxylate (**20**, 1.1 g, 4.4 mmol) in DCM (25 mL) at room temperature. After 2 h, the mixture was directly subjected to column chromatography (hexane: ethyl acetate = 20:1) to obtain the pure product as colorless oil (0.95 g, 88%). ¹H NMR (CDCl₃): δ 9.45 (t, *J* = 2.8 Hz, 1H), 7.38 (dd, *J* = 8.0 Hz, 1.6 Hz, 1H), 7.29-7.25 (m, 1H), 7.21-7.17 (m, 1H), 7.03 (dd, *J* = 8.0 Hz, 1.6 Hz, 1H), 2.81 (d, *J* = 2.8 Hz, 2H), 1.93-1.86 (m, 1H), 1.47 (s, 6H), 1.21-1.17 (m, 2H), 1.08-1.04 (m, 2H). ¹³C NMR (CDCl₃): δ 202.9, 173.4, 149.2, 137.6, 127.9, 127.7, 126.0, 124.5, 54.5, 36.3, 29.1, 13.5, 9.2. HRMS calcd for C₁₅H₁₈O₃ [M+Na]⁺ 269.1148, found: 269.1149.

Synthesis of 3-(2-((cyclopropanecarbonyl)oxy)phenyl)-3-methylbutanoic acid (22). To a solution of 2-(2-methyl-4-oxobutan-2-yl)phenyl cyclopropanecarboxylate (**21**, 900 mg, 3.6 mmol) in *t*-BuOH (20 mL) and 2-methylbut-2-ene (4 mL) NaClO₂ (496 mg, 5.4 mmol) in 0.67 M NaH₂PO₄ (4 mL) was added dropwise at room temperature. After 2 h, the reaction mixture was quenched with H₂O (20 mL), and extracted with ethyl acetate (2 × 100 ml). The combined organic phase was dried over anhydrous Na₂SO₄ and then evaporated under reduced pressure to give the crude product, which was purified by column chromatography (hexane: ethyl acetate =10:1) to yield a white solid (610 mg, 65%). ¹H NMR (MeOH): δ 7.42 (dd, *J* = 7.6 Hz, 1.6 Hz, 1H), 7.23-7.14 (m, 2H), 6.97 (dd, *J* = 7.6 Hz, 1.6 Hz, 1H), 2.80 (s, 2H), 1.99-1.93 (m, 1H), 1.47 (s, 6H), 1.13-1.07 (m, 4H). ¹³C NMR (CDCl₃) δ 177.6, 173.6, 149.1, 138.2, 127.8, 127.5, 125.8, 124.1, 45.8, 36.7, 28.4, 13.5, 9.2. HRMS calcd for C₁₅H₁₈O₄ [M+H]⁺263.1278, found: 263.1279.

Synthesis of sodium 3-(2-((cyclopropanecarbonyl)oxy)phenyl)-3-methylbutanethioate (HP-104). To a solution of 3-(2-((cyclopropanecarbonyl)oxy)phenyl)-3-methylbutanoic acid (**22**, 120 mg, 0.46 mmol) in DCM (5 mL) was added Lawesson's reagent (92 mg, 0.23 mmol). The mixture was heated in a microwave at 100 °C for 6 min. The mixture was directly subjected to column chromatography (hexane: ethyl acetate =20:1) to obtain the pure product as colorless oil, which was then dissolved in 5 ml methanol. Then 2.5 ml of 0.1 M NaOH methanol solution was added to the reaction solution at -78 °C. After 5 min, the mixture was allowed to warm to room temperature and the solvent was removed by vacuum. The final product was achieved by recrystallization in ether as a white solid (90 mg, 65%). ¹H NMR (CDCl₃): δ 7.38 (d, *J* = 7.2 Hz, 1H), 7.28-7.17 (m, 2H), 7.04 (d, *J* = 8.0 Hz, 1H), 4.41 (s, 1H), 3.11 (s, 2H), 1.97-1.90 (m, 1H), 1.48 (s, 6H), 1.22-1.20 (m, 2H), 1.09-1.06 (m, 2H); ¹³C NMR (CDCl₃): 195.8, 173.4, 149.1, 137.6,

128.0, 127.7, 125.9, 124.2, 56.3, 37.5, 28.4, 13.5, 9.3. HRMS calcd for C₁₅H₁₇NaO₃S [M+H]⁺ 301.0869, found: 301.0871.



Reagents and conditions (i) EDC/DMAP, DCM, rt, 2 h, 88%; (ii) AcOH/H₂O, THF, rt, 12 h, 87%; (iii) PCC, DCM, rt, 2 h, 81%; (iv) NaClO₂/NaH₂PO₄, 2-methylbut-2-ene, t-BuOH, rt, 2 h, 66%; (v) 1) Lawesson's reagent, DCM, microwave, 6 min; 2) NaOH, methanol, -78 °C, 65% for the last two steps

Scheme 1.9 Synthesis of HP-105.

Synthesis of 2-((tert-butyldimethylsilyl)oxy)-2-methylbutan-2-yl)-3,5-dimethylphenyl (S)-2-(6-methoxynaphthalen-2-yl)propanoate (23). To a solution of 2-((tert-butyldimethylsilyl)oxy)-2-methylbutan-2-yl)-3,5-dimethylphenol (**5**, 1.27 g, 3.9 mmol), (S)-2-(6-methoxynaphthalen-2-yl)propanoic acid (1.00 g, 4.4 mmol) and DMAP (100 mg, 0.8 mmol) in DCM (50 mL) was added EDC (1.62 g, 8.7 mmol). The mixture was stirred at room temperature for 2 h, then quenched with the addition of H₂O (50 mL), and extracted with DCM (2×50 mL). The combined organic phase

was dried over anhydrous Na₂SO₄ and evaporated under reduced pressure to give the crude product, which was purified by column chromatography (hexane: ethyl acetate =50:1) to give a colorless oil (1.86 g, 88%). ¹H NMR (CDCl₃): δ 7.77-7.72 (m, 3H), 7.50 (dd, *J* = 8.4 Hz, *J* = 1.6 Hz, 1H), 7.17-7.14 (m, 2H), 6.74 (d, *J* = 1.2 Hz, 1H), 6.32 (d, *J* = 1.2 Hz, 1H), 4.04 (q, , *J* = 7.2 Hz, 1H), 3.93 (s, 3H), 3.40 (t, *J* = 7.2 Hz, 2H), 2.48 (s, 3H), 2.14 (s, 3H), 1.91 (t, *J* = 7.2 Hz, 2H), 1.69 (d, *J* = 7.2 Hz, 3H), 1.36 (d, *J* = 7.2 Hz, 6H), 0.84 (s, 9H), -0.06 (s, 6H); ¹³C NMR (CDCl₃): 173.7, 157.8, 150.2, 138.3, 136.0, 134.9, 134.2, 134.0, 132.3, 129.5, 129.1, 127.4, 126.6, 126.5, 122.7, 119.2, 105.7, 60.9, 55.4, 46.3, 45.9, 39.2, 31.9, 31.9, 26.1, 25.4, 20.3, 18.6, 18.3, -5.2. HRMS calcd for C₃₃H₄₆O₄Si [M+H]⁺535.3238, found: 535.3239.

Synthesis of 2-(4-hydroxy-2-methylbutan-2-yl)-3,5-dimethylphenyl (S)-2-(6-methoxynaphthalen-2-yl)propanoate (24). To a solution of (2-(4-((tert-butyldimethylsilyl)oxy)-2-methylbutan-2-yl)-3,5-dimethylphenyl (S)-2-(6-methoxynaphthalen-2-yl)propanoate (**23**, 1.86 g, 3.5 mmol) in THF (15 mL) was added H₂O (20 mL) and AcOH (45 mL). The reaction mixture was stirred at room temperature for 12 h, quenched with H₂O (50 mL), and extracted with ethyl acetate (2 × 100 mL). The combined organic phase was dried over anhydrous Na₂SO₄ and evaporated under reduced pressure. Silica gel column chromatography (hexane: ethyl acetate =2:1) gave the product as colorless oil (1.27 g, 87%). ¹H NMR (CDCl₃): δ 7.79-7.74 (m, 3H), 7.52 (dd, *J* = 8.4 Hz, *J* = 1.6 Hz, 1H), 7.19-7.15 (m, 2H), 6.77 (d, *J* = 1.2 Hz, 1H), 6.35 (d, *J* = 1.2 Hz, 1H), 4.08 (q, *J* = 7.2 Hz, 1H), 3.93 (s, 3H), 3.44 (t, *J* = 7.2 Hz, 2H), 2.49 (s, 3H), 2.16 (s, 3H), 1.92-1.80 (m, 2H), 1.72 (d, *J* = 7.2 Hz, 3H), 1.37 (s, 6H); ¹³C NMR (CDCl₃): 174.2, 157.9, 150.2, 138.4, 136.3, 134.6, 134.0, 134.0, 132.5, 129.4, 129.1, 127.5, 126.7, 126.5, 122.8, 119.3, 105.7, 60.6, 55.4, 46.3, 45.6, 39.2, 32.0, 25.5, 20.2, 18.5. HRMS calcd for C₂₇H₃₂O₄ [M+Na]⁺443.2193, found: 443.2192.

Synthesis of 3,5-dimethyl-2-(2-methyl-4-oxobutan-2-yl)phenyl (S)-2-(6-methoxynaphthalen-2-yl)propanoate (25). To a solution of PCC (1.2 g, 5.6 mmol) in DCM (15 mL) was added dropwise the solution of 2-(4-hydroxy-2-methylbutan-2-yl)-3,5-dimethylphenyl (S)-2-(6-methoxynaphthalen-2-yl)propanoate (24, 1.2 g, 2.8 mmol) in DCM (20 mL) at room temperature. After 2 h, the mixture was directly subjected to column chromatography (hexane: ethyl acetate =5:1) to obtain the pure product as colorless oil (0.97 g, 81%). ^1H NMR (CDCl_3): δ 9.36 (d, J = 2.4 Hz, 1H), 7.77-7.73 (m, 3H), 7.49 (dd, J = 8.8 Hz, J = 1.6 Hz, 1H), 7.19-7.14 (m, 2H), 6.79 (s, 1H), 6.43 (s, 1H), 4.06 (q, J = 7.2 Hz, 1H), 3.93 (s, 3H), 2.54 (t, J = 2.4 Hz, 2H), 2.48 (s, 3H), 2.18 (s, 3H), 1.71 (d, J = 7.2 Hz, 3H), 1.40 (s, 3H), 1.35 (s, 3H); ^{13}C NMR (CDCl_3): 203.22, 173.5, 157.9, 149.9, 137.8, 136.9, 134.3, 134.0, 132.9, 132.7, 129.4, 129.1, 127.6, 126.7, 126.4, 123.0, 119.4, 105.7, 56.4, 55.4, 46.3, 38.2, 31.6, 31.4, 25.6, 20.3, 18.4. HRMS calcd for $\text{C}_{27}\text{H}_{30}\text{O}_4$ $[\text{M}+\text{Na}]^+$ 441.2036, found: 441.2033.

Synthesis of (S)-3-((2-(6-methoxynaphthalen-2-yl)propanoyl)oxy)-4,6-dimethylphenyl-3-methylbutanoic acid (26). To a solution of 3,5-dimethyl-2-(2-methyl-4-oxobutan-2-yl)phenyl (S)-2-(6-methoxynaphthalen-2-yl)propanoate (25, 0.96 g, 2.3 mmol) in *t*-BuOH (18 mL) and 2-methylbut-2-ene (3 mL) was added dropwise NaClO_2 (330 mg, 3.4 mmol) in 0.67 M NaH_2PO_4 (3.6 mL) at room temperature. After 2 h, the reaction mixture was quenched with H_2O (20 mL), and extracted with ethyl acetate (2×50 ml). The combined organic phase was dried over anhydrous Na_2SO_4 and then evaporated under reduced pressure to give the crude product, which was purified by column chromatography (hexane: ethyl acetate =2:1) to yield a white solid (650 mg, 66%). ^1H NMR (CDCl_3): δ 7.77-7.72 (m, 3H), 7.50 (dd, J = 8.8 Hz, J = 2.0 Hz, 1H), 7.16-7.13

(m, 2H), 6.75 (s, 1H), 6.40 (s, 1H), 4.09 (q, , $J = 7.2$ Hz, 1H), 3.92 (s, 3H), 2.68-2.55 (m, 2H), 2.49 (s, 3H), 2.15 (s, 3H), 1.70 (d, $J = 7.2$ Hz, 3H), 1.44 (s, 3H), 1.38 (s, 3H); ^{13}C NMR (CDCl_3): 176.8, 173.7, 157.9, 150.0, 138.1, 136.4, 134.5, 134.0, 133.5, 132.5, 129.5, 129.1, 127.5, 126.7, 126.5, 122.7, 119.2, 105.7, 55.4, 47.2, 46.3, 38.8, 31.4, 31.2, 25.5, 20.3, 18.4. HRMS calcd for $\text{C}_{27}\text{H}_{30}\text{O}_5$ $[\text{M}+\text{Na}]^+$ 457.1985, found: 457.1983.

Synthesis of Sodium (S)-3-((2-((6-methoxynaphthalen-2-yl)propanoyl)oxy)-4,6-dimethylphenyl)-3-methylbutanethioate (HP-105). To a solution of (S)-3-((2-((6-methoxynaphthalen-2-yl)propanoyl)oxy)-4,6-dimethylphenyl)-3-methylbutanoic acid (**26**, 180 mg, 0.41 mmol) in DCM (5 mL) was added Lawesson's reagent (83 mg). The mixture was heated in a microwave at 100 °C for 6 min. The mixture was directly subjected to column chromatography (hexane: ethyl acetate = 15:1) to obtain the pure product as colorless oil, which was then dissolved in 5 ml methanol. Then 2.6 ml 0.1 M NaOH methanol solution was added at -78 °C. After 5 min, the mixture was allowed to warm to room temperature and the solvent was removed by vacuum. The final product was achieved by recrystallization in ether as white solid (140 mg, 72%) ^1H NMR (CDCl_3): δ 7.81-7.74 (m, 3H), 7.52 (dd, $J = 8.8$ Hz, $J = 2.0$ Hz, 1H), 7.20-7.15 (m, 2H), 6.76 (d, $J = 1.6$ Hz 1H), 6.49 (d, $J = 1.6$ Hz 1H), 4.14 (q, $J = 7.2$ Hz, 1H), 3.94 (s, 3H), 2.80-2.64 (m, 2H), 2.48 (s, 3H), 2.18 (s, 3H), 1.74 (d, $J = 7.2$ Hz, 3H), 1.38 (s, 3H), 1.30 (s, 3H); ^{13}C NMR (CDCl_3): 196.2, 173.4, 158.0, 150.1, 138.1, 136.5, 134.4, 134.1, 132.8, 132.6, 129.5, 129.1, 17.7, 126.8, 126.5, 122.8, 119.4, 105.8, 58.1, 55.4, 46.4, 39.7, 31.5, 31.3, 25.6, 20.4, 18.3. HRMS calcd for $\text{C}_{27}\text{H}_{29}\text{O}_4\text{SNa}$ $[\text{M}+\text{H}]^+$: 473.1757, found: 473.1756.

1.4.2 H₂S release from HPs

Stock solution preparation. HPs stock solution: HPs were dissolved in DMSO to afford 20 mM HPs stock solutions. Esterase stock Solution: 6.0 mg Esterase (18 unit/mg esterase from porcine liver, PLE, Aldrich, E3019) was dissolved in 1.080 ml PBS to provide a 100 unit/mL esterase stock solution. WSP-5 stock solution: WSP-5 was dissolved in DMSO to prepare a 2.5 mM stock solution. CTAB was dissolved in ethanol to prepare a 100 mM stock solution.

H₂S concentration measurement by an electrode probe ISO-H2S-2.

HPs (Final Conc. 200 μM) was added to an incubation chamber (World Precision Instruments; WPI) containing phosphate buffer (10 mM; pH 7.4, 10 mL), and esterase (1 unit/ mL) at 37 °C. H₂S formation was detected with the use of a 2-mm H₂S-selective microelectrode (ISO-H2S-2; WPI) attached to an Apollo 1100 Free Radical Analyser (WPI) and shown as picoamps current generated. A standard curve (using Na₂S·9H₂O) was generated by following literature procedures,⁸⁹ but using PBS containing esterase at 37 °C .

H₂S measurement by a fluorescent probe WSP-5.

HP-101 (final concentration: 200 μM) or other control compounds were added to PBS (10 mL) buffer containing esterase (1 unit/ mL) at 37 °C. After 15 minutes, aliquots of 100 μL samples were taken out and added into 100 μL PBS containing 50 uM WSP-5 and 100 μM CTAB in 96-well plate. After mixing and standing for 5 min at room temperature, the fluorescent intensities at 535 nm were recorded by a plate reader with excitation at 485 nm.

H₂S release from HP-101 in cell culture media

HP-101 (200 μM) was added to an incubation chamber (World Precision Instruments; WPI) containing cell culture media (10mL) at 37 °C. H₂S formation was detected with the use of a ISO-

H_2S -2 attached to an Apollo 1100 Free Radical Analyser and shown as picoamps current generated (Figure 1.4.1). A standard curve (using $\text{Na}_2\text{S}\cdot 9\text{H}_2\text{O}$) was also generated under the same conditions.⁸⁹ The results (Figure 1.9) indicated that HP-101 in the DMEM did not release H_2S ; however, when HP-101 was added into the media collected after overnight of cell culturing, H_2S was released at a moderate rate, presumably due to the presence of esterases produced by the cells.

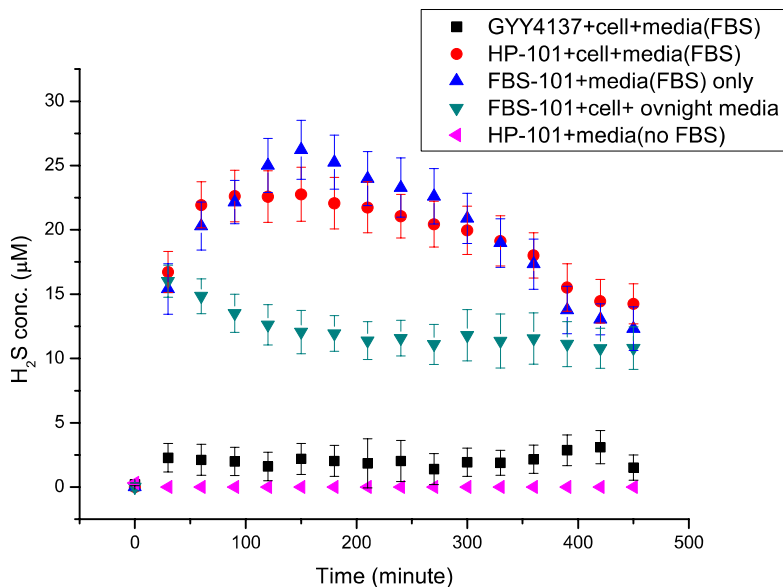


Figure 1.9. H_2S release from HP-101(200 μM) in cell culture media with or without FBS as detected using an electrode probe. ($n= 3$, $p= 0.95$)

H_2S release from HP-105 measurement

To 9.9 mL phosphate buffer (pH 7.4) solution was added 11.1 mg (200 unit) PLE, followed by the addition of 100 μL 20 mM HP-105 stock solution (Final Conc.: 200 μM). The resultant solution was sealed and stirred at 37 °C. At every 30 min, 200 μL of reaction solution was taken into a 1.5 mL vial containing 200 μL zinc acetate (1 %, w/v). Then the vial was centrifuged for 10 min. (14.5 \times 1000 rp). Removed the supernatant and washed the precipitation with PBS solution (100 μL \times 2). Then 600 μL N,N-dimethyl-1,4-phenylenediaminesulfate (0.2% w/v in 20% H_2SO_4 solution) and 50 μL ferric chloride (10% w/v in 0.2% H_2SO_4 solution) was added to the vial. Then

the vial was centrifuged for 5 min (14.5×1000 rp). The absorbance (at 740 nm) of the resulting solution was measured (after stirring for 10 min). H₂S concentration was calculated based on a calibration curve of NaHS.

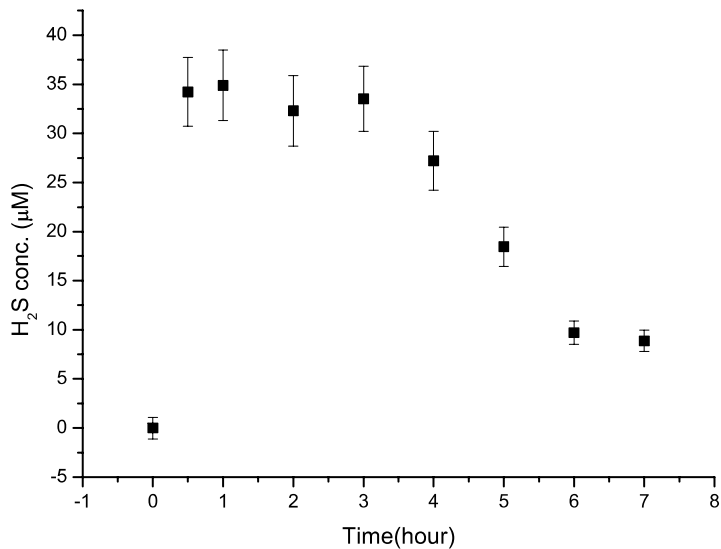


Figure 1.10. H₂S release from HP-105 (200 μM) in PBS at 37 °C with 20 unit/ mL PLE. (n= 3, p= 0.95)

1.4.3 Kinetic studies of esterase trigger lactone formation

Esterase triggered lactone formation from HP-101 as monitored by LC-MS/MS (Figure 8) HP-101 (final Conc. 200 μM) was added to PBS (10 mL) with 1 unit/mL esterase at 37 °C. Reaction mixture (10 μL) was taken out every 3 minutes and added into a vial containing 990 uL methanol at -78°C for 5 minutes. The mixture (14.5×1000 rp) was centrifuged, and the supernatant was used as the sample for LC-MS/MS analysis (Agilent 1100 LC, 6410 TripleQ MS/MS, Ion transition: 205.0/135.0, positive mode).

All LC-MS/MS samples were analyzed using liquid chromatography tandem mass spectrometric method (Agilent 6410 series). Auto-sampler temperature was set at 10 °C, a positive ionization

mode with multiple reaction monitoring (MRM, m/z Q1/Q3) of lactone (m/z 205.0/135.0, RT 1.4min) was employed. The ion spray voltage was set at 3500 V, ionization temperature set as 300 °C and drying gas flow rate at 10 L/min. Data acquisition and quantitation were performed using Mass Hunter software (Agilent Technologies). Separation was achieved using HP1100 series LC (Agilent Technologies, Wilmington, DE) equipped with a photodiode array (PDA) detector, using an Agilent Zorbax reversed-phase (SB-C18, 3.0×250 mm, 5.0 μm) column. A gradient method was employed to separate the individual GE components using mobile phase A (0.1% formic acid in water) and mobile phase B (ACN). The gradient elution method with 30% B at 0 min, 90% B at 20 min, held for 10 min, back to 30% B at 40 min with a flow rate of 0.4 mL/min. An injection volume of 10 μL was used for analysis.

The results (Figure 1.11) showed that about 190 μM of the lactone product was formed after treatment with esterase for 25 min. Such results indicate that about 95% of H₂S was released in that period.

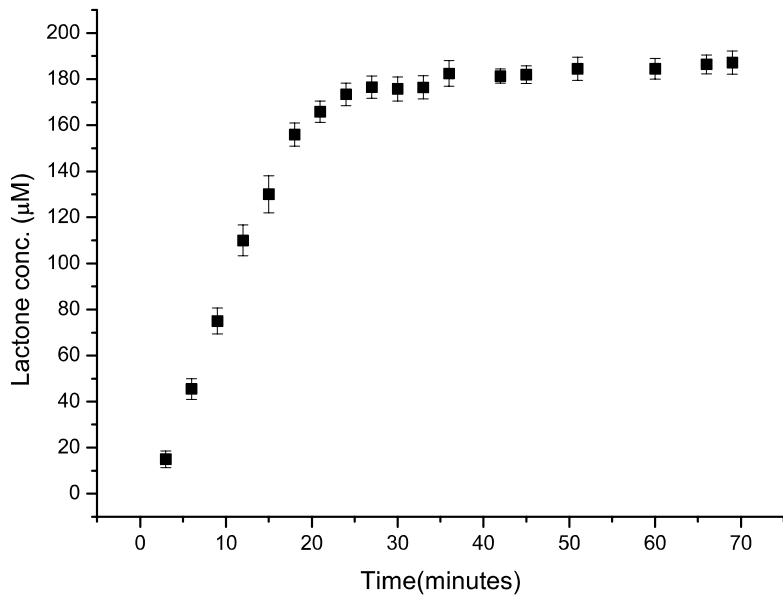


Figure 1.11. Esterase-triggered lactone formation from HP-101 as monitored with LC-MS/MS. (n= 3, p= 0.95)

Esterase triggering lactone formation from HPs as monitored with HPLC

HPs (final Conc. 200 μM) was added to PBS (10 mL) with 1 unit/mL esterase at 37 °C. 200 μL reaction mixture was taken out every 10 minutes and added into a vial containing 600 μL ethanol at -78 °C for 5 minutes. The mixture (14.5 ×1000 rp, 90 seconds) was centrifuged, and the supernatant was used as the sample for HPLC. 200 μL HPLC samples were injected into Shimadzu Prominence UFC (column: Waters C18 3.5 μM, 4.6×100 mm, injection loop volume: 20μL). The mobile phase was acetonitrile (ACN)/H₂O (pH=4.0) with ratios defined in the table below. (Table 1.2)

Table 1.2 HPLC monitored esterase triggering lactone formation of HPs. (n= 3, p= 0.95)

	HP-101	HP-102	HP-103	HP-104	HP-105
Eluent conditions	50% ACN 0~20 min	60% ACN 0~20 min	45% ACN 0~20 min	55% ACN 0~20min	Method b
Retention time of HPs (min)	13.6 ± 0.2	9.7 ± 0.2	7.7 ± 0.2	8.3 ± 0.2	20.7 ± 0.3
Retention time of the lactones (min)	10.7 ± 0.2	5.5 ± 0.2	8.5 ± 0.2	6.1 ± 0.2	9.6 ± 0.3

Method b: 45% ACN, 0~10min; 45%~75% ACN, 10~15 min; 75% CAN, 15-20min; 75%~45% CAN, 20~25min.

1.4.4 Stability Studies of the thioacid group

To a solution of 5 mL deuterated PBS (1X pH=7.4), 50.0 mg of potassium thioacetate (0.438 mmol) and 4.0 mg of acetic acid (0.0658 mmol) were added. The mixture was incubated at 37 °C for 48 hours. The mixture was analyzed by ¹H NMR at 0- and 48-hour time points, respectively. The spectra were shown below (Figure1.12). At 0 h, the integration ratio between the methyl protons in thioacetate (CH₃: 2.48 ppm) and that of acetic acid (CH₃: 1.94 ppm) is 6.7, which is

consistent of the ratio of the compounds we added, and after 48 hours, the ratio did not change. Such results indicate that the thioacid group is stable under the conditions of the study.

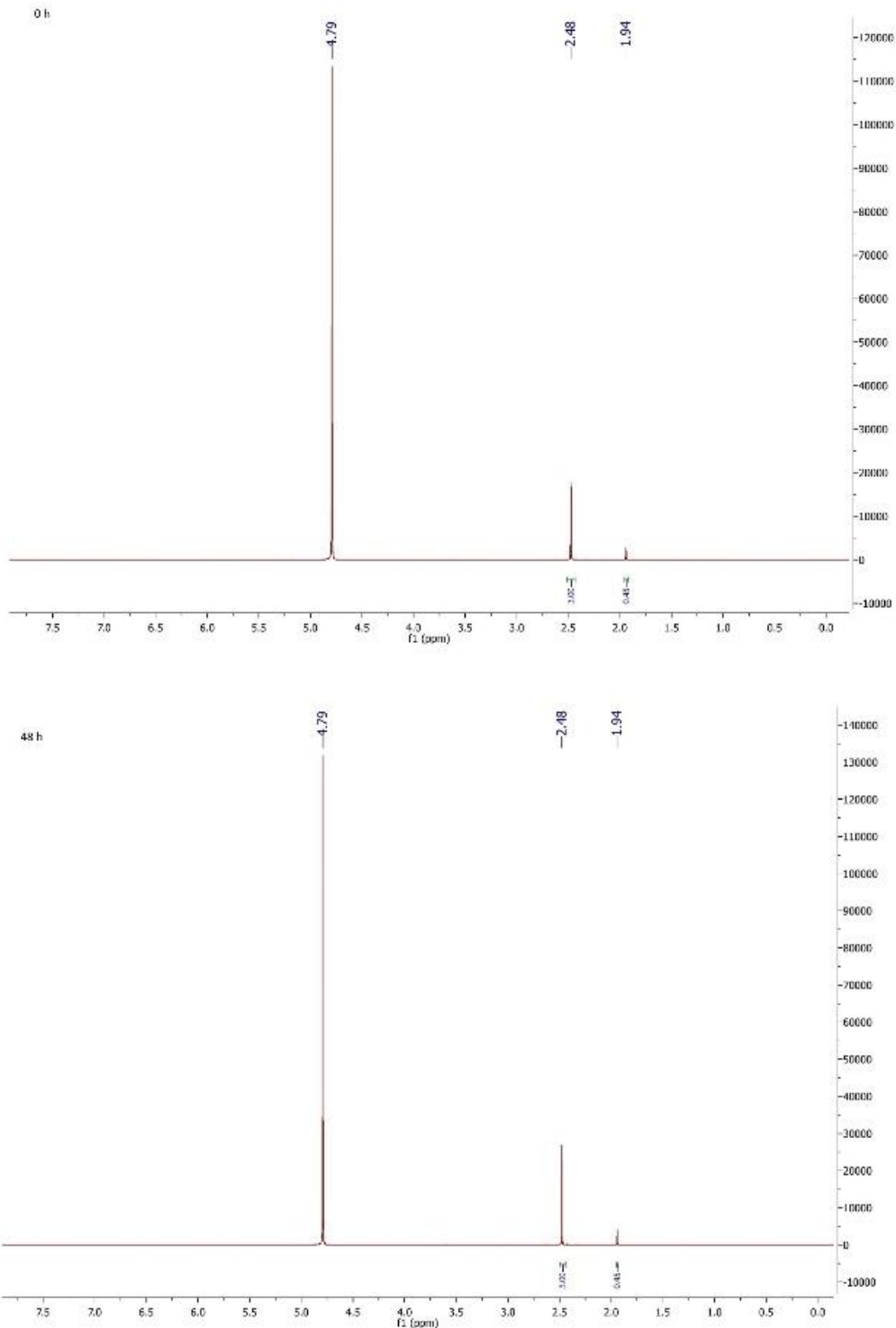


Figure 1.12. ^1H NMR spectra of reaction mixture at the 0- and 48-hour time points.

1.4.5 Cell culture

RAW 264.7 (ATCC® TIB-71™) mouse macrophage cells were used in the studies. The RAW 264.7 cells were maintained in DMEM (Dulbecco's Modified Eagle's Medium) supplemented with 10% fetal bovine serum (MidSci; S01520HI) and 1% penicillin-streptomycin (Sigma-Aldrich; P4333) at 37 °C with 5% CO₂.

1.4.5.1 Cytotoxicity study

The RAW 264.7 cells were seeded in 96-well plate one day before the experiment. Different concentrations of HP or iHP compounds was directly dissolved in cell culture media and added into the RAW 264.7 cell culture. The cells were then incubated with the compound for 24 hours at 37 °C with 5% CO₂. The cell viability was tested by the MTT assay. Specifically, after 24 hr of incubation, 0.5 mg/mL MTT (3-(4, 5-Dimethylthiazol-2-yl)-2, 5-Diphenyltetrazolium Bromide) was added into the cell culture for 4 hours. Thereafter, the supernatant was removed and 100 µL DMSO was added into the wells containing the cells. After shaking gently for 3 minutes, absorbance at 570 nm was read by a plate reader (Figure1.13).

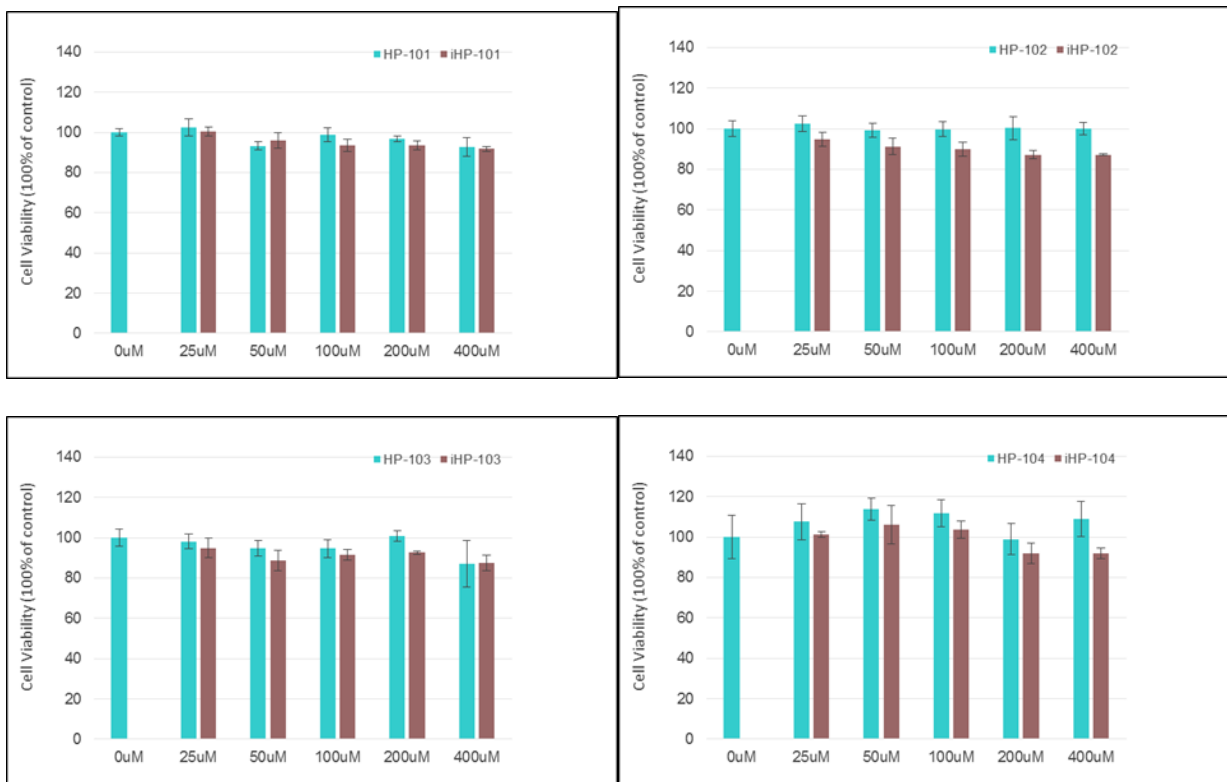


Figure 1.13. Cytotoxicity of HPs. (n= 4, p=0.95)

1.4.5.2 Anti-inflammation study

The RAW 264.7 cells were seeded in the 48-well plate one day before the experiment. Lipopolysaccharide was added into the cell culture to initiate the inflammatory response in RAW 264.7 cells and to trigger the expression of cytokines. RAW 264.7 cells were co-treat with HPs or iHPs, 1unit/mL esterase and 1 μ g/mL of LPS for 1 hour. Thereafter, the cell culture supernatant was collected. The concentrations of TNF- α in the cell culture supernatant was quantified by a commercial ELISA kit (ELISA Ready-SET-Go!® -eBioscience).

1.5 Acknowledgement

I would like to specially thank Dr. Siming Wang and Dr. Chunhua Yang for the MS work, Bingchen Yu, Zhixiang Pan and Vayou Chittavong for helping with some of the synthetic work, Dr. Kaili Ji for the cell culture work.

2 DEVELOPMENT OF A NOVEL ESTERASE-SENSITIVE PRODRUG APPROACH FOR CONTROLLABLE DELIVERY OF PERSULFIDE SPECIES

Abstract: This chapter is mainly based on my publications: *Angew. Chem. Int. Ed.* in 2017, from page 11749–11753. A new strategy to deliver a well-defined persulfide species in a biological medium is described herein. Under near physiological conditions, the persulfide prodrug can be activated by an esterase to generate a “hydroxyl methyl persulfide” intermediate, which rapidly collapses to form a defined persulfide. Such persulfide prodrugs can be used either as chemical tools to study persulfide chemistry and biology or for future development as H₂S-based therapeutic reagents. Using the persulfide prodrugs developed in this study, the reactivity between S-methyl methanethiosulfonate (MMTS) with persulfide was unambiguously demonstrated. In addition, a representative prodrug exhibited potent cardioprotective effects in a murine model of myocardial ischemia-reperfusion (MI/R) injury with a bell shape therapeutic profile.

2.1 Introduction

The physiologic and potentially therapeutic roles of hydrogen sulfide (H₂S) and related sulfur species are well accepted.^{117–123} However, the detailed mechanism(s) of action for these sulfur species is far from clear. Further, even the question of the “active” sulfur species is not always clear for a given biological response. To complicate this further, different donors of sulfur species without defined chemistry are often used in various studies, leading to difficulty in result interpretation and comparison. For example, polysulfides and garlic-derived sulfur species are often used in biological studies.^{124–125} The chemistry of such sulfur donors is not well defined; consequently, it is not always clear what the “active” species is and the relative ratio of the various species. To advance the field of sulfur biology, it is important to devise chemical strategies that allow for the precise production of various specific sulfur species for mechanistic studies at the

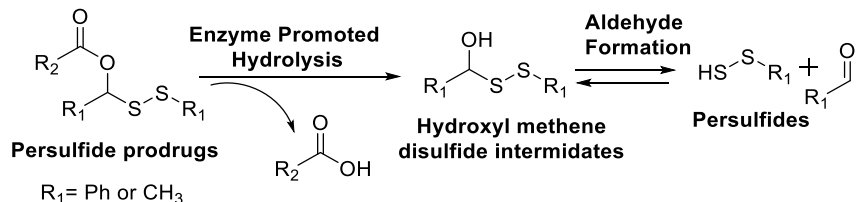
molecular level and for understanding the biology. Several labs have made significant contributions in developing prodrugs of hydrogen sulfide^{4, 126-128} and COS¹²⁹⁻¹³³ as well as sulfur donors at various oxidation states.^{95, 134-136} Along this line, one molecular pathway is known to play an important role in sulfur-mediated signaling, *S*-sulphydrylation.¹³⁷ Clearly, this is not the kind of chemistry that can be achieved with hydrogen sulfide *per se*. It would require sulfur species at the oxidation state of a persulfide or polysulfide. Indeed, perthiol species have drawn growing attention owing to its potentially dominant roles in H₂S-related signaling pathways.^{123, 138-139} There are already many studies that explore persulfide chemistry in biology. For example, it was reported that persulfide species such as glutathione persulfide (GSSH) have much stronger “reducing” ability for ferric-cytochrome *c* than H₂S and GSH.¹⁴⁰ Such results are puzzling in terms of the redox chemistry because chemically it is hard to understand how a persulfide species can be stronger reducing agents than sulfide. Such findings suggest that more work is needed at the molecular level to elucidate the mechanism of action. Other examples include the findings that reactive sulfur species (RSS) such as sulfane sulfurs or polysulfides are more effective in *S*-sulphydrylation than H₂S.^{123, 141-142} There is a clear need for investigation of persulfide chemistry and chemical biology in this field.¹³⁸ However, there are two major challenges that face the chemistry field. The first one is a lack of good persulfide precursors/prodrugs that allow for easy and reliable access to persulfides as research tools; and the second one is the limited availability of ‘easy to use’ detection methods for protein *S*-sulphydrylation.¹³⁸ There has been reported work to address the second issue.^{123, 137, 143-146} We herein focus on developing novel and easy to handle persulfide prodrugs to address the first issue.

The difficulty in developing persulfide prodrugs comes from the unstable nature of persulfide species, which can rapidly decompose to disulfides, polysulfides, elemental sulfur and

H_2S .¹⁴⁷ This is especially true if there is an exposed free sulfhydryl group (-SH). To achieve controlled delivery of persulfide in biological studies, the free sulfhydryl group has to be protected, and then regenerated when needed. One class of existing persulfide precursors contains the acyl disulfide group.^{126, 145} They were cleverly designed to release the persulfides through nucleophilic attack by a thiol group. However, the release of persulfide relies on the addition of an excess amount of thiol in solution.^{126, 146} Therefore, there is a mix of various sulfur species present at any given time. An approach to directly achieve “pure” persulfide species under physiological conditions without using other sulfide or thiol species is needed.

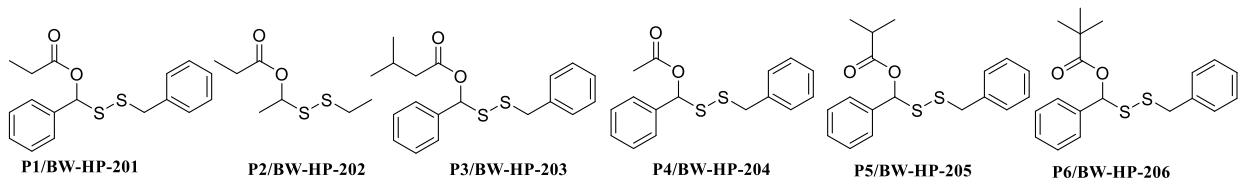
2.2 Results and Discussions

Enzyme-sensitive prodrugs have been widely used in drug delivery.¹⁴⁸ We are interested in designing esterase-sensitive persulfide prodrugs, which are stable under physiological conditions and can efficiently generate persulfide in the presence of an enzymatic trigger. Specifically, similar to the idea of using “hemiacetal” as an unstable intermediate in prodrug design,¹⁴⁹ we were interested in exploiting the “hydroxyl methyl disulfide” (HOCHRSSR) analog as a key intermediate in our design. In this design, an ester group is introduced to mask the hydroxyl group, leading to a stable precursor. Activation of this prodrug thus relies on the cleavage of this ester bond, resulting in an unstable HOCHRSSR intermediate, which would collapse to give an aldehyde and a persulfide (Scheme 2.1)



Scheme 2.1. General design of persulfide prodrugs, and their release mechanism.

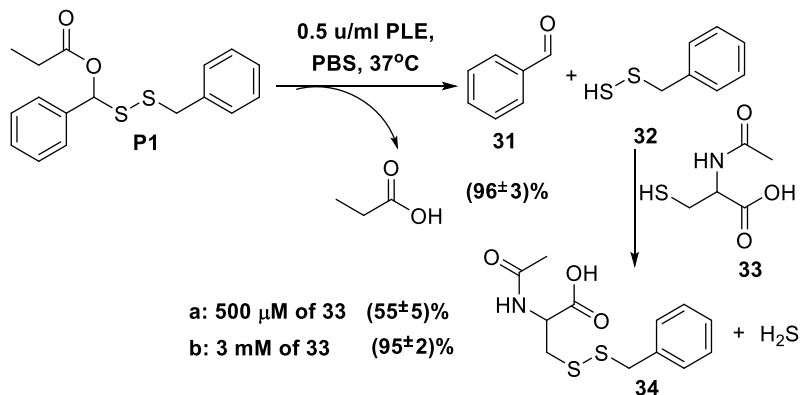
To test our design, persulfide prodrug **1** (**P1, BW-HP-201**, Scheme 2.2) was synthesized by a one-step reaction between 1,2-dibenzyl disulfane and propionic acid using KMnO₄ as the oxidant by following a similar literature procedure.¹⁵⁰ **P1** is a colorless oil without the characteristic smell of sulfide such as benzyl mercaptan and is stable at room temperature for 5 days and at -20 °C for 3 months. **P2~6** (BW-HP-202-206) were also synthesized using the same procedures.



Scheme 2.2. Structures of persulfide prodrugs.

We first studied the ability for **P1** to undergo the intended reaction by monitoring the formation of both benzyl persulfide and benzaldehyde by HPLC. It turned out that the benzyl persulfide (compound **32**) (Scheme 2.3) was not sufficiently stable for detection on an HPLC time scale. This further affirms the rationale for designing these prodrugs, i.e., without the protection of the terminal sulfhydryl group, the persulfide species would not be stable enough for long-term storage. For detection purpose, we therefore, trapped benzyl persulfide using *N*-acetyl-L-cysteine (compound **33**) to give compound **34**, which is stable for HPLC detection. Specifically, 100 μM **P1** was treated with porcine liver esterase (0.5 u/ml, PLE) for 10 min at 37 °C in the phosphate buffered saline (PBS, pH= 7.4) containing 500 μM compound **33** (Scheme 2.3). The results show that the amount of benzaldehyde **31** detected was the equivalent of 96% conversion. However, only 55% recovery of disulfide **34** were detected under such conditions, clearly indicating that the trapping reaction was not fast enough on the time scale of the study. By increasing the

concentration of **33** to 3 mM, we were able to detect about 95% recovery of disulfide **34** (Scheme 2.3). Such results clearly indicated that the release reaction occurred as designed.



*Scheme 2.3. Benzyl persulfide was released from **P1** and trapped by **33**.*

Besides using HPLC to detect the formation of **31** and **34**, we also used the standard methylene blue (MB) method to detect the H₂S release from **P1** (Figure 2.1) in the presence of **33**. The results showed no obvious H₂S generation in the absence of PLE, and only less than 5 μM H₂S (5%) were formed in the presence of 500 μM compound **33**, suggesting the possibility of a small percentage of the prodrug to undergo sulfur exchange. However, with the addition of 0.5 u/ml PLE at 37 °C in PBS **P1** generated about 23 μM, 33 μM and 45 μM H₂S in the presence of 0 μM, 500 μM and 3 mM compound **33**, respectively. Compared with H₂S release, the formation of benzaldehyde was not affected by compound **33** (Figure 2.1). More than 90% benzaldehyde was detected in 2 min in PLE-containing solution with or without compound **33**, and less than 5% benzaldehyde was detected in the solution with 500 μM compound **33** without the addition of PLE. Such results indicated that the prodrugs were most effectively activated by an esterase, which controlled the rate-determining step.

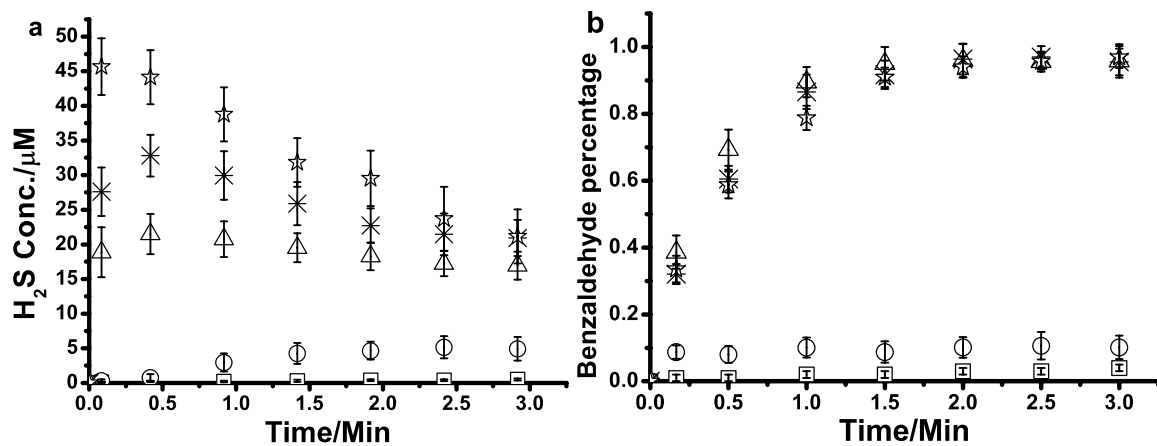


Figure 2.1. P1 hydrolysis at 37 °C in PBS (2% DMSO). □: 100 μM P1; ○: 100 μM P1 + 500 μM Compound 3; △: 100 μM P1 + PLE; *: 100 μM P1 + 500 μM Compound 3 + PLE; ☆: 100 μM P1 + 3 mM Compound 3 + PLE. a) H₂S release detection by MB method; b) Benzaldehyde formation detection by HPLC.

For small molecule bioregulators (SMBs), release rate is a very important factor in determining the sustained effective concentration and thus biological effect. Donors at the same concentration could lead to different biological effects when the release rates are different. Our earlier work on H₂S prodrugs demonstrated that varying the acyl moiety allows for tuning the esterase-catalyzed hydrolysis rates.⁷⁶ Thus we reasoned that similarly designed persulfide prodrugs should also show different release profiles. Therefore, we next examined release kinetics. Specifically, we treated all these precursors (100 μM) with 0.5 u/ml PLE in PBS containing 500 μM compound 33 at 37 °C. Aldehyde formation was monitored by HPLC (Table 2.1), and H₂S release was tested by the MB method.

Table 2.1 Total percentage of aldehyde formation (A%) and 50% aldehyde formation time (*t*_{1/2})

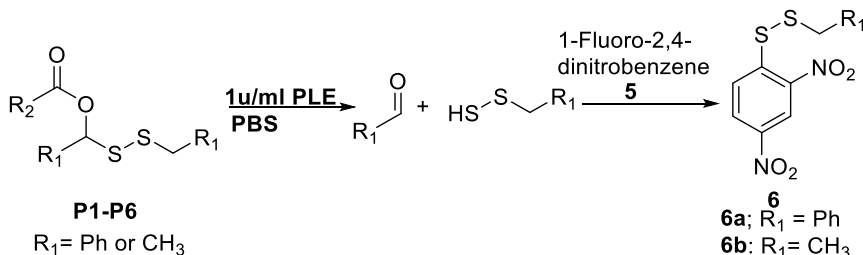
Compound	P1	P2	P3	P4	P5	P6
A%	96±3	Δ	91±4	97±3	97±2	89±6
t _{1/2} (s)	25±5	12±6*	85±9	17±6	29±6	145±12

Δ: not detectable because of low boiling point of acetaldehyde;*: 50% **P2** remaining at the time of sampling. n= 3 p=0.95.

The results demonstrated that all the prodrugs were sensitive to PLE with hydrolysis half-lives ranging from 12 to 145 s. As a consequence of their respective release rates, the peak concentrations and sustained concentrations are also different. For example, H₂S level released from **P1** reached a peak concentration of 33 μM within 30 s and then decreased slowly. On the other hand, the slowest prodrug **P6** showed a gradual increase in H₂S concentration, reaching a maximum of 15 μM after 3 min.

The above studies clearly demonstrated the chemical feasibility of the prodrug activation and allow for studies of reaction kinetics. However, such studies used benzaldehyde and hydrogen sulfide as surrogates for product detection. Next, it was important to demonstrate persulfide formation without the added the thiol species, **33**. In the field of designing detection methods for protein S-sulphydrylation, a key step is developing trapping reagents, which could efficiently trap the persulfide under physiological conditions.¹³⁸ For this study, we used dinitrofluorobenzene (DNFB, Compound **35**), which was known to trap persulfides (Scheme 2.4).¹⁵¹ Specifically, we incubated 100 μM of the prodrugs with 1u/ml PLE at 37 °C for 10 s and then added 4 mM of DNFB to the mixture. The resulting solution was further incubated for another 30 min. Then the formation of disulfide compound **36** was analyzed by HPLC (Table2.2). We were able to trap 70%-82% of the persulfide released from the prodrugs. There could be several reasons for the incomplete “conversion” to **36**. First, it is possible that the reaction rate between the released persulfide and **35** is not high enough for 100% conversion. However, the fact that all prodrugs gave similar percentages of **36** (Table 2.2) suggests that this is not controlled by reaction kinetics

at the trapping step because the various prodrugs gave substantially different peak concentrations, and trapping yields are not correlated with release rates. The second possible reason is the competition between trapping and disproportionation reaction of the persulfide released. We tend to think that the latter was the reason for the less than 100% conversion to **36**. To confirm this, we incubate 100 μM of the prodrug with 1u/ml PLE and 4 mM DNFB at r.t., and found that the trapping yields increased to 82%-93%. Clearly, at lower temperature (room temperature vs. 37 °C), the disproportion reaction was slower, allowing for the improved trapping efficiency. The results demonstrated that the prodrugs could efficiently afford persulfide for further studies.



Scheme 2.4. Persulfide released from precursors and trapped by DNFB

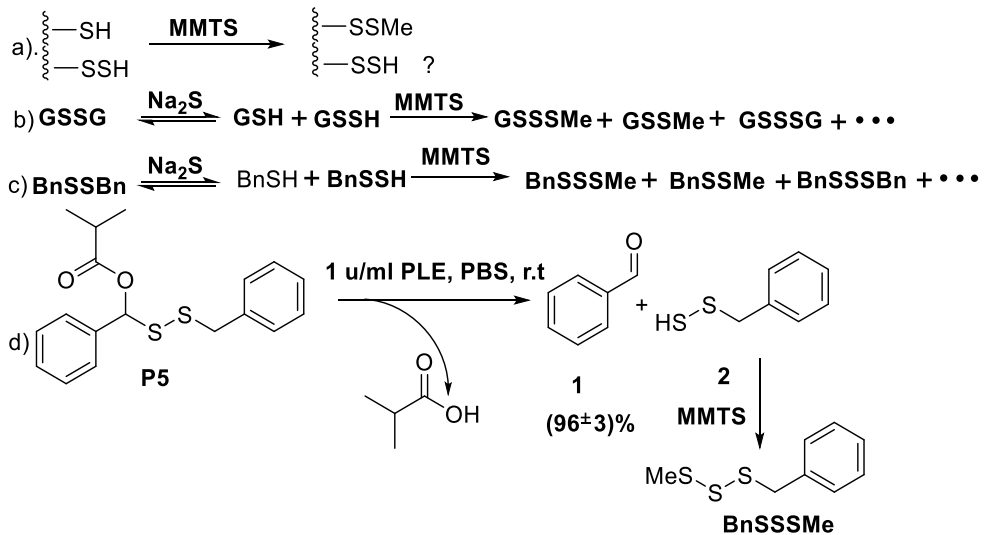
Table 2.2 Persulfide released from precursors and trapped by DNFB

Prodrugs	P1	P2	P3	P4	P5	P6
A (%)	79±5	70±4	71±5	80±4	82±5	78±4
B (%)	87±5	80±6	81±5	88±6	93±5	86±5

A: trapping yield at 37 °C, B: trapping yield at r.t. n= 3, p=0.95

As a research tool, the system can provide relatively “pure” persulfide, which is very unique and important in the field of protein S-sulphydrylation. In 2009, sulfide signaling through S-sulphydrylation was first demonstrated.¹³⁷ A modified biotin switch technique, using S-methyl methanethiosulfonate (MMTS) as an alkylating reagent, was used to identify a large number of proteins that may undergo S-sulphydrylation. The underlying chemical mechanism was based on the

assumption that MMTS would selectively react with thiol groups (RSH), but not persulfide group (RSSH) (Scheme 2.5a).



Scheme 2.5. Persulfides react with MMTS

However, later studies suggested that this assumption on the lack of reactivity between MMTS with RSSH was questionable (Scheme 2.5a).¹⁴⁶ One reported work in studying the reactivity between MMTS with RSSH used a mixture of GSSG and sodium sulfide (Scheme 2.5b). In doing so, a small peak of GSSSMe was indeed detected. However, the origin of this “trisulfide” peak could be interpreted in more than one way due to complexity of the mixture formed in the process of preparing GSSH (Scheme 2.5b). To further probe the reactivity between MMTS with RSSH, we conducted the reaction between MMTS and the persulfide released from **P5**. Specifically, 100 μM of the prodrug was incubated with 1u/ml PLE and 4 mM MMTS at r.t. for 30 min (Scheme 2.5d). Then LC-MS was applied to analyze product formation. For comparison, we also incubated 4 mM of MMTS with 1 mM dibenzyl disulfide BnSSBn and 1 mM of Na₂S (Scheme 2.5c). The results are shown in Figure 2.2a and 2.2b. The reaction in 2.5c led to BnSSSMe as the major product, and only a small amount of BnSSMe was formed. Such results are quite

similar to the product formation pattern in the reported reaction between MMTS with GSSG and Na₂S.¹⁴⁶ However in the reaction of MMTS with benzyl persulfide released from **P5** (Scheme 2.5d, Figure 2.2b), BnSSSMe clearly formed as the dominant product, and other possible sulfide products were only observed in minute quantities. The results here clearly demonstrated that MMTS could react with persulfide. By taking advantage of the unique property of our persulfide prodrug system, we reconfirmed that MMTS can efficiently react with persulfide.

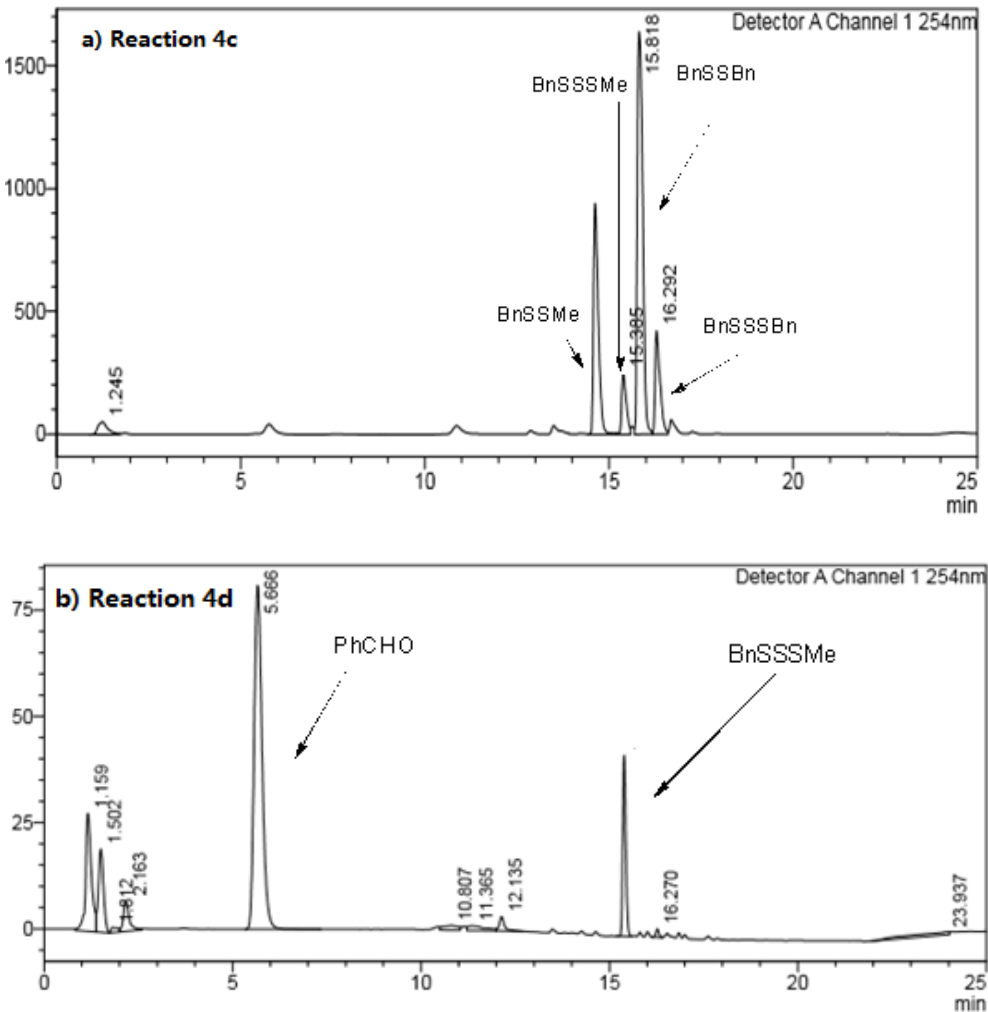


Figure 2.2. HPLC chromatography. a) HPLC trace of BnSSBn reacting with Na₂S and MMTS. b) HPLC trace of esterase mediate **P5** hydrolysis and persulfide trapping by MMTS.

Besides using the prodrugs as chemical tools to study persulfide chemistry under near physiological conditions, we also examined their biological effects. We first assessed the cytotoxicity of these prodrugs using the H9c2 cell line. All prodrugs showed no obvious toxicity at up to 100 μM after 24 h of incubation. Various sulfur species have been shown to exhibit protective effects in heart myocardial infarction reperfusion (MI/R) injury studies.^{122, 126, 152} As a test of the biological relevance of the prodrugs designed, we selected **P2**, which has a relative good water solubility and low toxicity of side product (acetaldehyde), as a representative for examination of its protective effect in a murine model of MI/R injury. The compounds were tested in a mouse heart ischemia reperfusion injury model. Mice were subjected to 45 min of ischemia induced by left coronary artery (LCA) occlusion followed by 24 h of reperfusion of **P2** (0, 12.5, 50, 100, 500 $\mu\text{g}/\text{kg}$) or vehicle, administered by intracardiac injection at the time of reperfusion. The LCA was re-occluded at 24h of reperfusion at the same position. Then Evans Blue dye was injected through right common carotid artery to delineate the area-at-risk (AAR). Due to the occlusion of LCA, AAR did not receive blood flow nor the Evans Blue dye, while the remainder of the heart was stained blue. Therefore, AAR were the non-blue regions in the mid-ventricular slice (Figure 2.3a). The infarct size (INF) was stained white by triphenyltetrazolium chloride solution. Thus, the white regions in the mid-ventricular slice represent INF (Figure 2.3a). Left ventricle (LV) is the sum of blue and non-blue regions. All of the animal groups displayed similar area-at-risk per left ventricle (AAR/LV), suggesting that the surgical procedure produced the same degree of ischemic damage. Compared with vehicle-treated mice, those receiving the prodrug displayed significant reductions in infarct size per area-at-risk (INF/AAR) at the dosage of 50 or 100 $\mu\text{g}/\text{kg}$ (Figure 2.3b). It is well-known that sulfide's protective effects are bell-shaped with regard to dosage.^{12, 127} It is important to note that indeed the prodrug's protective effect had an

optimal concentration of 50-100 $\mu\text{g}/\text{kg}$. Substantially lower (12.5 $\mu\text{g}/\text{kg}$) or higher (500 $\mu\text{g}/\text{kg}$) doses showed no protective effects. Moreover, circulating cardiac troponin I levels, a marker for acute myocardial infarction, paralleled the results of infarction area measurements (Figure 2.3c). In addition to that, we also validated the sulfane sulfur production from the prodrug *in vivo*. As shown in Figure 2.3d, administration of **P2** led to a significant increase of sulfane sulfur in blood. Such results strongly suggest that persulfide prodrug indeed serves as a persulfide donor.

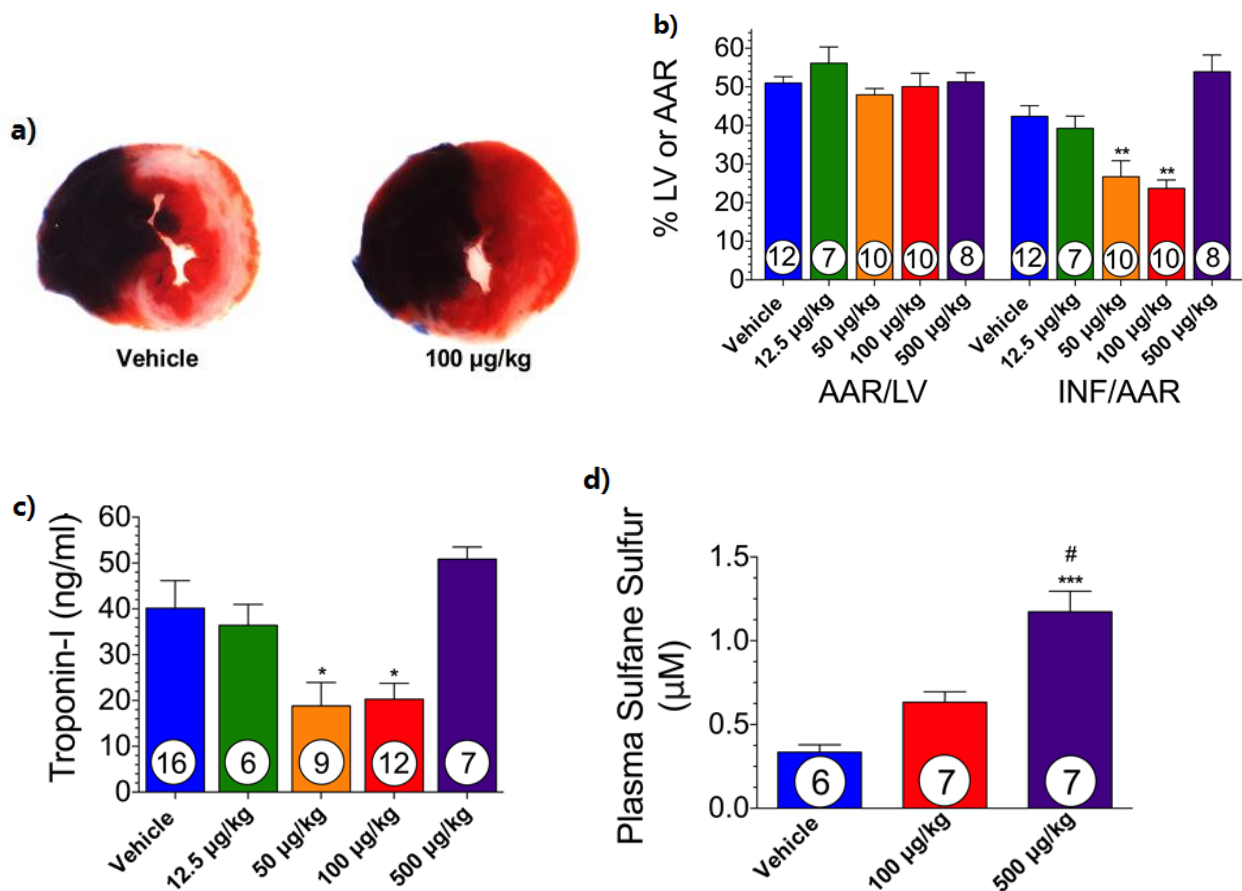


Figure 2.3. a) Representative photomicrographs of a mid-ventricular slice after MI/R and stained with Evan's blue and 2,3,5-triphenyltetrazolium chloride for both vehicle- and prodrug-(**P2**) treated hearts. *b)* AAR/LV and INF/AAR for **P2** treated or Vehicle treated mice. *c)* Circulating troponin I level for **P2** treated, or Vehicle treated mice. *d)* Plasma sulfane sulfur levels at 5 minutes post intracardiac injection. Values are means \pm SEM. *P < 0.05, **P < 0.01, ***P < 0.001 the vehicle group, #P < 0.01 vs the 100 $\mu\text{g}/\text{kg}$ of **P2** treated group.

2.3 Conclusions

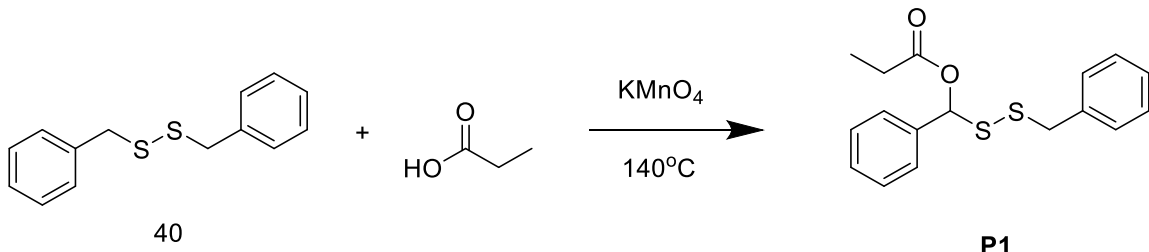
In summary, we have developed a series of persulfide prodrugs with controllable release rates. These persulfide prodrugs release persulfide through an esterase-mediated hydrolysis mechanism. In the presence of the PLE, the prodrugs efficiently released persulfides under near physiological conditions. Using the prodrug, we reaffirmed the reactivity between persulfide and MMTS. The protective effects of P2 in a murine model of MI/R injury have also been demonstrated. All the studies above demonstrate that this novel type of persulfide prodrugs not only can be used as research tools, but also are possible therapeutic agents.

2.4 Experimental part

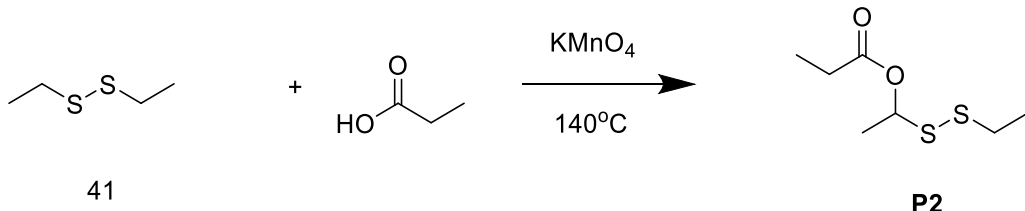
General Information. All solvents were of reagent grade and were purchased from Fisher Scientific and Aldrich. Reagents and were purchased from Aldrich, Oakwood, or VWR. Silica gel (230 × 400 mesh, Sorbtech) was used for column chromatography unless otherwise noted. Silica gel TLC plate was purchased from Sorbtech. ^1H -NMR (400 MHz) and ^{13}C -NMR (100 MHz) spectra were recorded on a Bruker Avance 400 MHz NMR spectrometer. Mass spectral analyses were performed on an ABI API 3200 (ESI-Triple Quadruple). HPLC was performed on a Shimadzu Prominence UFC (column: Waters C18 3.5 μM , 4.6×100 mm). UV-Vis absorption spectra were recorded on a Shimadzu PharmaSpec UV-1700 UV-Visible spectrophotometer. Fluorescence spectra were recorded on a Shimadzu RF-5301PC fluorometer. 96-Well plates were read and recorded on a PerkinElmer 1420 multi-label counter. Porcine liver esterase was purchased from Aldrich. WSP-5 was synthesized following literature procedures.¹ CHNS analysis were conducted by Atlantic Microlab.

2.1.1 Synthesis

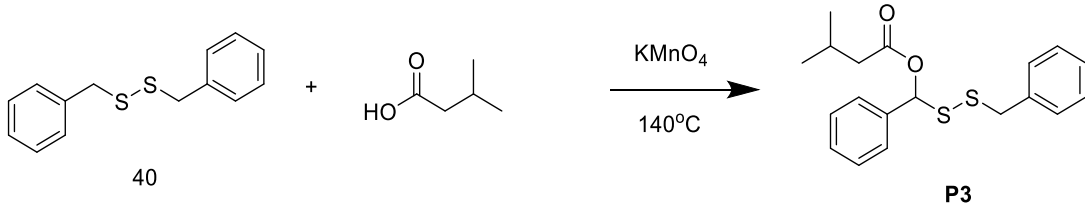
2.4.1.1 synthesis of persulfide prodrugs



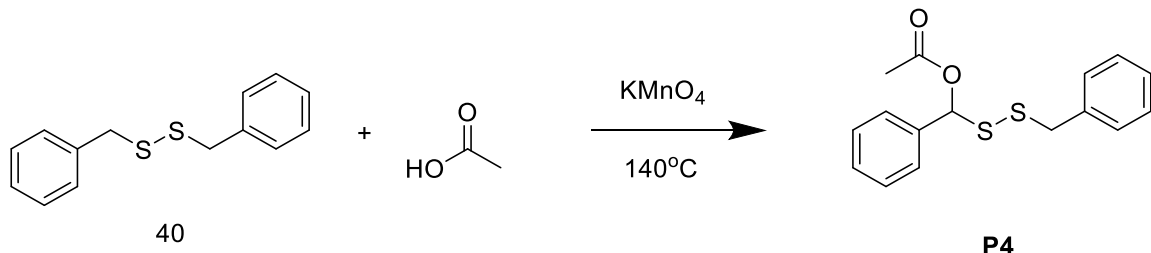
P1: To a 20-ml vial was added 1,2-dibenzyldisulfane (**40**, 500 mg, 2.0 mmol), KMnO_4 (316 mg, 2.0 mmol) and 4 ml propionic acid. The oil bath was preheated to 140°C and the mixture was stirred at this temperature for 5 min and then immediately cooled down to room temperature. The mixture was diluted with 100 ml ethyl acetate and then washed with 50 ml brine, 50 ml saturated NaHCO_3 and finally 50 ml brine. The organic phase was then dried over Na_2SO_4 and then solvent was evaporated under reduced pressure to give the crude product, which was purified by column chromatography (hexane: ethyl acetate =200:1) to yield a colorless oil ($R_f = 0.7$ in hexane: ethyl acetate =20:1). The colorless oil was further subjected to vacuum at room temperature for 2 h to yield the pure product as a colorless oil (35 mg, 9.5%, 213 mg of 1,2-dibenzyldisulfane was recovered). ^1H NMR (MeOD): δ 7.38-7.24 (m, 10H), 6.76 (s, 1H), 3.75 (s, 2H), 2.47 (q, $J = 7.6$ Hz, 2H), 1.17 (t, $J = 7.6$ Hz, 3H) ppm. ^{13}C NMR (MeOD): δ 174.4, 138.2, 138.0, 130.6, 130.0, 129.6, 128.6, 128.6, 127.8, 82.8, 44.2, 28.5, 9.4 ppm. HRMS calcd for $\text{C}_{17}\text{H}_{18}\text{O}_2\text{S}_2\text{Na} [\text{M}+\text{Na}]^+$ 341.0640, found: 341.0643. Elem. Anal.: calcd (%) for $\text{C}_{17}\text{H}_{18}\text{O}_2\text{S}_2$: C 64.12, H 5.70, N 0.00, S 20.14; Found C 64.38, H 5.74, N 0.00, S 20.35



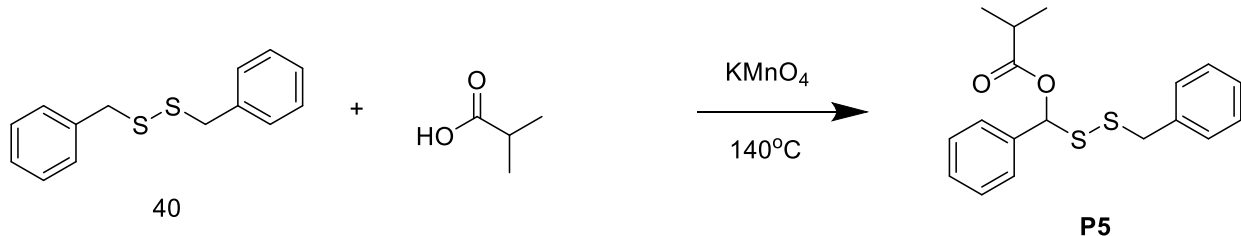
P2: To a 20-ml vial was added 1,2-diethyldisulfane (**41**, 244 mg, 2.0 mmol), KMnO₄ (316 mg, 2.0 mmol) and 4 ml propionic acid. The oil bath was preheated to 140 °C and the mixture was stirred at this temperature for 5 min and then immediately cooled down to room temperature. The mixture was diluted with 100 ml ethyl acetate and washed with 50 ml brine, 50 ml saturated NaHCO₃ and then 50 ml brine. The organic phase was dried over Na₂SO₄ and then evaporated under reduced pressure to give the crude product, which was purified by column chromatography (hexane: ethyl acetate =200:1) to yield a colorless oil (*R*_f = 0.6 in hexane: ethyl acetate =20:1). The colorless oil was further subjected to vacuum at room temperature for 2 h to yield the pure product as a colorless oil (20mg, 9.6%, 113 mg 1,2-diethyldisulfane was recovered). ¹H NMR (CDCl₃): δ 5.99 (q, *J* = 6.4 Hz, 1H), 2.73 (q, *J* = 7.2 Hz, 2H), 2.35 (q, *J* = 7.6 Hz, 2H), 1.60 (d, *J* = 6.4 Hz, 2H), 1.31 (t, *J* = 7.2 Hz, 3H), 1.17 (t, *J* = 7.6 Hz, 3H) ppm. ¹³C NMR (CDCl₃): δ 173.4, 77.6, 33.7, 27.9, 20.3, 14.4, 9.1 ppm. HRMS calcd for C₇H₁₄O₂S₂Na [M+Na]⁺ 217.0327, found: 217.0325. Elem. Anal.: calcd (%) for C₇H₁₄O₂S₂: C 43.27, H 7.26, N 0.00, S 33.00; Found C 43.41, H 7.13, N 0.00, S 32.84.



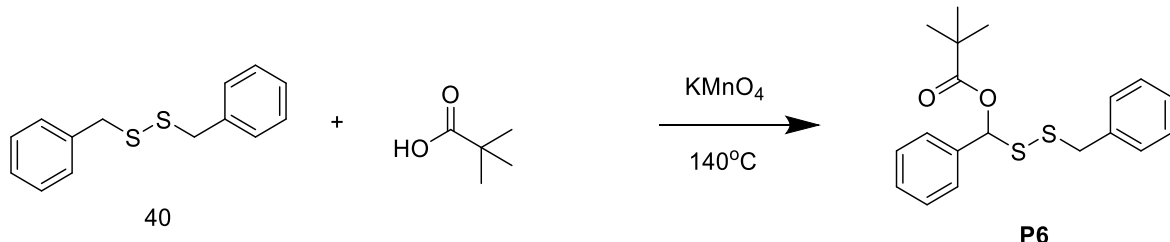
P3: To a 20-ml vial was added 1,2-dibenzyl disulfane (**40**, 500 mg, 2.0 mmol), KMnO_4 (316 mg, 2.0 mmol) and 4 ml 3-methylbutanoic acid. The oil bath was preheated to 140°C and the mixture was stirred at this temperature for 5 min and then immediately cooled down to room temperature. The mixture was diluted with 100 ml ethyl acetate and washed with 50 ml brine, 50 ml saturated NaHCO_3 and then 50 ml brine. The organic phase was dried over Na_2SO_4 and then evaporated under reduced pressure to give the crude product, which was purified by column chromatography (hexane: ethyl acetate = 200:1) to yield a colorless oil ($R_f = 0.7$ in hexane: ethyl acetate = 20:1). The colorless oil was subjected to vacuum at 70°C for 2 h to yield the pure product as a colorless oil (27 mg, 7.6 %, 248 mg 1,2-dibenzyl disulfane was recovered). ^1H NMR (CDCl_3): δ 7.40-7.31 (m, 8H), 7.25-7.24 (m, 2H), 6.78 (s, 1H), 3.70 (ABq, $J = 12.4$ Hz, $\Delta\delta_{\text{AB}} = 0.04$, 2H), 2.34-2.27 (m, 2H), 2.21-2.16 (m, 1H), 0.99 (d, $J = 3.2$ Hz, 3H), 0.97 (d, $J = 3.2$ Hz, 3H) ppm. ^{13}C NMR (CDCl_3): δ 171.7, 136.7, 136.6, 129.6, 129.1, 128.7, 128.6, 127.8, 126.9, 81.3, 43.6, 43.6, 25.9, 22.6 ppm. HRMS calcd for $\text{C}_{19}\text{H}_{23}\text{O}_2\text{S}_2$ [$\text{M}+\text{H}]^+$ 347.1134, found: 347.1303. Elem. Anal.: calcd (%) for $\text{C}_{19}\text{H}_{22}\text{O}_2\text{S}_2$: C 65.86, H 6.40, N 0.00, S 18.50; Found C 65.99, H 6.40, N 0.00, S 18.33.



P4: To a 20-ml vial was added 1,2-dibenzyldisulfane (**40**, 500 mg, 2.0 mmol), KMnO₄ (316 mg, 2.0 mmol), CH₃COONa (600mg, 7.3 mmol) and 4 ml acetic acid. The oil bath was preheated to 140 °C and the mixture was stirred at this temperature for 5 min and then immediately cooled down to room temperature. The mixture was diluted with 100 ml ethyl acetate and washed with 50 ml brine, 50ml saturated NaHCO₃ and then 50ml brine. The organic phase was dried over Na₂SO₄ and then evaporated under reduced pressure to give the crude product, which was purified by column chromatography (hexane: ethyl acetate =200:1) to yield a colorless oil (R_f = 0.7 in hexane: ethyl acetate =20:1). The colorless oil was further subjected to vacuum at room temperature for 2 h to yield the pure product as a colorless oil (35mg, 10.8 %, 237 mg 1,2-dibenzyldisulfane was recovered). ¹H NMR (CDCl₃): δ 7.40-7.29 (m, 9H), 7.26-7.24 (m, 1H), 6.78 (s, 1H), 3.73 (ABq, J = 12.0 Hz, Δδ_{AB} = 0.04, 2H), 2.18 (s, 3H) ppm. ¹³C NMR (CDCl₃): δ 169.6, 136.6, 136.5, 129.6, 129.2, 128.7, 128.7, 127.8, 126.9, 81.6, 43.6, 21.3 ppm. HRMS calcd for C₁₆H₁₆O₂S₂Na [M+Na]⁺ 327.0484, found: 327.0494. Elem. Anal.: calcd (%) for C₁₆H₁₆O₂S₂: C 63.13, H 5.30, N 0.00, S 21.06; Found C 63.23, H 5.30, N 0.00, S 21.10.

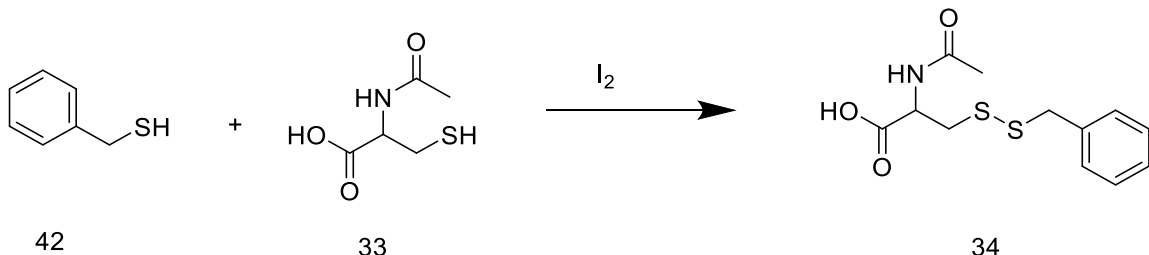


P5: To a 20-ml vial was added 1,2-dibenzyldisulfane (**40**,500 mg, 2.0 mmol), KMnO_4 (316 mg, 2.0 mmol) and 4 ml isobutyric acid. The oil bath was preheated to 140°C and the mixture was stirred at this temperature for 5 min and then immediately cooled down to room temperature. The mixture was diluted with 100 ml ethyl acetate and washed with 50 ml brine, 50 ml saturated NaHCO_3 and then 50ml brine. The organic phase was then dried over Na_2SO_4 and then evaporated under reduced pressure to give the crude product, which was purified by column chromatography (hexane: ethyl acetate =200:1) to yield a colorless oil ($R_f = 0.7$ in hexane: ethyl acetate =20:1). The colorless oil was further subjected to vacuum at 55°C for 2 h to yield the pure product as a colorless oil (20 mg, 5.6 %, 233 mg of 1,2-dibenzyldisulfane was recovered). ^1H NMR (CDCl_3): δ 7.42-7.29 (m, 9H), 7.26-7.24 (m, 1H), 6.79 (s, 1H), 3.72 (ABq, $J = 12.0$ Hz, $\Delta\delta_{\text{AB}} = 0.05$, 2H), 2.73-2.66 (m, 1H), 1.27 (d, $J = 7.2$ Hz, 3H), 1.24 (d, $J = 7.2$ Hz, 3H) ppm. ^{13}C NMR (CDCl_3): δ 175.6, 136.7, 136.6, 129.6, 129.0, 128.7, 128.6, 127.8, 126.8, 81.2, 43.6, 34.4, 19.1, 19.0 ppm. HRMS calcd for $\text{C}_{18}\text{H}_{20}\text{O}_2\text{S}_2\text{Na}$ $[\text{M}+\text{Na}]^+$ 355.0797, found: 355.0818. Elel. Anal.: calcd (%) for $\text{C}_{18}\text{H}_{20}\text{O}_2\text{S}_2$: C 65.03, H 6.06, N 0.00, S 19.29; Found C 65.16, H 6.18, N 0.00, S 19.42.



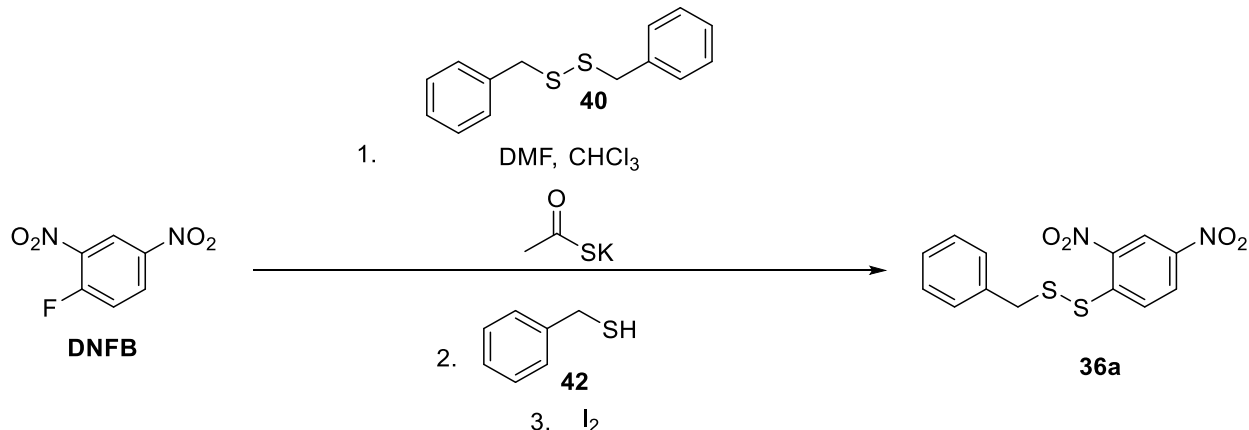
P6: To a 20-ml vial was added 1,2-dibenzyl disulfane (**40**, 1000 mg, 4.0 mmol), KMnO_4 (600 mg, 3.8 mmol) and 4 ml isobutyric acid. The oil bath was preheated to 140°C and the mixture was stirred at this temperature for 5 min and then immediately cooled down to room temperature. The mixture was diluted with 100 ml ethyl acetate and washed with 50 ml brine, 50 ml saturated NaHCO_3 and then 50 ml brine. The organic phase was then dried over Na_2SO_4 and then evaporated under reduced pressure to give the crude product, which was purified by column chromatography (hexane: ethyl acetate = 200:1) to yield a colorless oil ($R_f = 0.7$ in hexane : ethyl acetate = 20:1). The colorless oil was further subjected to vacuum at 70°C for 2 h to yield the pure product as a colorless oil (20 mg, 5.6 %, 233 mg 1,2-dibenzyl disulfane was recycled). ^1H NMR (CDCl_3): δ 7.40–7.30 (m, 8H), 7.26–7.24 (m, 2H), 6.77 (s, 1H), 3.68 (ABq, $J = 12.0$ Hz, $\Delta\delta_{\text{AB}} = 0.05$, 2H), 1.29 (s, 9H) ppm. ^{13}C NMR (CDCl_3): δ 177.0, 136.8, 136.6, 129.6, 129.0, 128.7, 128.6, 127.7, 126.8, 81.2, 43.6, 39.2, 27.3 ppm. HRMS calcd for $\text{C}_{19}\text{H}_{22}\text{O}_2\text{S}_2\text{Na} [\text{M}+\text{Na}]^+$ 369.0953, found: 369.0971. Elem. Anal.: calcd (%) for $\text{C}_{19}\text{H}_{22}\text{O}_2\text{S}_2$: C 65.86, H 6.40, N 0.00, S 18.50; Found C 65.96, H 6.38, N 0.00, S 18.62.

2.4.1.2 Synthesis of *N*-acetyl-*S*-(benzylthio)cysteine

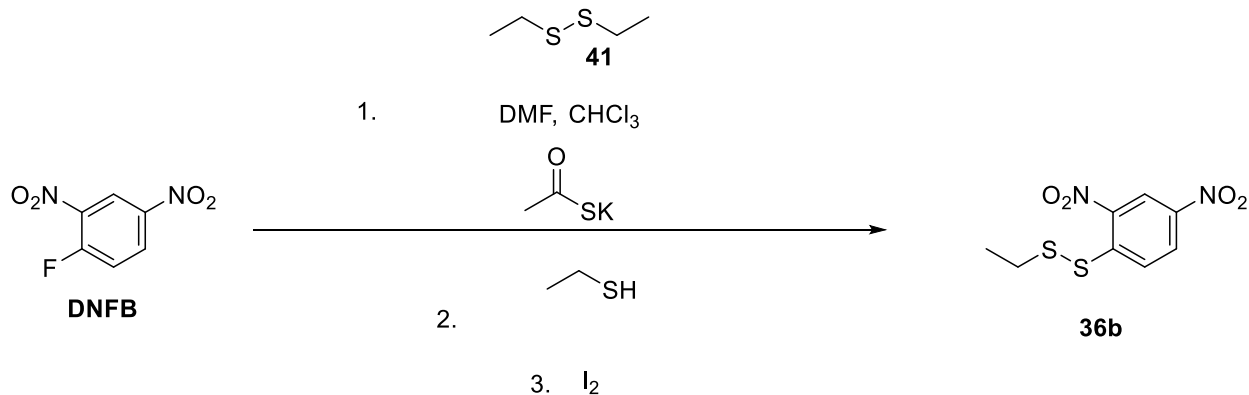


N-acetyl-*S*-(benzylthio)cysteine (**34**): To a 20-ml vial was added benzyl mercaptan (**42**, 100 mg, 0.8 mmol), acetylcysteine (**33**, 130 mg, 0.8 mmol), sodium acetate (131 mg, 1.6 mmol), 4 ml tetrahydrofuran and 2 ml water. The reaction mixture was stirred for 5 min and then iodine (101 mg, 0.4 mmol) was added. After stirring for another 10 min, the mixture was diluted with 30 ml ethyl acetate and 10 ml water. To the mixture was then added saturated sodium thiosulfate solution until the solution became colorless. The organic phase was washed with 10 ml brine and then concentrated to give the crude product, which was purified by column chromatograph to yield the pure product as pale yellow oil ($R_f = 0.7$ in Methanol: Dichloromethane = 1:5, 150 mg, 66 %). 1H NMR (CD_3OD): δ 7.36-7.24 (m, 5H), 4.64 (dd, $J = 8.8$ Hz, $J = 4.4$ Hz, 1H), 3.93 (ABq, $J = 12.8$ Hz, $\Delta\delta_{AB} = 0.02$, 2H), 2.89 (dd, $J = 14.0$ Hz, $J = 4.4$ Hz, 1H), 2.71 (dd, $J = 14.0$ Hz, $J = 8.8$ Hz, 1H), 1.99 (s, 3H) ppm. ^{13}C NMR (CD_3OD): δ 173.6, 173.3, 138.8, 130.5, 129.6, 128.5, 53.0, 44.1, 40.5, 22.4 ppm. HRMS calcd for $C_{12}H_{16}NO_3S_2^+ [M+H]^+$: 286.0566, found: 286.0569.

2.4.1.3 Synthesis of disulfide compound 36a and 36b



1-benzyl-2-(2,4-dinitrophenyl)disulfane (36a): To a solution of 2,4-Dinitro-1-fluorobenzene (**DNFB**, 186mg, 1mmol), compound **40** (50mg, 0.2 mmol) in 3 ml chloroform was added a solution of potassium thiolacetate (116mg , 1mmol) in 1ml DMF. The reaction was stirred at r.t for 15 min. Then compound **42** (500mg, 4mmol) was added to the reaction mixture. The reaction was stirred at r.t for another 10 min, then iodine (259mg, 1mmol) was added to the reaction mixture. The reaction mixture was stirred at r.t for 2 h, diluted with ethyl acetate (30 ml), and washed with 1N HCl (20 ml), H₂O (20 ml) and brine (10 ml). The organic layer was dried over NaSO₄ and solvent was removed by rotavapor to afford a crude product, which was purified by column chromatograph (Rf = 0.6 in hexane : ethyl acetate =10:1) to yield the pure product as a yellow solid (31 mg, 10%). ¹H NMR (CDCl₃): δ 8.97 (d, J = 2.4 Hz, 1H), 8.13 (dd, J=2.4 Hz, H= 9.2 Hz, 1H), 8.04 (d, J = 9.2 Hz, 1H), 7.13-7.25(m, 5H), 4.00(s, 2H). ¹³C NMR (CDCl₃): δ 146.1, 145.2, 144.9, 135.5, 129.3, 128.9, 128.8, 128.1, 126.6, 121.1, 43.5. HRMS calcd for C₁₃H₁₀AgN₂O₄S₂⁺ [M+Ag]⁺: 428.9127, found: 428.9132 .



1-(2,4-dinitrophenyl)-2-ethyldisulfane (36b**):** Following the same procedure for preparing compound **36a**, the product was obtained as a yellow solid ($R_f = 0.5$ in hexane : ethyl acetate = 10:1, 15 mg, 6%). ^1H NMR (CDCl_3): δ 9.12 (d, $J = 2.4$ Hz, 1H), 8.54 (d, $J = 8.8$ Hz, 1H), 8.47 (dd, $J = 2.4$ Hz, $J = 8.8$ Hz, 1H), 2.82 (q, $J = 6.4$ Hz, 2H), 1.36 (t, $J = 6.4$ Hz, 2H). ^{13}C NMR (CDCl_3): δ 147.0, 145.6, 145.2, 128.9, 127.4, 121.8, 32.7, 14.5. HRMS calcd for $\text{C}_8\text{H}_8\text{AgN}_2\text{O}_4\text{S}_2^+ [\text{M}+\text{Ag}]^+$: 366.8971, found: 366.8979.

2.4.2 Kinetic studies of P1-6 (Ps) in the presence of esterase.

Stock solution preparation: HPs stock solution: HPs were dissolved in DMSO to afford 5 mM HPs stock solutions. Disulfide compound stock solution: Compound **36a** and **36b** were dissolved in DMSO to afford 5 mM stock solutions. Esterase stock solution: 6.0 mg Esterase (18 u/mg esterase from porcine liver, PLE, Aldrich, E3019) was dissolved in 108 ml phosphate buffer (PBS, pH 7.4) to provide a 1 u/ml PLE stock solution. Acetylcysteine stock solution: 163 mg acetylcysteine was dissolved in 100 ml PBS to afford 10mM stock solution; 50 mg acetylcysteine was dissolved in 2.0 ml DMSO to afford 150 mM stock solution. WSP-5 stock solution: WSP-5 was dissolved in DMSO to prepare a 2.5 mM stock solution. CTAB was dissolved

in ethanol to prepare a 100 mM stock solution. DNFB stock solution: DNFB was dissolved in DMSO to afford 200 mM stock solution.

H_2S release from HP detected by Methylene Blue Method. At each time point, 100 μL of reaction solution was taken into a 1.5 mL vial containing 100 μL zinc acetate (1%, w/v). Then the vial was centrifuged for 10 min (14.5×1000 rp). The supernatant was removed. Then 200 μL *N,N*-dimethyl-1,4-phenylenediaminesulfate (0.2% w/v in 20% H_2SO_4 solution) and 200 μL ferric chloride (1% w/v in 0.2% H_2SO_4 solution) were added to the vial. After 6 min, the absorbance (at 740 nm) of the resulting solution was measured. H_2S concentration was calculated based on a calibration curve of $\text{Na}_2\text{S} \cdot 9\text{H}_2\text{O}$.

HPLC sample preparation. At each time point, 200 μL of reaction solution was taken into a 1.5 mL vial containing 600 μL acetonitrile (ACN). The mixture was incubated in an acetone dry ice bath (-78 ° C) for 5 min, and centrifuged for 10 min (14.5×1000 rp). The supernatant was analyzed by HPLC with method A.

HPLC with Method A: mobile phase A (10 mM NaH_2PO_4 in water, pH= 5.0) and mobile phase B (ACN), flow rate: 1mL/min, running time: 25min, the gradient elution method: 30% B from 0 to 8 min, 30% to 95% B from 8 to 15 min, 95% B from 15 to20 min, 95% to 30% B from 20 to 24 min, 30% B from 24 to 25 min. Detection wavelength: 254 nm. Column: Waters C18 3.5 μM , 4.6×100 mm. Injection volume: 20 μL

HPLC with Method B: mobile phase A (H_2O) and mobile phase B (ACN), flow rate: 1mL/min, running time: 25min, the gradient elution method: 30% B from 0 to 8 min, 30% to 95% B from 8 to 15 min, 95% B from 15 to20 min, 95% to 30% B from 20 to 24 min, 30% B from 24 to 25 min. Detection wavelength: 254 nm. Column: Waters C18 3.5 μM , 4.6×100 mm. Injection volume: 200 μL

HPLC with Method C: mobile phase A (H_2O , pH = 3.0, CF_3COOH) and mobile phase B (ACN), flow rate: 1 mL/min, running time: 35 min, the gradient elution method: 30% B from 0 to 10 min, 30% to 80% B from 10 to 25 min, 80% to 30% B from 25 to 35 min. Detection wavelength: 254 nm. Column: Waters C18 3.5 μM , 4.6×100 mm. Injection volume: 200 μL

Table 2.3. Retention times table with Method A.

Compound	P1	P2	P3	P4	P5	P6	31	6a	6b
Time /min	15.9	4.3	16.6	15.2	16.3	16.6	5.8	14.7	15.4

Time points at which samples were taken for kinetic studies: 10s, 30s, 1min, 1.5 min, 2min, 2.5 min, 3min.

Reaction set up procedure: To a 20-ml vial was added various volumes of PLE stock solution, acetylcysteine stock solution and pure PBS (Table 2.4.2). The mixture was stirred at 37 °C for 30 min. Then 100 μl HPs was added to the mixture. The reaction mixture was stirred at 37 °C, and at each time point, 100 μl or 200 μl reaction mixture was taken out for H_2S release detection or HPLC sample preparation.

Table 2.4 Reaction conditions.

Condition	PLE stock solution(1unit/ml)	Acetylcysteine stock solution (10mM)	Pure PBS	Substrates
1	2.5 ml	250 μl	2.25ml	201
2	2.5 ml	500 μl	2 ml	201
3	2.5 ml	1.5 ml	1 ml	201
4	0	250 μl	4.75 ml	201
5	2.5 ml	0	2.5 ml	201
6	2.5 ml	250 μl	2.25 ml	202

7	2.5 ml	250 µl	2.25 ml	203
8	2.5 ml	250 µl	2.25 ml	204
9	2.5 ml	250 µl	2.25 ml	205
10	2.5 ml	250 µl	2.25 ml	206
11	2.5 ml	0	2.5 ml	202
12	2.5 ml	0	2.5 ml	203
13	2.5 ml	0	2.5 ml	204
14	2.5 ml	0	2.5 ml	205
15	2.5 ml	0	2.5 ml	206

Persulfide trapping reaction: To a 20-ml vial was added 5 ml PLE stock solution (1 unit/ml). The solution was incubated at 37 °C for 30 min, then 100 µl HPs were added to the mixture. After 10 s, 200 µl DNFB stock solution was added. The reaction mixture was stirred at 37 °C for another 30 min. 200 µl reaction mixture was taken out for HPLC sample preparation.

2.4.3 Mechanism study of H₂S release from “acetal” based H₂S prodrugs using HPLC.

For the H₂S release mechanism study, HPLC with method C was used.

Procedure: To a 20-ml vial was added 1.9 ml PLE stock solution (5 unit/ml) and 40 µl 150 mM acetylcysteine. Then 40 µl **P1** (5 mM in DMSO) was added. The solution was incubated at 37 °C for 3 h. The 200 µL of reaction solution was taken into a 1.5 mL vial containing 600 µL ACN. The mixture was incubated in an acetone dry ice bath (-78 °C) for 5 min, and centrifuged for 10 min (14.5 × 1000 rp). The supernatant was analyzed by HPLC with method C.

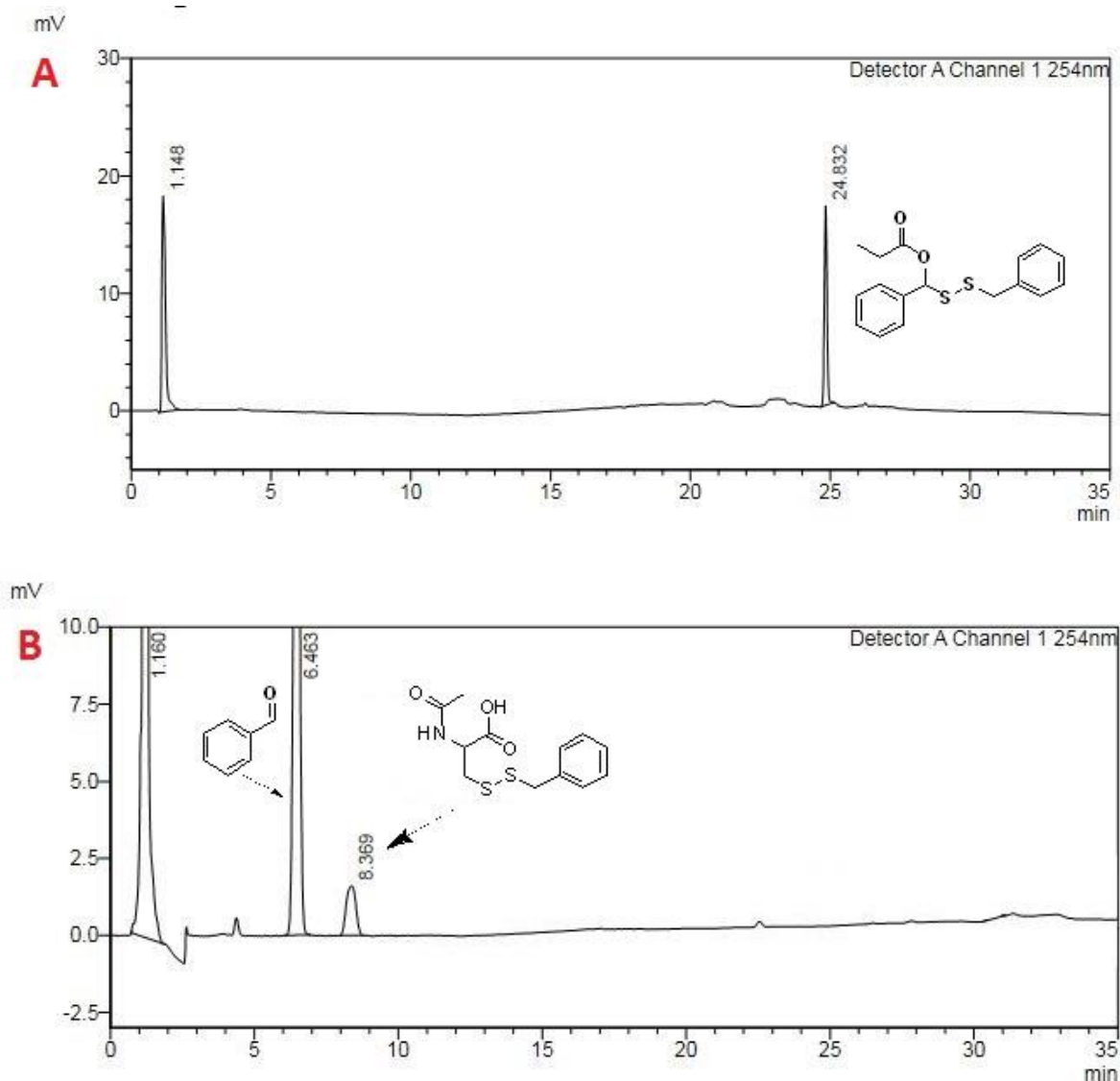


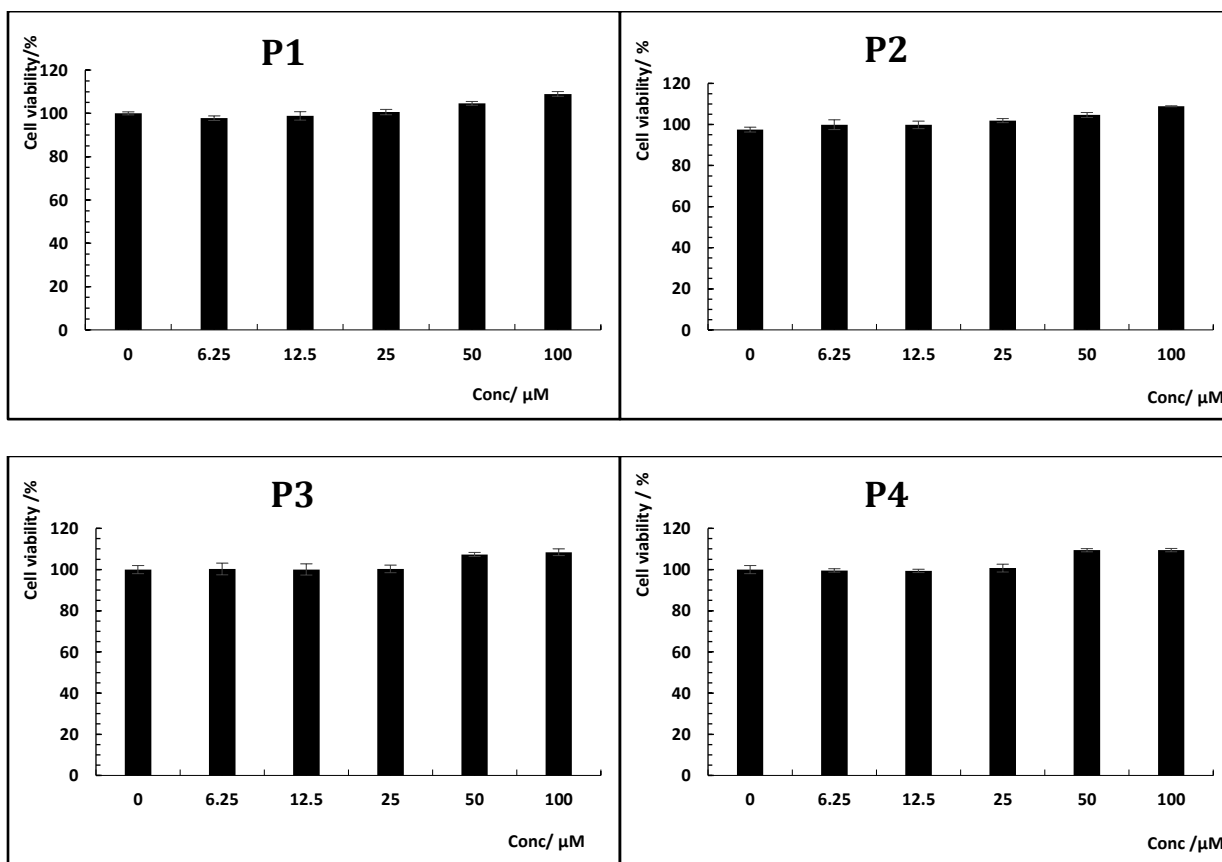
Figure 2.4. Persulfide release mechanism study. a), 100 μM P1 in PBS. b), 100 μM P1 in PBS (4% DMSO) was incubated with 5 U/ml PLE and 3 mM L- acetylcysteine at 37 °C, after 3 hours the mixture was subjected to HPLC.

2.4.4 Cell culture

H₉C₂ (ATCC®CRL-1446™) cells were used in the studies. The H₉C₂ cells were maintained in DMEM (Dulbecco's Modified Eagle's Medium) supplemented with 10% fetal bovine serum (MidSci; S01520HI) and 1% penicillin-streptomycin (Sigma-Aldrich; P4333) at 37 °C with 5% CO₂.

2.4.4.1 Cytotoxicity study (Without added PLE)

The H₉C₂ cells were seeded in 96-well plate one day before the experiment. Different concentrations of prodrugs were added into the H₉C₂ cells. The cells were then incubated with the compounds for 24 hours at 37 °C with 5% CO₂. Cell viability was tested by the cell counting kit-8 (Dojindo; KH677). Specifically, after 24 h of incubation, cell culture media was changed and 10 μl cell counting kit-8 solution was added. Absorbance at 450 nm was read by a plate reader after 3 h.



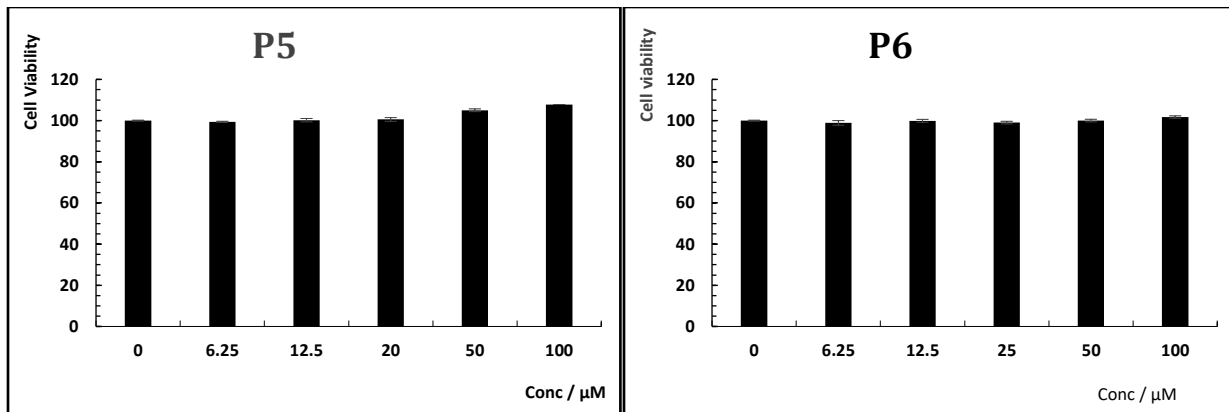
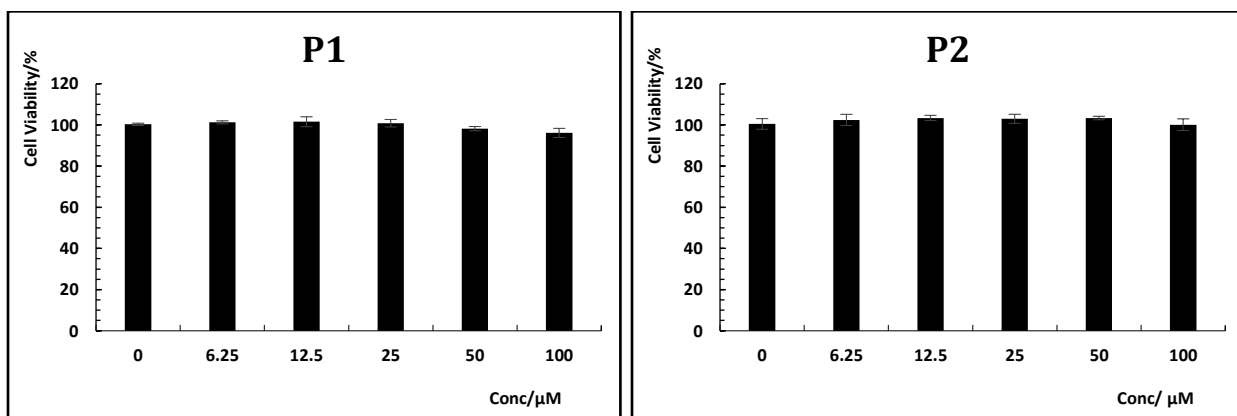


Figure 2.5. Cytotoxicity of various perthiol prodrugs. H9C2 cells were treated with perthiol prodrugs with various concentrations for 24h.

2.4.4.2 Cytotoxicity studies (With adding PLE)

The H₉C₂ cells were seeded in 96-well plate one day before the experiment. Cell was cultured in DMEM supplemented with 10% fetal bovine serum, 1% penicillin-streptomycin and 1u/ml PLE.

Different concentrations of prodrugs were added into the H₉C₂ cells. The cells were then incubated with the compounds for 24 hours at 37 °C with 5% CO₂. Cell viability was tested by the cell counting kit-8 (Dojindo; KH677). Specifically, after 24 h of incubation, cell culture media was changed and 10 ul cell counting kit-8 solution was added. Absorbance at 450 nm was read by a plate reader after 3 h.



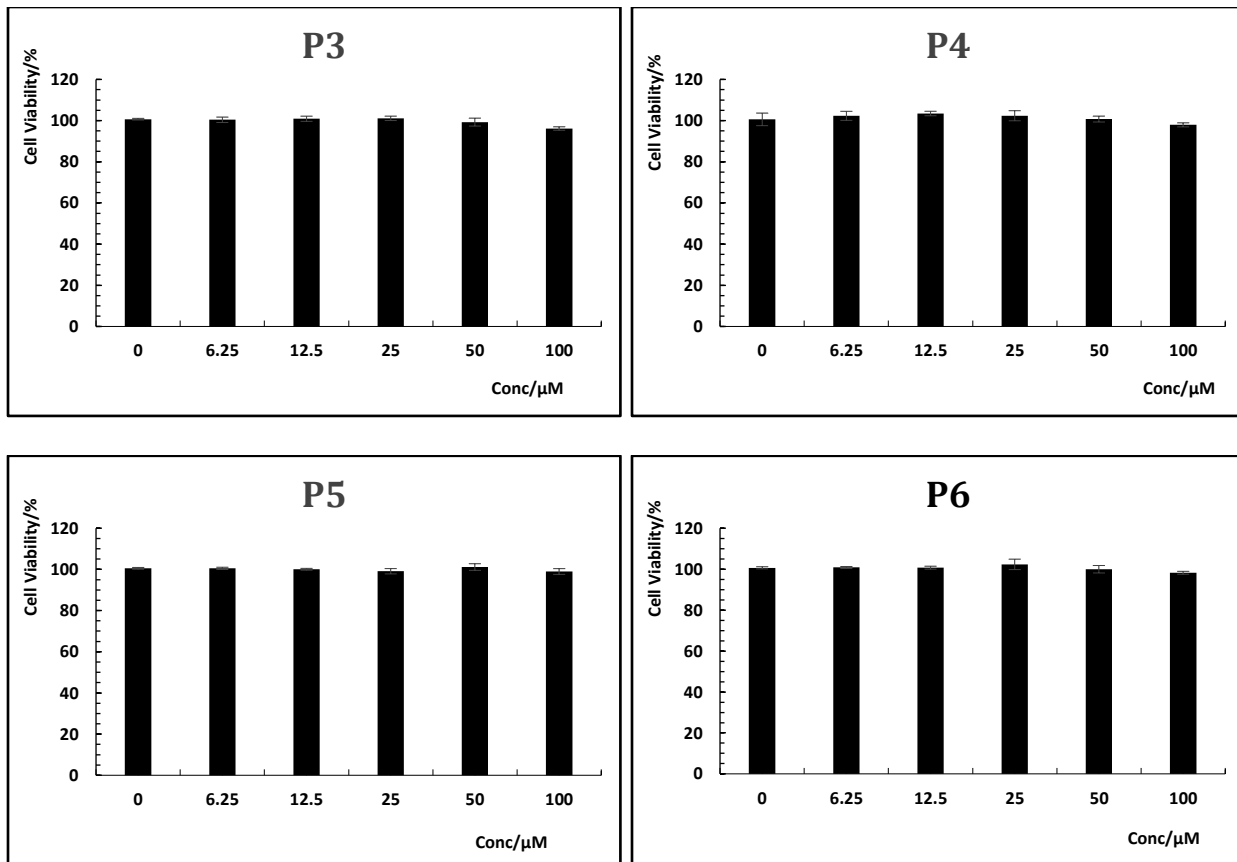


Figure 2.6. Cytotoxicity of various perthiol prodrugs. H9C2 cells were treated with perthiol prodrugs with various concentrations for 24h.

2.4.4.3 H₂S release validation by fluorescent probe WSP-5 in cultured cell

H₉C₂ cells were cultured in DMEM supplemented with 10% FBS (v/v), penicillin (100 U/mL) and streptomycin (100 ug/mL) at 37 °C with 5% CO₂. Cells were seeded to culture dished one day before use. Cells were washed by FBS free DMEM media before use. Cells were treated with 100 μM **P5** or 100 μM Na₂S or vehicle in PBS buffer (containing 300 μM L-cysteine) with PLE (5 U/ml) or without PLE for 10 min. The cell culture media was removed and washed by PBS. Cells were incubated with 10 μM WSP-5 in PBS (containing 100 μM CTAM) for 10 minutes. Then culture solution was removed and cell imaging was performed.

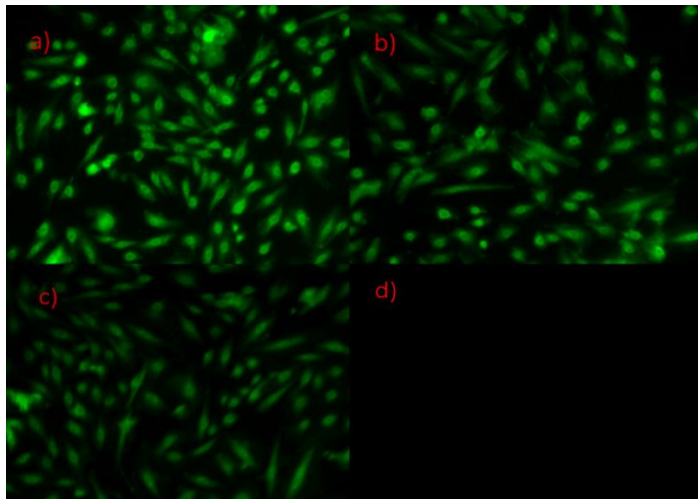


Figure 2.7. Fluorescence images of P5 in cultured cells. H9C2 cells were treated with different prodrugs under various conditions, and then washed and treated with 10 μ M WSP-5 for 10 min. (a) P5 100 μ M + esterase 5 u/ml (b) P5 100 μ M (c) 100 μ M $\text{Na}_2\text{S}\cdot 9\text{H}_2\text{O}$ (d) No prodrug.

2.4.5 LC-MS studies of persulfide reactivity with S-methyl methanethiosulfonate (MMTS).

Sample preparation A: To a 20-ml vial was added 5 ml PBS containing 1u/ml PLE, 100 μ l P5 stock solution (5 mM in DMSO), and 100 μ l MMTS (200 mM in DMSO). The mixture was stirred at r.t for 30 min. Then 200 μ l reaction mixture was taken out and added to a vial containing 600 μ l ACN, and the mixture was centrifuged for 4 min (14.5×1000 rp). The supernatant was analyzed by HPLC with method B. The fraction at 15.3 min retention time was collected. 1 μ l of AgNO_3 (1 mg/ml in ACN) solution was added to the fraction, and the mixture was injected to the MS.

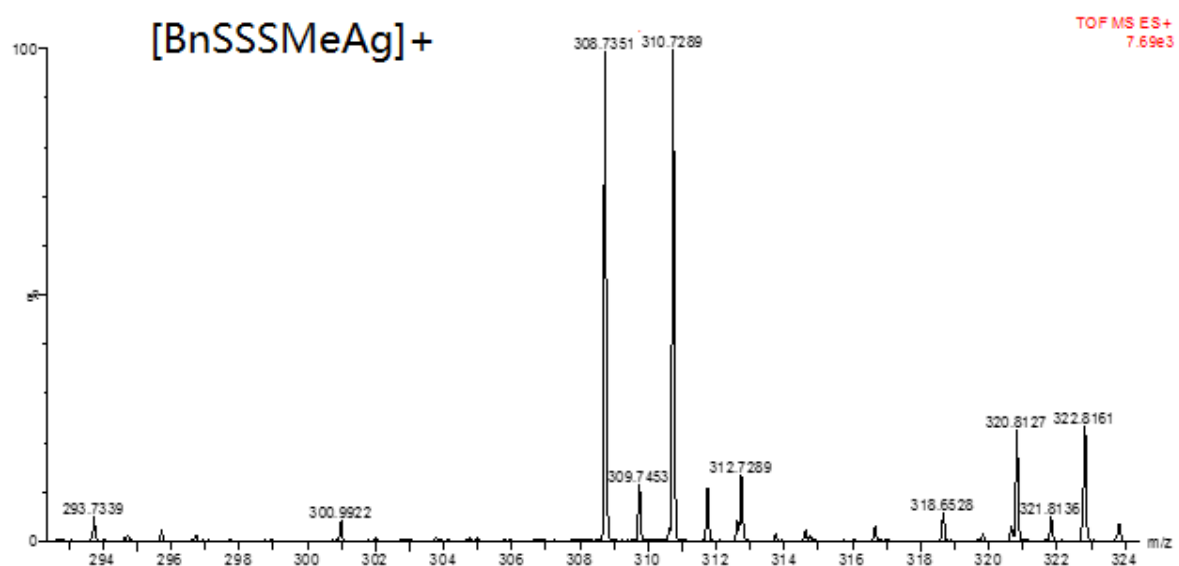
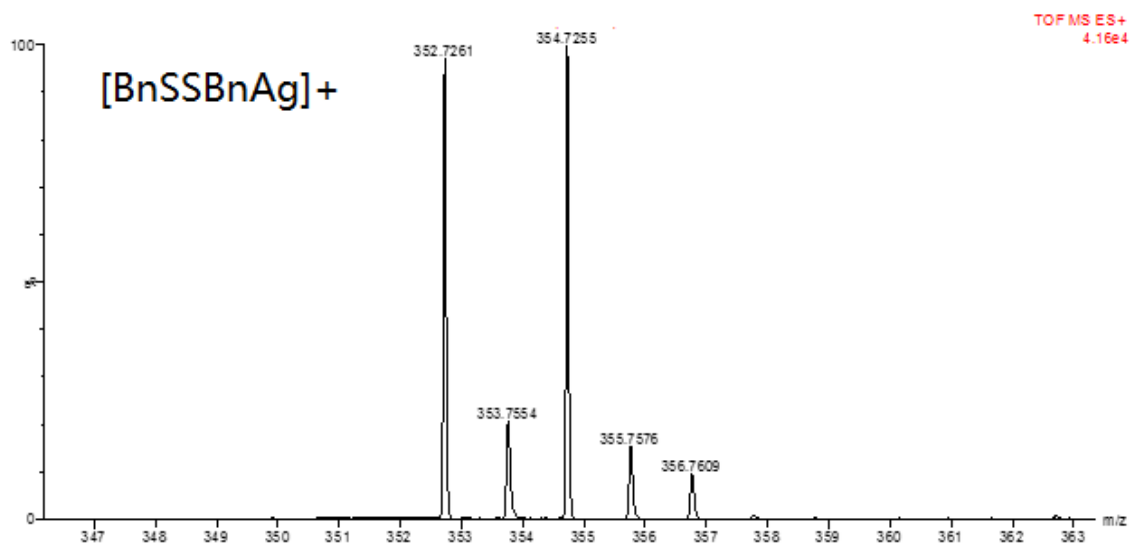
Sample preparation B: To a 20-ml vial was added 1 ml H_2O , 100 μ l dibenzyl disulfide (BnSSBn , 10 mM in DMSO), 100 μ l Na_2S solution (10 mM in H_2O), and 100 μ l MMTS (200 mM in DMSO). The mixture was stirred at r.t for 30 min. Then 200 μ l reaction mixture was taken out and added to a vial containing 600 μ l ACN, and the mixture was centrifuged for 4 min (14.5×1000 rp). The supernatant was analyzed by HPLC with method B. The fractions at 14.6 min, 15.3

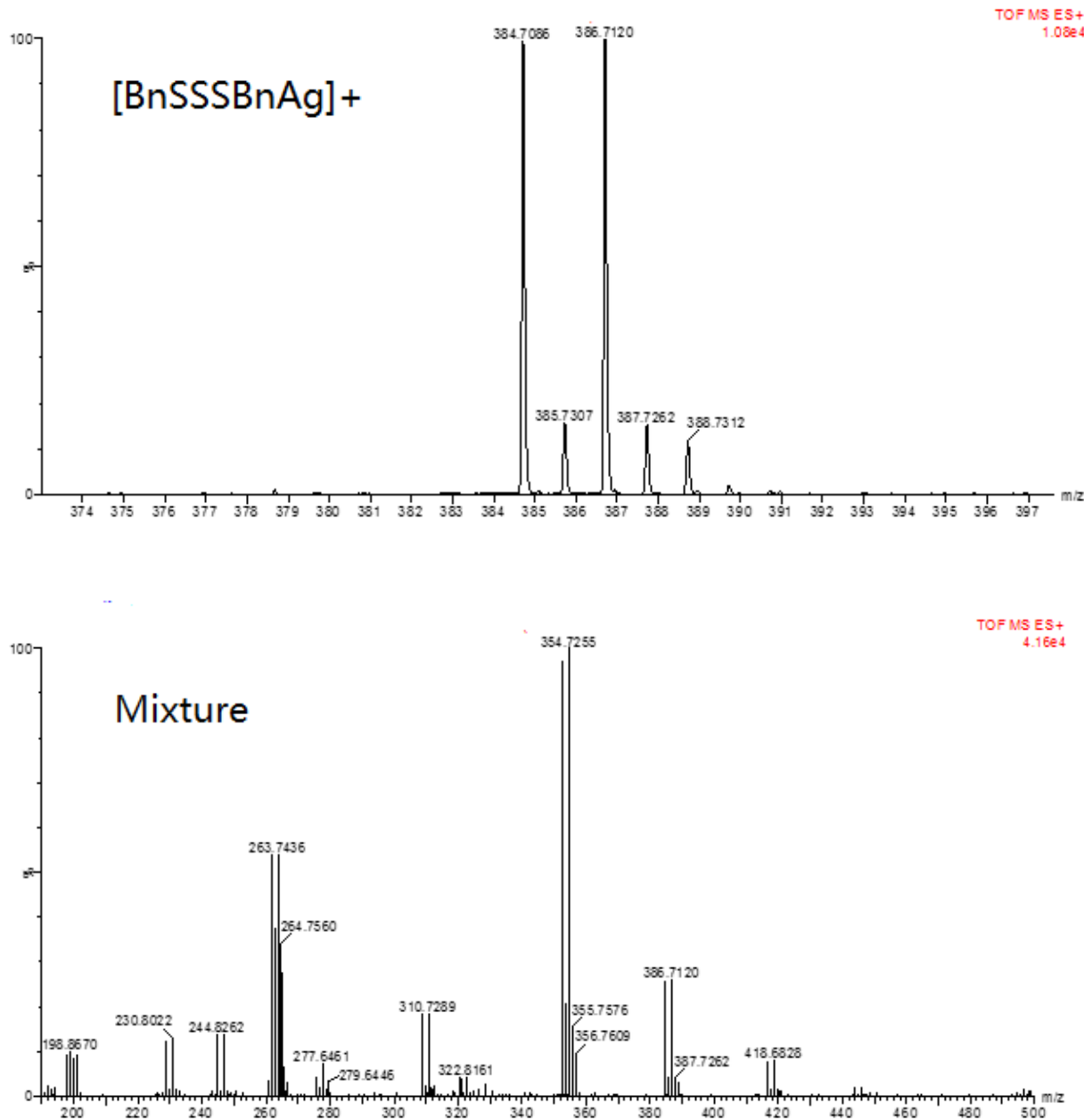
min, 15.8 min and 16.3 min was collected separately, and all samples was added 1 ul of AgNO₃ (1 mg/ml in ACN) solution and then was injected to the MS respectively.

It needs to be noted that all spectrums shown below is the original spectrum before calibrated by the internal standards. The HRMS of these compounds are shown in Table 2.4.3:

Table 2.5 HRMS of sulfide compounds

Compound	Formula	Calcd.	Found
[BnSSMe+Ag] ⁺	C ₈ H ₁₀ AgS ₂ ⁺	276.9269	276.9273
[BnSSSMe+Ag] ⁺	C ₈ H ₁₀ AgS ₃ ⁺	308.8990	308.8997
[BnSSBn+Ag] ⁺	C ₁₄ H ₁₄ AgS ₂ ⁺	352.9582	352.9588
[BnSSSBn+Ag] ⁺	C ₁₄ H ₁₄ AgS ₃ ⁺	384.9303	384.9307
[BnSSSBn+Ag] ⁺	C ₁₄ H ₁₄ AgS ₃ ⁺	384.9303	384.9307





2.4.6 Methylene blue (MB) method to detect the H₂S release from P1-P6

To 4.9 mL 500 μM Compound **33** in phosphate buffer (pH 7.4) solution was added 5unit PLE, followed by the addition of 100 μL 5 mM prodrugs stock solution (Final Conc.: 100 μM). The resultant solution was stirred at 37 °C. At each time point, 200 μL of reaction solution was taken into a 1.5 mL vial containing 200 μL zinc acetate (1 %, w/v). Then the vial was centrifuged

for 10 min. (14.5×1000 rp). Removed the supernatant and washed the precipitation with PBS solution ($100 \mu\text{L} \times 2$). Then $600 \mu\text{L}$ N,N-dimethyl-1,4-phenylenediaminesulfate (0.2% w/v in 20% H_2SO_4 solution) and $50 \mu\text{L}$ ferric chloride (10% w/v in 0.2% H_2SO_4 solution) was added to the vial. Then the vial was centrifuged for 5 min (14.5×1000 rp). The absorbance (at 740 nm) of the resulting solution was measured (after stirring for 10 min). H_2S concentration was calculated based on a calibration curve of NaHS.

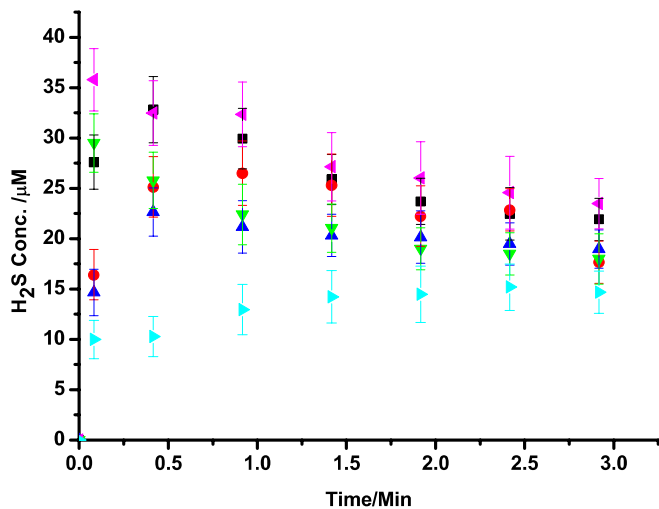


Figure 2.8. H_2S release from $100 \mu\text{M}$ P1 to P6 at 37°C in PBS in the presence of $500 \mu\text{M}$ compound 33 (2% DMSO) and $0.5 \mu\text{M}$ PLE. The H_2S concentrations were detected by MB method. ■ P1; ● P2; ▲ P3; ▼ P4; ▲ P5 ▶ P6.

2.4.7 Myocardial Ischemia-Reperfusion Protocol

Male c57/b6j mice (Jaxon Laboratory) were used at 10-12 weeks of age. The surgery was performed under aseptic conditions. Instruments were steam autoclaved or undergo cold sterilization (MaxiCide, Henry Schein). The surgical area was cleaned and wiped down with 70% ethanol before and after surgery. The mice were anesthetized with intraperitoneal injections of ketamine (50mg/kg) and sodium pentobarbital (60 mg/kg). Subsequent to anesthesia, the mice were orally intubated with polyethylene-60 (PE-60) tubing, connected via loose junction to a rodent ventilator (MiniVent Type 845, Hugo-Sachs Elektronik) set at a tidal volume $250 \mu\text{L}$ of and

a rate of ~130 breaths per minute, and supplemented with 100% oxygen (0.1-0.2 liters/minute flow rate). Body temperature was maintained at ~37 °C using a mouse monitor pad (Indus, MouseMonitor). Hair remover (i.e., Nair®) was placed on the chest with a cotton swab and then removed along with the chest hair. Betadine solution was placed on the chest wall prior to any skin incision. We applied alternating applications of betadine and alcohol to be applied with a cotton swab at least once each with a final application of betadine. An incision was made in the skin along the midline to expose the sternum. A median sternotomy was performed and the wound edges were cauterized with an electrocautery device. The proximal left coronary artery (LCA) was visualized and ligated for 45 min with 7-0 silk suture mounted on a tapered needle (BV-1, Ethicon). A short segment of PE-10 tubing was placed in between the LCA and the 7-0 silk suture to minimize damage to the coronary artery and allow for complete reperfusion following the ischemic period. Ischemia was confirmed by the appearance of hypokinesis and pallor distal to the occlusion, as well as ST segment elevation shown on the Mouse Monitor. Following the prescribed period of LCA occlusion, the ligature was removed, and reperfusion was visually confirmed. Following reperfusion, the chest wall and the skin incision will be carefully closed with 5-0 Polysorb® (Braided Lactomer 9-1) suture mated to a CV-23 (1/2 inch, 17 mm) tapered needle.

The duration of myocardial ischemia was for 45 min in all experiments and the duration of the reperfusion was 24 hours. 5 mins prior to reperfusion, experimental compound or vehicle was administered via intracardiac injection.

In the myocardial ischemia-reperfusion experiments blood (~50 µL) was collected from a subset of mice via tail vein at 4 hours of reperfusion for the subsequent measurement of plasma markers of cardiac injury (Troponin-I).

At 24 hours of reperfusion, mice were anesthetized as previously described. An endotracheal tube was placed in the trachea following a tracheostomy and the mice were ventilated as described previously. The common carotid artery was fully dissected and then cannulated with PE-10 tubing for injection of Evan's blue dye to delineate the area of myocardium at risk. Next, the left coronary artery was fully ligated again at the same location as in ischemic phase. Then Evan's blue dye (0.5 mL) was injected into the carotid artery catheter.

The Evan's blue dye was only distributed in regions of the heart that receive normal blood flow and therefore provided a very accurate method to delineate the non-ischemic (normal) myocardium from the ischemic myocardium (area at risk). The heart then was rapidly excised and sliced for further analysis with 2,3,5-triphenyltetrazolium (TTC). In non-infarcted myocardium, TTC was enzymatically reduced to 1,3,5-triphenylformazan, which is in red color. In the necrosis core (Infarction), TTC remained in white color. In general, on the slices of a properly stained heart, the left ventricle (LV) was divided into three regions: the dark-blue region as the normal myocardium, the non-blue region as the area at risk (AAR), and the white region as the infarction (INF). Pictures of each slice were taken and analyzed using ImageJ software (NIH) in a blinded manner.

2.4.8 Sulfane Sulfur Measurement Protocol

Male c57bl/6j mice (Jaxon Laboratory) were used at 10-12 weeks of age. The mice were anesthetized with intraperitoneal injections of ketamine (50 mg/kg) and sodium pentobarbital (60 mg/kg). An incision was made in the skin along the midline to expose the sternum. A median sternotomy was performed and the wound edges were cauterized with an electrocautery device. Experimental compound solution or vehicle was administered through intracardiac injection. 5-min post injection, blood was collected for further analysis.

For sulfane sulfur measurement, 50 μ L of plasma sample was mixed with equal volume of 15 mM DTT in 0.1 mM Tris/HCl, pH 9.0 in a small glass vial (5182-0553, Agilent), sealed with a rubber top, and incubated at 37 °C for 50 minutes. After the incubation, 200 μ L of 1M sodium citrate (pH 6.0) was injected into the vial through the rubber top. Then the mixture was incubated at 37 °C for 10 minutes with shaking at 125 rpm. After shaking, 200 μ L of head-space gas was applied to a gas-chromatograph (7890A GC System, Agilent) equipped with a dual plasma controller and sulfur chemiluminescence detector (355, Agilent). Chromatographs were captured and analyzed with Agilent ChemStation software (B.04.03).

2.5 Acknowledgement

I would like to specially thank Bingchen Yu for a large amount of synthetic work as well as for extensive discussions. I also like thank Zhengnan Yuan for helping with the synthesis and the cell culture work. The animal model work was conducted in the lab of Dr. David Lefer with Zhen li, Chelsea L. Organ, and Rishi K. Trivedi assisting with the experimental work. I also would like to thank Dr. Siming Wang for the MS work.

3 AN ENRICHMENT-TRIGGERED PRODRUG ACTIVATION STRATEGY DEMONSTRATED USING A CLICK, CYCLIZE, AND RELEASE SYSTEM FOR DELIVERY OF DOXORUBICIN IN MITOCHONDRIA

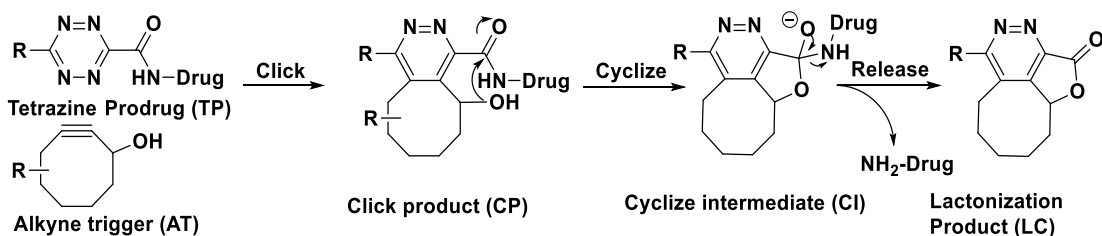
Abstract: This chapter is mainly based on my publications: Nat. Chem. 2017 in revision. A critical component of an effective prodrug approach is achieving delivery to and drug release at the desired site. Through the use of targeting molecules such as antibodies, selective delivery of a drug to the desired site can be readily achieved. However, achieving triggered drug release only at the site of action while ensuring prodrug stability in the general circulation is a challenging task. We designed a novel approach of prodrug activation through enrichment by taking advantage of reaction kinetics, which is directly correlated with concentration. Specifically, we have designed a “Click, Cyclize and Release” (CCR) system for drug delivery using tetrazine-alkyne pairs as a model system to initiate the release cascade. In demonstrating the feasibility of this prodrug system, we prepared prodrugs of doxorubicin conjugated to triphenylphosphonium for targeted enrichment in mitochondria. It was found that indeed, enrichment allowed the proper chemistry to happen, leading to doxorubicin release and thus cytotoxicity. This method should be generally applicable to targeted drug delivery using a variety of targeting molecules.

3.1 Introduction

Prodrug strategies have been widely used to address delivery problems with pharmaceuticals.^{80, 153-160} Essentially all such approaches have one goal, i.e. to deliver the drug to the desired location at a sufficiently high concentration. Prodrug efforts focused on improving physicochemical properties allow for enhanced permeability and solubility. Site-selective activations allow for targeting based on environmental factors such as pH,¹⁶¹⁻¹⁶² unique redox chemistry including levels of H₂O₂¹⁶³⁻¹⁶⁵ glutathione¹⁶⁶⁻¹⁷⁰ and other thiol species,¹⁷¹⁻¹⁷² and

elevated levels of enzymes such as esterases,^{116, 173-174} proteases,¹⁷⁵⁻¹⁷⁷ and phosphatases.¹⁷⁸⁻¹⁷⁹ In addition, gut bacteria also present unique redox chemistry and an active enzymatic environment for site-selective targeting.¹⁸⁰ In recent years, targeted drug delivery has quickly gained attention with some remarkable success,¹⁸¹ especially in the field of cancer with the goal being minimizing toxicity.¹⁸² For example, antibody-drug conjugates allow for targeted delivery of drugs to the desired site.^{181, 183-184} There are many other targeting molecules that can be used to hone in on biomarkers such as the high affinity folate receptor,¹⁸⁵⁻¹⁸⁶ carbohydrate biomarkers,¹⁸⁷ and prostate-specific membrane antigen (PSMA).¹⁸⁸⁻¹⁹⁰ Such targeted approaches work very well in enriching the concentration of the drug conjugates and prodrugs at the desired site. However, targeted release after enrichment is still a significant challenge.

Herein we describe a novel concentration-sensitive platform approach to prodrug activation based on controls by reaction kinetics using bioorthogonal click chemistry, which has been applied in prodrug preparation with excellent success.^{130, 156-157, 191-197} Ideally, one would like to use linker chemistry that tethers the active drug to the targeting molecule in a stable fashion, and allow for selective cleavage at the desired site of action.^{157, 198-201} Through the use of click chemistry and the concept of co-localization,²⁰²⁻²⁰⁴ the linker can be very stable until enrichment-triggered release (ETR). The applicability of the approach is not limited to cell surface as in the case of antibody-mediated delivery because of the use of small molecules for both targeting and cleavage.



Scheme 3.1. General concept of the CCR system.

3.2 Results and Discussions

To establish the proof of concept, we designed a pair of prodrug-release trigger partners that can undergo a bioorthogonal reaction with tunable release rates, which should set the stage for subsequent release of a drug moiety. Specifically, we used the tetrazine-cyclooctyne chemistry as the prodrug-trigger pair for the click reaction,²⁰⁵⁻²⁰⁶ a lactonization reaction of the cycloaddition intermediate (**CI**) for drug release (Scheme 3.1),⁹⁷ and mitochondria-targeting as a way to achieve enrichment, which is discussed later.²⁰⁷ Tetrazines are known to react with transcyclooctene²⁰⁸⁻²⁰⁹ and strained cyclooctyne²⁰⁵⁻²⁰⁶ with second order rate constants ranging from $0.0001\text{ M}^{-1}\text{s}^{-1}$ to more than $1000\text{ M}^{-1}\text{s}^{-1}$. As a proof of principle study, we contemplated a scenario where the prodrug could be used at a concentration of $10\text{ }\mu\text{M}$ in cell culture without cytotoxicity until triggered release is achieved based on control by reaction kinetics. For this design, we desire the second order rate constant to be below $0.25\text{ M}^{-1}\text{s}^{-1}$, which would result in the first half-life being over 100 h without enrichment at $10\text{ }\mu\text{M}$. Triphenylphosphine conjugation is known to enrich its “payload” to about $500\mu\text{M}$ or higher in mitochondria,^{207, 210} which would lead to a decrease in its first half-life to about 2.2 h. What this means is that the prodrug would be non-toxic to cells until enrichment-triggered release. The general idea is presented in Figure 3.1, which depicts a trigger-prodrug pair going through targeted enrichment, reaction kinetics-controlled click reaction, and spontaneous cyclization-based release.

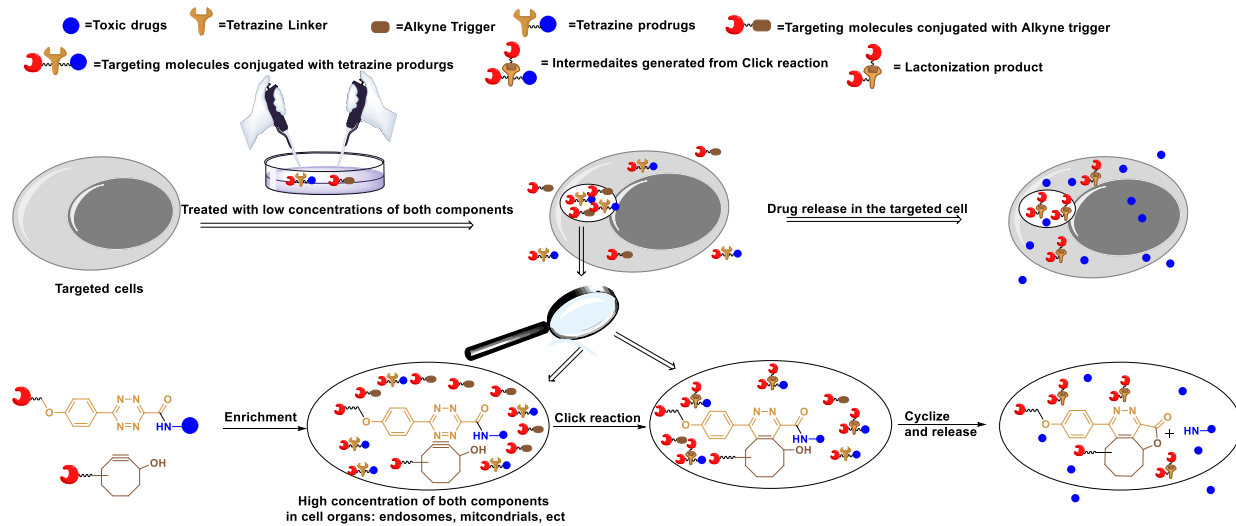
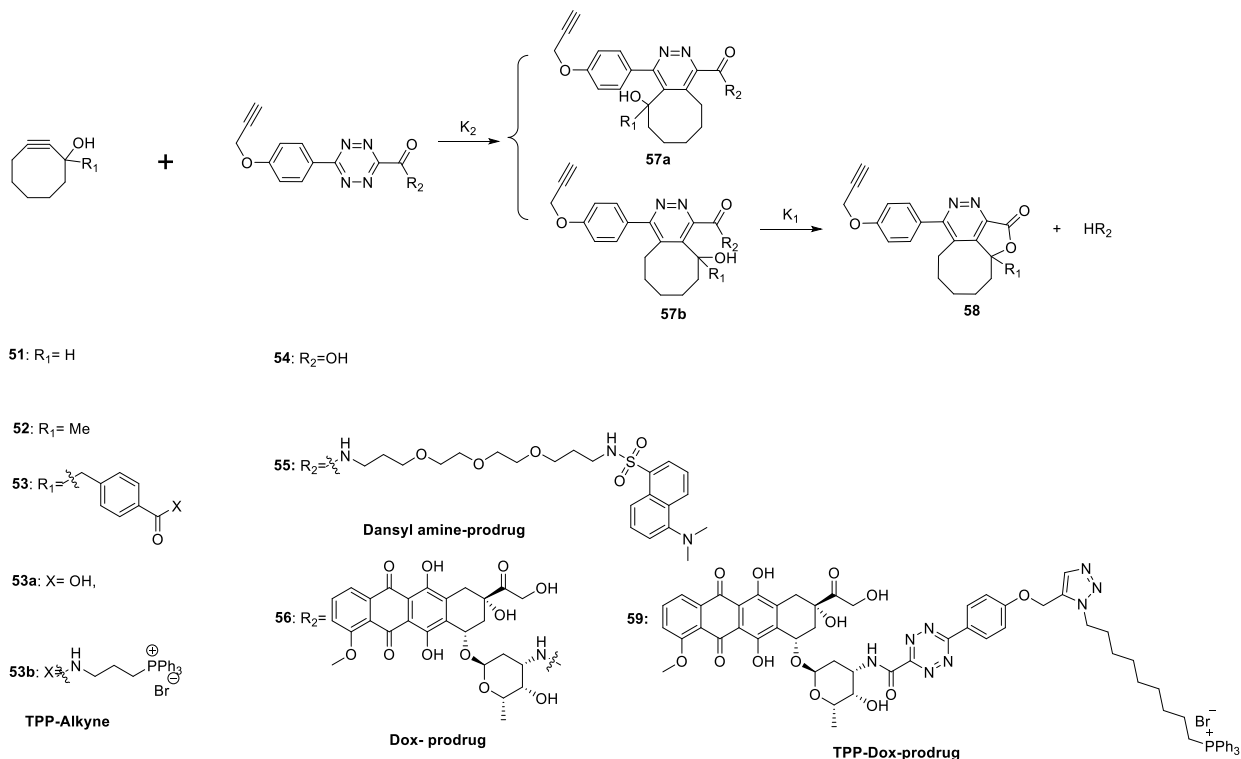


Figure 3.1. General approach for drug release based on reaction kinetics, leading to enrichment triggered release (ETR)

First, we studied the chemical feasibility of the designed system using Dox. Thus, we synthesized the two components of this drug release system: alkyne triggers (AT, **51-53**) with an appropriately positioned hydroxyl group to initiate lactonization, model tetrazine-prodrugs (**TP, 54 and 55**), and tetrazine-linked prodrugs of Dox (**56 and 59**; Table 3.1). The reason that we also prepared a tetrazine conjugate (**55**) with dansyl amine was to take advantage of the strong fluorescence of dansyl amine as a marker to easily monitor and also check feasibility of the click, cyclization and release (CCR) sequence of events for amine containing prodrugs.



*Table 3.1 Evaluation of the reaction kinetics of the CCR system. All reactions were conducted in PBS containing 10% DMSO. *not detectable because of the slow second order reaction and fast lactonization reaction. No intermediates were observed. Δ: not detectable because of Dox decomposition in PBS. ($n = 3, p = 0.95$).*

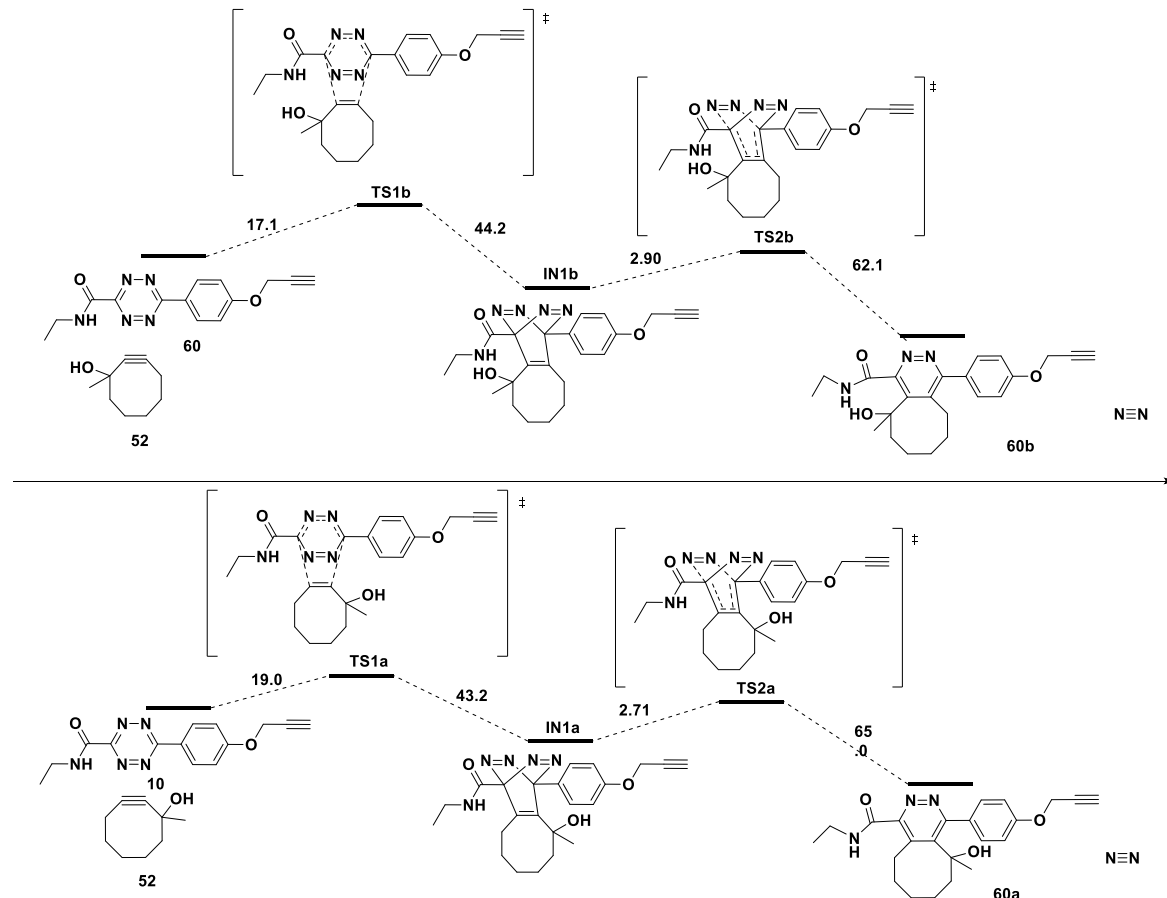
Tetrazine	Alkyne	k_2 at r.t ($M^{-1}s^{-1}$)	k_2 at 37 °C ($M^{-1}s^{-1}$)	k_1 at r.t (h^{-1})	Dox Peak % within 48 h, at r.t (%)
55	51	0.25 ± 0.06	1.9 ± 0.4	0.029 ± 0.006	60 ± 6 (48 h)
	52	0.0075 ± 0.0009	0.021 ± 0.005	*	90 ± 5 (20 h)
	53b	0.042 ± 0.012	0.14 ± 0.04	0.16 ± 0.04	90 ± 3 (16 h)
56	51	0.36 ± 0.07	2.1 ± 0.4	Δ	20 ± 5 (48 h)
	52	0.0078 ± 0.0009	0.025 ± 0.006	*	85 ± 5 (21 h)
	53b	0.065 ± 0.013	0.19 ± 0.04	0.20 ± 0.04	80 ± 5 (18 h)
	53a	0.061 ± 0.013	0.17 ± 0.05	0.21 ± 0.04	80 ± 5 (19 h)

59	53b	0.091±0.013	0.25±0.05	0.22±0.05	78±6 (18 h)
-----------	------------	-------------	-----------	-----------	-------------

As the first step, we studied the basic chemical feasibility of the proposed approach. Thus, we treated 25 μM of the prodrugs **55** or **56** with alkynes **51**, **52** or **53** at different concentrations at room temperature (r.t.) or 37 °C respectively, and monitored prodrug consumption and the release of the parent drug by HPLC (Table 3.1). There are three issues in this study: i.) cycloaddition regiochemistry, ii.) substituent effect at the R₁ position, and iii.) the effect of the “drug” on the reaction rates and regiochemistry.

On the issue of regiochemistry, one can see from Scheme 1 that the cycloaddition chemistry has two possible regiosomeric products, but only one would lead to lactonization and drug release. For the strategy to work, it is critical that the correct regiosomer (**57b**) is the predominant product. Fortunately, it was found that more than 80% Dox or dansyl amine was released within 48 h of the prodrug treatment with alkyne **52** or **53**. Such results indicate that the regiochemistry of the Inverse Electron Demand Diels-Alder reaction (DA_{inv}) is such that it favors the reaction leading to **57b** with the hydroxyl group on the cyclooctyne positioned on the same side of the amide group linked to the parent drug. This allows for subsequent lactonization and drug release. To acquire initial insight into the observed regiochemistry, we performed theoretical calculations. Specifically, we used reported methods to calculate possible transition state(s) and activation energies for two regio-isomers.²⁰⁵ Schematic representations of the energy profiles for the tetrazine alkyne reactions are shown in Scheme 3.2. All of the QM energies are in kcal· mol⁻¹. To simplify the calculation process, we used tetrazine **60** and alkyne **52** as models.²⁰⁵ The results showed that the activation energy for the first step of the DA_{inv} between **60** and **52** via transition state **TS1b** is

17.1 kcal·mol⁻¹ as compared to 19.0 kcal·mol⁻¹ for the reaction via transition state **TS1a**. The qualitative difference in activation energy correlates well with our observed regiochemistry outcome.



Scheme 3.2. Schematic representations of the reaction between tetrazine 60 and alkyne 52 (kcal·mol⁻¹)

There are several reasons that we needed to understand the effect of the R₁ group on the alkyne trigger for this project. First, we are interested in understanding factors that would allow us to tune the reaction rate. It is easy to intuitively understand that the R₁ group would have an effect on both the DA_{inv} reaction and the subsequent lactonization. Second, for eventual applications, we need to conjugate both the tetrazine and alkyne to a targeting moiety. This means that we need a

“handle” for such conjugation chemistry. For the tetrazine part, this can be easily accomplished through the phenolic hydroxyl group. For the cyclooctyne, we need to introduce an additional “handle” for such conjugations. For this reason, the R₁ group is essential as a handle for further conjugation. Thus, we need to understand the substituent effect at this position. It was found that a methyl group or a benzyl group significantly reduced the rate of the DA_{inv} reaction. For example, when R₁ was a hydrogen, the second order rate constant was 0.25 M⁻¹s⁻¹ at r.t and 1.9 M⁻¹s⁻¹ at 37 °C when dansyl amine-prodrug **55** was used. In comparison, the second order rate constant was 0.0075 M⁻¹s⁻¹ and 0.021 M⁻¹s⁻¹ at r.t and 37 °C, respectively, for alkyne **52** with a methyl substituent; and 0.042 M⁻¹s⁻¹ and 0.14 M⁻¹s⁻¹ at r.t and 37 °C, respectively, for alkyne **53** with a phenyl substituent. Such results indicate that the DA_{inv} reaction rates can easily be tuned over a range of more than 30-fold by using different R₁ groups on the alkyne. Additionally, varying the temperature from r.t to 37 °C can afford another 3- to 10-fold of reaction rate variations. Besides, the reaction rate (0.25 M⁻¹s⁻¹) between **59** and **53b** is similar to that for the reaction between **56** and **53a** (0.17 M⁻¹ s⁻¹), confirming that the introduction of the TPP moiety would not significantly affect the reaction kinetics. As discussed earlier, the second order rate constant was targeted to be below 0.25 M⁻¹s⁻¹. The range of second order rate constants that can be tuned falls exactly where needed. It should also be noted that the R₁ substituent accelerated the rate of the lactonization, as expected due to added conformational constraints. Therefore, all the reaction studies thus far clearly demonstrate one thing, i.e., the designed CCR system can be used for prodrug release for the intended purpose.

Regarding the third issue of the effect of the “drug” moiety on the reaction outcomes, it was found that dansylamine-prodrug **55** and Dox-prodrug **56** did not show statistically significant differences in terms of reaction rates. For example, the second order rate constant for the reaction

of alkyne **51** with tetrazine **55** or **56** at 37 °C is 1.9 or 2.1 M⁻¹s⁻¹, respectively. Similarly, the second order rate constant for the reaction of alkyne **53b** with tetrazine **55** or **56** at 37 °C is 0.14 or 0.19 M⁻¹s⁻¹, respectively. Such results are expected since the “drug” portion is positioned away from all reaction centers, and thus would not be expected to have a major effect on reaction rates. The only issue is that if the lactonization rate is slow, it may only lead to partial drug release within a reasonable period of time. This is the case with alkyne trigger **51**. For example, only 60% dansylamine and 20% Dox was detected after treating prodrugs with alkyne **51** (1 mM) for 48 h. This low percentage Dox recovery was likely because of the slow lactonization rate of **57b** ($t_{1/2} = 24$ h) when R₁ was hydrogen, and decomposition of Dox in PBS ($t_{1/2} = 50$ h).²¹¹ In contrast, with alkyne **52**, the lactonization rate was so fast that the HPLC method did not detect the accumulation of the intermediate (CI). This also led to 85-90% release of the active drug at the 48-h point. For alkyne **53**, the situation was similar with 80-90% drug release. All such results indicate the importance of the R₁ group not only for tethering a targeting molecule, but also for an improved lactonization rate.

In addition to the three chemical feasibility issues discussed above, we were also interested in understanding the stability of the tetrazine-linked prodrugs in the presence of high concentrations of thiol species, due to the electron deficient nature of the tetrazine moiety. It is important to note that we did not encounter stability problems.

Next, we were interested in testing the drug delivery system in a cellular environment. We first chose the alkyne **51** and **53b**. HeLa cells were incubated with different concentrations of Dox-prodrug and alkynes, or doxorubicin, for 48 hours at 37 °C. The IC₅₀ values are shown in Table 3.2. After modification, the Dox-prodrug **56** lost its activity with IC₅₀ well over 100 μM, while the IC₅₀ of the parent drug Dox was about 1.0 μM. Such results were expected and desirable

because the activity of the prodrug means that it would not be cytotoxic before Dox is released through the CCR process. As designed, the IC₅₀ of Dox-prodrug **56** is about 1.5 μM in the presence of 50 μM alkyne **51** and 2.0 μM in the presence of 50 μM alkyne **53b**. Such results indicate efficient release of the parent drug, Dox, by alkynes **51** and **53b**.

Table 3.2 IC₅₀ in Hela cell line. (n = 3, p = 0.95)

Compounds	IC ₅₀ (μM)
Dox-prodrug 56	>100
Alkyne 51	>100
Alkyne 53b	>50
Dox	1.0±0.2
Dox-prodrug 56 + 50 μM 51	1.5±0.3
Dox-prodrug 56 + 100 μM 51	1.3±0.2
Dox-prodrug 56 + 50 μM 53b	2.3±0.4
Tetrazine 54 + 100 μM 51	>100

Having established a well-defined release system, we next examined the feasibility of using reaction kinetics to control drug release. Our goal was thus to target and enrich the prodrug at a particular location within the mammalian cell. It is well-known that folic acid, Arg-Asp-Asp (RGD), and many other molecules can target cancer, and be used for drug delivery.²¹² We chose mitochondrion-targeting through the use of a well-known triphenylphosphonium (TPP) moiety, which is known to enrich in mitochondria by approximately 100 to 500 fold.²¹⁰ We elected to use mitochondria targeting because this can easily be assessed in a cell culture system. Thus, we conjugated the tetrazine prodrug and the alkyne trigger with triphenylphosphine to give **59** and

53b, respectively. HeLa cells were treated with 10 μM or 20 μM TPP-alkyne **53b** and various concentrations of TPP-Dox-prodrug **59** (0, 1.2, 2.5, 5 and 10 μM) for 48 hours. It is clear that the IC_{50} ($\sim 1.5 \mu\text{M}$) for TPP-Dox **59** in the presence of 20 μM of TPP-alkyne **53b** is much lower than that of its non-TPP conjugated counterpart Dox prodrug **56** ($\sim 10 \mu\text{M}$) in the presence of 20 μM alkyne **53a** (**Figure 3.2a**). We see a similar trend when the alkyne concentration was decreased to 10 μM . For example, the IC_{50} for TPP-Dox prodrug **59** was about 2 μM in the presence of **53b**, while the IC_{50} for Dox prodrug **56** was well over 10 μM in the presence of 10 μM of the alkyne trigger **53a** (**Figure 3.2b**). As controls, both the IC_{50} values of **59** and **53b** alone are higher than 40 μM , and the treatment of 20 μM of alkyne **53a** or **53b** alone had no effect on cell viability. Such dose-dependent results strongly support the underlying hypothesis that conjugation with TPP (**53b** and **59**) allows for the enhanced release of Dox through enrichment of the prodrug in mitochondria, which subsequently led to an enhanced bimolecular reaction rate and facilitated CCR-mediated activation of the prodrug. Without such an enrichment, the reaction is expected to be slow, resulting in a lower level of active Dox being released. Specifically, the second order rate constant of the reaction between the Dox-prodrug **56** and alkyne **53a** was determined to be $0.17 \text{ M}^{-1}\text{s}^{-1}$, with the first half-life at 10 μM concentration of **56** and 10 μM concentration of **53a** being about 163 h. Such results also mean that only 22% of the drug is released at the 48-h time point. If the concentrations of both the tetrazine prodrug (**59**) and alkyne (**53b**) are enriched to 500 μM in the mitochondria, the first half-life of the reaction would be 2.0 h (confirmed by experiments), which means almost complete Dox release at the 48-h time point. As a consequence, major differences in the apparent potency of the two prodrugs was observed with and without conjugation to TPP. Therefore, we conclude that enrichment in the mitochondria indeed led to triggered release of the

drug, as designed. The same concept is applicable to the delivery of drugs through other targeting approaches such as receptor-mediated drug delivery.

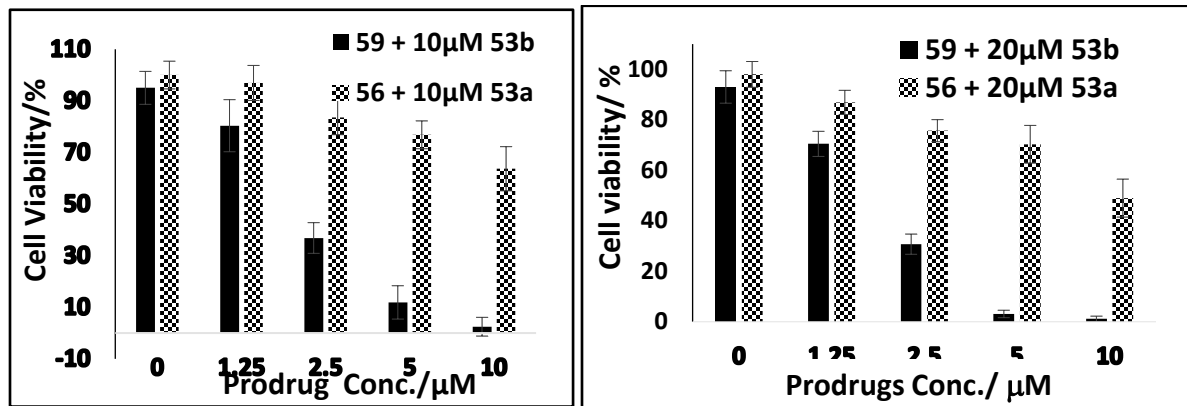


Figure 3.2. Cytotoxicity evaluation of various prodrugs($n = 4$, $p = 0.95$)

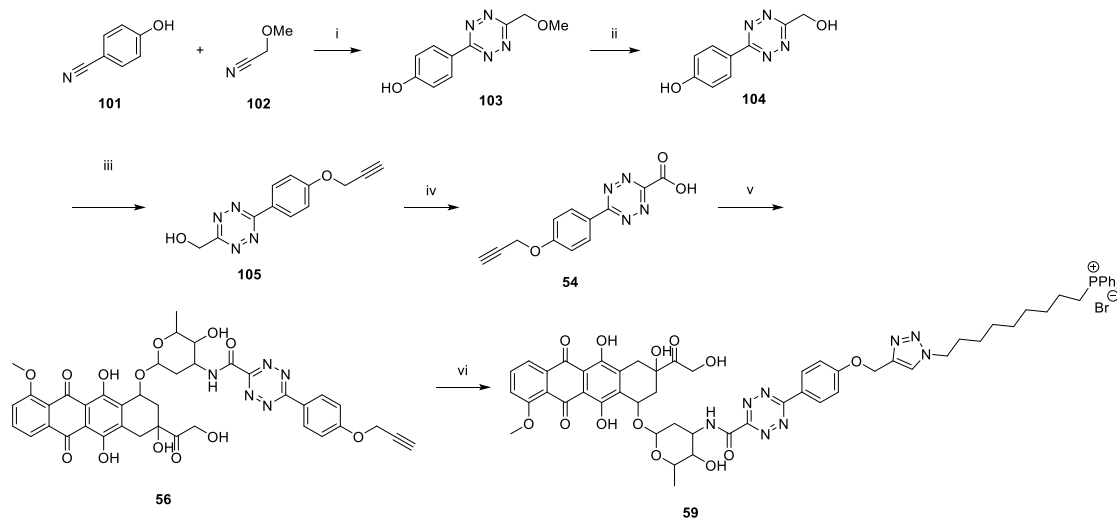
3.3 Conclusion

In conclusion, in targeted therapy, there is a strong need for the development of new chemistry to achieve selective delivery, which would complement existing ones. In this study, we have developed a new concept and a platform approach, which relies on concentration-sensitive chemistry to allow for selective drug release upon enrichment. This is achieved by taking advantage of reaction kinetics, which allows for accelerated cleavage at an elevated concentration. Such an approach will be very useful in delivering small molecules through targeting including the use of antibody drug conjugates and receptor-mediated drug delivery. As a result, the delivery is not limited to cell surface and can be used for sub-cellular delivery, with enriched concentrations, which could not be achieved by ADC based delivery. Collectively, we describe a method that could be leveraged for biologic and medicinal efforts in treating disease.

3.4 Experiment part

General Information. All reagents and solvents were of reagent grade and were purchased from Aldrich. ^1H -NMR (400 MHz) and ^{13}C -NMR (100 MHz) spectra were recorded on a Bruker Avance 400 MHz NMR spectrometer. Mass spectral analyses were performed on an ABI API 3200 (ESI-Triple Quadruple) instrument. HPLC was performed on a Shimadzu Prominence UFC (column: Waters C18 3.5 μM , 4.6 \times 100 mm). UV-Vis absorption spectra were recorded on a Shimadzu PharmaSpec UV-1700 UV-Visible spectrophotometer. Fluorescence spectra were recorded on a Shimadzu RF-5301PC fluorometer. 96-Well plates were read and recorded on a PerkinElmer 1420 multi-label counter.

3.4.1 Synthesis



Reagents and conditions (i). (1) N_2H_4 , $\text{Zn}(\text{OTf})_2$, 60 °C, 24 h, (2) NaNO_2 , H_2O , HCl ; (ii). dichloromethane (DCM), BBr_3 , 0 °C, 0.5 h; (iii) propargyl bromide, acetonitrile, K_2CO_3 , 60 °C, 3 h; (iv). (1) DCM, Dess–Martin periodinane, room temperature (r.t.), 10 min; (2) $\text{NaClO}_2/\text{NaH}_2\text{PO}_4$, 2-methylbut-2-ene, t-BuOH , r.t., 2h; (v). (1) $\text{C}_2\text{O}_2\text{Cl}_2$, DMF, DCM, r.t., (2) NHS , Et_3N , DCM, r.t. 1h (3) Dox, Et_3N , DMF, DCM, r.t.. (vi). $\text{CuSO}_4 \cdot 5\text{H}_2\text{O}$, sodium ascorbate, DMSO , t-BuOH , $\text{N}_3(\text{CH}_2)_9\text{PPh}_3\text{Br}$, TBTA, 6 h r.t.

Scheme 3.3 Synthesis of 59.

*Synthesis of 4-(6-(methoxymethyl)-1,2,4,5-tetrazin-3-yl)phenol (**103**):* To a solution of 4-hydroxybenzonitrile (**101**, 1.785 g, 15.0 mmol) and 2-methoxyacetonitrile (**102**, 3.195 g, 45.0 mmol) in N₂H₄ (13.5 ml) was added Zn(OTf) (1.812 g, 6 mmol). The reaction mixture was stirred at 60 °C for 24 h and cooled down to the room temperature (r.t). Then 40 mL of ethyl acetate (EtOAc), 20mL H₂O, and NaNO₂ (10 g, 145 mmol) were added to the mixture. HCl (10 M, 10 ml) was added slowly to the mixture over a period of 1 h. The reaction mixture was extracted with EtOAc (3 × 40 ml). The combined organic layer was washed with brine (50 mL), and dried over Na₂SO₄. The solvent was removed under reduced pressure to afford the crude product. The final product was obtained as a purple solid by recrystallization with hexane and EtOAc (2.18 g, 67%).
¹H NMR (CD₃OD): δ 8.41 (d, *J* = 8.8 Hz, 2H), 6.96 (d, *J* = 8.8 Hz, 2H), 4.99 (s, 2H), 3.56 (s, 3H).
¹³C NMR (CD₃OD): δ 166.8, 166.0, 163.5, 131.1, 124.0, 117.2, 73.2, 59.6. HRMS (ESI): m/z [M + H]⁺ calcd for C₁₀H₁₁N₄O₂ 219.0882; found, 219.0898.

*Synthesis of 4-(6-(hydroxymethyl)-1,2,4,5-tetrazin-3-yl)phenol (**104**):* To a solution of compound **103** (410 mg, 1.9 mmol) in dichloromethane (DCM, 20 ml) was added BBr₃ solution (1 M, 5 ml, 5.0 mmol) dropwise. The mixture was stirred at 0 °C for 30 min, and then the reaction was quenched with water (20 ml) and extracted with EtOAc (3 × 30 ml). The combined organic phase was dried over Na₂SO₄ and evaporated under reduced pressure. The pure product was achieved by chromatography as a purple solid (230 mg, 60%).
¹H NMR (CD₃OD): δ 8.45 (d, *J* = 8.8 Hz, 2H), 7.00 (d, *J* = 8.8 Hz, 2H), 5.14 (s, 2H).
¹³C NMR (CD₃OD): δ 168.8, 166.1, 163.4, 131.0, 124.2, 117.2, 63.5. HRMS (ESI): m/z [M + H]⁺ calcd for C₉H₉N₄O₂, 205.0726; found, 205.0756.

Synthesis of (6-(4-(prop-2-yn-1-yloxy)phenyl)-1,2,4,5-tetrazin-3-yl)methanol (105): To a solution of compound **104** (230 mg, 1.1 mmol) in acetonitrile (ACN) (10 ml), 3-bromoprop-1-yne (250 mg, 2.1 mmol) and K₂CO₃ (690 mg, 5.0 mmol) were added at r. t. The reaction was stirred at 60 °C for 2 h, cooled down to r.t, quenched with the HCl solution (1M, 10 ml), and then extracted with EtOAc (2 × 50 ml). The combined organic phase was dried over Na₂SO₄ and evaporated under reduced pressure. The pure product was achieved by chromatography as a purple solid (230 mg, 86%). ¹H NMR (CD₃OD): δ 8.46 (d, *J* = 8.8 Hz, 2H), 7.26 (d, *J* = 8.8 Hz, 2H), 5.99 (t, *J* = 6.4 Hz, 1H), 5.02 (d, *J* = 6.4 Hz, 2H), 4.95 (d, *J* = 2.4 Hz, 2H), 3.64 (t, *J* = 2.4 Hz, 1H). ¹³C NMR (CD₃OD): δ 168.0, 163.7, 160.8, 129.5, 124.7, 115.8, 78.8, 78.7, 62.0, 55.8. [M + H]⁺ calcd for C₁₂H₁₁N₄O₂, 243.0882; found, 243.0895.

Synthesis of 6-(4-(prop-2-yn-1-yloxy)phenyl)-1,2,4,5-tetrazine-3-carboxylic acid (54): To a solution of compound **105** (100 mg, 0.41 mmol) in DCM (5 ml) was added Dess–Martin periodinane (260 mg, 0.62 mmol) at r.t. After 20 min, the mixture was loaded into a silica column and eluted with DCM/EtOAc (2/1) to afford a purple solid (98 mg). The solid was dissolved in a solution of *t*-BuOH (3 mL) and 2-methylbut -2-ene (0.5 mL). Then a solution of NaClO₂ (74 mg, 0.82 mmol) in 0.67M NaH₂PO₄ (0.7 mL) was added slowly to the reaction mixture at r.t. After 2 h, the reaction mixture was quenched with HCl (1 M, 10 mL), and extracted with ethyl acetate (2 × 20 mL). The combined organic phase was dried over Na₂SO₄ and then evaporated under reduced pressure to give the crude product, which was purified by column chromatography to yield a purple solid (73 mg, 70%). ¹H NMR (DMSO-D6): δ 8.53 (d, *J* = 8.8 Hz, 2H), 7.29 (d, *J* = 8.8 Hz, 2H), 4.97 (d, *J* = 2.4 Hz, 2H), 3.63 (t, *J* = 2.4 Hz, 1H). ¹³C NMR (DMSO-D6): δ 163.5, 163.2., 161.3,

160.2, 130.2, 124.6, 116.0, 78.9, 78.8, 55.9. $[M + H]^+$ calcd for $C_{12}H_9N_4O_3$, 257.0675, found; 257.0689.

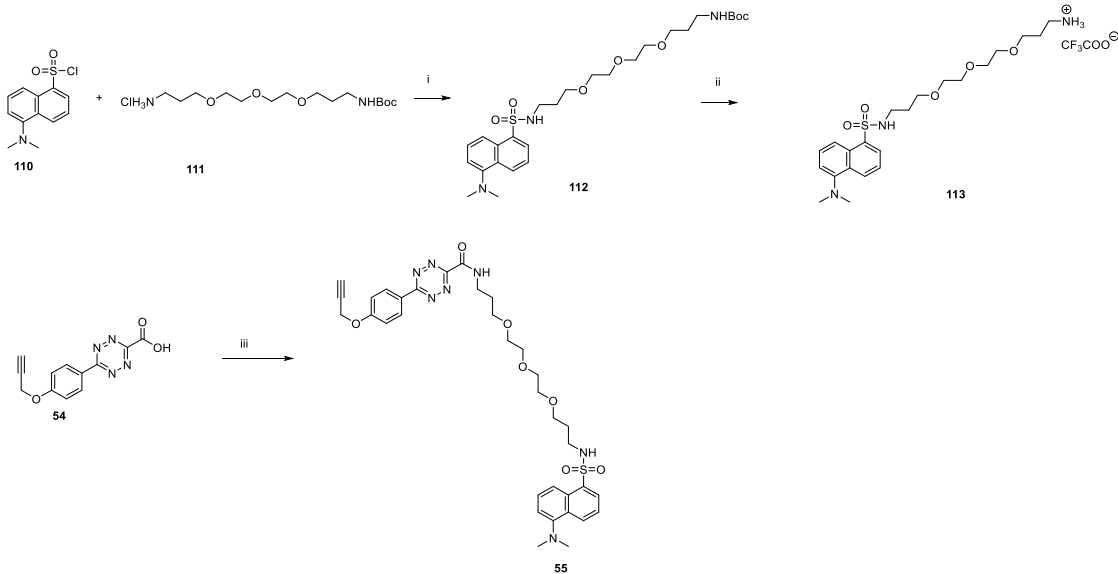
Synthesis of N-(3-hydroxy-2-methyl-6-((3,5,12-trihydroxy-3-(2-hydroxyacetyl)-10-methoxy-6,11-dioxo-1,2,3,4,6,11-hexahydrotetracen-1-yl)oxy)tetrahydro-2H-pyran-4-yl)-6-(4-(prop-2-yn-1-yloxy)phenyl)-1,2,4,5-tetrazine-3-carboxamide (56): To a solution of **54** (32 mg, 0.125 mmol) in 1.5 ml DCM was added oxalyl chloride (32 mg, 0.25 mmol); then DMF (2 μ L) was added. The reaction was stirred at r.t. for 20 min. The solvent was removed by rotavapor. The residue was dissolved in 1 ml DCM. A solution of *N*-hydroxysuccinimide (NHS, 29 mg, 0.25 mmol) in 2 mL DCM was added to the reaction mixture, followed by triethylamine (Et_3N , 16 μ L). The reaction mixture was stirred at r.t. for 1 h; then a solution of doxorubicin hydrochloride (68 mg, 0.125 mmol) in 2 mL DMF was added to the reaction mixture. Then Et_3N (16 μ L) was added to the mixture. The reaction was stirred at r.t. for 20 min and diluted with 20 mL DCM, and washed with H_2O (10 mL) and brine (10 mL). The organic layer was dried over Na_2SO_4 , and then evaporated under reduced pressure to give the crude product, which was purified by column chromatography to yield a red solid (50 mg, 51%). 1H NMR ($CDCl_3$): δ 13.97 (s, 1H), 13.21 (s, 1H), 8.56 (d, $J = 8.8$ Hz, 2H), 8.19 (d, $J = 8.8$ Hz, 1H), 8.00 (d, $J = 8.0$ Hz, 1H), 7.76 (t, $J = 8.0$ Hz, 2H), 7.36 (d, $J = 8.0$ Hz, 2H), 7.13 (d, $J = 8.8$ Hz, 2H), 5.57 (d, $J = 3.2$ Hz, 1H), 5.30 (d, $J = 1.6$ Hz, 1H), 4.80-4.79 (m, 4H), 4.54 (s, 1H), 4.52-4.48 (m, 1H), 4.27 (q, $J = 6.4$ Hz, 1H), 4.05 (s, 3H), 3.84 (d, $J = 5.6$ Hz, 1H), 3.26-3.28 (m 1H), 2.98-3.02 (m, 2H), 2.59 (t, $J = 2.4$ Hz, 1H), 2.42-2.37 (m, 2H), 2.22-1.99 (m, 3H), 1.34 (d, $J = 9.6$ Hz, 3H). ^{13}C NMR ($CDCl_3$): δ 214.0, 187.2, 186.8, 164.9, 162.3, 161.2, 158.7, 157.4, 156.3, 155.8, 135.9, 135.6, 133.8, 133.6, 131.0, 124.1, 121.0

120.0, 118.6, 116.0, 111.8, 111.6, 100.7, 100.1, 77.7, 77.4, 76.8, 76.6, 70.0, 69.3, 67.3, 65.7, 56.8, 56.1, 46.3, 35.8, 34.1, 29.9, 17.0. [M - H]⁻ calcd for C₃₉H₃₄N₅O₁₃. 780.2159. found; 780.2140.

*Synthesis of (9-azidononyl)triphenylphosphonium bromide (**109**)*. To a solution of 1, 9-dibromononane (2 ml, 10 mmol) in toluene (5 ml) was added triphenylphosphine (262 mg). The reaction was stirred at 110 °C for 24 h, and then cooled down to r.t. The solvent was removed under reduced pressure, and the residue was purified by column (DCM/MeOH= 50/1) to afford colorless oil (400 mg). Then the oil was dissolved in ethanol (5 ml), and followed by addition of NaN₃ (325 mg, 5 mmol). The reaction was stirred at 70 °C for 48 h, and cooled down to r.t. The solvent was removed under reduced pressure, and the residue was washed with H₂O (10 ml), and extracted with EtOAc (3 × 20 ml). The combined organic phase was washed with brine (10 ml) and dried over Na₂SO₄, and then evaporated under reduced pressure to give the crude product, which was purified by column chromatography (DCM/MeOH= 20/1) to yield a red solid (300 mg, 62%). ¹H NMR (CDCl₃): δ 7.65-7.85 (m, 15H), 3.78-3.70 (m, 2H), 3.20 (t, J = 7.0 Hz, 2H), 1.46-1.58 (m, 6H), 1.13-1.25 (m, 8H). ¹³C NMR (CDCl₃): δ 135.0 (d, J = 3 Hz), 133.7 (d, J = 10 Hz), 130.5 (d, J = 12 Hz), 118.4 (d, J = 85 Hz), 51.4, 30.4 (d, J = 15 Hz), 29.0, 28.9, 28.8, 26.6, 22.7, 22.6 (d, J = 50 Hz) 22.6, [M - Br]⁺ calcd for C₂₇H₃₃N₃P, 430.2407. found: 430.2406.

*Synthesis of (7-((4-((4-((6-((3-hydroxy-2-methyl-6-((3,5,12-trihydroxy-3-(2-hydroxyacetyl)-10-methoxy-6,11-dioxo-1,2,3,4,6,11-hexahydrotetracen-1-yl)oxy)tetrahydro-2H-pyran-4-yl)carbamoyl)-1,2,4,5-tetrazin-3-yl)phenoxy)methyl)-1H-1,2,3-triazol-1-yl)heptyl)triphenylphosphonium bromide(**59**)*: To a solution of **56** (30 mg, 0.038 mmol), **109** (39

mg, 0.076 mmol), tris[(1-benzyl-1H-1,2,3-triazol-4-yl)methyl]amine (TBTA, 1 mg) in *t*-BuOH (1.5 mL), and DMSO (0.5 mL) was added a solution of CuSO₄ 5H₂O (1 mg) and sodium ascorbate (1.5 mg) in 0.5 mL H₂O. The reaction mixture was stirred at r.t. for 6 h, diluted with DCM (20 mL) and H₂O (10 mL), and extracted with DCM (2 × 20 ml). The combined organic layer was washed with EDTA (20 mM, 10 mL) and brine (10 mL), dried over Na₂SO₄, and then evaporated under reduced pressure to give the crude product, which was purified by column chromatography (DCM/MeOH= 9/1) to yield a red solid (28 mg, 57%). ¹H NMR (DMSO-D6): δ 14.07 (s, 1H), 13.29 (s, 1H), 8.63 (d, J = 8.4 Hz, 1H), 8.48 (d, J = 8.0 Hz, 2H), 8.29 (s, 1H), 7.60-7.90 (m, 18H), 7.33 (d, J = 8.0 Hz, 2H), 5.57 (s, 1H), 5.25-5.30 (m, 3H), 5.20 (d, J = 6.0 Hz, 1H), 4.94-5.02 (m, 1H), 4.89 (t, J = 6.0 Hz, 1H), 4.61 (d, J = 6.0 Hz, 2H), 4.30-4.37 (m, 3H), 3.97 (s, 3H), 3.50-3.60 (m, 2H), 2.94-3.07 (m, 2H), 2.00-2.33 (m, 4H), 1.71-1.78 (m, 4H), 1.41-1.50 (m, 4H), 1.16-1.23 (m, 11H). ¹³C NMR (DMSO-D6): δ 213.9, 186.5, 186.5, 163.9, 162.3, 160.8, 158.9, 158.1, 156.2, 154.6, 142.0, 136.2, 135.5, 134.9 (d, J = 3.0Hz), 134.7, 134.2, 133.6 (d, J = 10 Hz), 133.4, 130.2 (d, J = 12 Hz), 130.2, 124.7, 123.7, 120.0, 119.8, 118.6 (d, J = 85 Hz), 115.9, 110.8, 110.7, 100.1, 75.0, 70.1, 67.8, 66.6, 63.7, 61.5, 56.6, 49.4, 46.0, 36.7, 32.1, 29.8, 29.8, 29.6, 28.5, 28.2, 27.9, 25.7, 21.6(d, J = 4 Hz), 20.2 (d, J = 50 Hz), 17.0. [M - Br]⁺ calcd for C₆₆H₆₈N₈O₁₃P, 1211.4638 found: 1211.4692.



Reagents and conditions: (i) DCM, Et₃N, r.t 1 h; (ii) DCM, TFA, 30 min. r.t.; (iii) (1) C₂O₂Cl₂, DMF, DCM, r.t. 30 min; (2) NHS, Et₃N, DCM, 1 h, r.t., (3) 113, Et₃N, DCM, r.t. 20 min.

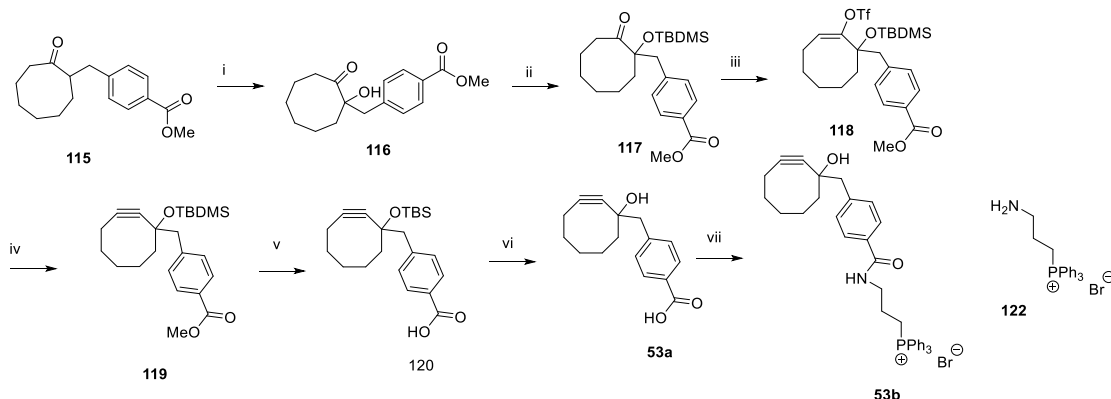
Scheme 3.4 Synthesis of Dansylamine prodrugs.

Synthesis of tert-butyl(3-(2-(2-(3-((5-(dimethylamino)naphthalene)-1-sulfonamido)propoxy)-ethoxy)ethoxy)propyl)carbamate (112). To a solution of dansyl chloride (**110**, 270 mg, 1 mmol) in DCM (2 mL) was add a solution of NH₂-PEG-NHBoc (**111**, 352 mg, 1.1 mmol) and then Et₃N (180 uL). The reaction mixture was stirred at r.t. for 30 min and evaporated under reduced pressure to give the crude product, which was purified by column chromatography (DCM/MeOH= 50/1) to give a yellow oil (590 mg). ¹H NMR (CDCl₃): δ 8.51 (d, J = 8.4 Hz, 1H), 8.31 (d, J = 8.4 Hz, 1H), 8.22 (dd, J₁ = 7.2 Hz, J₂ = 1.2 Hz, 1H), 7.50-7.54 (m, 2H), 7.16 (d, J = 7.6 Hz, 1H), 5.70-5.78 (m, 1H), 4.90-4.98(m, 1H), 3.40-3.65 (m, 12H), 3.13-3.23 (m 2H), 3.02(q, J = 6.4 Hz), 2.87 (s, 6H), 1.65-1.75 (m, 2H), 1.58-1.64 (m, 2H), 1.44 (s, 9H). ¹³C NMR (CDCl₃): δ 156.14 152.0, 135.0, 130.2, 130.0, 129.8, 129.6, 128.3, 123.3, 119.2, 115.2, 78.9, 70.7, 70.7, 70.6, 70.4, 70.2, 70.0, 45.5, 42.2, 38.6, 29.7, 28.8, 28.6. [M +H]⁺ calcd for C₂₇H₄₄N₃O₇S. 554.2894 found: 554.2890.

Synthesis of N-(3-(2-(2-(3-aminopropoxy)ethoxy)ethoxy)propyl)-5-(dimethylamino)naphthalene-1-sulfonamide (113). To a solution of **112** (300 mg) in DCM (2 mL) was added TFA (2 mL) at r.t. The reaction mixture was stirred at r.t for 30 min and then the solvent was evaporated under reduced pressure to give the crude product, which was purified by column chromatography (DCM/MeOH= 10/1) to afford a green oil (292 mg, 95%). ¹H NMR (CDCl_3): δ 8.51 (d, J = 8.4 Hz, 1H), 8.32 (d, J = 8.4 Hz, 1H), 8.21 (dd, J_1 = 7.2 Hz, J_2 = 0.8Hz, 1H), 7.82-7.95 (m, 2H), 7.48-7.56 (m, 2H), 7.18 (d, J = 7.6 Hz, 1H) 6.48-6.55 (m, 1H), 3.55-3.68 (m, 8H), 3.44-3.50 (m, 4H), 3.15-3.22 (m, 2h), 2.95-3.00 (m 2H), 2.88(s, 6H), 1.90-1.95(m, 2H), 1.62-1.69(m, 2H). ¹³C NMR (CDCl_3) δ 151.6, 135.0, 130.2, 129.9, 129.8, 129.5, 128.4, 123.4, 119.5, 115.5, 70.4, 70.4, 70.0, 69.9, 69.8, 69.6, 45.6, 41.7, 40.0, 28.8, 26.4. $[\text{M} + \text{H}]^+$ calcd for $\text{C}_{22}\text{H}_{36}\text{N}_3\text{O}_5\text{S}$ 454.2370 found: 454.2359.

Synthesis of N-(3-(2-(2-(3-((5-(dimethylamino)naphthalene)-1-sulfonamido)propoxy)ethoxy)-ethoxy)propyl)-6-(4-(prop-2-yn-1-yloxy)phenyl)-1,2,4,5-tetrazine-3-carboxamide(55). To a solution of **54** (16 mg, 0.0625 mmol) in 1ml DCM was added oxalyl chloride (16 mg, 0.125 mmol) and DMF (2 μL). The reaction was stirred at r.t for 20 min. Then the solvent was removed by rotavapor. The residue was dissolved in 1 mL DCM. A solution of NHS in 2 mL DCM was added to the reaction mixture, followed by the addition of Et_3N (16 μL). The reaction mixture was stirred at r.t for 1 h; then a solution of dansylamine (96 mg, 0.125 mmol) in 2 mL DCM was added, followed by the addition of Et_3N (32 μL). The reaction was stirred at r.t for 20 min, diluted with 20 mL DCM, and washed with H_2O (10 mL) and brine (10 mL). The organic layer was separated, dried over Na_2SO_4 , and evaporated under reduced pressure. The residue was purified by column (DCM/MeOH= 50/1) to afford a purple solid 25 mg (60%). ¹H

NMR (CDCl_3): δ 8.63 (dd, $J_1 = 6.8$ Hz, $J_2 = 2$ Hz, 2H), 8.55-8.61 (m 1H), 8.49 (d, $J = 8.4$ Hz, 1H), 8.31 (d, $J = 8.4$ Hz, 1H), 8.21 (dd, $J_1 = 7.2$ Hz, $J_2 = 1.2$ Hz, 1H), 7.46-7.54 (m, 2H), 7.18 (dd, $J_1 = 6.8$ Hz, $J_2 = 2$ Hz, 2H), 7.14 (d, $J = 7.2$, 1H), 5.73-5.78 (m, 1H), 4.82 (d, $J = 2.4$ Hz, 2H), 3.64-3.76 (m, 10H), 3.47-3.49 (m 2H), 3.40 (t, $J = 6.4$ Hz 2H), 3.02 (q, $J = 6.0$ Hz, 2H), 2.87 (s, 6H), 2.59 (t, $J = 2.4$ Hz, 1H), 1.92-1.99 (m, 2H), 1.58-1.64 (m, 2H). ^{13}C NMR (CDCl_3): δ 164.9, 162.2, 159.32, 157.8, 152.0, 135.1, 131.0, 130.3, 123.0, 129.8, 129.6, 128.3, 124.3, 123.3, 119.3, 116.0, 115.2, 77.4, 76.5, 70.9, 70.7, 70.6, 70.3, 70.2, 70.1, 56.1, 45.5, 42.3, 39.0, 28.9, 28.7. [M +H]⁺ calcd for $\text{C}_{34}\text{H}_{42}\text{N}_7\text{O}_7\text{S}$, 692.2861 found: 692.2846.



Reagents and conditions: (i) Cs_2CO_3 , $\text{P}(\text{OMe})_3$, DMSO , O_2 , r.t., 24 h; (ii) TBDMSCl , Et_3N , DCM , r.t., 6 h; (iii) (1) KHMDS , THF , -78°C , 1 h; (2) Tf_2NPh , THF , -78°C -r.t., 1 h; (iv) LDA , THF , 0°C , 2.5 h. (v) LiOH , $\text{dioxane}/\text{H}_2\text{O}$ (5:1), 60°C , 3 h; (vi) TBAF , THF , r.t., 2 h; (vii) (1) EDC , NHS , DCM , r.t., 1 h; (2) **122**, DCM , Et_3N , r.t., 3 h.

Scheme 3.5 Synthesis of TPP-Alkyne.

Compound **115**²¹³ and **122**²¹⁴ are known compounds.

*Synthesis of methyl 4-((1-hydroxy-2-oxocyclooctyl)methyl)benzoate (**116**):* To the solution of **115** (4.6 g, 16.8 mmol) in 20 ml of DMSO was added Cs_2CO_3 (821 mg, 2.52 mmol) and $\text{P}(\text{OMe})_3$ (5.2 g, 42 mmol). The reaction was stirred at r.t under O_2 for 24 h, quenched with H_2O

(40 mL), and extracted with EtOAc (2×200 ml). The combined organic phase was dried over Na₂SO₄ and then evaporated under reduced pressure to give the crude product, which was purified by column chromatography to yield a white solid (3.1 g, 64%). ²¹⁵¹H NMR (CDCl₃): δ 7.91 (d, *J* = 8.3 Hz, 2H), 7.18 (d, *J* = 8.3 Hz, 2H), 3.88 (s, 3H), 3.84 (d, *J* = 1.2 Hz, 1H), 2.94 – 2.82 (m, 3H), 2.42 – 2.31 (m, 1H), 2.22–2.27 (m, 1H), 2.00 – 1.86 (m, 2H), 1.83 – 1.54 (m, 4H), 1.47 – 1.20 (m, 2H), 0.98 – 0.78 (m, 1H). ¹³C NMR (CDCl₃): δ 218.1, 167.1, 140.9, 1302, 129.5, 128.9, 81.0, 52.1, 46.3, 36.8, 33.3, 30.5, 25.5, 24.5, 23.0. [M +H]⁺ calcd for C₁₇H₂₃O₄, 291.1591 found: 291.1586.

Synthesis of methyl 4-((1-((tert-butyldimethylsilyl)oxy)-2-oxocyclooctyl)methyl)-benzoate(117). To a solution of **116** (3.1 g, 10.7 mmol) in 50 ml of DCM, was added TBDMSOTf (3.4 g, 12.84 mmol) and Et₃N (1.3 g, 12.84 mmol). The reaction was stirred at r.t for 6 h. Then solvent was evaporated under reduced pressure to give the crude product, which was purified by column chromatography to yield a white solid (1.7 g, 33%). ¹H NMR (CDCl₃): δ 7.91 (d, *J* = 7.2 Hz, 2H), 7.16 (d, *J* = 7.6 Hz, 2H), 3.90 (d, *J* = 1.0 Hz, 3H), 3.05 (d, *J* = 13.6 Hz, 1H), 2.90 (d, *J* = 13.6 Hz, 1H), 2.56 – 2.15 (m, 3H), 1.92 – 1.20 (m, 8H), 1.11 – 1.01 (m, 1H), 0.86 (d, *J* = 0.9 Hz, 9H), 0.05 (s, 3H), -0.12 (s, 3H). ¹³C NMR (CDCl₃): δ 216.3, 167.2, 141.6, 130.8, 129.4, 128.8, 85.1, 52.2, 47.8, 38.7, 35.9, 30.5, 26.6, 25.7, 24.8, 23.4, 19.4, -2.1, -2.4. [M +H]⁺ calcd for C₂₃H₃₇O₄Si, 405.2456 found: 405.2468.

Synthesis of methyl (E)-4-((1-((tert-butyldimethylsilyl)oxy)-2-(((trifluoromethyl)sulfonyl)oxy)cyclooct-2-en-1-yl)methyl)benzoate(118). To a solution of **117**(1.7 g, 4.2 mmol) in 50 ml of THF was added a solution of potassium bis(trimethylsilyl)amide(KHMDS) in THF (0.5 M, 9.2 ml) over a period of 10 min under the protection of argon at -78 °C. The reaction was stirred

at -78 °C for 1 h, and a solution of *N*-phenyl-bis(trifluoromethanesulfonimide) (Tf_2NPh , 1.6 g, 4.62 mmol) in 20 ml of THF was added slowly over 10 min. The reaction was stirred for another 10 min at -78 °C, then warmed to r.t, and then stirred for another 30 min. The solvent was removed by a rotavapor and the residue was purified by chromatography to give a colorless oil (1.0 g, 47%). ^1H NMR (CDCl_3): δ 7.93 (d, J = 8.1 Hz, 2H), 7.22 (d, J = 8.1 Hz, 2H), 5.57 (t, J = 9.4 Hz, 1H), 3.91 (s, 3H), 3.36 (d, J = 12.4 Hz, 1H), 2.91 (d, J = 12.4 Hz, 1H), 1.69-2.01 (m, 6H), 1.53 – 1.32 (m, 4H), 0.96 (s, 9H), 0.27 (m, 6H). ^{13}C NMR (CDCl_3) δ 167.1, 152.3, 141.6, 130.5, 129.4, 128.7, 120.5, 118.6 (q, J = 317 Hz), 80.1, 52.2, 35.9, 26.5, 25.4, 23.5, 23.4, 22.1, 19.0, -1.3, -1.5. [M +H]⁺ calcd for $\text{C}_{24}\text{H}_{36}\text{F}_3\text{O}_6\text{SSi}$, 537.1948 found: 537.1970.

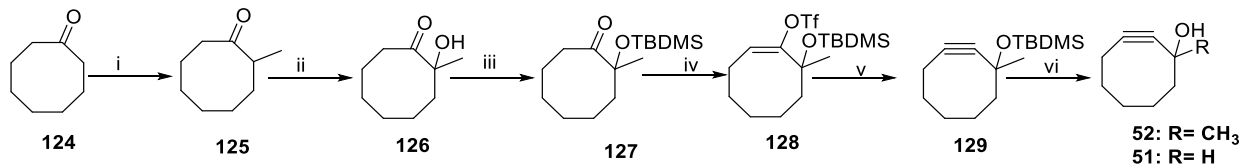
Synthesis of methyl 4-((1-((tert-butyldimethylsilyl)oxy)cyclooct-2-yn-1-yl)methyl)benzoate(119) To a solution of **118** (450 mg, 0.84 mmol) in 10 ml of THF was added a solution of LDA in THF (2M, 0.53 ml) drop-wise over a period of 2.5 h under the protection of argon at 0 °C. Then the reaction was quenched with H_2O (40 mL), and extracted with ethyl acetate (2×50 ml). The combined organic phase was dried over Na_2SO_4 and then evaporated under reduced pressure to give the crude product, which was purified by column chromatography to yield a colorless oil (200 mg, 62%). ^1H NMR (CDCl_3): δ 7.93 (d, J = 8.0 Hz, 2H), 7.37 (d, J = 8.0 Hz, 2H), 3.89 (s, 3H), 2.97 (d, J = 13.0 Hz, 1H), 2.78 (d, J = 13.0 Hz, 1H), 1.36-2.32 (m, 10H), 0.83 (s, 9H), 0.12 (s, 3H), -0.26 (s, 3H). ^{13}C NMR (CDCl_3): δ 167.6, 143.6, 131.2, 129.0, 128.3, 99.5, 94.9, 75.9, 52.1, 52.0, 48.3, 34.5, 30.1, 27.2, 26.1, 20.7, 18.3, -2.7, -3.6. [M +H]⁺ calcd $\text{C}_{23}\text{H}_{35}\text{O}_3\text{Si}$ 387.2350 found: 387.2365.

Synthesis of *4-((1-((tert-butyldimethylsilyl)oxy)cyclooct-2-yn-1-yl)methyl)benzoic acid (120)*. To a solution of **119** (100 mg, 0.26 mmol) in dioxane (3 mL) and H₂O (0.75 mL) was added finely crushed LiOH (200 mg, 8.3 mmol). The suspension was heated to 50 °C and then stirred for 3 h. The dioxane was removed on a rotary evaporator and the reaction mixture was diluted with DCM (20 mL). The organic layer was washed with 1 N HCl (2 × 10 mL), H₂O (3 x 10 mL), and brine (1 × 10 mL), and dried over Na₂SO₄, yielding a white solid (86 mg 89%). ¹H NMR (CDCl₃): δ 8.02 (d, J = 8.0 Hz, 2H), 7.42 (d, J = 8.0 Hz, 2H), 3.00 (d, J = 13Hz, 1H), 2.82 (d, J = 13Hz, 1H), 2.05- 2.28 (m, 2H), 1.51-2.01 (m, 6H), 1.26-1.50 (m, 2H), 0.84 (s, 9H), 0.13 (s, 3H), -0.25 (s, 3H) ¹³C NMR (CDCl₃): δ 172.4, 144.6, 131.3, 129.6, 127.4, 99.6, 94.6, 75.7, 52.1, 48.4, 34.5, 30.1, 27.2, 26.0, 20.7, 18.2, -2.7, -3.6. [M +H]⁺ calcd C₂₂H₃₃O₃Si 373.2193 found: 373.2204.

Synthesis of *4-((1-hydroxycyclooct-2-yn-1-yl)methyl)benzoic acid (53a)*. To a solution of **120** (68 mg, 0.18 mmol) in 0.2 ml of THF was added tetra-*n*-butylammonium fluoride (TBAF) solution (2M in THF/hexane, 1 mL). The reaction was stirred at r.t for 2 h, and then the solvent was removed under reduced pressure. The residue was purified by chromatography (DCM/EtOAc=2/1) to give a white sticky solid (46 mg, 99%). ¹H NMR (CDCl₃): δ 8.03 (d, J = 8.0 Hz, 2H), 7.44 (d, J = 8.0 Hz, 2H), 3.01 (d, J=13 Hz, 1H), 2.88 (d, J=13 Hz, 1H), 2.08-2.21(m, 3H), 1.72-2.03 (m, 6H), 1.36-1.44 (m, 1H). ¹³C NMR (CDCl₃): δ 172.0, 143.6, 130.7, 130.1, 127.9, 100.5, 94.4, 74.4, 50.7, 46.9, 34.5, 29.9, 26.5, 20.7. [M +H]⁺ calcd C₁₆H₁₉O₃ 259.1329 found: 259.1325.

Synthesis of *(3-(4-((1-hydroxycyclooct-2-yn-1-yl)methyl)benzamido)propyl)-triphenylphosphonium bromide (53b)*. To a solution of **53a** (38 mg, 0.15 mmol) in DCM, was

added *N*-(3-dimethylaminopropyl)-*N*-ethylcarbodiimide hydrochloride (EDC 42 mg, 0.225 mmol) and NHS (35 mg, 0.3 mmol). The reaction was stirred at r.t for 1 h, diluted with DCM (10 mL), and then washed with H₂O (5 mL) and brine (5 mL). The organic phase was dried over Na₂SO₄, and evaporated under reduced pressure to afford a white solid. The solid was dissolved in 2mL DCM, followed by the addition of a solution of **122** (90 mg, 0.225 mmol) in 2mL DCM. Then Et₃N (30 mg, 0.3 mmol) was added into the reaction mixture. The reaction was stirred at r.t for 3 h, and diluted with DCM (15 mL). The organic layer was washed with H₂O (5 mL) and brine (5 mL), dried over Na₂SO₄, and evaporated under reduced pressure to afford the crude product, which was purified by chromatography (DCM/MeOH =10/1) to give a white solid (57 mg, 60 %). ¹H NMR (CDCl₃): δ 9.43 (t, J = 6.0 Hz, 1H), 8.14 (d, J = 8.0 Hz, 2H) 7.69-7.74 (m, 9H), 7.56-7.61 (m, 6H), 7.39 (d, J = 8.0 Hz, 2H), 3.89-3.82 (m, 2H), 3.71-3.70 (m, 2H), 2.97 (d, J=13 Hz, 1H), 2.82 (d, J=13 Hz, 1H), 2.16 (t, J = 6.0 Hz, 2H), 2.12-1.67 (m, 10H), 1.43-1.38 (m, 1H). ¹³C NMR (CDCl₃): δ 167.8, 140.6, 135.1 (d, J = 3 Hz), 133.5 (d, J = 10 Hz), 132.4, 130.6, 130.6 (d, J = 12 Hz), 127.9, 118.4 (d, J = 85 Hz), 100.1, 99.7, 94.9, 74.3, 50.8, 46.9, 39.4 (d, J = 17 Hz), 34.6, 30.0, 26.7, 22.6 (d, J = 4 Hz), 20.7, 20.6 (d, J = 52 Hz). [M +H]⁺ calcd : C₃₇H₃₉NO₂P, 560.2713 found: 560.2717



Reagents and conditions: (i) 1) LDA, THF, -78 °C, 1h; 2) methyl iodide, THF, r.t, 40 min; (ii) Cs₂CO₃, P(OEt)₃, DMSO, O₂ (1.0 atm), r.t, 36 h; (iii) TBDMSCl, Et₃N, DCM, r.t, 6 h; (iv) 1) KHMDS, THF, 46 °C, 1 h; 2) Tf₂NPh, THF, r.t, 1 h; (v) LDA, THF, 0 °C, 2.5 h, 89%; (vi) TBAF, THF, r.t, 2 h.

Scheme 3.6 Synthesis of Alkyne 52.

Compound **124** is commercially available, and compound **51**²¹⁶ is a known compound.

*Synthesis of 2-methylcyclooctan-1-one (**125**)*. To a solution of cyclooctanone (**124**, 3.2g, 25.3 mmol) in 50 ml of THF, a solution of LDA in THF (2M, 15.1 mL) was added dropwise under the protection of argon at -78 °C. The reaction was stirred at -78 °C for 1 h, and then methyl iodide (1.6 ml, 25.7 mmol) was added slowly over 10 min. The reaction was stirred for another 30 min after being warmed to r.t. The solvent was removed on a rotavapor, and the residue was purified by chromatography to give a colorless oil (1.9 g, 56%). ¹H NMR (CDCl₃): δ 2.63-2.52 (m, 1H), 2.43-2.30 (m, 2H), 1.33-1.95 (m, 9H), 1.25-1.12 (m, 1H), 1.01 (d, *J*=6.8 Hz, 3H). ¹³C NMR (CDCl₃): δ 220.4, 45.3, 40.4, 33.1, 26.9, 26.6, 25.7, 24.6, 16.6. [M +H]⁺ calcd: C₉H₁₇O 141.1274 found: 141.1286

*Synthesis of 2-hydroxy-2-methylcyclooctan-1-one (**126**)*. The mixture of **125** (1.9 g, 13.5 mmol), Cs₂CO₃ (1.3 g, 4.0 mmol) and P(OEt)₃ (6.9 ml, 40.5 mmol) in 20 ml of DMSO was stirred at r.t under O₂ for 36 h. Then the reaction was quenched with H₂O (40 mL), and extracted with EtOAc (2 × 200 ml). The combined organic phase was dried over Na₂SO₄ and then evaporated under reduced pressure to give the crude product, which was purified by column chromatography to yield a colorless liquid (0.75 g, 35%). ¹H NMR (CDCl₃): δ 3.91 (s, 1H), 2.83-2.72 (m, 1H), 2.35-2.24 (m, 2H), 1.99-1.83 (m, 2H), 1.82-1.67 (m, 3H), 1.67-1.56 (m, 1H), 1.39-1.28 (m, 2H), 1.27 (s, 3H), 0.96-0.83 (m, 1H). ¹³C NMR (CDCl₃): δ 219.8, 77.8, 35.8, 34.4, 30.3, 27.4, 25.4, 24.3, 23.1. [M +Na]⁺ calcd: C₉H₁₆NaO₂, 179.1048 found: 179.1055.

Synthesis of 2-((tert-butyldimethylsilyl)oxy)-2-methylcyclooctan-1-one (127). To a solution of **126** (0.75 g, 4.8 mmol) in 50 ml of DCM were added TBDMsOTf (1.6ml, 7.2 mmol) and Et₃N (0.73 ml, 5.3 mmol). The reaction was stirred at r.t for 6 h before solvent evaporation under reduced pressure to give the crude product, which was purified by column chromatography to yield a white solid (0.42 g, 33%). ¹H NMR (CDCl₃): δ 2.71-2.61 (m, 1H), 2.44-2.35 (m, 1H), 2.08-1.99 (m, 1H), 1.96-1.78 (m, 3H), 1.77-1.54 (m, 1H), 1.53-1.37 (m, 2H), 1.37-1.29 (m, 5H), 0.90 (s, 9H), 0.14 (d, J = 6.7 Hz, 6H). ¹³C NMR (CDCl₃): δ 217.4, 80.8, 38.6, 36.9, 29.3, 26.2, 25.9, 25.6, 24.6, 23.1, 18.5, -2.3, -2.6. [M +Na]⁺ calcd: C₁₅H₃₀NaO₂Si, 293.1913 found: 293.1913.

Synthesis of (E)-8-((tert-butyldimethylsilyl)oxy)-8-methylcyclooct-1-en-1-yl trifluoromethanesulfonate (128). To a solution of **127** (0.42 g, 1.58 mmol) in 50 ml of THF was added a solution of KHMDS in THF (0.5 M, 3.4 mL) slowly over 10 min under the protection of argon at -78 °C. After the reaction was stirred at -78 °C for 1 h, a solution of Tf₂NPh, (0.62 g, 1.73 mmol) in 10 ml of THF was added slowly over 10 min. The reaction was stirred for another 1 h after warming to r.t. The solvent was removed on a rotavapor and the residue was purified by column chromatography to give a colorless oil (0.32 g, 50%). ¹H NMR (CDCl₃): δ 6.18 (dd, J=12.8, 4.7 Hz, 1H), 2.65-2.47 (m, 1H), 2.30-2.20 (m, 1H), 2.11-1.99 (m, 1H), 1.92-1.65 (m, 4H), 1.57-1.42 (m, 4H), 1.24-1.08 (m, 1H), 0.95 (s, 9H), 0.84-0.71 (m, 1H), 0.15 (d, J = 6.6 Hz, 6H). ¹³C NMR (CDCl₃): δ 155.5, 118.6 (q, J = 318 Hz), 118.0, 76.6, 40.1, 28.8, 26.3, 26.2, 23.7, 23.5, 22.1, 18.7, -2.0, -2.0. [M +H]⁺ calcd: C₁₆H₃₀F₃O₄SSi, 403.1586; found 403.1575.

Synthesis of tert-butyldimethyl((1-methylcyclooct-2-yn-1-yl)oxy)silane (129). To a solution of **128** (0.32, 0.80 mmol) in 10 ml of THF, a solution of LDA in THF (2 M, 0.8 ml) was added

drop-wise over a period of 20 minutes under the protection of argon at 0 °C. After being warmed to r.t., the reaction was quenched with H₂O (10 mL), and extracted with ethyl acetate (2 × 30 ml). The combined organic phase was dried over Na₂SO₄ and then evaporated under reduced pressure to give the crude product, which was purified by column chromatography to yield a colorless oil (179 mg, 89%). ¹H NMR (CDCl₃): δ 2.29-2.10 (m, 2H), 2.08-1.98 (m, 1H), 1.92-1.82 (m, 3H), 1.80-1.68 (m, 2H), 1.61-1.51 (m, 2H), 1.36 (s, 3H), 0.88 (s, 9H), 0.19 (d, J=16.6Hz, 6H). ¹³C NMR (CDCl₃): δ97.7, 96.8, 71.9, 53.9, 34.8, 30.2, 29.6, 27.1, 25.9, 20.8, 18.1, -3.0, -3.0. [M +H]⁺ calcd: C₁₅H₂₉OSi, 253.1988, found: 253.1972

Synthesis of *1-methylcyclooct-2-yn-1-ol (52)*. To a solution of **129** (179 mg, 0.71 mmol), TBAF (1 M, 2.1 ml) was added. After stirring at r.t. for 2 h, the solvent was removed under reduced pressure and was purified by chromatography to give a colorless oil (51 mg, 52%). ¹H NMR (CDCl₃): δ2.29-2.12 (m, 2H), 2.10-2.01 (m, 1H), 1.99-1.75 (m, 5H), 1.74-1.61 (m, 2H), 1.58-1.47 (m, 1H), 1.42(s, 3H). ¹³C NMR (CDCl₃): δ 98.3, 96.1, 70.9, 52.5, 34.7, 30.0, 28.2, 27.0, 20.7. M +H]⁺ calcd: C₉H₁₅O, 139.1117 found 139.1109.

3.4.2 Kinetic studies of the CCR system

Stock solution preparation.

Each of the tetrazine prodrugs (compounds **55**, **56** and **59**) was dissolved in DMSO to afford a 500-μM stock solution. Each of the alkynes (compounds **51**, **52**, **53a** and **53b**) was dissolved in DMSO to afford a 50-mM stock solution. Doxorubicin (Dox) and dansylamino compound (DA) **113** were each dissolved in DMSO to afford 1mM stock solutions

HPLC method A: mobile phase A (10 mM NaH₂PO₄ in water, pH = 5.0) and mobile phase B (ACN), flow rate: 1 mL/min, running time: 30 min, the gradient elution method: 25% B from 0 to 6 min, 25% to 50 % B from 6 to 8 min, 50% B from 8 to 15 min, 50% to 99% B from 15 to 20 min, 99% B from 20 to 25 min, 99% to 25% B from 25 to 30 min. Detection wavelength: 256 nm. Column: Waters C18 3.5 μ M, 4.6 \times 100 mm. Injection volume: 20 μ L.

HPLC method B: mobile phase A (10 mM NaH₂PO₄ in water, pH = 5.0) and mobile phase B (ACN), flow rate: 1 mL/min, running time: 30 min, the gradient elution method: 30% B from 0 to 6 min, 30% to 50 % B from 6 to 8 min, 50% B from 8 to 15 min, 50% to 99% B from 15 to 20 min, 99% B from 20 to 25 min. 99% to 30 % B from 25 to 30 min. Detection wavelength 1: 256, detection wavelength 2: 337 nm. Column: Waters C18 3.5 μ M, 4.6 \times 100 mm. Injection volume: 20 μ L.

Standard curve of Dox concentration measurement.

To four HPLC vials containing 0.9 mL PBS (size: 1.5 mL) were added 25, 15, 20, 10 μ L Dox stock solution (1 mM) respectively. Then defined amounts DMSO (975, 985, 980, and 990 μ L) were added to each vial to afford final concentration of four vials were 25, 15, 20, 10 μ M in PBS (10% DMSO), respectively. The samples were analyzed with HPLC method A. Dox retention time: 4.0 min.

Standard curve for DA concentration measurement.

To four HPLC vials containing 0.9 mL PBS (size: 1.5 mL) were added 25, 15, 20, 10 μ L Dox stock solution (1 mM) respectively. Then defined amounts DMSO (975, 985, 980, and 990 μ L) were added to each vial to afford final concentration of four vials were 25, 15, 20, 10 μ M in PBS (10% DMSO), respectively. The samples were analyzed with HPLC method B. DA retention time: 5.8 min.

General procedures HPLC studies of reaction kinetic.

To three 20-ml vials with 9 mL PBS were added a solution of tetrazine prodrug (500 μ L, 500 μ M). 350 μ L, 300 μ L and 250 μ L DMSO were added to vial respectively, and then 150 μ L, 200 μ L and 250 μ L of the alkyne solution (50 mM in DMSO) were added to the vials to afford final concentrations of alkyne 0.75 mM, 1 mM and 1.25 mM in PBS (10% DMSO, 25 μ M prodrug) respectively. The reaction was stirred at r.t or 37 °C respectively. Every 30 min about 500 μ L reaction mixtures were taken out and 20 μ L of them were injected into the HPLC by the autosampler; the rest of them were poured back to the reaction mixture. (Note: In the cases of prodrugs **55** or **56** reacting with alkyne **51** at 37 °C, the final concentrations of **51** in the kinetic studies were 250 μ M, 300 μ M and 350 μ M).

Table 3.3 Retention time from the kinetic studies

Method	Prodrugs	Alkyne	Prodrugs retention time (min)	Dox/DA retention time (min)	Intermediates retention time (min)
A	6	1	13.7	3.9	13.9/14.5
		2	13.7	3.9	NO
		3a	13.7	4.0	18.5
		3b	13.7	4.0	22.8
	9	3b	11.0	4.0	23.1
B	5	1	11.7	5.7	11.5/12.1
		2	11.7	5.7	no
		3b	11.7	5.7	23.5

Determination of second-order rate constants:

The reaction rate constant, k_{obs} , was calculated for each concentration of the alkyne by fitting the prodrug areas versus time using eq. 1

$$Y = A \exp(-k_{\text{obs}}t) \text{ eq. 1}$$

Where Y is the prodrug area, and t is time. The pseudo-first-order rate constant, k_{obs} , was then plotted against the concentration of alkyne to yield the second-order rate constant using eq 2.

$$k_{\text{obs}} = k_2[\text{Alkyne}] \text{ eq. 1}$$

where k_2 is the second-order rate constant. The results are shown in Table 3.4.

Table 3.4 K_{obs} table from the kinetic studies.

Temp.	Prodrugs(25 μM)	Alkyne	Concentratio n of Alkyne (mM)	Expt. 1	Expt. 2	Expt. 3
				$K_{\text{obs}} (\text{h}^{-1})$		
r.t	55	51	0.75	0.752	0.704	0.756
		51	1.00	0.980	0.802	1.01
		51	1.25	1.20	1.10	1.26
37 °C	55	51	0.25	1.82	1.64	1.90
		51	0.3	2.15	1.94	2.26
		51	0.35	2.53	2.25	2.65
r.t	55	52	0.75	0.0203	0.0201	0.0217
		52	1.00	0.0273	0.0269	0.0289
		52	1.25	0.0339	0.0324	0.0359
37 °C	55	52	0.75	0.0506	0.0584	0.0599
		52	1.00	0.0670	0.0781	0.0801
		52	1.25	0.083	0.0978	0.101

r.t	55	53b	0.75	0.125	0.115	0.13
		53b	1.00	0.155	0.148	0.175
		53b	1.25	0.199	0.180	0.22
37 °C	55	53b	0.75	0.411	0.388	0.353
		53b	1.00	0.548	0.511	0.453
		53b	1.25	0.695	0.636	0.561
r.t	56	51	0.75	0.894	0.976	0.993
		51	1.00	1.18	1.30	1.34
		51	1.25	1.47	1.62	1.69
37 °C	56	51	0.25	1.90	1.81	1.97
		51	0.3	2.28	2.15	2.38
		51	0.35	2.65	2.48	2.78
r.t	56	52	0.75	0.0202	0.0209	0.0207
		52	1.00	0.0282	0.0262	0.0278
		52	1.25	0.0353	0.0341	0.0344
37 °C	56	52	0.75	0.0607	0.0671	0.0696
		52	1.00	0.0798	0.0895	0.0941
		52	1.25	0.0986	0.112	0.119
r.t	56	53b	0.75	0.201	0.195	0.197
		53b	1.00	0.261	0.257	0.261
		53b	1.25	0.309	0.318	0.326
37 °C	56	53b	0.75	0.486	0.503	0.533
		53b	1.00	0.635	0.672	0.622

		53b	1.25	0.783	0.846	0.905
r.t	56	53a	0.75	0.183	0.191	0.185
		53a	1.00	0.235	0.246	0.247
		53a	1.25	0.289	0.295	0.307
37 °C	56	53a	0.75	0.418	0.438	0.495
		53a	1.00	0.546	0.598	0.678
		53a	1.25	0.673	0.739	0.857
r.t	59	53b	0.75	0.296	0.305	0.291
		53b	1.00	0.331	0.356	0.359
		53b	1.25	0.445	0.465	0.474
37 °C	59	53b	0.75	0.711	0.701	0.714
		53b	1.00	0.921	0.902	0.871
		53b	1.25	1.21	1.15	1.09

General procedure for the determination of the lactonization rate constants.

To a 9 mL PBS in a 20-mL vial was added a solution of the respective tetrazine prodrug (500 µL, 500 µM). Then 1 mL of the respective alkyne (50 mM in DMSO) was added to afford a final concentration of 5 mM in PBS (15% DMSO). The reaction was stirred at r.t. Every 30 min about 500 µL the reaction mixture was taken out and 20 µL of them was injected into the HPLC by an autosampler; the rest of them was poured back to the reaction mixture. The reaction rate constant, k_1 , was determined by fitting the area in HPLC chromatogram of the intermediate versus time using eq. 3.

$$Y = A \exp(-k_1 t) \text{ eq. 3}$$

Where Y is the intermediate areas, and t is the time. The results are shown in Table 3.5.

Table 3.5 Lactonization rate constants

Tetrazines prodrugs	Alkyne	First point time*	k ₁ (h ⁻¹)		
			Expt 1	Exp 2	Expt. 3
55	51	1 h	0.0253	0.0291	0.0332
55	53b	4 h	0.162	0.184	0.142
56	53b	4 h	0.223	0.179	0.196
56	53a	4 h	0.185	0.206	0.229
59	53b	4h	0.225	0.191	0.265

*: The time point that more than 90% prodrug were consumed. .

General procedure of prodrug stability studies.

To a 9.5 mL of PBS or 1 mM cysteine solution in PBS in a 20-mL vial was added a solution of tetrazine prodrug (500 μL, 500 μM). The solution was stirred at r.t. or 37 °C for 24 h. The reaction solution was injected into HPLC, and analyzed with Method A for prodrugs **56** and **59**, and Method B for prodrug **55**.

Prodrug (**55** or **56**, 25 μM in PBS alone or in the presence of 1 mM cysteine (Cys) in PBS) was incubated at r.t or 37 °C for 24 h. Then HPLC was used to monitor the concentration of the remaining prodrug (Table 3.6). (Note: there are literature reports of Dox decomposition by itself²¹¹).²¹⁷

Table 3.6 Stability studies of prodrugs 55 and 56 in PBS. (5% DMSO, n = 4, p = 0.95).

Prodrugs remaining	24 h in PBS at r.t (%)	24 h in PBS at 37 °C (%)	24 h in PBS with 1mM 1mM Cys at r.t (%)	24 h in PBS with 1mM Cys at 37 °C (%)

555	91±5	85±5	88±5	81±5
56	85±5	78±5	80±5	76±5

3.4.3 Cell culture

Hela cells (ATCC) were used in the studies. Hela cells were maintained in DMEM (Dulbecco's Modified Eagle's Medium) supplemented with 10% fetal bovine serum (MidSci; S01520HI), and 1% penicillin-streptomycin (Sigma-Aldrich; P4333) at 37 °C with 5% CO₂.

3.4.3.1 Studies of cytotoxicity

Test compound was dissolved in DMSO to afford a stock solution. The final concentration of DMSO in cell culture was 1% (v/v) in PBS. Hela cells were seeded in 96-well plates one day before the experiment. Different concentrations of prodrug was added into the cell culture. The cells were then incubated for 48 h at 37 °C with 5% CO₂. The cell viability was tested by the MTT assay.²¹⁸ Specifically, after 48 h of incubation, 5 mg/mL MTT (3-(4, 5-dimethylthiazol-2-yl)-2, 5-diphenyltetrazolium bromide) was added into the cell culture. After incubation for 4 h, the supernatant was removed and 100 µL DMSO was added into the wells containing the cells. After shaking gently for 3 min, absorbance at 605 nm was read by a plate reader. Some of the result were shown in Figure 3. 3.

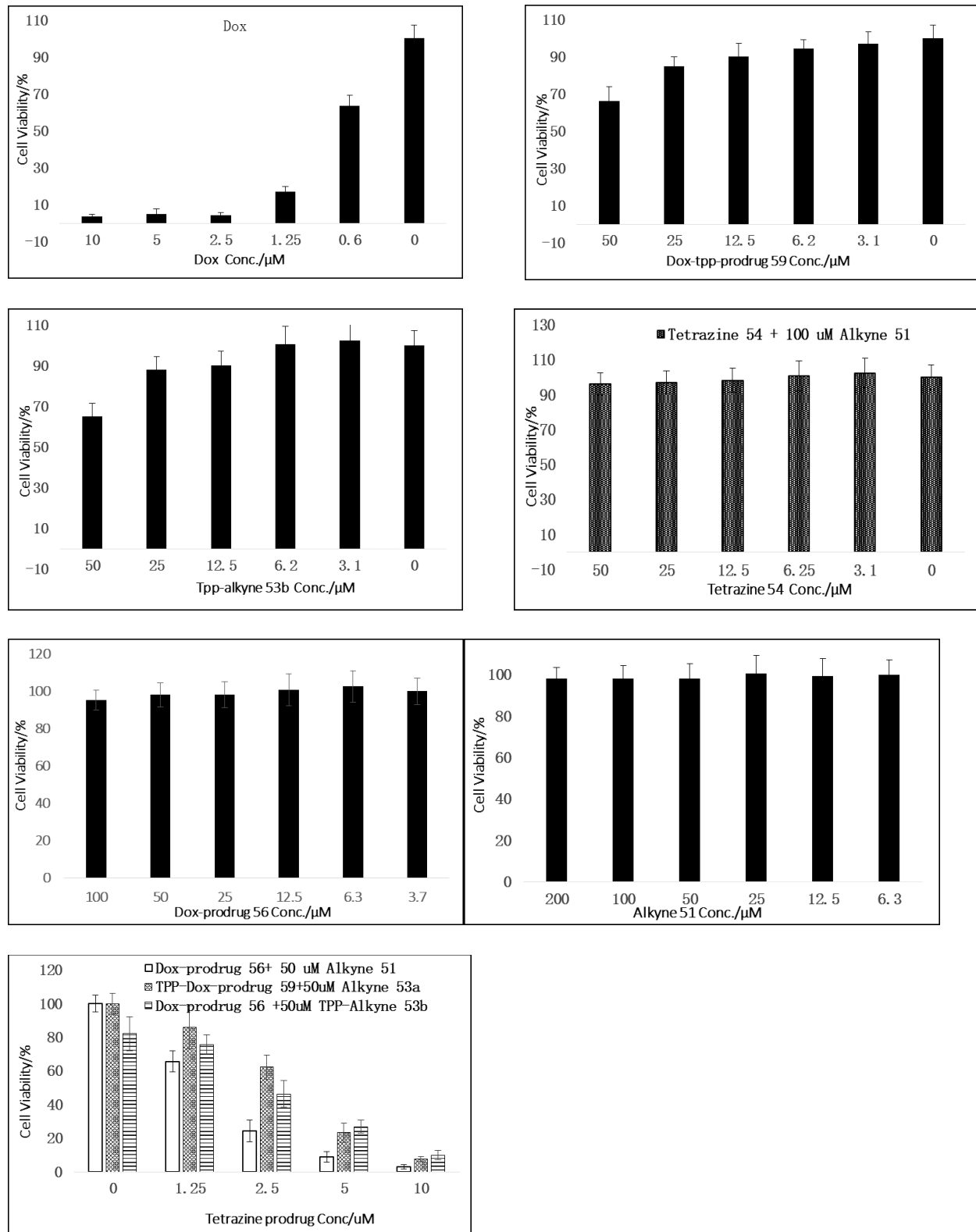


Figure 3.3. Studies of cytotoxicity ($n = 4$).

3.4.4 Computational studies

All calculations were performed using the Gaussian 09 program.²¹⁹ Initial geometry optimizations were carried out by DFT calculations with use of the B3LYP²²⁰⁻²²¹ with the standard 6-31G(d,p) basis set. The transition state geometries were obtained using the QST3 method. Energies are shown in Table S4. The stationary points are characterized by frequency calculations to verify that TSs has one and only one imaginary frequency (Scheme S8). All calculations were conducted on Georgia State University cluster Orion with 8 CPU cores.²²²

Coordinates and connections of **60**

N	-3.33510000	1.54220000	-0.14430000
C	4.67560000	0.52310000	-0.31910000
C	5.21030000	-0.72150000	0.01340000
C	4.36190000	-1.79170000	0.29720000
C	2.97890000	-1.61720000	0.24860000
C	2.44420000	-0.37260000	-0.08380000
C	3.29260000	0.69760000	-0.36770000
C	1.11850000	-0.20540000	-0.13030000
N	0.63990000	1.04560000	-0.00410000
N	-0.69490000	1.21400000	-0.05090000
C	-1.45900000	0.11980000	-0.22080000
N	-0.98040000	-1.13120000	-0.34700000
N	0.35440000	-1.29960000	-0.30010000
C	-2.79850000	0.28880000	-0.26790000
O	6.55380000	-0.89100000	0.06070000

C 6.87730000 -2.20900000 0.41250000
C 8.33880000 -2.36090000 0.45530000
C 9.54380000 -2.48610000 0.49060000
O -3.52290000 -0.66600000 -0.41910000
C -4.77280000 1.72360000 -0.19480000
C -5.10480000 3.20130000 -0.03400000
H -2.72830000 2.34220000 -0.01760000
H 5.34460000 1.36700000 -0.54300000
H 4.78350000 -2.77330000 0.55940000
H 2.30990000 -2.46120000 0.47240000
H 2.87090000 1.67910000 -0.62990000
H 6.45130000 -2.44030000 1.41440000
H 6.45370000 -2.90890000 -0.34230000
H 10.62750000 -2.59870000 0.52230000
H -5.15760000 1.36200000 -1.17460000
H -5.24880000 1.14490000 0.62820000
H -6.20830000 3.34050000 -0.07280000
H -4.72000000 3.56290000 0.94580000
H -4.62880000 3.78000000 -0.85700000

1 14 1.0 20 1.0 22 1.0

2 3 1.0 7 2.0 23 1.0

3 4 2.0 15 1.0

4 5 1.0 24 1.0

5 6 2.0 25 1.0

6 7 1.0 8 1.0

7 26 1.0

8 9 1.0 13 2.0

9 10 2.0

10 11 1.0

11 12 2.0 14 1.0

12 13 1.0

13

14 19 2.0

15 16 1.0

16 17 1.0 27 1.0 28 1.0

17 18 3.0

18 29 1.0

19

20 21 1.0 30 1.0 31 1.0

21 32 1.0 33 1.0 34 1.0

22

23

24

25

26

27

28

29

30

31

32

33

34

Coordinates and connections of 52

C	-4.18010000	-2.30160000	0.09260000
C	-5.19150000	-1.18990000	-0.25300000
C	-4.97230000	0.16130000	0.47260000
C	-4.06550000	1.19260000	-0.25130000
C	-2.63920000	1.37760000	0.32480000
C	-1.55430000	0.46390000	-0.28050000
C	-2.01330000	-0.91580000	-0.20460000
C	-2.83370000	-1.77920000	-0.09320000
C	-0.25860000	0.61690000	0.50520000
O	-1.32060000	0.81810000	-1.61670000
H	-4.33910000	-3.17460000	-0.57920000
H	-4.31920000	-2.62770000	1.14760000
H	-6.20830000	-1.55850000	0.00950000
H	-5.05560000	-0.97980000	-1.33750000
H	-4.51330000	-0.05680000	1.46290000

H -5.97760000 0.63600000 0.52550000
H -3.96310000 0.86830000 -1.31100000
H -4.56920000 2.17600000 -0.11720000
H -2.68330000 1.17830000 1.41890000
H -2.33920000 2.41850000 0.06930000
H 0.54860000 0.97060000 -0.17450000
H -0.40610000 1.35810000 1.32230000
H 0.02850000 -0.36580000 0.94190000
H -2.13710000 0.71350000 -2.07460000

1 2 1.0 8 1.0 11 1.0 12 1.0

2 3 1.0 13 1.0 14 1.0

3 4 1.0 15 1.0 16 1.0

4 5 1.0 17 1.0 18 1.0

5 6 1.0 19 1.0 20 1.0

6 7 1.0 9 1.0 10 1.0

7 8 3.0

8

9 21 1.0 22 1.0 23 1.0

10 24 1.0

11

12

13

14

15

16

17

18

19

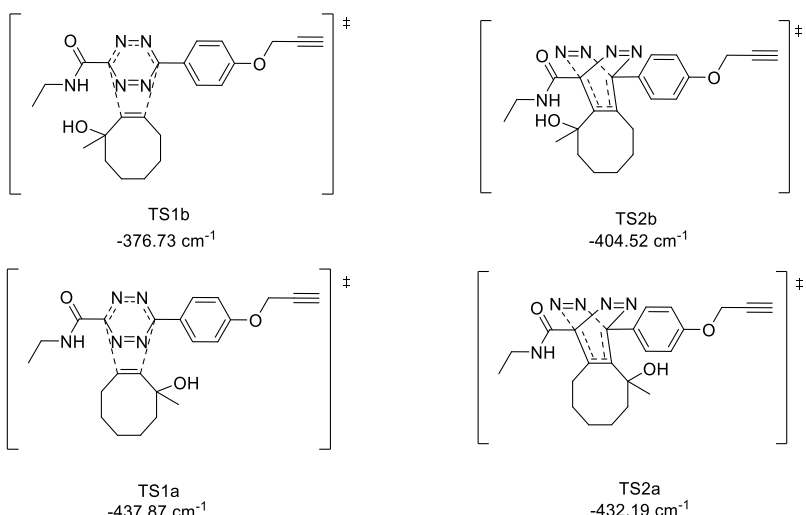
20

21

22

23

24

*Scheme 3.7. Unique imaginary frequencies.**Table 3.7 Calculated energies.*

Structure	Energy (Hartree)
60	-965.3956

52	-426.5493
TS1b:	-1391.9178
IN1b:	-1391.9879
TS2b:	-1391.9833
60b	-1282.5577
N2:	-109.5241
TS1a:	-1391.9147
IN1a:	-1391.9832
TS2a:	-1391.9789
60a	-1282.5579

3.5 Acknowledgement

We gratefully acknowledge the use of Orion that is supported by Georgia State University's Research Solutions. I also would like to specially thank Bingchen Yu for the synthesis and cell culture, Manjusha Roy Choudhury for the kinetic studies and synthesis, Zhixiang Pan for the synthesis, Mengyuan Zhu for the computational study, Dr. Xingyue Ji Dr. Chaofeng Dai, and Dr. Weixuan Chen for the discussion, Dr. Kaili Ji and Jun Zhang for the cell culture work, and Dr. Siming Wang and Ms. Lenong Wang Allison for the MS work.

4 CONCLUSIONS

In conclusion, we successfully investigated a new strategy of making H₂S prodrugs by using an esterase catalyzed lactonization prodrug system. Compared to existing H₂S prodrugs/donors, the new H₂S prodrugs described show several unique features. First of all, they have controlled H₂S release rates. This aspect seems to be the most challenging and important issue in the field of H₂S donors. Secondly, the trigger is an enzyme ubiquitous in the biological system.²²³ Thirdly, the prodrugs require a specific type of enzyme to trigger H₂S release, which afford the potential for controlled release at preferred sites. Fourthly, as research tools, the prodrugs described have well-defined negative controls. Fifthly, this strategy provides the first H₂S-NSAIDs hybrids with controllable release rates. We believe that these new H₂S prodrugs will be very useful research tools to others working in this field.

We have developed a series of persulfide prodrugs with controllable release rates. These persulfide prodrugs release persulfide through an esterase-mediated hydrolysis mechanism. In the presence of the PLE, the prodrugs efficiently released persulfides under near physiological conditions. Using the prodrug, we reaffirmed the reactivity between persulfide and MMTS. The protective effects of P2 in a murine model of MI/R injury have also been demonstrated. All the studies above demonstrate that this novel type of persulfide prodrugs not only can be used as research tools, but also are possible therapeutic agents.

In targeted therapy, there is a strong need for the development of new chemistry to achieve selective delivery, which would complement existing ones. In the chapter 2 study, we have developed a new concept and a platform approach, which relies on concentration-sensitive chemistry to allow for selective drug release upon enrichment. This is achieved by taking advantage of reaction kinetics, which allows for accelerated cleavage at an elevated concentration.

Such an approach will be very useful in delivering small molecules through targeting including the use of antibody drug conjugates and receptor-mediated drug delivery. As a result, the delivery is not limited to cell surface and can be used for sub-cellular delivery, with enriched concentrations, which could not be achieved by ADC based delivery. Collectively, we describe a method that could be leveraged for biologic and medicinal efforts in treating disease.

REFERENCES

1. Wang, R., Two's company, three's a crowd: can H₂S be the third endogenous gaseous transmitter? *FASEB J.* **2002**, *16* (13), 1792-8.
2. Gadalla, M. M.; Snyder, S. H., Hydrogen Sulfide as a Gasotransmitter. *J. Neurochem.* **2010**, *113* (1), 14-26.
3. Wallace, J. L.; Wang, R., Hydrogen sulfide-based therapeutics: exploiting a unique but ubiquitous gasotransmitter. *Nat. Rev. Drug Discov.* **2015**, *14* (5), 329-345.
4. Li, L.; Whiteman, M.; Guan, Y. Y.; Neo, K. L.; Cheng, Y.; Lee, S. W.; Zhao, Y.; Baskar, R.; Tan, C. H.; Moore, P. K., Characterization of a novel, water-soluble hydrogen sulfide-releasing molecule (GYY4137): new insights into the biology of hydrogen sulfide. *Circulation* **2008**, *117* (18), 2351-60.
5. Li, T.; Zhao, B.; Wang, C.; Wang, H.; Liu, Z.; Li, W.; Jin, H.; Tang, C.; Du, J., Regulatory effects of hydrogen sulfide on IL-6, IL-8 and IL-10 levels in the plasma and pulmonary tissue of rats with acute lung injury. *Exp. Biol. Med. (Maywood)* **2008**, *233* (9), 1081-7.
6. Andruski, B.; McCafferty, D. M.; Ignacy, T.; Millen, B.; McDougall, J. J., Leukocyte trafficking and pain behavioral responses to a hydrogen sulfide donor in acute monoarthritis. *Am. J. Physiol. Regul. Integr. Comp. Physiol.* **2008**, *295* (3), R814-20.
7. Sidhapuriwala, J. N.; Hegde, A.; Ang, A. D.; Zhu, Y. Z.; Bhatia, M., Effects of S-propargyl-cysteine (SPRC) in caerulein-induced acute pancreatitis in mice. *PLOS ONE* **2012**, *7* (3), e32574.
8. Hellmich, M. R.; Szabo, C., Hydrogen sulfide and cancer. *Handb. Exp. Pharmacol.* **2015**, *230*, 233-241.
9. Shrotriya, S.; Kundu, J. K.; Na, H. K.; Surh, Y. J., Diallyl trisulfide inhibits phorbol ester-induced tumor promotion, activation of AP-1, and expression of COX-2 in mouse skin by blocking JNK and Akt signaling. *Cancer Res.* **2010**, *70* (5), 1932-40.
10. Hellmich, M. R.; Coletta, C.; Chao, C.; Szabo, C., The therapeutic potential of cystathionine beta-synthetase/hydrogen sulfide inhibition in cancer. *Antioxid. Redox Signal.* **2015**, *22* (5), 424-48.
11. Wu, B.; Teng, H.; Yang, G.; Wu, L.; Wang, R., Hydrogen sulfide inhibits the translational expression of hypoxia-inducible factor-1alpha. *Br. J. Pharmacol.* **2012**, *167* (7), 1492-505.
12. Szabo, C., Gasotransmitters in cancer: from pathophysiology to experimental therapy. *Nat. Rev. Drug Discov.* **2016**, *15* (3), 185-203.
13. Zhao, W.; Zhang, J.; Lu, Y.; Wang, R., The vasorelaxant effect of H(2)S as a novel endogenous gaseous K(ATP) channel opener. *EMBO J.* **2001**, *20* (21), 6008-16.
14. Liu, L.; Liu, H.; Sun, D.; Qiao, W.; Qi, Y.; Sun, H.; Yan, C., Effects of H(2)S on myogenic responses in rat cerebral arterioles. *Circ. J.* **2012**, *76* (4), 1012-9.
15. Buckler, K. J., Effects of exogenous hydrogen sulphide on calcium signalling, background (TASK) K channel activity and mitochondrial function in chemoreceptor cells. *Pflugers Arch., EJP* **2012**, *463* (5), 743-54.
16. Elies, J.; Scragg, J. L.; Dallas, M. L.; Huang, D.; Huang, S.; Boyle, J. P.; Gamper, N.; Peers, C., Inhibition of T-type Ca²⁺ Channels by Hydrogen Sulfide. *Adv. Exp. Med. Biol.* **2015**, *860*, 353-60.
17. Lisjak, M.; Srivastava, N.; Teklic, T.; Civale, L.; Lewandowski, K.; Wilson, I.; Wood, M. E.; Whiteman, M.; Hancock, J. T., A novel hydrogen sulfide donor causes stomatal opening and reduces nitric oxide accumulation. *Plant Physiol. Biochem.* **2010**, *48* (12), 931-5.

18. Liu, M. H.; Zhang, Y.; He, J.; Tan, T. P.; Wu, S. J.; Guo, D. M.; He, H.; Peng, J.; Tang, Z. H.; Jiang, Z. S., Hydrogen sulfide protects H9c2 cardiac cells against doxorubicin-induced cytotoxicity through the PI3K/Akt/FoxO3a pathway. *Int. J. Mol. Med.* **2016**, *37* (6), 1661-8.
19. Yuan, G.; Peng, Y.-J.; Khan, S. A.; Nanduri, J.; Singh, A.; Vasavda, C.; Semenza, G. L.; Kumar, G. K.; Snyder, S. H.; Prabhakar, N. R., H2S production by reactive oxygen species in the carotid body triggers hypertension in a rodent model of sleep apnea. *Sci. Signal.* **2016**, *9* (441), ra80.
20. Wang, R.; Szabo, C.; Ichinose, F.; Ahmed, A.; Whiteman, M.; Papapetropoulos, A., The role of H2S bioavailability in endothelial dysfunction. *Trends Pharmacol. Sci.* **2015**, *36* (9), 568-78.
21. Osborne, N. N.; Ji, D.; Majid, A. S.; Del Soldato, P.; Sparatore, A., Glutamate oxidative injury to RGC-5 cells in culture is necrostatin sensitive and blunted by a hydrogen sulfide (H2S)-releasing derivative of aspirin (ACS14). *Neurochem. Int.* **2012**, *60* (4), 365-78.
22. Xie, L.; Feng, H.; Li, S.; Meng, G.; Liu, S.; Tang, X.; Ma, Y.; Han, Y.; Xiao, Y.; Gu, Y.; Shao, Y.; Park, C. M.; Xian, M.; Huang, Y.; Ferro, A.; Wang, R.; Moore, P. K.; Wang, H.; Ji, Y., SIRT3 Mediates the Antioxidant Effect of Hydrogen Sulfide in Endothelial Cells. *Antioxid. Redox Signal.* **2016**, *24* (6), 329-43.
23. Soma, M.; Nakayama, T.; Kanmatsuse, K., Nitric oxide synthase gene polymorphism and its influence on cardiovascular disease. *Curr. Opin. Nephrol. Hypertens.* **1999**, *8* (1), 83-7.
24. Huerta, S.; Chilka, S.; Bonavida, B., Nitric oxide donors: novel cancer therapeutics (review). *Int. J. Oncol.* **2008**, *33* (5), 909-27.
25. Ji, X.; Damera, K.; Zheng, Y.; Yu, B.; Otterbein, L. E.; Wang, B., Toward Carbon Monoxide-Based Therapeutics: Critical Drug Delivery and Developability Issues. *J. Pharm. Sci.* **2016**, *105* (2), 406-16.
26. Song, Z. J.; Ng, M. Y.; Lee, Z.-W.; Dai, W.; Hagen, T.; Moore, P. K.; Huang, D.; Deng, L.-W.; Tan, C.-H., Hydrogen sulfide donors in research and drug development. *Med. Chem. Commun.* **2014**, *5* (5), 557-570.
27. Guo, W.; Cheng, Z.-y.; Zhu, Y.-z., Hydrogen sulfide and translational medicine. *Acta Pharmacol. Sin.* **2013**, *34* (10), 1284-1291.
28. Li, L.; Rose, P.; Moore, P. K., Hydrogen sulfide and cell signaling. *Annu. Rev. Pharmacol. Toxicol.* **2011**, *51*, 169-87.
29. Zhao, Y.; Biggs, T. D.; Xian, M., Hydrogen sulfide (H2S) releasing agents: chemistry and biological applications. *Chem. Commun.* **2014**, *50* (80), 11788-11805.
30. Szabó, C., Hydrogen sulphide and its therapeutic potential. *Nat. Rev. Drug Discov.* **2007**, *6* (11), 917-935.
31. Martelli, A.; Testai, L.; Breschi, M. C.; Blandizzi, C.; Virdis, A.; Taddei, S.; Calderone, V., Hydrogen sulphide: novel opportunity for drug discovery. *Med. Res. Rev.* **2012**, *32* (6), 1093-130.
32. Calderone, V.; Martelli, A.; Testai, L.; Citi, V.; Breschi, M. C., Using hydrogen sulfide to design and develop drugs. *Expert. Opin. Drug. Discov.* **2016**, *11* (2), 163-75.
33. Chou, S. *Syracuse research corporation, and United States. Agency for toxic substances and disease registry. Toxicological profile for hydrogen sulfide: update, U.S. Dept. of Health and Human Services Public Health Service Agency for Toxic Substances and Disease Registry [Atlanta, GA.]*; 2006.
34. Stein, A.; Bailey, S. M., Redox biology of hydrogen sulfide: Implications for physiology, pathophysiology, and pharmacology. *Redox Biol.* **2013**, *1* (1), 32-39.

35. Ungerer, P. W.; Aurelie; Demoulin, Gregoire; Bourasseau, Emeric; Mougin, Pascal, Application of Gibbs ensemble and NPT Monte Carlo simulation to the development of improved processes for H₂S-rich gases. *Mol. Simul.* **2004**, *30* (10), 631-648.
36. Hughes, M. N.; Centelles, M. N.; Moore, K. P., Making and working with hydrogen sulfide: The chemistry and generation of hydrogen sulfide in vitro and its measurement in vivo: a review. *Free Radic. Biol. Med.* **2009**, *47* (10), 1346-53.
37. Li, J.; Meng, Z., The role of sulfur dioxide as an endogenous gaseous vasoactive factor in synergy with nitric oxide. *Nitric Oxide* **2009**, *20* (3), 166-74.
38. Huang, Y.; Tang, C.; Du, J.; Jin, H., Endogenous Sulfur Dioxide: A New Member of Gasotransmitter Family in the Cardiovascular System. *Oxid. Med. Cell. Longev.* **2016**, *2016*, 8961951.
39. Ono, K.; Akaike, T.; Sawa, T.; Kumagai, Y.; Wink, D. A.; Tantillo, D. J.; Hobbs, A. J.; Nagy, P.; Xian, M.; Lin, J.; Fukuto, J. M., Redox chemistry and chemical biology of H₂S, hydopersulfides, and derived species: implications of their possible biological activity and utility. *Free Radic. Biol. Med.* **2014**, *77*, 82-94.
40. Pan, J.; Carroll, K. S., Persulfide Reactivity in the Detection of Protein S-Sulphydratation. *ACS Chem. Biol.* **2013**, *8* (6), 1110-1116.
41. Kimura, H., Hydrogen sulfide and polysulfides as signaling molecules. *Proc. Jpn. Acad. Ser. B Phys. Biol. Sci.* **2015**, *91* (4), 131-59.
42. Kimura, H., Signaling of hydrogen sulfide and polysulfides. *Antioxid. Redox Signal.* **2015**, *22* (5), 347-9.
43. Yamanishi, M.; Kabil, O.; Sen, S.; Banerjee, R., Structural insights into pathogenic mutations in heme-dependent cystathione-beta-synthase. *J. Inorg. Biochem.* **2006**, *100* (12), 1988-95.
44. Teng, H.; Wu, B.; Zhao, K.; Yang, G.; Wu, L.; Wang, R., Oxygen-sensitive mitochondrial accumulation of cystathione beta-synthase mediated by Lon protease. *Proc. Natl. Acad. Sci. USA* **2013**, *110* (31), 12679-84.
45. Renga, B., Hydrogen sulfide generation in mammals: the molecular biology of cystathione-beta-synthase (CBS) and cystathione-gamma-lyase (CSE). *Inflamm. Allergy Drug Targets* **2011**, *10* (2), 85-91.
46. Nagahara, N.; Okazaki, T.; Nishino, T., Cytosolic mercaptopyruvate sulfurtransferase is evolutionarily related to mitochondrial rhodanese. Striking similarity in active site amino acid sequence and the increase in the mercaptopyruvate sulfurtransferase activity of rhodanese by site-directed mutagenesis. *J. Biol. Chem.* **1995**, *270* (27), 16230-5.
47. Kolluru, G. K.; Shen, X.; Bir, S. C.; Kevil, C. G., Hydrogen Sulfide Chemical Biology: Pathophysiological roles and detection. *Nitric Oxide* **2013**, *35*, 5-20.
48. Bartholomew, T. C.; Powell, G. M.; Dodgson, K. S.; Curtis, C. G., Oxidation of sodium sulphide by rat liver, lungs and kidney. *Biochem. Pharmacol.* **1980**, *29* (18), 2431-7.
49. Powell, M. A.; Somero, G. N., Hydrogen Sulfide Oxidation Is Coupled to Oxidative Phosphorylation in Mitochondria of *Solemya reidi*. *Science* **1986**, *233* (4763), 563-6.
50. Kabil, O.; Banerjee, R., Redox biochemistry of hydrogen sulfide. *J. Biol. Chem.* **2010**, *285* (29), 21903-7.
51. Jackson, M. R.; Melideo, S. L.; Jorns, M. S., Human sulfide:quinone oxidoreductase catalyzes the first step in hydrogen sulfide metabolism and produces a sulfane sulfur metabolite. *Biochemistry* **2012**, *51* (34), 6804-15.

52. Wilson, K.; Mudra, M.; Furne, J.; Levitt, M., Differentiation of the roles of sulfide oxidase and rhodanese in the detoxification of sulfide by the colonic mucosa. *Dig. Dis. Sci.* **2008**, *53* (1), 277-83.
53. Jackson, M. R.; Melideo, S. L.; Jorns, M. S., Role of human sulfide: quinone oxidoreductase in H₂S metabolism. *Methods Enzymol.* **2015**, *554*, 255-70.
54. Hildebrandt, T. M.; Grieshaber, M. K., Three enzymatic activities catalyze the oxidation of sulfide to thiosulfate in mammalian and invertebrate mitochondria. *FEBS J.* **2008**, *275* (13), 3352-61.
55. Weber, R. E.; Vinogradov, S. N., Nonvertebrate hemoglobins: functions and molecular adaptations. *Physiol. Rev.* **2001**, *81* (2), 569-628.
56. Nicoletti, F. P.; Comandini, A.; Bonamore, A.; Boechi, L.; Boubeta, F. M.; Feis, A.; Smulevich, G.; Boffi, A., Sulfide binding properties of truncated hemoglobins. *Biochemistry* **2010**, *49* (10), 2269-78.
57. Bostelaar, T.; Vitvitsky, V.; Kumutima, J.; Lewis, B. E.; Yadav, P. K.; Brunold, T. C.; Filipovic, M.; Lehnert, N.; Stemmler, T. L.; Banerjee, R., Hydrogen Sulfide Oxidation by Myoglobin. *J. Am. Chem. Soc.* **2016**, *138* (27), 8476-8488.
58. Mustafa, A. K.; Gadalla, M. M.; Sen, N.; Kim, S.; Mu, W.; Gazi, S. K.; Barrow, R. K.; Yang, G.; Wang, R.; Snyder, S. H., H₂S signals through protein S-sulfhydration. *Sci. Signal.* **2009**, *2* (96), ra72.
59. Mishanina, T. V.; Libiad, M.; Banerjee, R., Biogenesis of reactive sulfur species for signaling by hydrogen sulfide oxidation pathways. *Nat. Chem. Biol.* **2015**, *11* (7), 457-64.
60. Paul, B. D.; Snyder, S. H., H₂S: A Novel Gasotransmitter that Signals by Sulfhydration. *Trends Biochem. Sci.* **2015**, *40* (11), 687-700.
61. Kimura, Y.; Mikami, Y.; Osumi, K.; Tsugane, M.; Oka, J.; Kimura, H., Polysulfides are possible H₂S-derived signaling molecules in rat brain. *FASEB J.* **2013**, *27* (6), 2451-7.
62. Longen, S.; Richter, F.; Köhler, Y.; Wittig, I.; Beck, K.-F.; Pfeilschifter, J., Quantitative Persulfide Site Identification (qPerS-SID) Reveals Protein Targets of H(2)S Releasing Donors in Mammalian Cells. *Sci. Rep.* **2016**, *6*, 29808.
63. Doka, E.; Pader, I.; Biro, A.; Johansson, K.; Cheng, Q.; Ballago, K.; Prigge, J. R.; Pastor-Flores, D.; Dick, T. P.; Schmidt, E. E.; Arner, E. S.; Nagy, P., A novel persulfide detection method reveals protein persulfide- and polysulfide-reducing functions of thioredoxin and glutathione systems. *Sci. Adv.* **2016**, *2* (1), e1500968.
64. Mustafa, A. K.; Sikka, G.; Gazi, S. K.; Steppan, J.; Jung, S. M.; Bhunia, A. K.; Barodka, V. M.; Gazi, F. K.; Barrow, R. K.; Wang, R.; Amzel, L. M.; Berkowitz, D. E.; Snyder, S. H., Hydrogen Sulfide as Endothelial Derived Hyperpolarizing Factor Sulfhydrates Potassium Channels. *Circ. Res.* **2011**, *109* (11), 1259-1268.
65. Yang, G.; Zhao, K.; Ju, Y.; Mani, S.; Cao, Q.; Puukila, S.; Khaper, N.; Wu, L.; Wang, R., Hydrogen sulfide protects against cellular senescence via S-sulfhydration of Keap1 and activation of Nrf2. *Antioxid. Redox Signal.* **2013**, *18* (15), 1906-19.
66. Francoleon, N. E.; Carrington, S. J.; Fukuto, J. M., The reaction of H(2)S with oxidized thiols: generation of persulfides and implications to H(2)S biology. *Arch. Biochem. Biophys.* **2011**, *516* (2), 146-53.
67. Vasas, A.; Doka, E.; Fabian, I.; Nagy, P., Kinetic and thermodynamic studies on the disulfide-bond reducing potential of hydrogen sulfide. *Nitric Oxide* **2015**, *46*, 93-101.

68. Kimura, Y.; Toyofuku, Y.; Koike, S.; Shibuya, N.; Nagahara, N.; Lefer, D.; Ogasawara, Y.; Kimura, H., Identification of H₂S₃ and H₂S produced by 3-mercaptopyruvate sulfurtransferase in the brain. *Sci. Rep.* **2015**, *5*, 14774.
69. Greiner, R.; Palinkas, Z.; Basell, K.; Becher, D.; Antelmann, H.; Nagy, P.; Dick, T. P., Polysulfides link H₂S to protein thiol oxidation. *Antioxid. Redox Signal.* **2013**, *19* (15), 1749-65.
70. Artaud, I.; Galardon, E., A persulfide analogue of the nitrosothiol SNAP: formation, characterization and reactivity. *Chembiochem* **2014**, *15* (16), 2361-4.
71. Helmy, N.; Prip-Buus, C.; Vons, C.; Lenoir, V.; Abou-Hamdan, A.; Guedouari-Bounihi, H.; Lombes, A.; Bouillaud, F., Oxidation of hydrogen sulfide by human liver mitochondria. *Nitric Oxide* **2014**, *41*, 105-12.
72. Collman, J. P.; Ghosh, S.; Dey, A.; Decreau, R. A., Using a functional enzyme model to understand the chemistry behind hydrogen sulfide induced hibernation. *Proc. Natl. Acad. Sci. USA* **2009**, *106* (52), 22090-5.
73. Artaud, I.; Galardon, E., A Persulfide Analogue of the Nitrosothiol SNAP: Formation, Characterization and Reactivity. *ChemBioChem* **2014**, *15* (16), 2361-2364.
74. Lin, V. S.; Chen, W.; Xian, M.; Chang, C. J., Chemical probes for molecular imaging and detection of hydrogen sulfide and reactive sulfur species in biological systems. *Chem. Soc. Rev.* **2015**, *44* (14), 4596-618.
75. Wang, K.; Peng, H.; Wang, B., Recent advances in thiol and sulfide reactive probes. *J. Cell. Biochem.* **2014**, *115* (6), 1007-22.
76. Zheng, Y.; Yu, B.; Ji, K.; Pan, Z.; Chittavong, V.; Wang, B., Esterase-Sensitive Prodrugs with Tunable Release Rates and Direct Generation of Hydrogen Sulfide. *Angew. Chem. Int. Ed.* **2016**, *55* (14), 4514-8.
77. Borchardt, R. T.; Kerns, E. H.; Lipinski, C. A.; Thakker, D. R.; Wang, B., *Pharmaceutical Profiling In Drug Discovery for Lead Selection*. AAPS Press: Arlington, VA, 2004.
78. Han, C.; David, C.; Wang, B., *Evaluation of Drug Candidates for Preclinical Development: Pharmacokinetics, Metabolism, Pharmaceutics, and Toxicology* John Wiley and Sons,: New York, 2010.
79. Han, C.; Wang, B., Factors that Impact the Developability of Drug Candidates-An Overview. In *Drug Delivery: Principles and Applications*, Wang, B.; Siahaan, T.; Soltero, R., Eds. John Wiley and Sons: New York, 2005; pp 1-15.
80. Wang, B.; Hu, L.; Siahaan, T., *Drug Delivery: Principles and Applications*. 2nd Edition ed.; John Wiley and Sons: Hoboken, New Jersey, 2016.
81. Kashfi, K.; Olson, K. R., Biology and therapeutic potential of hydrogen sulfide and hydrogen sulfide-releasing chimeras. *Biochem. Pharmacol.* **2013**, *85* (5), 689-703.
82. Zhao, Y.; Biggs, T. D.; Xian, M., Hydrogen sulfide (H₂S) releasing agents: chemistry and biological applications. *Chem. Commun. (Camb.)* **2014**, *50* (80), 11788-805.
83. Pluth, M. D.; Bailey, T. S.; Hammers, M. D.; Hartle, M. D.; Henthorn, H. A.; Steiger, A. K., Natural Products Containing Hydrogen Sulfide Releasing Moieties. *Synlett* **2015**, *26* (19), 2633-2643.
84. Zheng, Y.; Ji, X.; Ji, K.; Wang, B., Hydrogen sulfide prodrugs—a review. *Acta Pharm. Sin. B* **2015**, *5* (5), 367-377.
85. Benavides, G. A.; Squadrito, G. L.; Mills, R. W.; Patel, H. D.; Isbell, T. S.; Patel, R. P.; Darley-Usmar, V. M.; Doeller, J. E.; Kraus, D. W., Hydrogen sulfide mediates the vasoactivity of garlic. *Proc. Natl. Acad. Sci. U. S. A.* **2007**, *104* (46), 17977-82.

86. Baskar, R.; Sparatore, A.; Del Soldato, P.; Moore, P. K., Effect of S-diclofenac, a novel hydrogen sulfide releasing derivative inhibit rat vascular smooth muscle cell proliferation. *Eur. J. Pharmacol.* **2008**, 594 (1-3), 1-8.
87. Qandil, A. M., Prodrugs of Nonsteroidal Anti-Inflammatory Drugs (NSAIDs), More Than Meets the Eye: A Critical Review. *Int. J. Mol. Sci.* **2012**, 13 (12), 17244-17274.
88. Liang, D.; Wu, H.; Wong, M. W.; Huang, D., Diallyl Trisulfide Is a Fast H₂S Donor, but Diallyl Disulfide Is a Slow One: The Reaction Pathways and Intermediates of Glutathione with Polysulfides. *Org. Lett.* **2015**, 17 (17), 4196-4199.
89. Zhao, Y.; Wang, H.; Xian, M., Cysteine-activated hydrogen sulfide (H₂S) donors. *J. Am. Chem. Soc.* **2011**, 133 (1), 15-7.
90. Zhao, Y.; Bhushan, S.; Yang, C.; Otsuka, H.; Stein, J. D.; Pacheco, A.; Peng, B.; Devarie-Baez, N. O.; Aguilar, H. C.; Lefer, D. J.; Xian, M., Controllable hydrogen sulfide donors and their activity against myocardial ischemia-reperfusion injury. *ACS Chem. Biol.* **2013**, 8 (6), 1283-90.
91. Martelli, A.; Testai, L.; Citi, V.; Marino, A.; Pugliesi, I.; Barresi, E.; Nesi, G.; Rapposelli, S.; Taliani, S.; Da Settimo, F.; Breschi, M. C.; Calderone, V., Arylthioamides as H₂S Donors: l-Cysteine-Activated Releasing Properties and Vascular Effects in Vitro and in Vivo. *ACS Med. Chem. Lett.* **2013**, 4 (10), 904-8.
92. Devarie-Baez, N. O.; Bagdon, P. E.; Peng, B.; Zhao, Y.; Park, C. M.; Xian, M., Light-induced hydrogen sulfide release from "caged" gem-dithiols. *Org. Lett.* **2013**, 15 (11), 2786-9.
93. Fukushima, N.; Ieda, N.; Sasakura, K.; Nagano, T.; Hanaoka, K.; Suzuki, T.; Miyata, N.; Nakagawa, H., Synthesis of a photocontrollable hydrogen sulfide donor using ketoprofenate photocages. *Chem. Commun. (Camb.)* **2014**, 50 (5), 587-9.
94. Zhou, Z.; von Wantoch Rekowski, M.; Coletta, C.; Szabo, C.; Bucci, M.; Cirino, G.; Topouzis, S.; Papapetropoulos, A.; Giannis, A., Thioglycine and L-thiovaline: biologically active H(2)S-donors. *Bioorg. Med. Chem.* **2012**, 20 (8), 2675-8.
95. Kondo, K.; Bhushan, S.; King, A. L.; Prabhu, S. D.; Hamid, T.; Koenig, S.; Murohara, T.; Predmore, B. L.; Gojon, G.; Gojon, G.; Wang, R.; Karusula, N.; Nicholson, C. K.; Calvert, J. W.; Lefer, D. J., H(2)S Protects Against Pressure Overload Induced Heart Failure via Upregulation of Endothelial Nitric Oxide Synthase (eNOS). *Circulation* **2013**, 127 (10), 1116-1127.
96. Whiteman, M.; Li, L.; Rose, P.; Tan, C. H.; Parkinson, D. B.; Moore, P. K., The effect of hydrogen sulfide donors on lipopolysaccharide-induced formation of inflammatory mediators in macrophages. *Antioxid. Redox Signal.* **2010**, 12 (10), 1147-54.
97. Shan, D.; Nicolaou, M. G.; Borchardt, R. T.; Wang, B., Prodrug Strategies Based on Intramolecular Cyclization Reactions. *J. Pharm. Sci.* **1997**, 86, 765-767.
98. Wang, B.; Zhang, H.; Wang, W., Chemical Feasibility Studies of a Potential Coumarin-Based Prodrug System. *Bioorg. Med. Chem. Lett.* **1996**, 6, 945-950.
99. Zych, L.; Yang, W.; Griffin, K.; Liao, Y.; Wang, B., Coumarin-based Cyclic Prodrugs of Peptides-The Effect of Substitution. *Bioorg. Chem.* **2004**, 32, 109-123.
100. Borchardt, R. T.; Cohen, L. A., Stereopopulation control. 3. Facilitation of intramolecular conjugate addition of the carboxyl group. *J. Am. Chem. Soc.* **1972**, 94 (26), 9175-82.
101. Borchardt, R. T.; Cohen, L. A., Stereopopulation control. II. Rate enhancement of intramolecular nucleophilic displacement. *J. Am. Chem. Soc.* **1972**, 94 (26), 9166-74.
102. Amsberry, K. L.; Borchardt, R. T., The Lactonization of 2'-Hydroxyhydrocinnamic Acid Amides: Potential Prodrugs for Amines. *J. Org. Chem.* **1990**, 55, 5867-5877.
103. Amsberry, K. L.; Borchardt, R. T., Amine Prodrugs which Utilize Hydroxy Amide Lactonization. I. A Potential Redox-Sensitive Amide Prodrug. *Pharm. Res.* **1991**, 8 (3), 323-330.

104. Schowen, K. B.; Schowen, R. L.; Borchardt, S. E.; Borchardt, P. M.; Artursson, P.; Audus, K. L.; Augustijns, P.; Nicolazzo, J. A.; Raub, T. R.; Schöneich, C.; Siahaan, T. J.; Takakura, Y.; Thakker, D. R.; Wolfe, M. S., A Tribute to Ronald T. Borchardt—Teacher, Mentor, Scientist, Colleague, Leader, Friend, and Family Man. *J. Pharm. Sci.* **2016**, *105*, published on-line, DOI: 10.1002/jps.24687.
105. Amsberry, K. L.; Gerstenberger, A. E.; Borchardt, R. T., Amine prodrugs which utilize hydroxy amide lactonization. II. A potential esterase-sensitive amide prodrug. *Pharm. Res.* **1991**, *8* (4), 455-61.
106. Rao, Y.; Li, X.; Nagorny, P.; Hayashida, J.; Danishefsky, S. J., A Simple Method for the Conversion of Carboxylic Acids into Thioacids with Lawesson's Reagent. *Tetrahedron lett.* **2009**, *50* (48), 6684-6686.
107. Peng, B.; Chen, W.; Liu, C.; Rosser, E. W.; Pacheco, A.; Zhao, Y.; Aguilar, H. C.; Xian, M., Fluorescent probes based on nucleophilic substitution-cyclization for hydrogen sulfide detection and bioimaging. *Chemistry* **2014**, *20* (4), 1010-6.
108. Elleby, B.; Sjöblom, B.; Lindskog, S., Changing the efficiency and specificity of the esterase activity of human carbonic anhydrase II by site-specific mutagenesis. *Eur. J. Biochem.* **1999**, *262* (2), 516-21.
109. Roberts, T. K.; Masson, P. L.; Lauwers, R.; Heremans, J. F., Two Esterases Common to Seminal Plasma, other External Secretions and Leucocytes in Man. *Andrologia* **1976**, *8* (1), 67-71.
110. Levine, M. N.; Raines, R. T., Trimethyl lock: a trigger for molecular release in chemistry, biology, and pharmacology. *Chem. Sci.* **2012**, *3* (8), 2412-2420.
111. Shan, D.; Nicolaou, M. G.; Borchardt, R. T.; Wang, B., Prodrug strategies based on intramolecular cyclization reactions. *J. Pharm. Sci.* **1997**, *86* (7), 765-767.
112. Milstien, S.; Cohen, L. A., Rate Acceleration by Stereopopulation Control: Models for Enzyme Action. *Proc. Natl. Acad. Sci. U. S. A.* **1970**, *67* (3), 1143-1147.
113. Milstien, S.; Cohen, L. A., Stereopopulation control. I. Rate enhancement in the lactonizations of O-hydroxyhydrocinnamic acids. *J. Am. Chem. Soc.* **1972**, *94* (26), 9158-65.
114. Sparatore, A.; Santus, G.; Giustarini, D.; Rossi, R.; Del Soldato, P., Therapeutic potential of new hydrogen sulfide-releasing hybrids. *Expert. Rev. Clin. Pharmacol.* **2011**, *4* (1), 109-21.
115. Li, L.; Rossoni, G.; Sparatore, A.; Lee, L. C.; Del Soldato, P.; Moore, P. K., Anti-inflammatory and gastrointestinal effects of a novel diclofenac derivative. *Free Radic. Biol. Med.* **2007**, *42* (5), 706-719.
116. Amsberry, K. L.; Borchardt, R. T., The lactonization of 2'-hydroxyhydrocinnamic acid amides: a potential prodrug for amines. *J. Org. Chem.* **1990**, *55* (23), 5867-5877.
117. Zheng, Y.; Ji, X.; Ji, K.; Wang, B., Hydrogen sulfide prodrugs—a review. *Acta. Pharm. Sin. B* **2015**, *5* (5), 367-77.
118. Wang, R., Physiological implications of hydrogen sulfide: a whiff exploration that blossomed. *Physiol. Rev.* **2012**, *92* (2), 791-896.
119. Ono, K.; Akaike, T.; Sawa, T.; Kumagai, Y.; Wink, D. A.; Tantillo, D. J.; Hobbs, A. J.; Nagy, P.; Xian, M.; Lin, J.; Fukuto, J. M., Redox chemistry and chemical biology of H₂S, hydrosulfides, and derived species: implications of their possible biological activity and utility. *Free Radic. Biol. Med.* **2014**, *77*, 82-94.
120. Whiteman, M.; Winyard, P. G., Hydrogen sulfide and inflammation: the good, the bad, the ugly and the promising. *Expert Rev. Clin. Pharmacol.* **2011**, *4* (1), 13-32.

121. Steiger, A. K.; Pardue, S.; Kevil, C. G.; Pluth, M. D., Self-Immulative Thiocarbamates Provide Access to Triggered H₂S Donors and Analyte Replacement Fluorescent Probes. *J. Am. Chem. Soc.* **2016**, *138* (23), 7256-9.
122. Kang, J.; Li, Z.; Organ, C. L.; Park, C. M.; Yang, C. T.; Pacheco, A.; Wang, D.; Lefer, D. J.; Xian, M., pH-Controlled Hydrogen Sulfide Release for Myocardial Ischemia-Reperfusion Injury. *J. Am. Chem. Soc.* **2016**, *138* (20), 6336-9.
123. Ida, T.; Sawa, T.; Ihara, H.; Tsuchiya, Y.; Watanabe, Y.; Kumagai, Y.; Suematsu, M.; Motohashi, H.; Fujii, S.; Matsunaga, T.; Yamamoto, M.; Ono, K.; Devarie-Baez, N. O.; Xian, M.; Fukuto, J. M.; Akaike, T., Reactive cysteine persulfides and S-polythiolation regulate oxidative stress and redox signaling. *Proc. Natl. Acad. Sci. USA* **2014**, *111* (21), 7606-11.
124. Bradley, J. M.; Organ, C. L.; Lefer, D. J., Garlic-Derived Organic Polysulfides and Myocardial Protection. *J. Nutr.* **2016**, *146* (2), 403s-409s.
125. Iciek, M.; Bilska-Wilkosz, A.; Górný, M.; Sokołowska-Jeżewicz, M.; Kowalczyk-Pachel, D., The Effects of Different Garlic-Derived Allyl Sulfides on Anaerobic Sulfur Metabolism in the Mouse Kidney. *Antioxidants* **2016**, *5* (4), 46.
126. Zhao, Y.; Bhushan, S.; Yang, C.; Otsuka, H.; Stein, J. D.; Pacheco, A.; Peng, B.; Devarie-Baez, N. O.; Aguilar, H. C.; Lefer, D. J.; Xian, M., Controllable hydrogen sulfide donors and their activity against myocardial ischemia-reperfusion injury. *ACS Chem. Biol.* **2013**, *8* (6), 1283-90.
127. Zheng, Y.; Yu, B.; De La Cruz, L. K.; Roy Choudhury, M.; Anifowose, A.; Wang, B., Toward Hydrogen Sulfide Based Therapeutics: Critical Drug Delivery and Developability Issues. *Med. Res. Rev.* **2017**, *10*.1002/med.21433.
128. Zhao, Y.; Pacheco, A.; Xian, M., Medicinal Chemistry: Insights into the Development of Novel H₂S Donors. *Handb. Exp. Pharmacol.* **2015**, *230*, 365-88.
129. Steiger, A. K.; Pardue, S.; Kevil, C. G.; Pluth, M. D., Self-Immulative Thiocarbamates Provide Access to Triggered H₂S Donors and Analyte Replacement Fluorescent Probes. *J. Am. Chem. Soc.* **2016**, *138* (23), 7256-7259.
130. Steiger, A. K.; Yang, Y.; Royzen, M.; Pluth, M. D., Bio-orthogonal "click-and-release" donation of caged carbonyl sulfide (COS) and hydrogen sulfide (H₂S). *Chem. Commun.* **2017**, *53* (8), 1378-1380.
131. Zhao, Y.; Pluth, M. D., Hydrogen Sulfide Donors Activated by Reactive Oxygen Species. *Angew. Chem. Int. Ed.* **2016**, *55* (47), 14638-14642.
132. Chauhan, P.; Bora, P.; Ravikumar, G.; Jos, S.; Chakrapani, H., Esterase Activated Carbonyl Sulfide/Hydrogen Sulfide (H₂S) Donors. *Org. Lett.* **2017**, *19* (1), 62-65.
133. Powell, C. R.; Foster, J. C.; Okyere, B.; Theus, M. H.; Matson, J. B., Therapeutic Delivery of H₂S via COS: Small Molecule and Polymeric Donors with Benign Byproducts. *J. Am. Chem. Soc.* **2016**, *138* (41), 13477-13480.
134. Liang, D.; Wu, H.; Wong, M. W.; Huang, D., Diallyl Trisulfide Is a Fast H₂S Donor, but Diallyl Disulfide Is a Slow One: The Reaction Pathways and Intermediates of Glutathione with Polysulfides. *Org. Lett.* **2015**, *17* (17), 4196-4199.
135. Martelli, A.; Testai, L.; Citi, V.; Marino, A.; Pugliesi, I.; Barresi, E.; Nesi, G.; Rapposelli, S.; Taliani, S.; Da Settimo, F.; Breschi, M. C.; Calderone, V., Arylthioamides as H₂S Donors: l-Cysteine-Activated Releasing Properties and Vascular Effects in Vitro and in Vivo. *ACS Med. Chem. Lett.* **2013**, *4* (10), 904-8.
136. Ozturk, T.; Ertas, E.; Mert, O., Use of Lawesson's reagent in organic syntheses. *Chem. Rev.* **2007**, *107* (11), 5210-78.

137. Mustafa, A. K.; Gadalla, M. M.; Sen, N.; Kim, S.; Mu, W.; Gazi, S. K.; Barrow, R. K.; Yang, G.; Wang, R.; Snyder, S. H., H₂S signals through protein S-sulfhydration. *Sci. Signal.* **2009**, 2 (96), ra72.
138. Park, C. M.; Weerasinghe, L.; Day, J. J.; Fukuto, J. M.; Xian, M., Persulfides: current knowledge and challenges in chemistry and chemical biology. *Mol. Biosyst.* **2015**, 11 (7), 1775-85.
139. Yadav, P. K.; Martinov, M.; Vitvitsky, V.; Seravalli, J.; Wedmann, R.; Filipovic, M. R.; Banerjee, R., Biosynthesis and Reactivity of Cysteine Persulfides in Signaling. *J. Am. Chem. Soc.* **2016**, 138 (1), 289-99.
140. Francoleon, N. E.; Carrington, S. J.; Fukuto, J. M., The reaction of H(2)S with oxidized thiols: generation of persulfides and implications to H(2)S biology. *Arch. Biochem. Biophys.* **2011**, 516 (2), 146-53.
141. Mishanina, T. V.; Libiad, M.; Banerjee, R., Biogenesis of reactive sulfur species for signaling by hydrogen sulfide oxidation pathways. *Nat. Chem. Biol.* **2015**, 11 (7), 457-64.
142. Kimura, H., Signaling of hydrogen sulfide and polysulfides. *Antioxid. Redox. Signal.* **2015**, 22 (5), 347-9.
143. Doka, E.; Pader, I.; Biro, A.; Johansson, K.; Cheng, Q.; Ballago, K.; Prigge, J. R.; Pastor-Flores, D.; Dick, T. P.; Schmidt, E. E.; Arner, E. S.; Nagy, P., A novel persulfide detection method reveals protein persulfide- and polysulfide-reducing functions of thioredoxin and glutathione systems. *Sci. Adv.* **2016**, 2 (1), e1500968.
144. Massey, V.; Edmondson, D., On the mechanism of inactivation of xanthine oxidase by cyanide. *J. Biol. Chem.* **1970**, 245 (24), 6595-8.
145. Zhang, D.; Macinkovic, I.; Devarie-Baez, N. O.; Pan, J.; Park, C. M.; Carroll, K. S.; Filipovic, M. R.; Xian, M., Detection of protein S-sulfhydration by a tag-switch technique. *Angew. Chem. Int. Ed. Engl.* **2014**, 53 (2), 575-81.
146. Pan, J.; Carroll, K. S., Persulfide reactivity in the detection of protein s-sulfhydration. *ACS Chem. Biol.* **2013**, 8 (6), 1110-6.
147. Tsurugi, J.; Kawamura, S.; Horii, T., Aryl hydrodisulfides. *J. Org. Chem.* **1971**, 36 (24), 3677-3680.
148. Rooseboom, M.; Commandeur, J. N.; Vermeulen, N. P., Enzyme-catalyzed activation of anticancer prodrugs. *Pharmacol. Rev.* **2004**, 56 (1), 53-102.
149. Hu, L., Prodrug Approaches to Drug Delivery. In *Drug Delivery*, John Wiley & Sons, Inc: 2016; pp 227-271.
150. Langler, R. F.; Angus Ryan, D.; Verma, S. D., Permanganate Oxidation of Disulfides: Monodesulfurization vs Oxygenation at S or alpha-C. *Sulfur Lett.* **2000**, 24 (2), 22.
151. Sawahata, T.; Neal, R. A., Use of 1-fluoro-2,4-dinitrobenzene as a probe for the presence of hydrodisulfide groups in proteins. *Anal. Biochem.* **1982**, 126 (2), 360-4.
152. Elrod, J. W.; Calvert, J. W.; Morrison, J.; Doeller, J. E.; Kraus, D. W.; Tao, L.; Jiao, X.; Scalia, R.; Kiss, L.; Szabo, C.; Kimura, H.; Chow, C. W.; Lefer, D. J., Hydrogen sulfide attenuates myocardial ischemia-reperfusion injury by preservation of mitochondrial function. *Proc. Natl. Acad. Sci. USA* **2007**, 104 (39), 15560-5.
153. Stella, V.; Borchardt, R.; Hageman, M.; Oliyai, R.; Maag, H.; Tilley, J., *Prodrugs: Challenges and Rewards*. 2007th ed.; Springer: New York City, New York, 2007.
154. Lin, C.; Sunkara, G.; Cannon, J. B.; Ranade, V., Recent advances in prodrugs as drug delivery systems. *Am. J. Ther.* **2012**, 19 (1), 33-43.

155. Rautio, J.; Kumpulainen, H.; Heimbach, T.; Oliyai, R.; Oh, D.; Jarvinen, T.; Savolainen, J., Prodrugs: design and clinical applications. *Nat. Rev. Drug. Discov.* **2008**, *7* (3), 255-270.
156. Matikonda, S. S.; Orsi, D. L.; Staudacher, V.; Jenkins, I. A.; Fiedler, F.; Chen, J.; Gamble, A. B., Bioorthogonal prodrug activation driven by a strain-promoted 1,3-dipolar cycloaddition. *Chem. Sci.* **2015**, *6* (2), 1212-1218.
157. Versteegen, R. M.; Rossin, R.; ten Hoeve, W.; Janssen, H. M.; Robillard, M. S., Click to release: instantaneous doxorubicin elimination upon tetrazine ligation. *Angew. Chem. Int. Ed. Engl.* **2013**, *52* (52), 14112-6.
158. Weiss, J. T.; Carragher, N. O.; Unciti-Broceta, A., Palladium-mediated dealkylation of N-propargyl-floxuridine as a bioorthogonal oxygen-independent prodrug strategy. *Sci. Rep.* **2015**, *5*, 9329.
159. Azoulay, M.; Tuffin, G.; Sallem, W.; Florent, J. C., A new drug-release method using the Staudinger ligation. *Bioorg. Med. Chem. Lett.* **2006**, *16* (12), 3147-9.
160. van Brakel, R.; Vulders, R. C.; Bokdam, R. J.; Grull, H.; Robillard, M. S., A doxorubicin prodrug activated by the staudinger reaction. *Bioconjug. Chem.* **2008**, *19* (3), 714-8.
161. Khan, M. Z.; Prebeg, Z.; Kurjakovic, N., A pH-dependent colon targeted oral drug delivery system using methacrylic acid copolymers. I. Manipulation Of drug release using Eudragit L100-55 and Eudragit S100 combinations. *J. Control. Release* **1999**, *58* (2), 215-22.
162. Madhusudhan, A.; Reddy, G. B.; Venkatesham, M.; Veerabhadram, G.; Kumar, D. A.; Natarajan, S.; Yang, M. Y.; Hu, A.; Singh, S. S., Efficient pH dependent drug delivery to target cancer cells by gold nanoparticles capped with carboxymethyl chitosan. *Int. J. Mol. Sci.* **2014**, *15* (5), 8216-34.
163. Chen, H.; Tian, J.; He, W.; Guo, Z., H₂O₂-Activatable and O₂-Evolving Nanoparticles for Highly Efficient and Selective Photodynamic Therapy against Hypoxic Tumor Cells. *J. Am. Chem. Soc.* **2015**, *137* (4), 1539-1547.
164. Peng, X.; Gandhi, V., ROS-activated anticancer prodrugs: a new strategy for tumor-specific damage. *Ther Deliv.* **2012**, *3* (7), 823-833.
165. Liu, J.; Pang, Y.; Zhu, Z.; Wang, D.; Li, C.; Huang, W.; Zhu, X.; Yan, D., Therapeutic Nanocarriers with Hydrogen Peroxide-Triggered Drug Release for Cancer Treatment. *Biomacromolecules* **2013**, *14* (5), 1627-1636.
166. Latorre, A.; Somoza, A., Glutathione-triggered drug release from nanostructures. *Curr. Top. Med. Chem.* **2014**, *14* (23), 2662-71.
167. Huang, X.; Zhang, T.; Goswami, A.; Luo, F.; Asefa, T., Glutathione-triggered release of model drug molecules from mesoporous silica nanoparticles via a non-redox process. *RSC Adv.* **2015**, *5* (36), 28836-28839.
168. Wang, T.; Ng, D. Y.; Wu, Y.; Thomas, J.; TamTran, T.; Weil, T., Bis-sulfide bioconjugates for glutathione triggered tumor responsive drug release. *Chem. Commun. (Camb)* **2014**, *50* (9), 1116-8.
169. Ock, K.; Jeon, W. I.; Ganbold, E. O.; Kim, M.; Park, J.; Seo, J. H.; Cho, K.; Joo, S.-W.; Lee, S. Y., Real-Time Monitoring of Glutathione-Triggered Thiopurine Anticancer Drug Release in Live Cells Investigated by Surface-Enhanced Raman Scattering. *Anal. Chem.* **2012**, *84* (5), 2172-2178.
170. Wang, X.; Cai, X.; Hu, J.; Shao, N.; Wang, F.; Zhang, Q.; Xiao, J.; Cheng, Y., Glutathione-Triggered “Off-On” Release of Anticancer Drugs from Dendrimer-Encapsulated Gold Nanoparticles. *J. Am. Chem. Soc.* **2013**, *135* (26), 9805-9810.

171. Hong, R.; Han, G.; Fernández, J. M.; Kim, B.-j.; Forbes, N. S.; Rotello, V. M., Glutathione-Mediated Delivery and Release Using Monolayer Protected Nanoparticle Carriers. *J. Am. Chem. Soc.* **2006**, *128* (4), 1078-1079.
172. Al-Nahain, A.; Lee, S. Y.; In, I.; Lee, K. D.; Park, S. Y., Triggered pH/redox responsive release of doxorubicin from prepared highly stable graphene with thiol grafted Pluronic. *Int. J. Pharm.* **2013**, *450* (1-2), 208-17.
173. Conda-Sheridan, M.; Lee, S. S.; Preslar, A. T.; Stupp, S. I., Esterase-activated release of naproxen from supramolecular nanofibres. *Chem. Commun. (Camb)* **2014**, *50* (89), 13757-60.
174. Amsberry, K. L.; Borchardt, R. T., Amine prodrugs which utilize hydroxy amide lactonization. I. A potential redox-sensitive amide prodrug. *Pharm. Res.* **1991**, *8* (3), 323-30.
175. van Rijt, S. H.; Böülübas, D. A.; Argyo, C.; Datz, S.; Lindner, M.; Eickelberg, O.; Königshoff, M.; Bein, T.; Meiners, S., Protease-Mediated Release of Chemotherapeutics from Mesoporous Silica Nanoparticles to ex Vivo Human and Mouse Lung Tumors. *ACS Nano* **2015**, *9* (3), 2377-2389.
176. Hamilton, J. R.; Trejo, J., Challenges and Opportunities in Protease-Activated Receptor Drug Development. *Annu. Rev. Pharmacol. Toxicol.* **2016**.
177. Choi, K. Y.; Swierczewska, M.; Lee, S.; Chen, X., Protease-activated drug development. *Theranostics* **2012**, *2* (2), 156-78.
178. Ji, C.; Miller, M. J., Chemical syntheses and in vitro antibacterial activity of two desferrioxamine B-ciprofloxacin conjugates with potential esterase and phosphatase triggered drug release linkers. *Bioorg. Med. Chem.* **2012**, *20* (12), 3828-3836.
179. Nam, N. H.; Kim, Y.; You, Y. J.; Hong, D. H.; Kim, H. M.; Ahn, B. Z., Water soluble prodrugs of the antitumor agent 3-[(3-amino-4-methoxy)phenyl]-2-(3,4,5-trimethoxyphenyl)cyclopent-2-ene-1-one. *Bioorg. Med. Chem.* **2003**, *11* (6), 1021-9.
180. Philip, A. K.; Philip, B., Colon Targeted Drug Delivery Systems: A Review on Primary and Novel Approaches. *Oman Med. J.* **2010**, *25* (2), 79-87.
181. Rossin, R.; van Duijnhoven, S. M. J.; ten Hoeve, W.; Janssen, H. M.; Kleijn, L. H. J.; Hoeben, F. J. M.; Versteegen, R. M.; Robillard, M. S., Triggered Drug Release from an Antibody–Drug Conjugate Using Fast “Click-to-Release” Chemistry in Mice. *Bioconjug. Chem.* **2016**, *27* (7), 1697-1706.
182. Agarwal, P.; Bertozzi, C. R., Site-Specific Antibody–Drug Conjugates: The Nexus of Bioorthogonal Chemistry, Protein Engineering, and Drug Development. *Bioconjug. Chem.* **2015**, *26* (2), 176-192.
183. Kern, J. C.; Cancilla, M.; Dooney, D.; Kwasnjuk, K.; Zhang, R.; Beaumont, M.; Figueroa, I.; Hsieh, S.; Liang, L.; Tomazela, D.; Zhang, J.; Brandish, P. E.; Palmieri, A.; Stivers, P.; Cheng, M.; Feng, G.; Geda, P.; Shah, S.; Beck, A.; Bresson, D.; Firdos, J.; Gately, D.; Knudsen, N.; Manibusan, A.; Schultz, P. G.; Sun, Y.; Garbaccio, R. M., Discovery of Pyrophosphate Diesters as Tunable, Soluble, and Bioorthogonal Linkers for Site-Specific Antibody–Drug Conjugates. *J. Am. Chem. Soc.* **2016**, *138* (4), 1430-1445.
184. Chudasama, V.; Maruani, A.; Caddick, S., Recent advances in the construction of antibody-drug conjugates. *Nat. Chem.* **2016**, *8* (2), 114-119.
185. Zwicke, G. L.; Mansoori, G. A.; Jeffery, C. J., Utilizing the folate receptor for active targeting of cancer nanotherapeutics. *Nano Rev.* **2012**, *3*, 18496-18507.
186. Zhao, X.; Li, H.; Lee, R. J., Targeted drug delivery via folate receptors. *Expert. Opin. Drug. Deliv.* **2008**, *5* (3), 309-19.

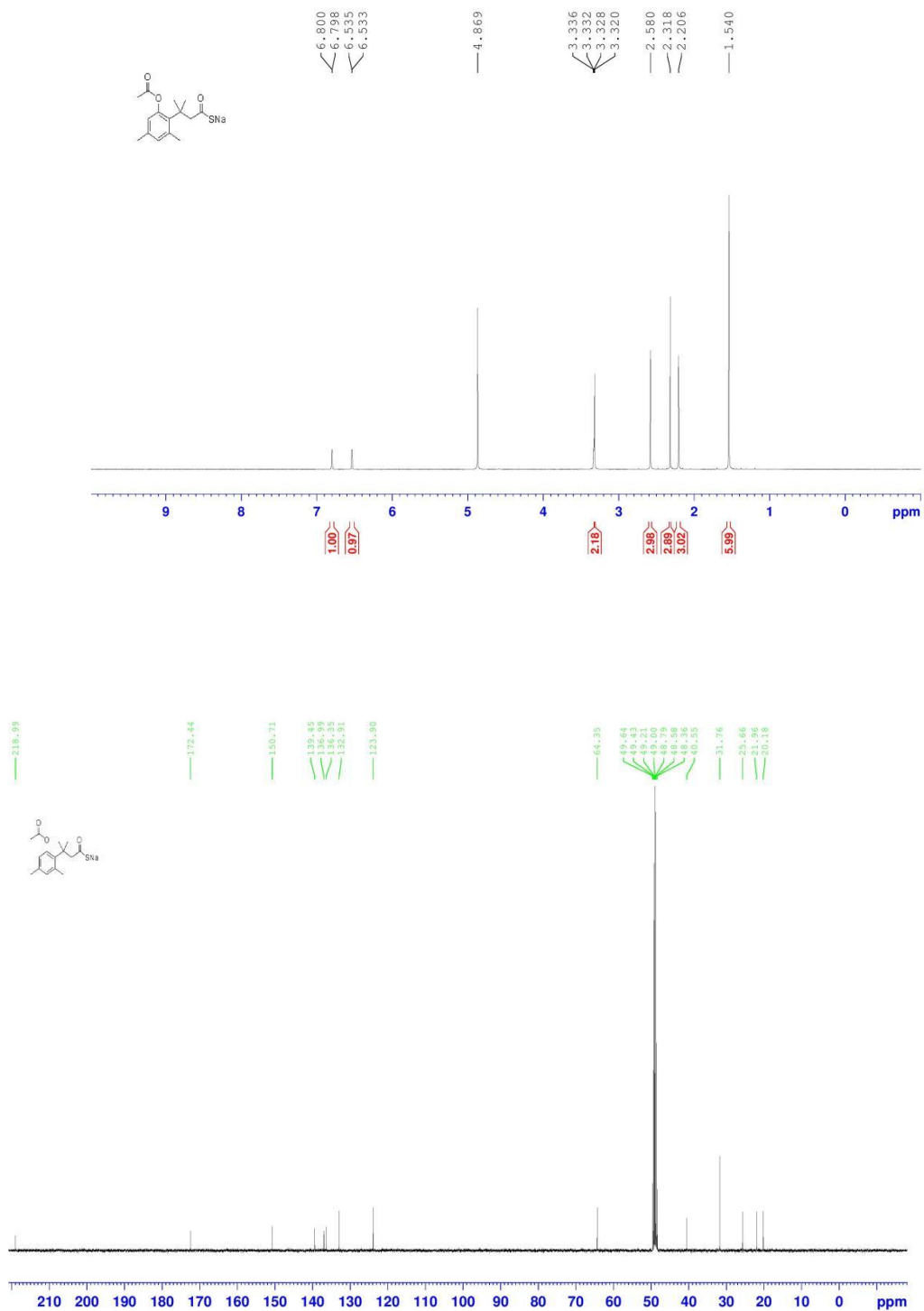
187. Ahmed, M.; Narain, R., Carbohydrate-based materials for targeted delivery of drugs and genes to the liver. *Nanomedicine (London, England)* **2015**, 10 (14), 2263-88.
188. DiPippo, V. A.; Olson, W. C.; Nguyen, H. M.; Brown, L. G.; Vessella, R. L.; Corey, E., Efficacy studies of an antibody-drug conjugate PSMA-ADC in patient-derived prostate cancer xenografts. *Prostate* **2015**, 75 (3), 303-13.
189. Jin, W.; Qin, B.; Chen, Z.; Liu, H.; Barve, A.; Cheng, K., Discovery of PSMA-specific peptide ligands for targeted drug delivery. *Int. J. Pharm.* **2016**, 513 (1-2), 138-147.
190. Dassie, J. P.; Hernandez, L. I.; Thomas, G. S.; Long, M. E.; Rockey, W. M.; Howell, C. A.; Chen, Y.; Hernandez, F. J.; Liu, X. Y.; Wilson, M. E.; Allen, L.-A.; Vaena, D. A.; Meyerholz, D. K.; Giangrande, P. H., Targeted Inhibition of Prostate Cancer Metastases with an RNA Aptamer to Prostate-specific Membrane Antigen. *Mol. Ther.* **2014**, 22 (11), 1910-1922.
191. Ji, X.; Zhou, C.; Ji, K.; Aghoghovbia, R. E.; Pan, Z.; Chittavong, V.; Ke, B.; Wang, B., Click and Release: A Chemical Strategy toward Developing Gasotransmitter Prodrugs by Using an Intramolecular Diels-Alder Reaction. *Angew. Chem. Int. Ed. Engl.* **2016**, 55 (51), 15846-15851.
192. Wang, D.; Viennois, E.; Ji, K.; Damera, K.; Draganov, A.; Zheng, Y.; Dai, C.; Merlin, D.; Wang, B., A click-and-release approach to CO prodrugs. *Chem. Commun. (Camb)* **2014**, 50 (100), 15890-3.
193. Wang, W.; Ji, X.; Du, Z.; Wang, B., Sulfur dioxide prodrugs: triggered release of SO₂ via a click reaction. *Chem. Commun. (Camb)* **2017**, 53 (8), 1370-1373.
194. Rossin, R.; van Duijnhoven, S. M.; Ten Hoeve, W.; Janssen, H. M.; Kleijn, L. H.; Hoeben, F. J.; Versteegen, R. M.; Robillard, M. S., Triggered Drug Release from an Antibody-Drug Conjugate Using Fast "Click-to-Release" Chemistry in Mice. *Bioconjug. Chem.* **2016**, 27 (7), 1697-706.
195. Ji, X.; El-labbad, E. M.; Ji, K.; Lasheen, D. S.; Serya, R. A. T.; Abouzid, K. A.; Wang, B., Click and Release: SO₂ Prodrugs with Tunable Release Rates. *Org. Lett.* **2017**, 19 (4), 818-821.
196. Ji, X.; Ji, K.; Chittavong, V.; Aghoghovbia, R. E.; Zhu, M.; Wang, B., Click and Fluoresce: A Bioorthogonally Activated Smart Probe for Wash-Free Fluorescent Labeling of Biomolecules. *J. Org. Chem.* **2017**, 82 (3), 1471-1476.
197. Jimenez-Moreno, E.; Guo, Z.; Oliveira, B. L.; Albuquerque, I. S.; Kitowski, A.; Guerreiro, A.; Boutureira, O.; Rodrigues, T.; Jimenez-Oses, G.; Bernardes, G. J., Vinyl Ether/Tetrazine Pair for the Traceless Release of Alcohols in Cells. *Angew. Chem. Int. Ed. Engl.* **2017**, 56 (1), 243-247.
198. Li, J.; Jia, S.; Chen, P. R., Diels-Alder reaction-triggered bioorthogonal protein decaging in living cells. *Nat. Chem. Biol.* **2014**, 10 (12), 1003-5.
199. Eising, S.; Lelivelt, F.; Bonger, K. M., Vinylboronic Acids as Fast Reacting, Synthetically Accessible, and Stable Bioorthogonal Reactants in the Carboni-Lindsey Reaction. *Angew. Chem. Int. Ed. Engl.* **2016**, 55 (40), 12243-7.
200. Luo, J.; Liu, Q.; Morihiro, K.; Deiters, A., Small-molecule control of protein function through Staudinger reduction. *Nat. Chem.* **2016**, 8 (11), 1027-1034.
201. Anseth, K. S.; Klok, H.-A., Click Chemistry in Biomaterials, Nanomedicine, and Drug Delivery. *Biomacromolecules* **2016**, 17 (1), 1-3.
202. Kang, J.; Hilmersson, G.; Santamaría, J.; Rebek, J., Diels–Alder Reactions through Reversible Encapsulation. *Journal of the American Chemical Society* **1998**, 120 (15), 3650-3656.
203. Kang, J.; Santamaría, J.; Hilmersson, G.; Rebek, J., Self-Assembled Molecular Capsule Catalyzes a Diels–Alder Reaction. *Journal of the American Chemical Society* **1998**, 120 (29), 7389-7390.

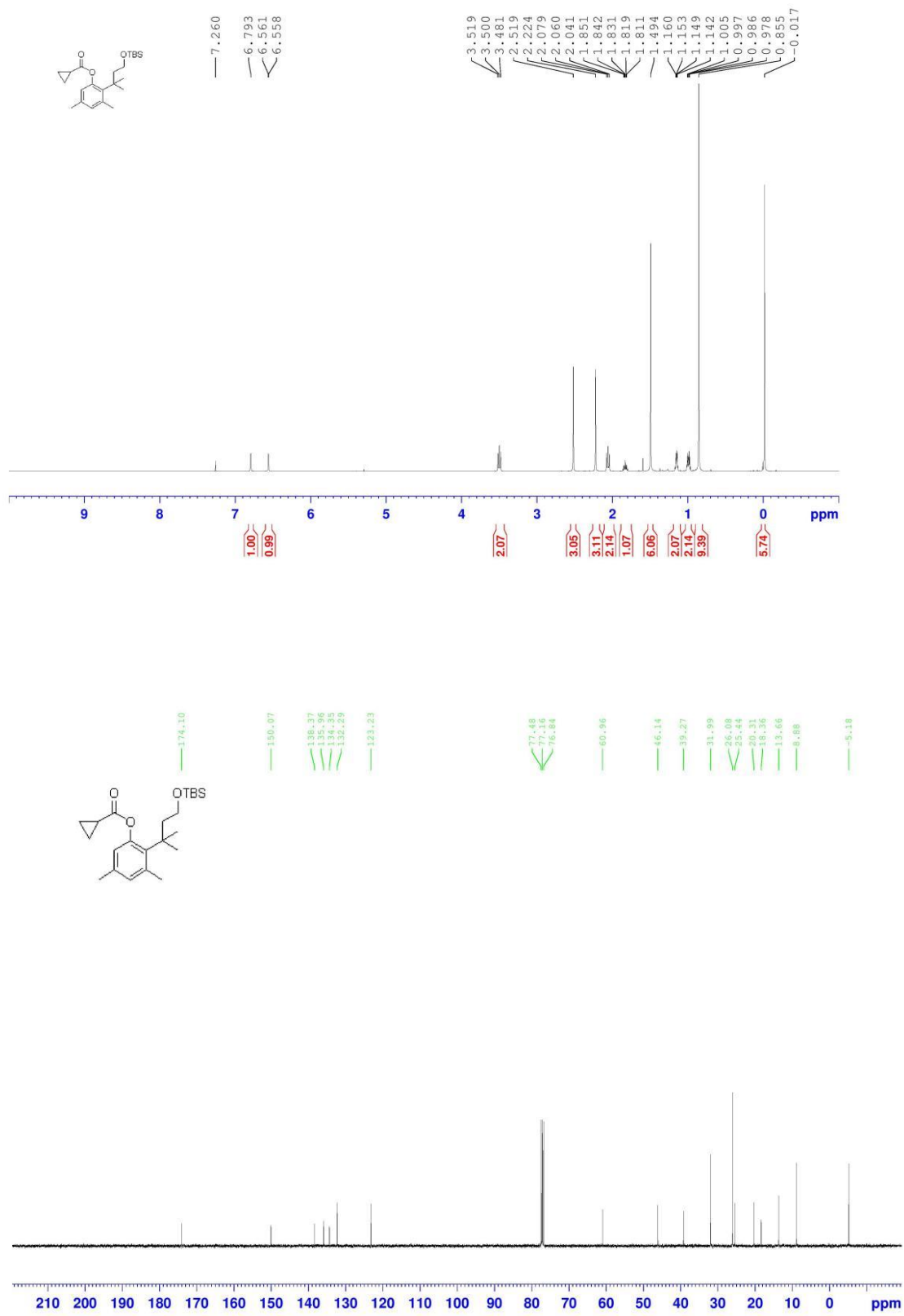
204. Murase, T.; Horiuchi, S.; Fujita, M., Naphthalene Diels–Alder in a Self-Assembled Molecular Flask. *Journal of the American Chemical Society* **2010**, *132* (9), 2866-2867.
205. Chen, W.; Wang, D.; Dai, C.; Hamelberg, D.; Wang, B., Clicking 1,2,4,5-Tetrazine and Cyclooctynes with Tunable Reaction Rates. *Chem. Commun.* **2012**, (48), 1736-1738
206. Wang, D.; Chen, W.; Zhang, Y.; Dai, C.; Wang, B., 3,6-Substituted-1,2,4,5-tetrazines: Tuning Reaction Rates for Staged Labeling Applications. *Org. Biomol. Chem.* **2014**, *12*, 3950-3955.
207. Murphy, M. P.; Smith, R. A. J., Targeting Antioxidants to Mitochondria by Conjugation to Lipophilic Cations. *Ann. Rev. Pharmacol. Toxicol.* **2007**, *47*, 629-656.
208. Blackman, M. L.; Royzen, M.; Fox, J. M., Tetrazine Ligation: Fast Bioconjugation Based on Inverse-Electron-Demand Diels–Alder Reactivity. *J. Am. Chem. Soc.* **2008**, *130* (41), 13518-13519.
209. Devaraj, N. K.; Weissleder, R.; Hilderbrand, S. A., Tetrazine-based cycloadditions: application to pretargeted live cell imaging. *Bioconjug. Chem.* **2008**, *19* (12), 2297-2299.
210. Smith, R. A. J.; Porteous, C. M.; Gane, A. M.; Murphy, M. P., Delivery of bioactive molecules to mitochondria *in vivo*. *Proc. Natl. Acad. Sci. USA* **2003**, *100* (9), 5407-5412.
211. Janssen, M. J. H.; Crommelin, D. J. A.; Storm, G.; Hulshoff, A., Doxorubicin decomposition on storage. Effect of pH, type of buffer and liposome encapsulation. *Int. J. Pharm.* **1985**, *23* (1), 1-11.
212. Wang, B.; Hu, L.; Siahaan, T. J., *Drug Delivery: Principles and Applications*, 2nd Edition. 2016.
213. Agard, N. J.; Baskin, J. M.; Prescher, J. A.; Lo, A.; Bertozzi, C. R., A Comparative Study of Bioorthogonal Reactions with Azides. *ACS Chem. Biol.* **2006**, *1* (10), 644-648.
214. Zhou, P.; Yao, J.; Hu, G.; Fang, J., Naphthalimide Scaffold Provides Versatile Platform for Selective Thiol Sensing and Protein Labeling. *ACS Chem. Biol.* **2016**, *11* (4), 1098-1105.
215. Liang, Y.-F.; Jiao, N., Highly Efficient C \square H Hydroxylation of Carbonyl Compounds with Oxygen under Mild Conditions. *Angew. Chem. Int. Ed. Engl.* **2014**, *53* (2), 548-552.
216. Hagendorf, T.; Bräse, S., A Route to Cyclooct-2-ynol and Its Functionalization by Mitsunobu Chemistry. *Eur. J. Org. Chem.* **2014**, *2014* (6), 1280-1286.
217. Perez, H. L.; Cardarelli, P. M.; Deshpande, S.; Gangwar, S.; Schroeder, G. M.; Vite, G. D.; Borzilleri, R. M., Antibody-drug conjugates: current status and future directions. *Drug Discov. Today* **2014**, *19* (7), 869-81.
218. Levitz, S. M.; Diamond, R. D., A rapid colorimetric assay of fungal viability with the tetrazolium salt MTT. *J. Infect. Dis.* **1985**, *152* (5), 938-45.
219. Frisch, M. J.; Trucks, G. W.; Schlegel, H. B.; Scuseria, G. E.; Robb, M. A.; Cheeseman, J. R.; Scalmani, G.; Barone, V.; Mennucci, B.; Petersson, G. A.; Nakatsuji, H.; Caricato, M.; Li, X.; Hratchian, H. P.; Izmaylov, A. F.; Bloino, J.; Zheng, G.; Sonnenberg, J. L.; Hada, M.; Ehara, M.; Toyota, K.; Fukuda, R.; Hasegawa, J.; Ishida, M.; Nakajima, T.; Honda, Y.; Kitao, O.; Nakai, H.; Vreven, T.; Montgomery Jr., J. A.; Peralta, J. E.; Ogliaro, F.; Bearpark, M. J.; Heyd, J.; Brothers, E. N.; Kudin, K. N.; Staroverov, V. N.; Kobayashi, R.; Normand, J.; Raghavachari, K.; Rendell, A. P.; Burant, J. C.; Iyengar, S. S.; Tomasi, J.; Cossi, M.; Rega, N.; Millam, N. J.; Klene, M.; Knox, J. E.; Cross, J. B.; Bakken, V.; Adamo, C.; Jaramillo, J.; Gomperts, R.; Stratmann, R. E.; Yazyev, O.; Austin, A. J.; Cammi, R.; Pomelli, C.; Ochterski, J. W.; Martin, R. L.; Morokuma, K.; Zakrzewski, V. G.; Voth, G. A.; Salvador, P.; Dannenberg, J. J.; Dapprich, S.; Daniels, A. D.; Farkas, Ö.; Foresman, J. B.; Ortiz, J. V.; Cioslowski, J.; Fox, D. J. *Gaussian 09, Revision C.01*, Gaussian, Inc.: Wallingford, CT, USA, 2009.

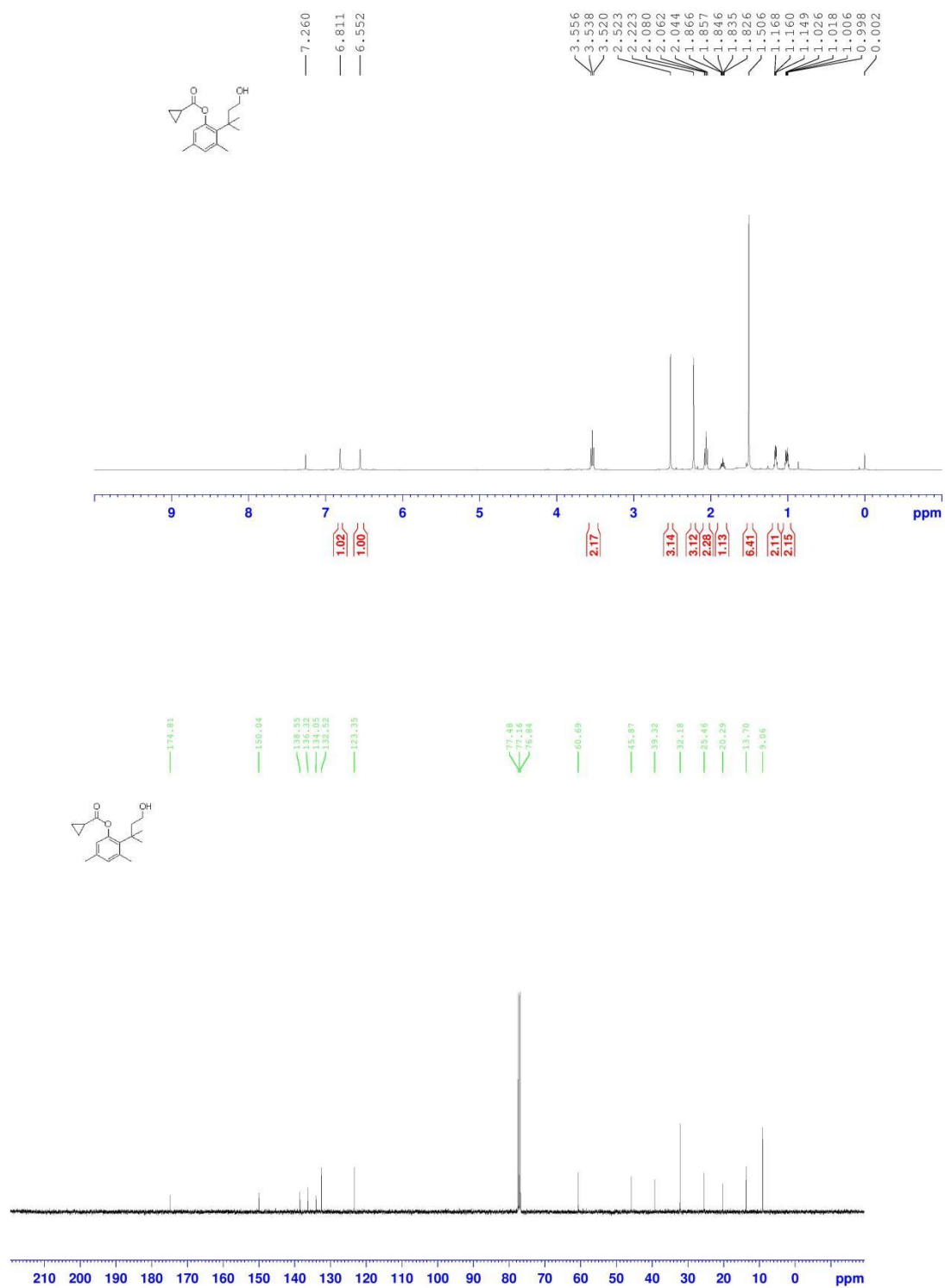
220. Becke, A. D., Density - functional thermochemistry. III. The role of exact exchange. *J. Chem. Phys.* **1993**, *98* (7), 5648-5652.
221. Lee, C.; Yang, W.; Parr, R. G., Development of the Colle-Salvetti correlation-energy formula into a functional of the electron density. *Phys. Rev. B* **1988**, *37* (2), 785-789.
222. Sarajlic;, S.; Edirisinghe;, N.; Lukinov;, Y.; Walters;, M.; Davis;, B.; Faroux, G., Orion: Discovery Environment for HPC Research and Bridging XSEDE Resources. In *Proceedings of the XSEDE16 Conference on Diversity, Big Data, and Science at Scale (XSEDE16)*, ACM: NY, USA, 2016; Vol. Article 54, p 5.
223. Bahar, F. G.; Ohura, K.; Ogihara, T.; Imai, T., Species difference of esterase expression and hydrolase activity in plasma. *J. Pharm. Sci.* **2012**, *101*, 3979-88.

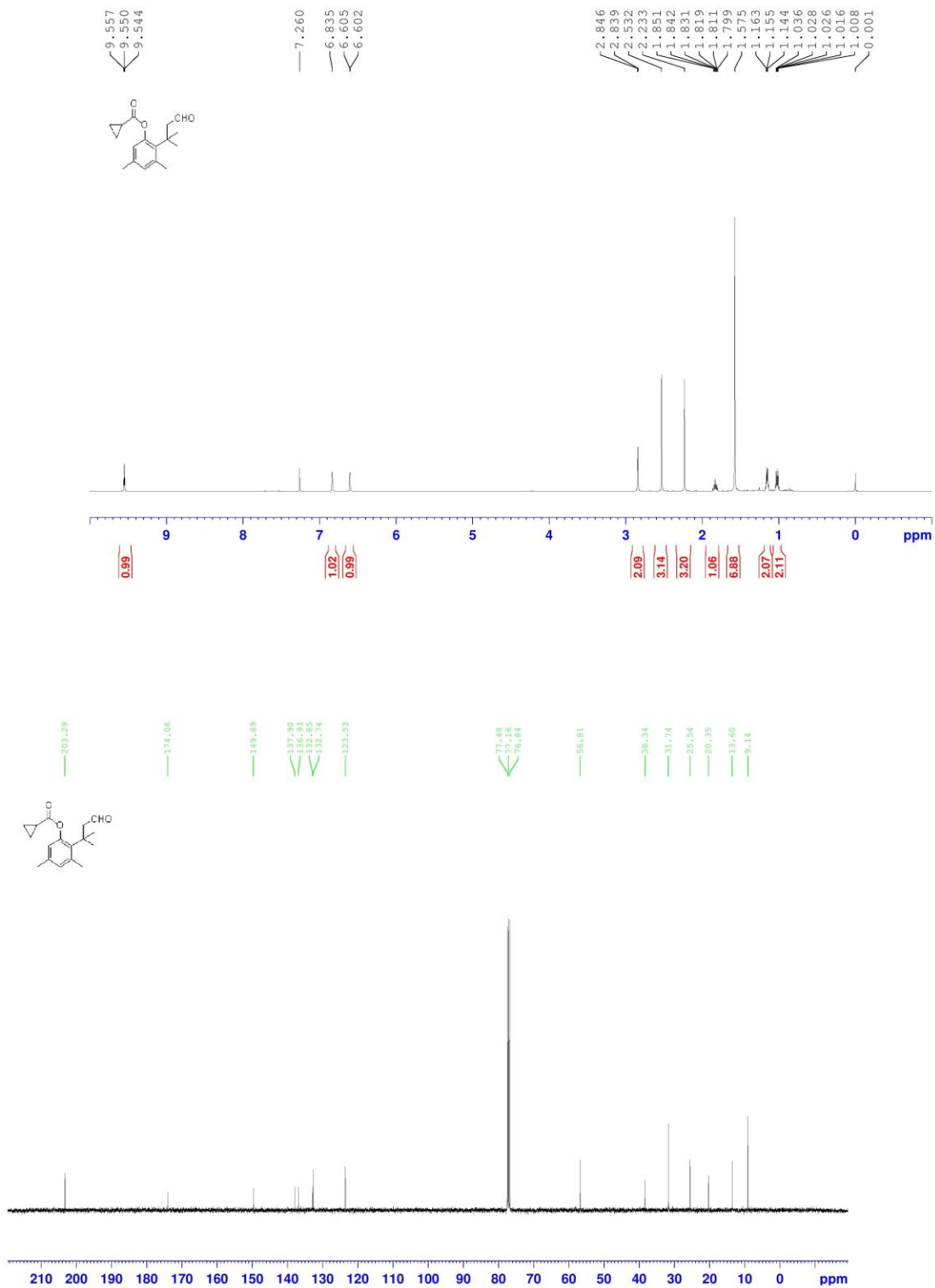
APPENDICS

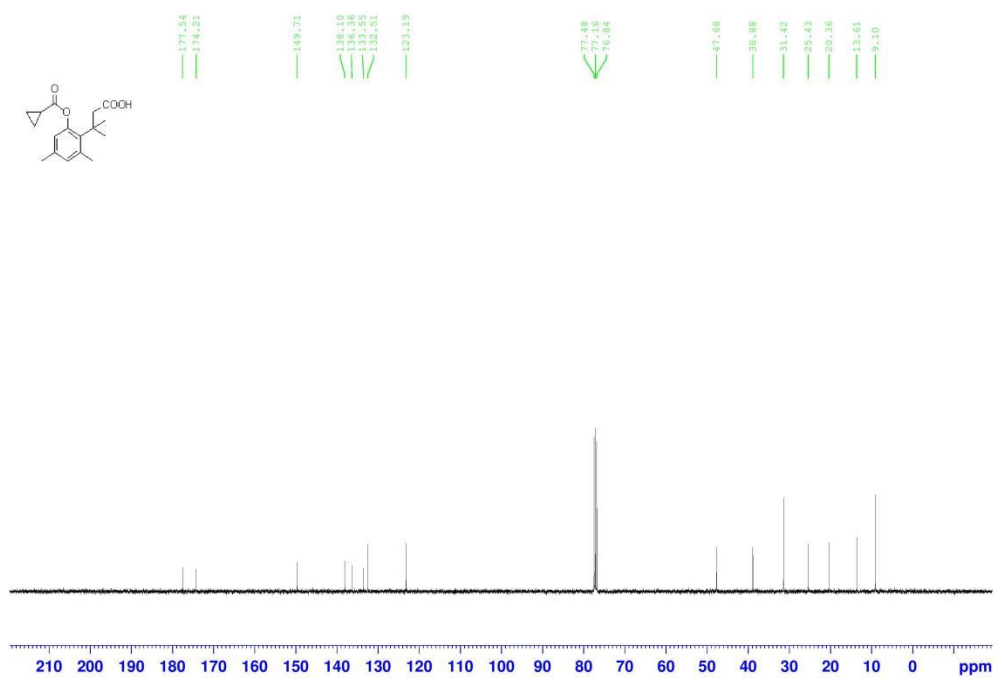
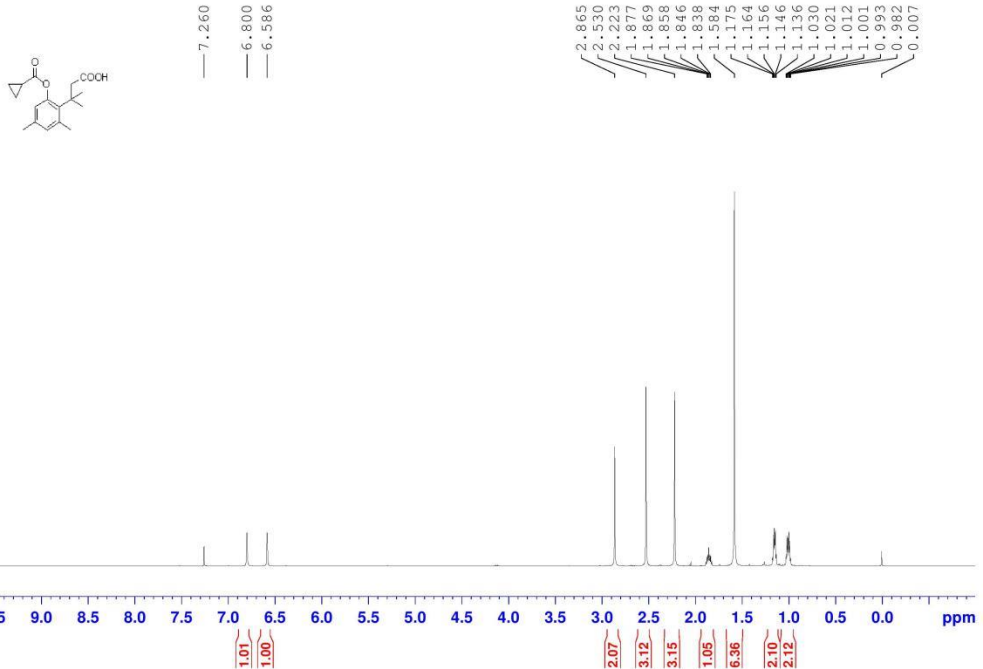
Appendix A. ^1H and ^{13}C Spectra of compounds in chapter 1

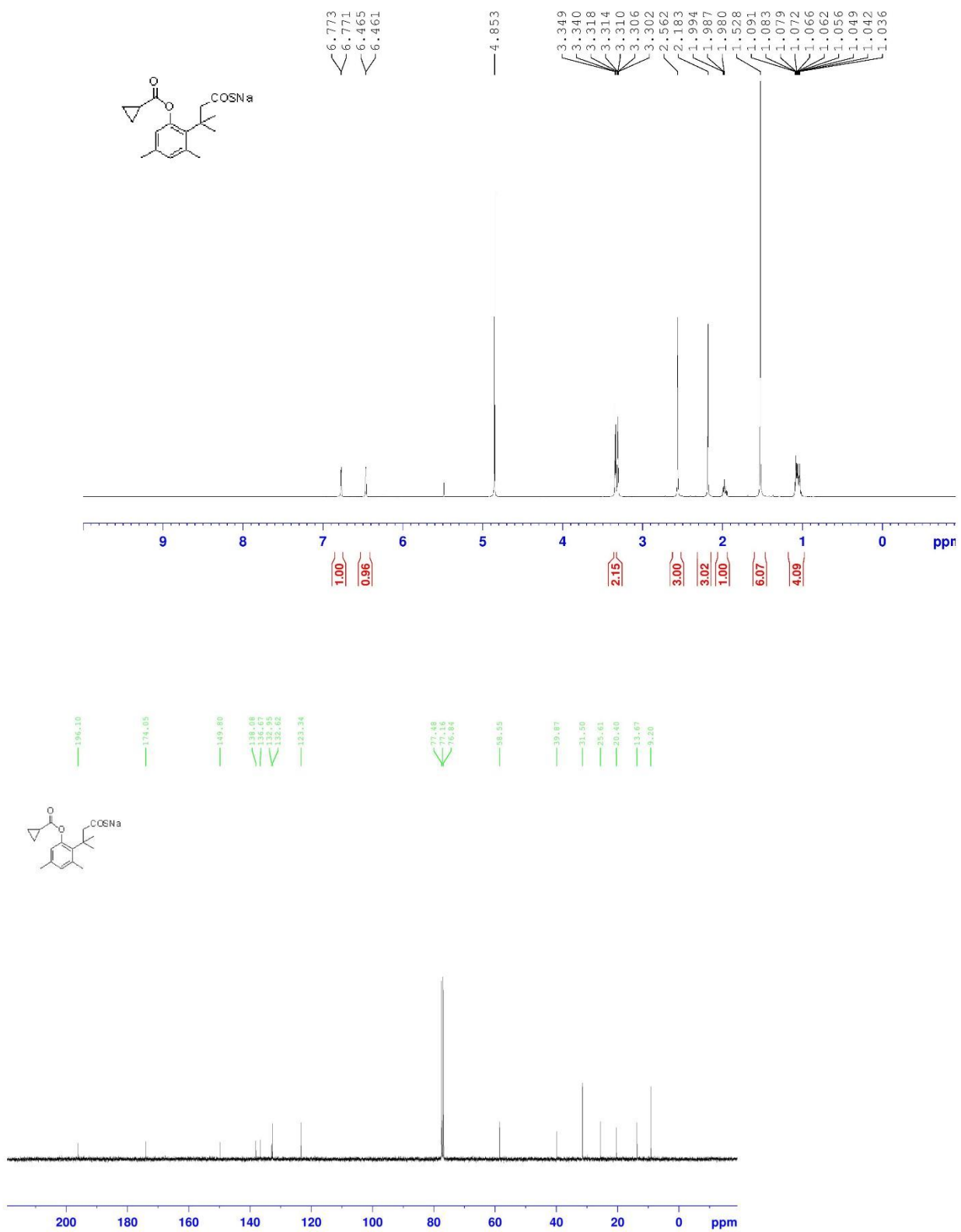


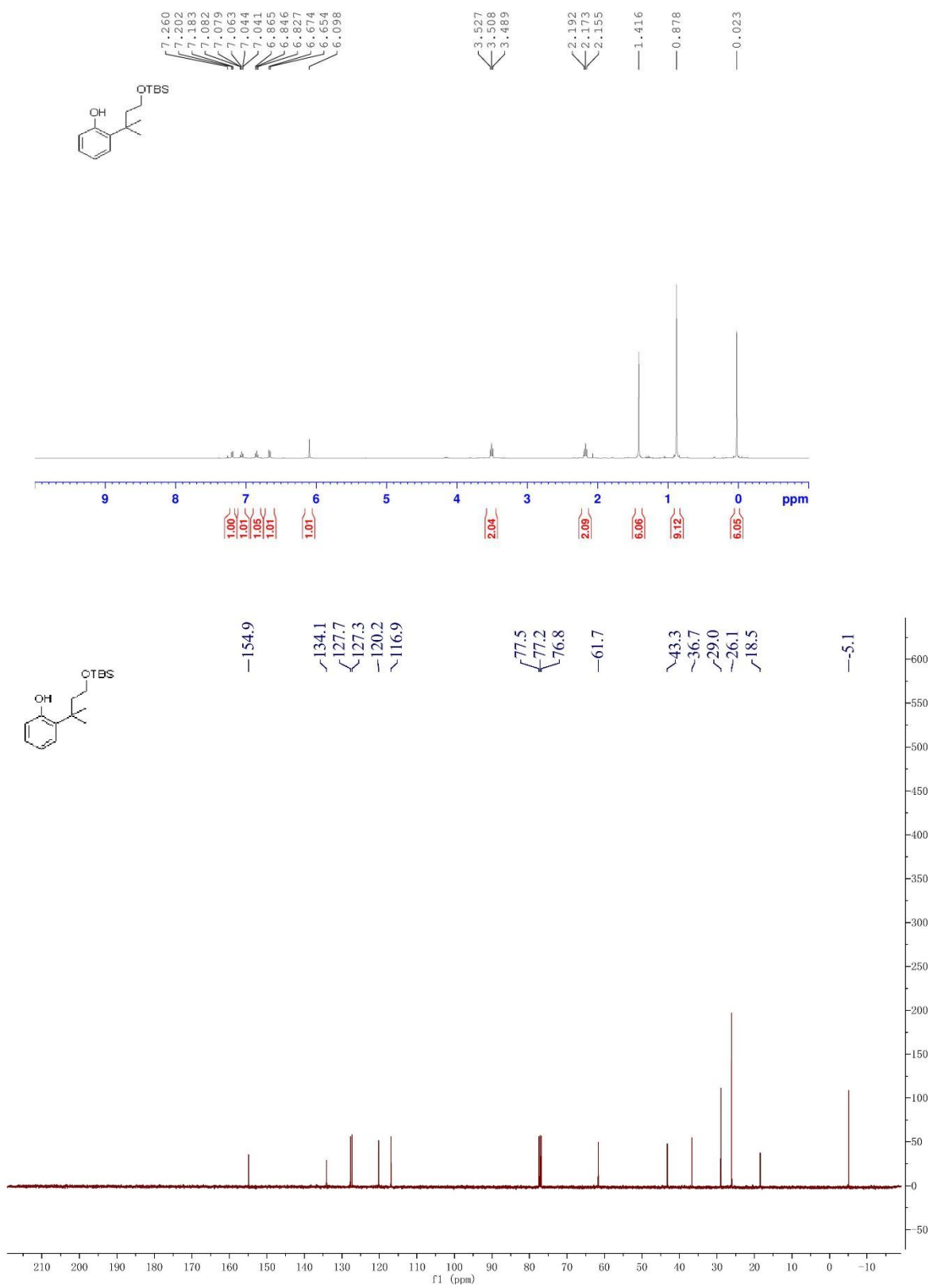


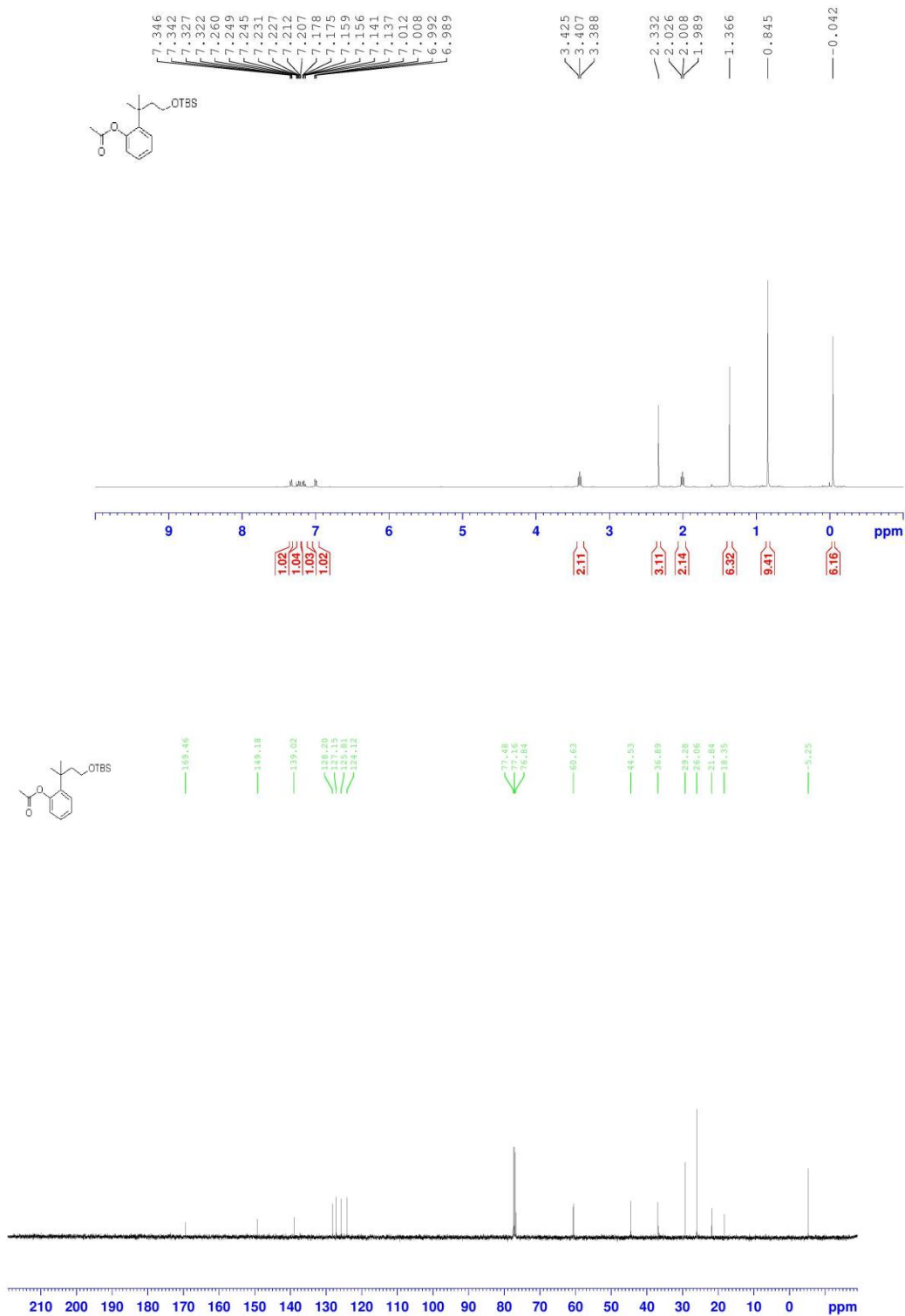


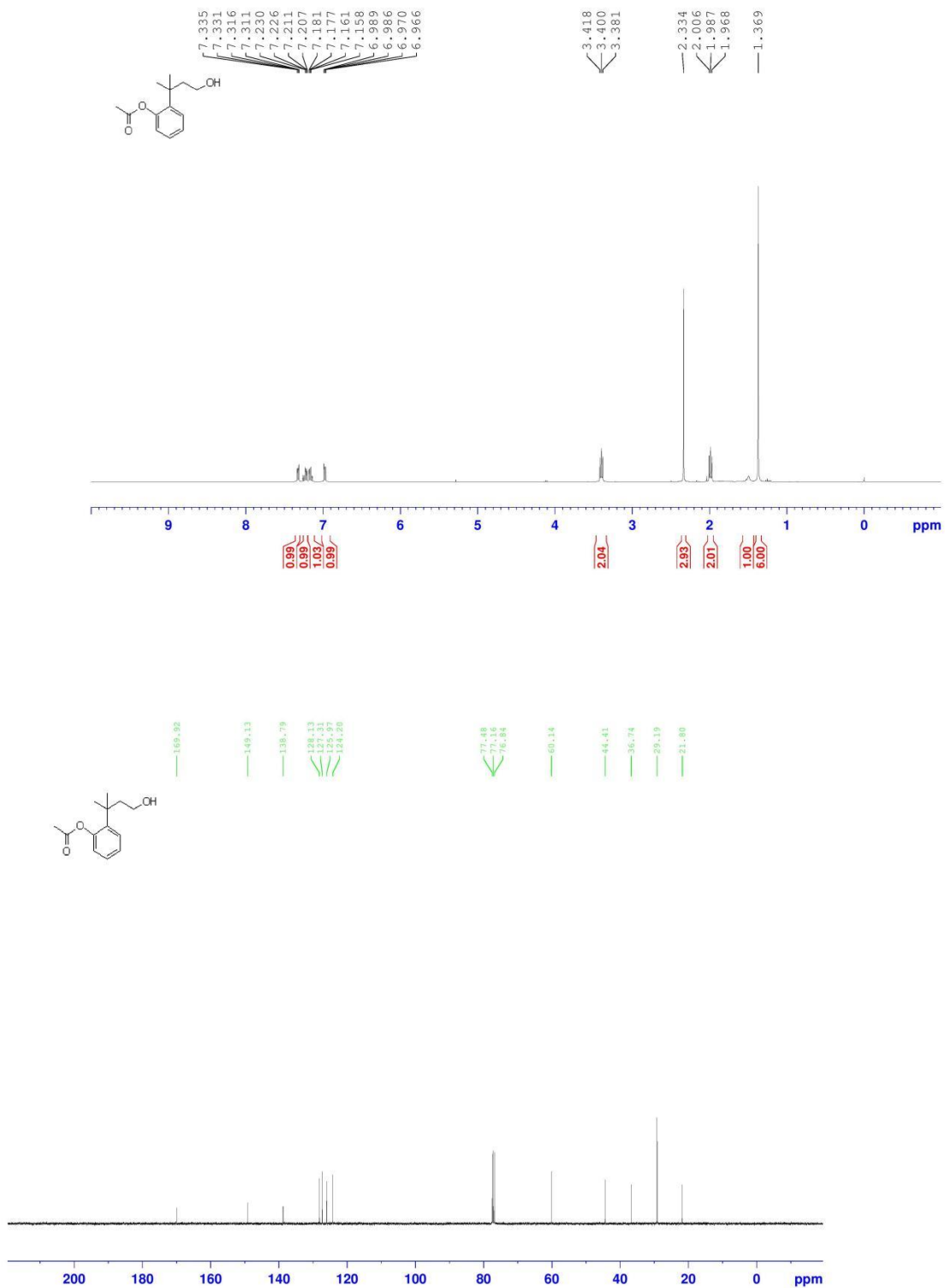


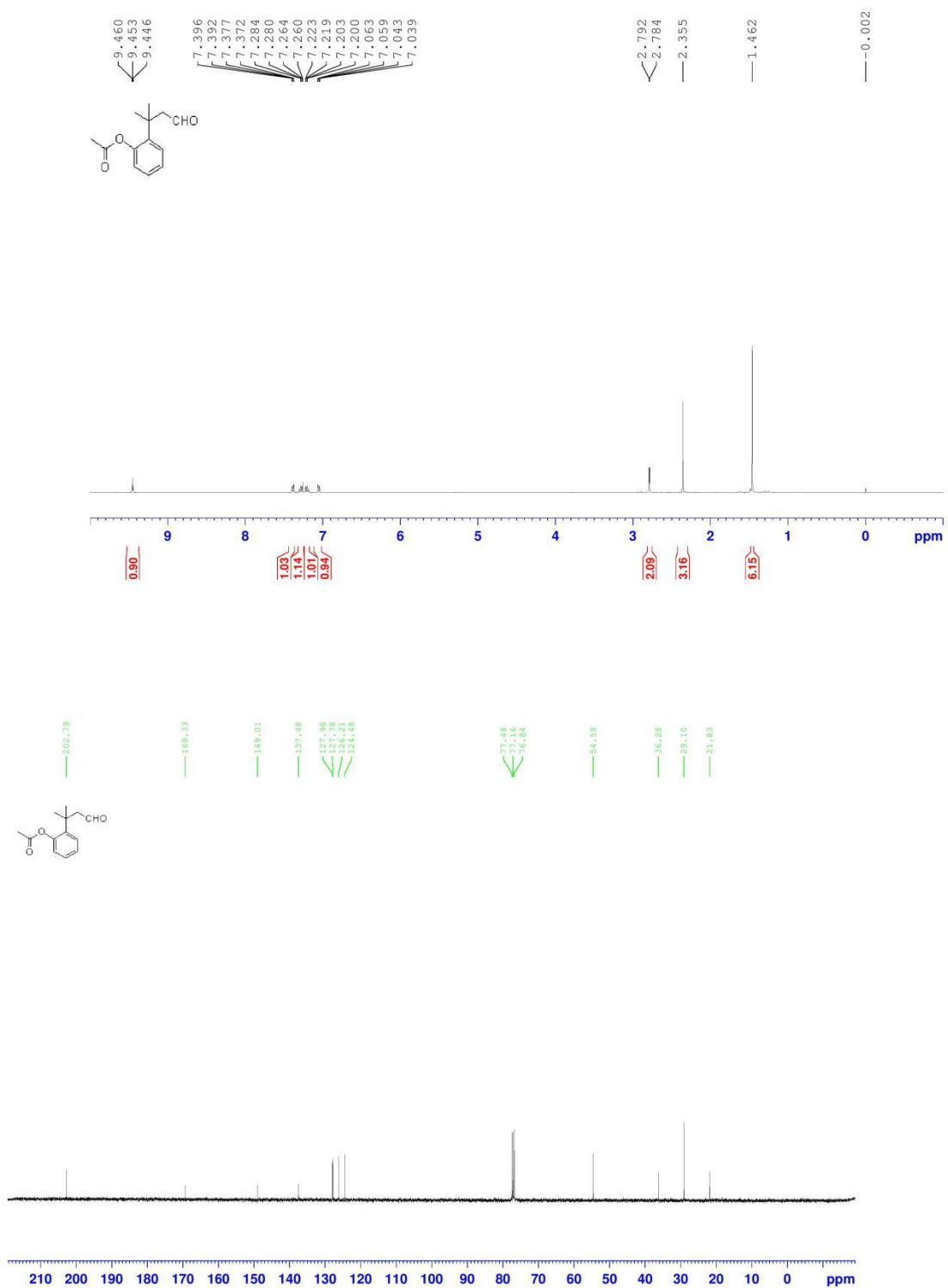


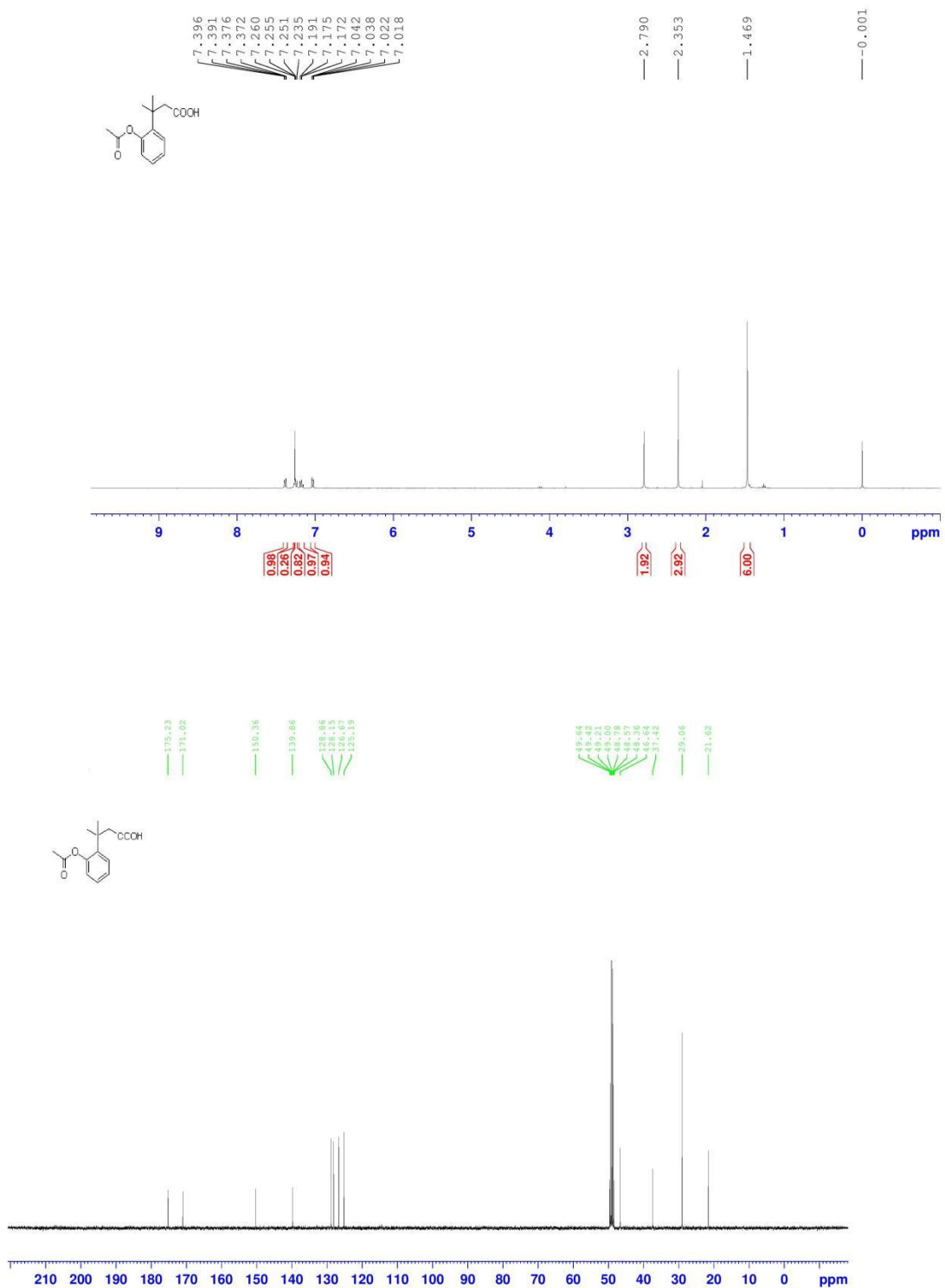


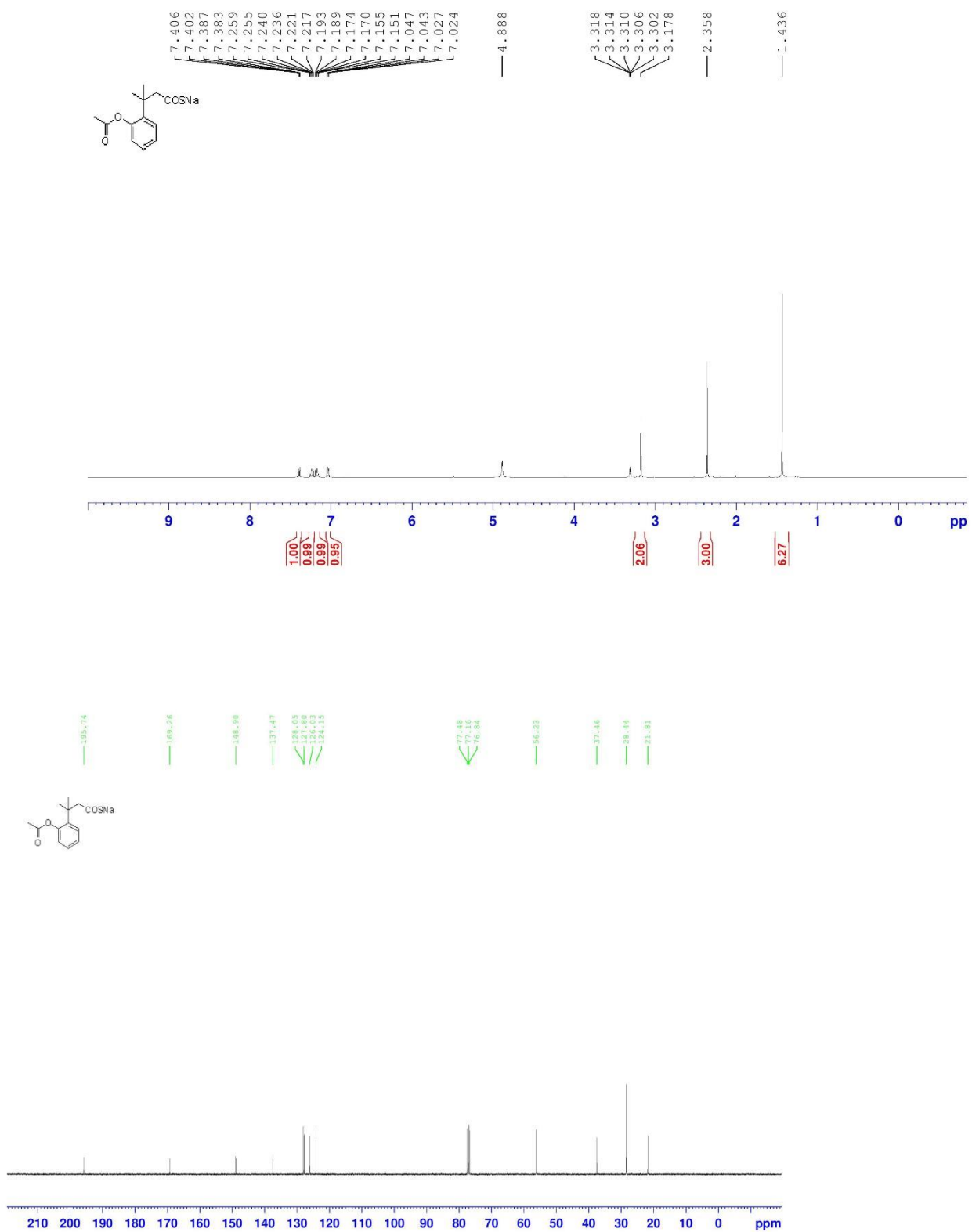


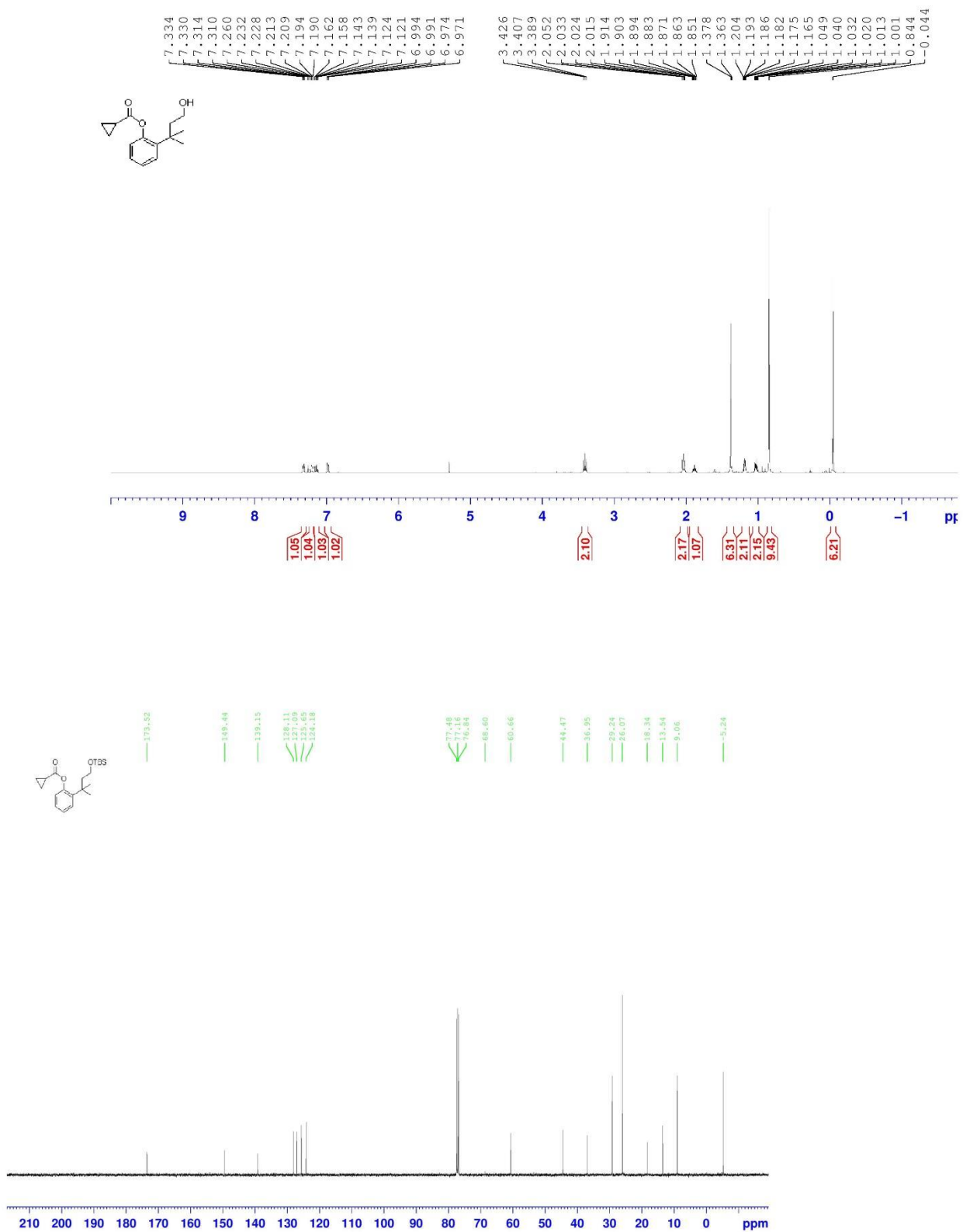


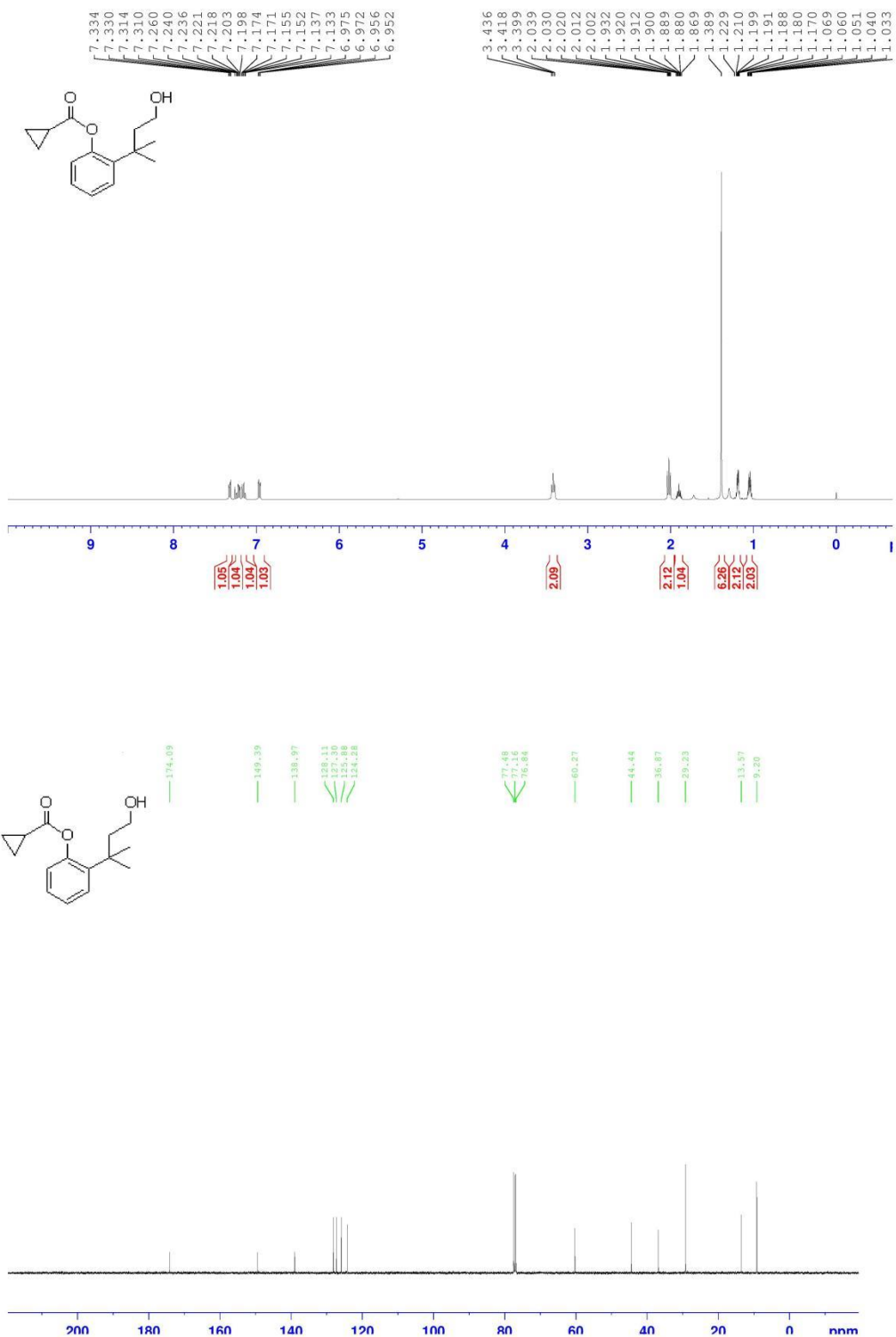


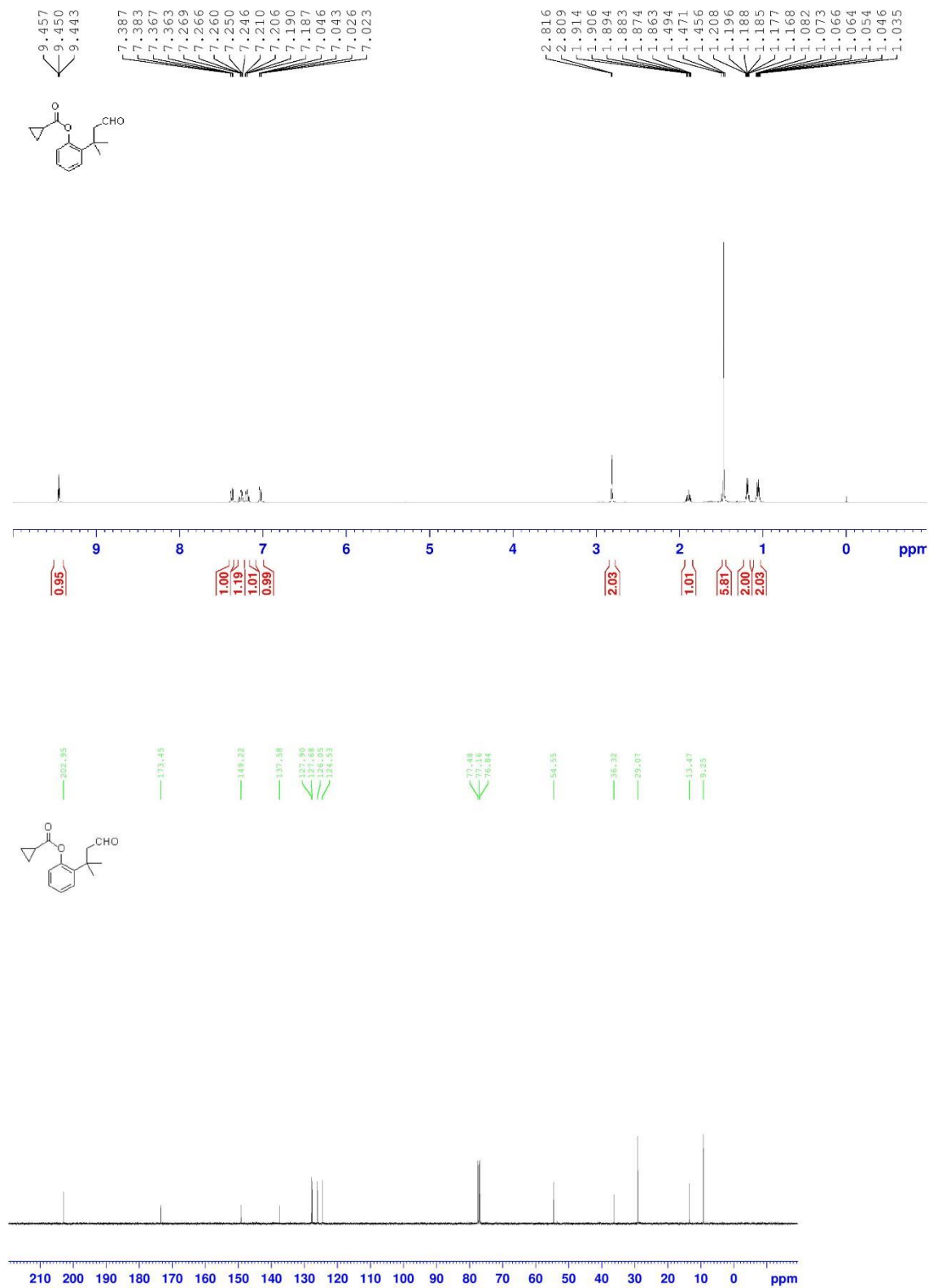


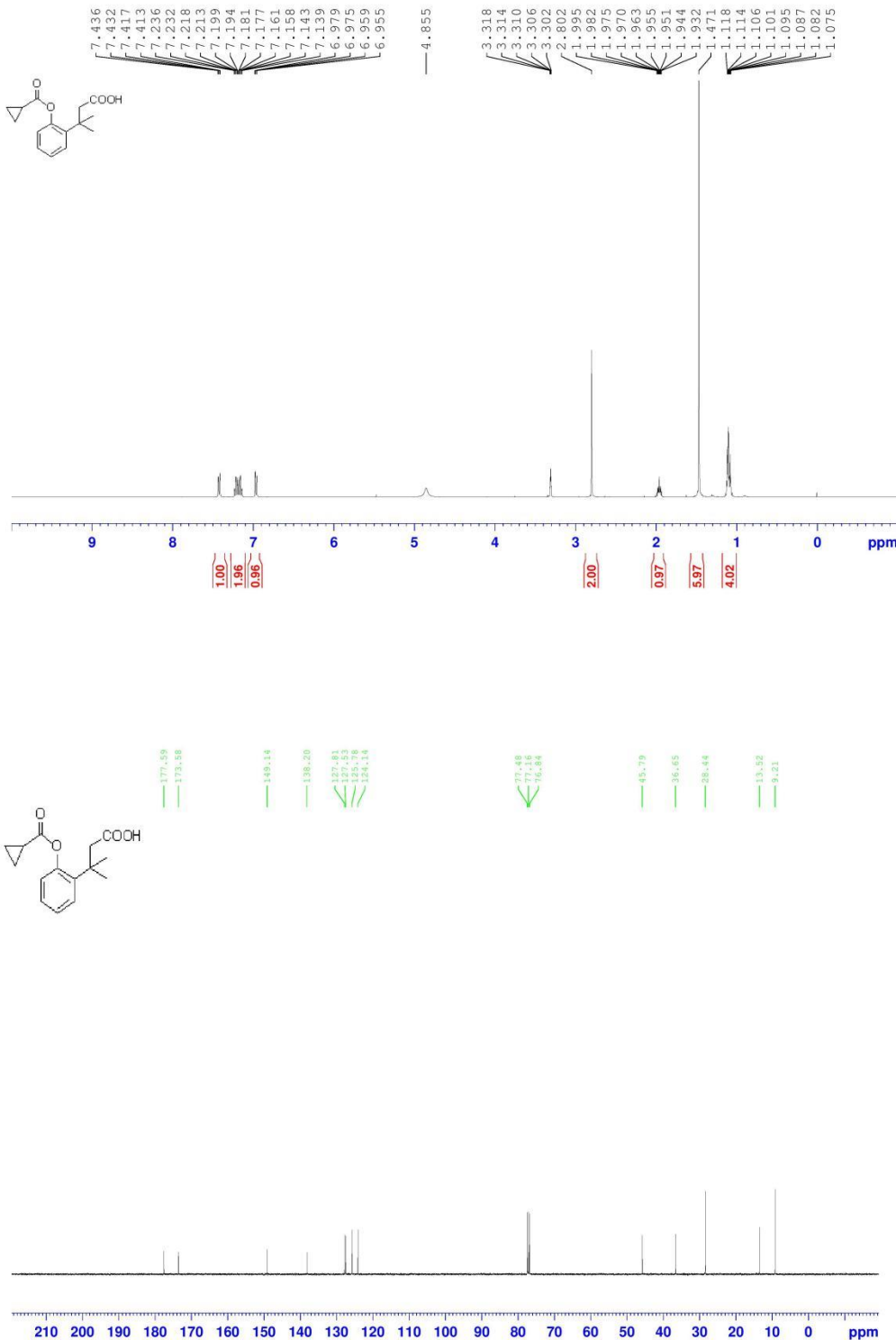


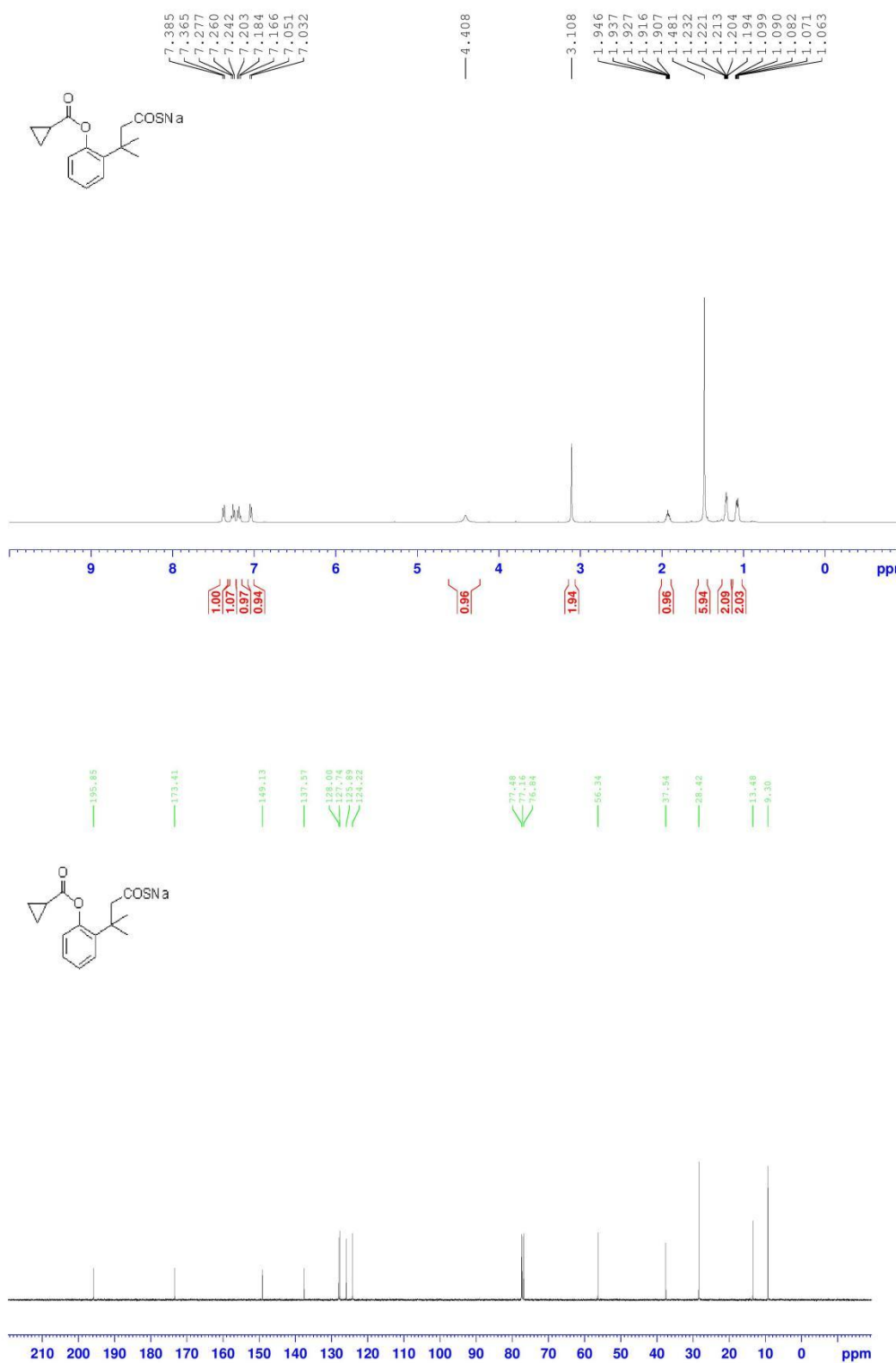


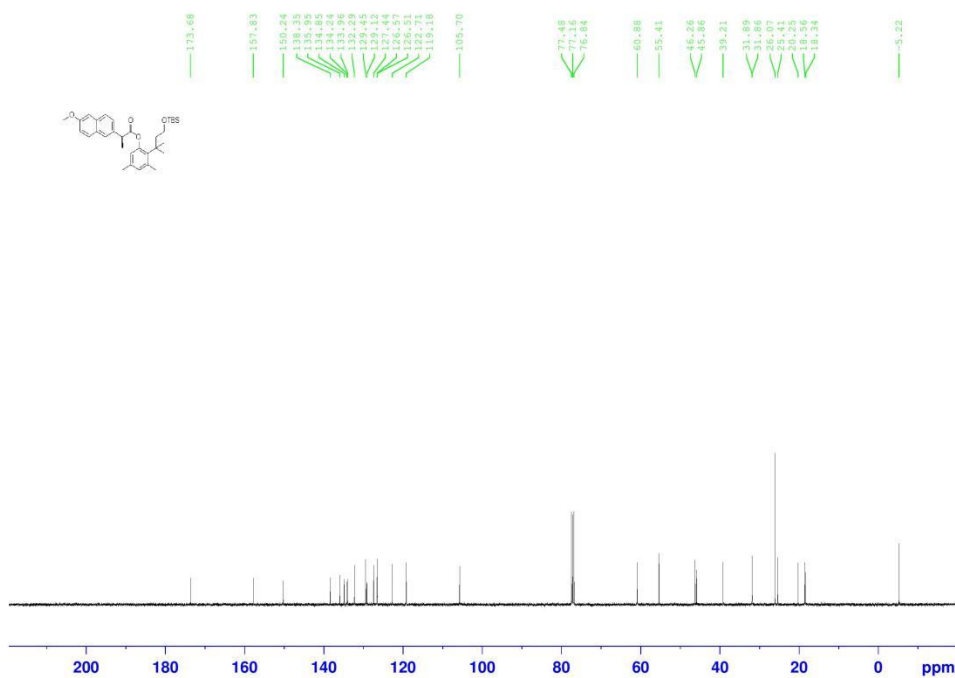
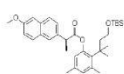
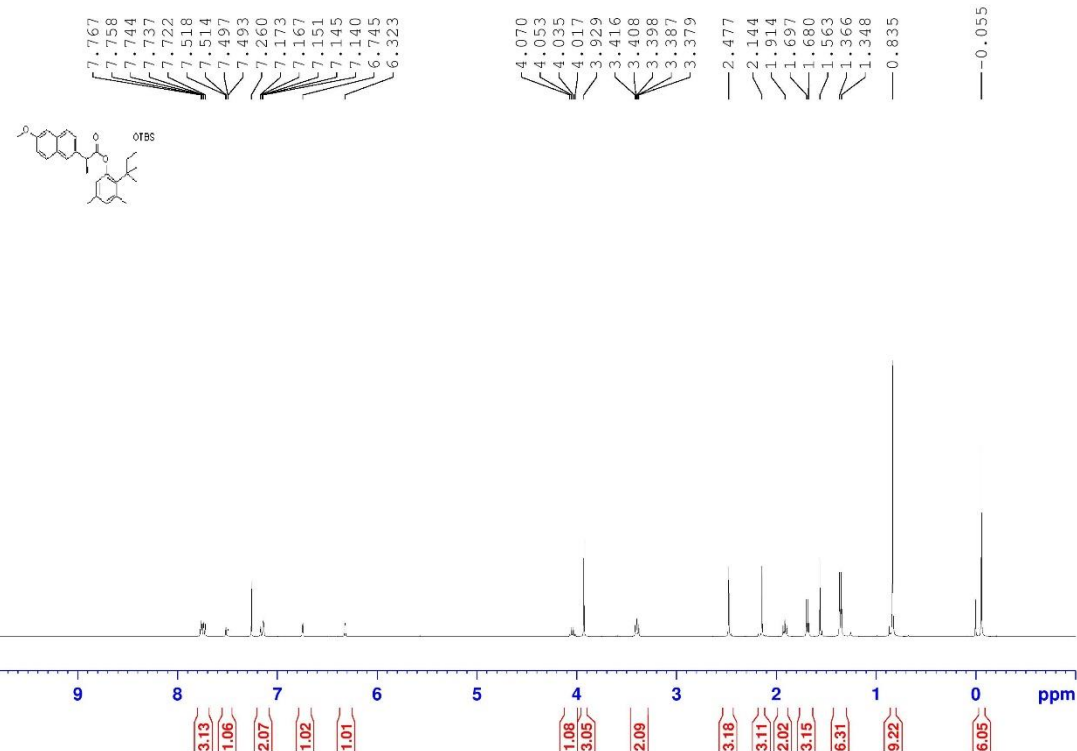


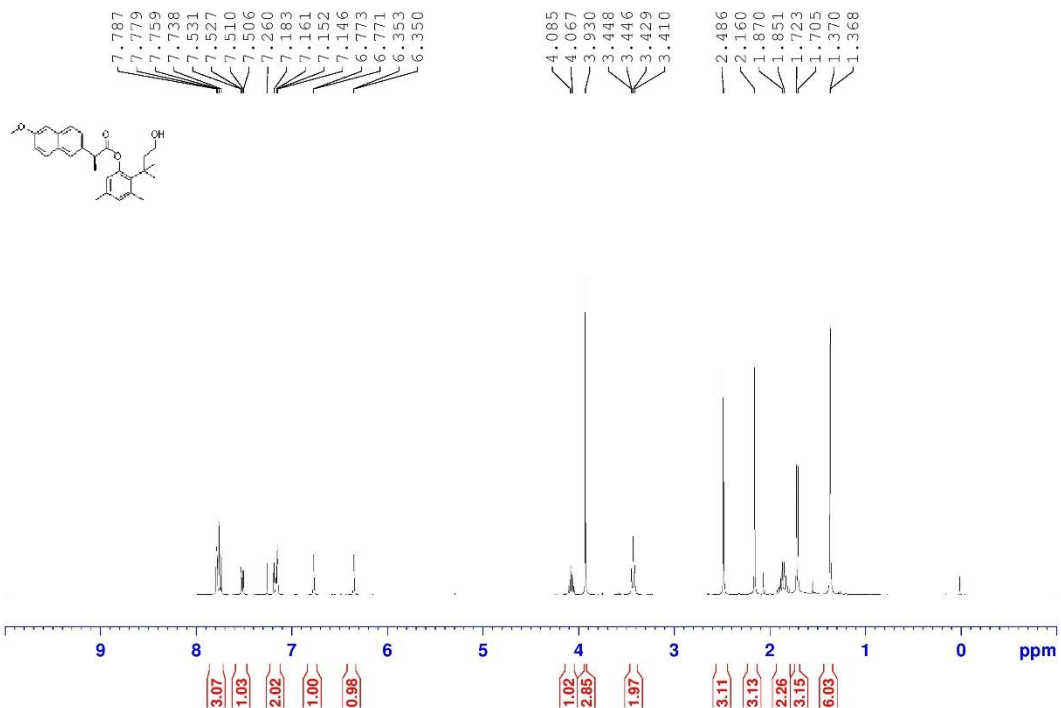


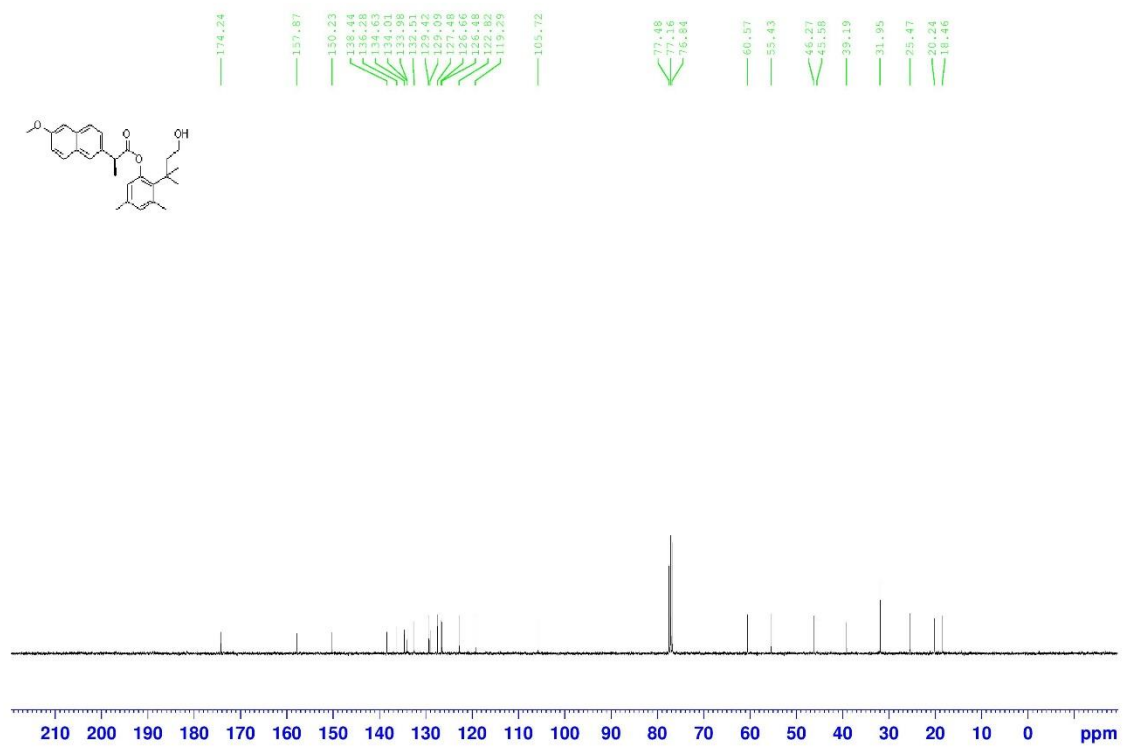


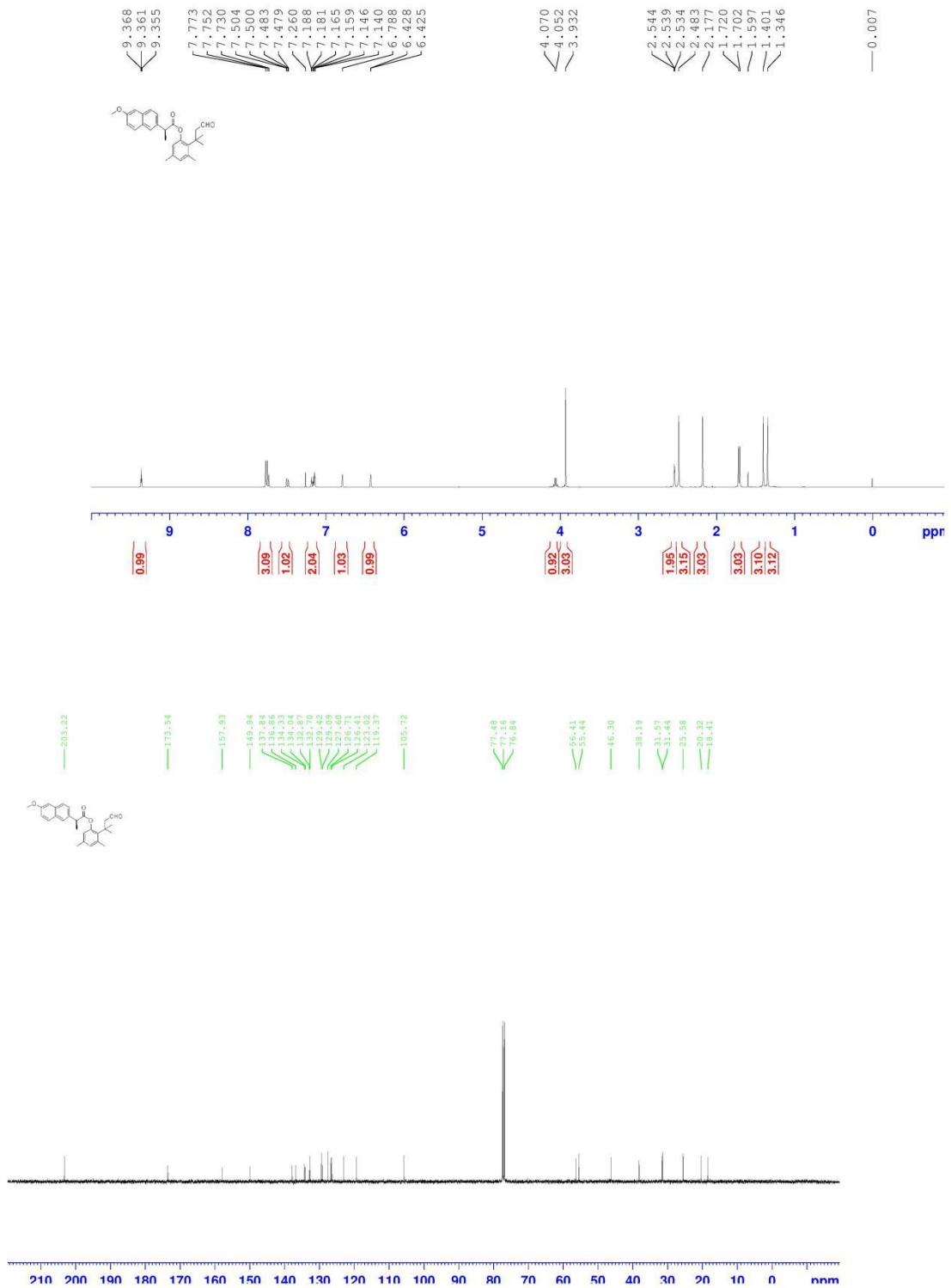


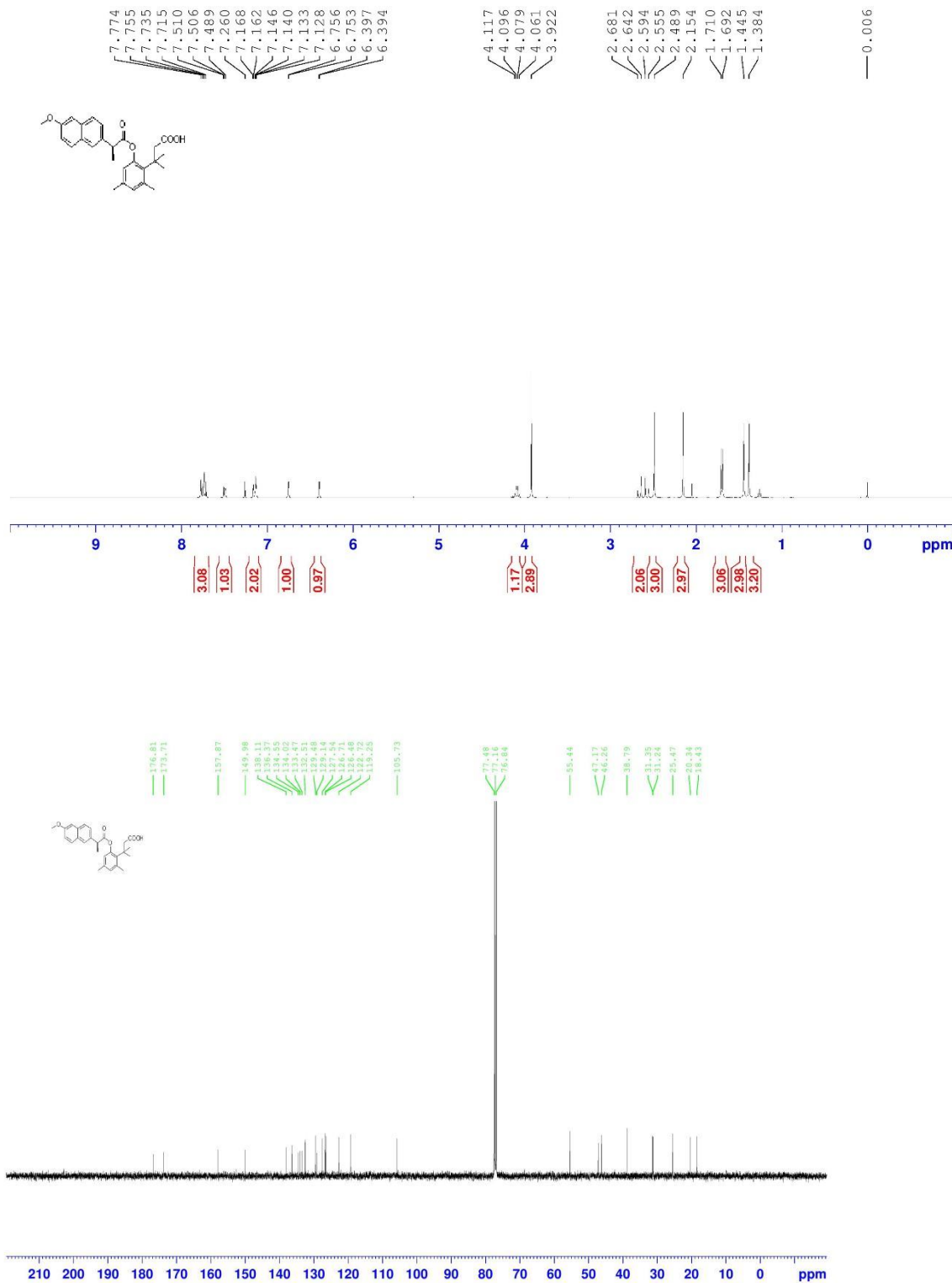


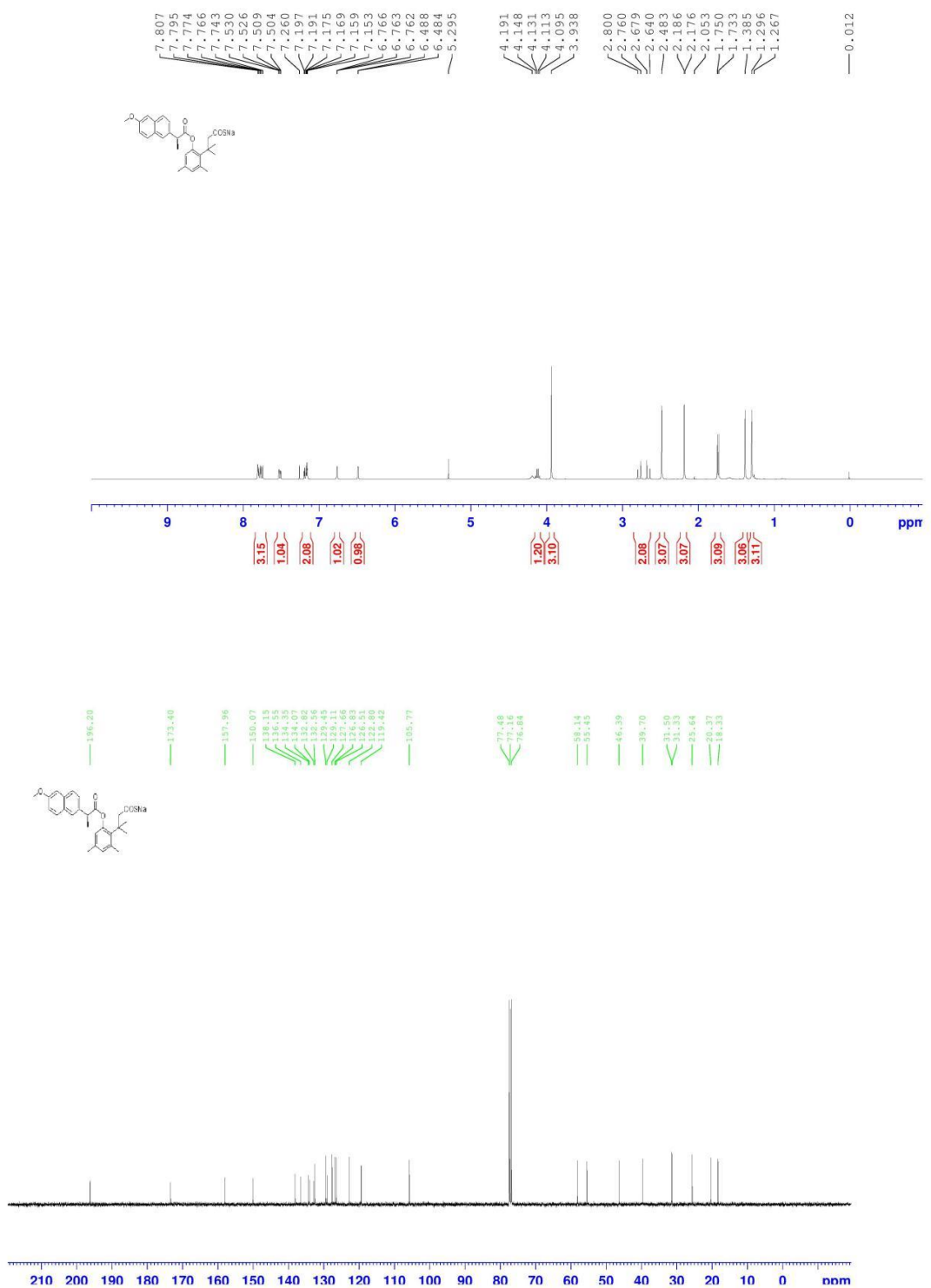




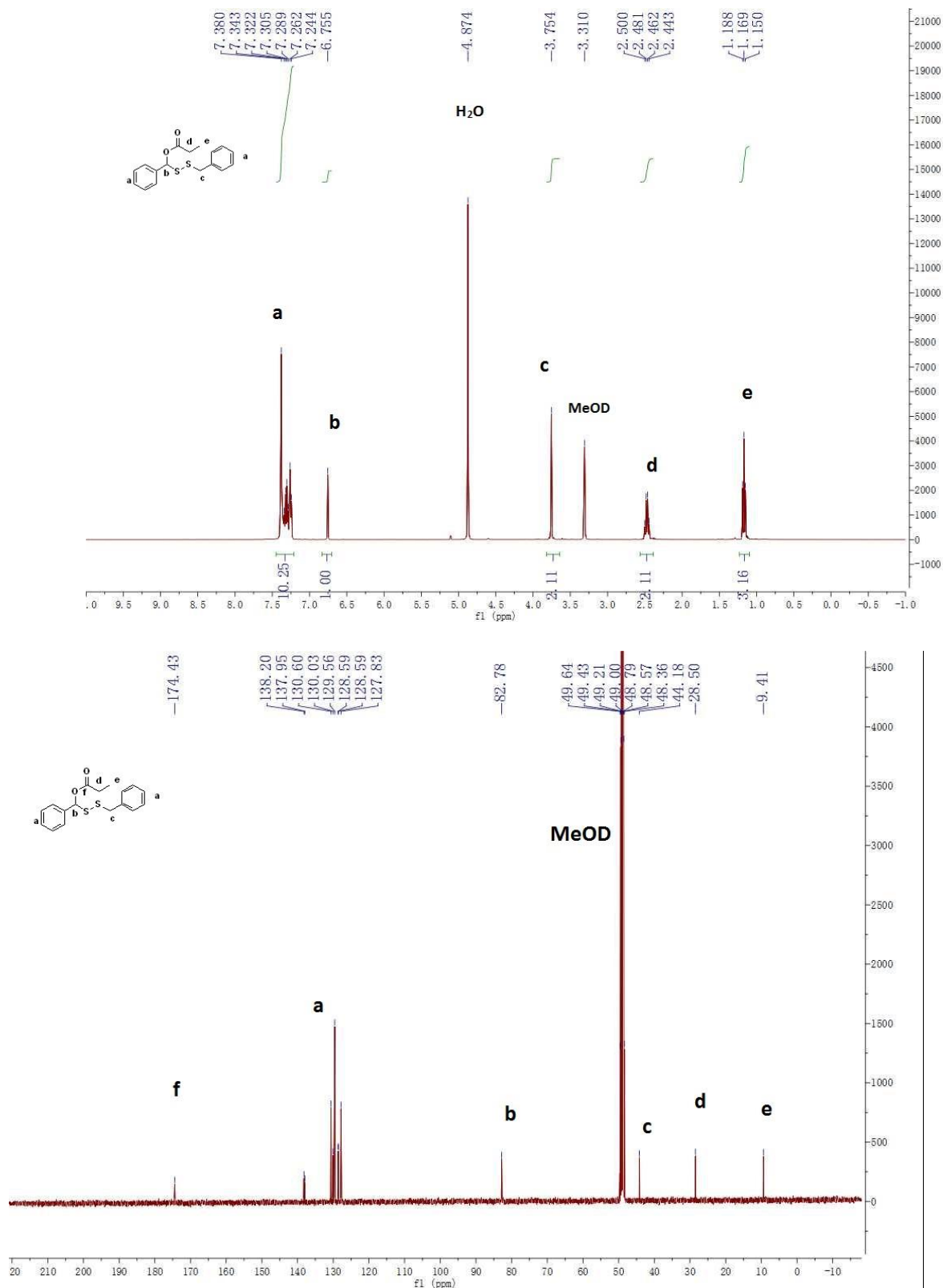


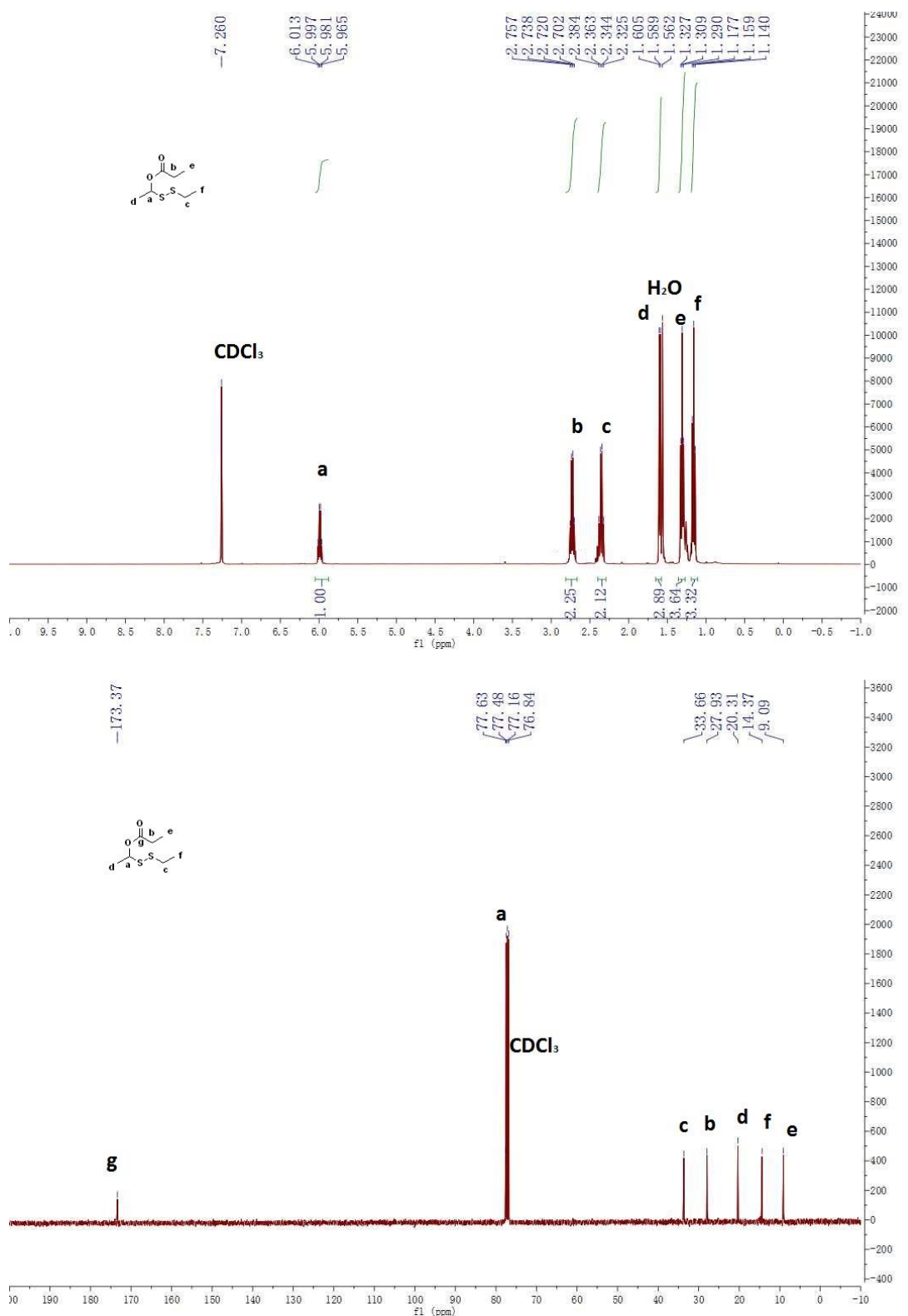


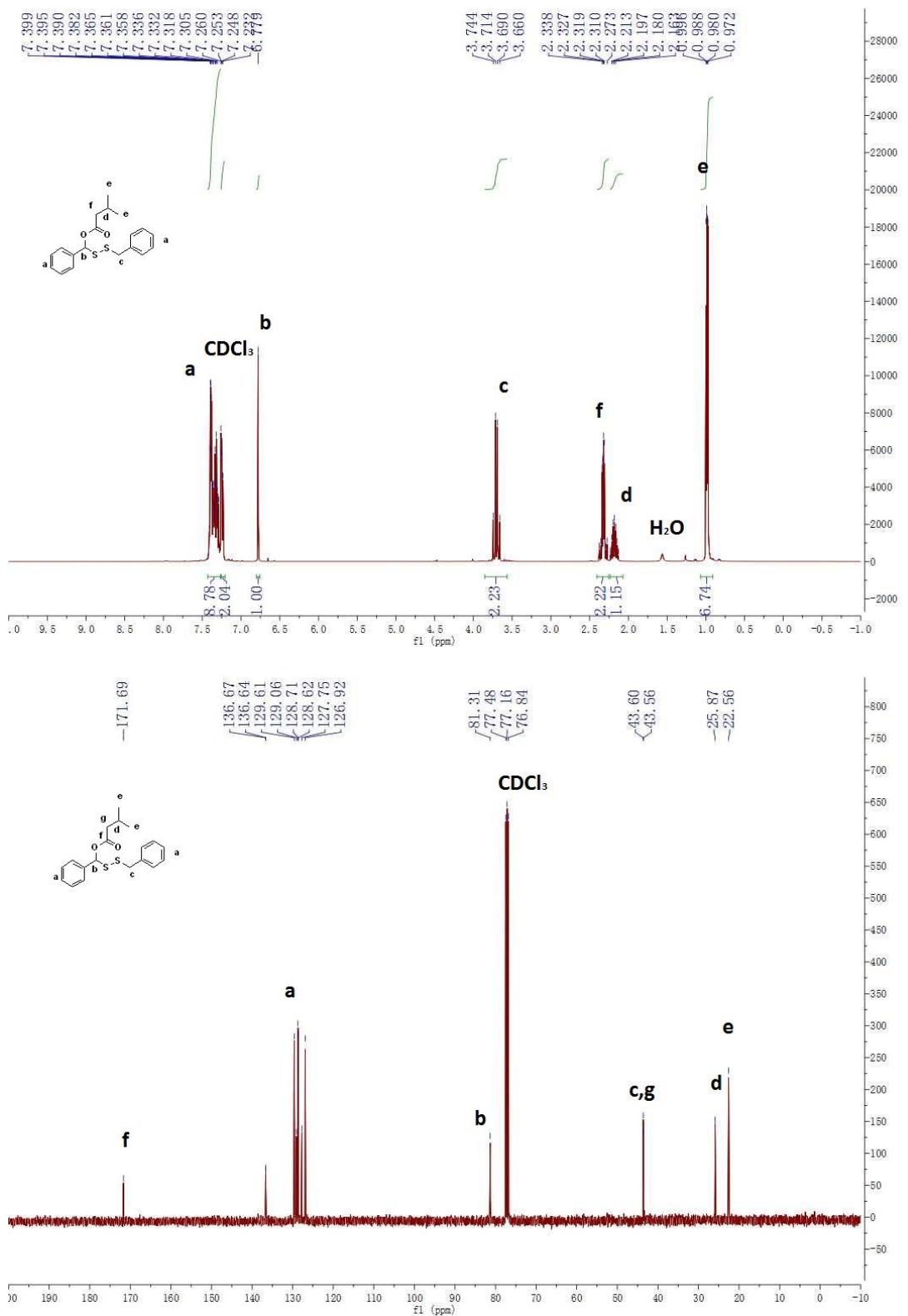


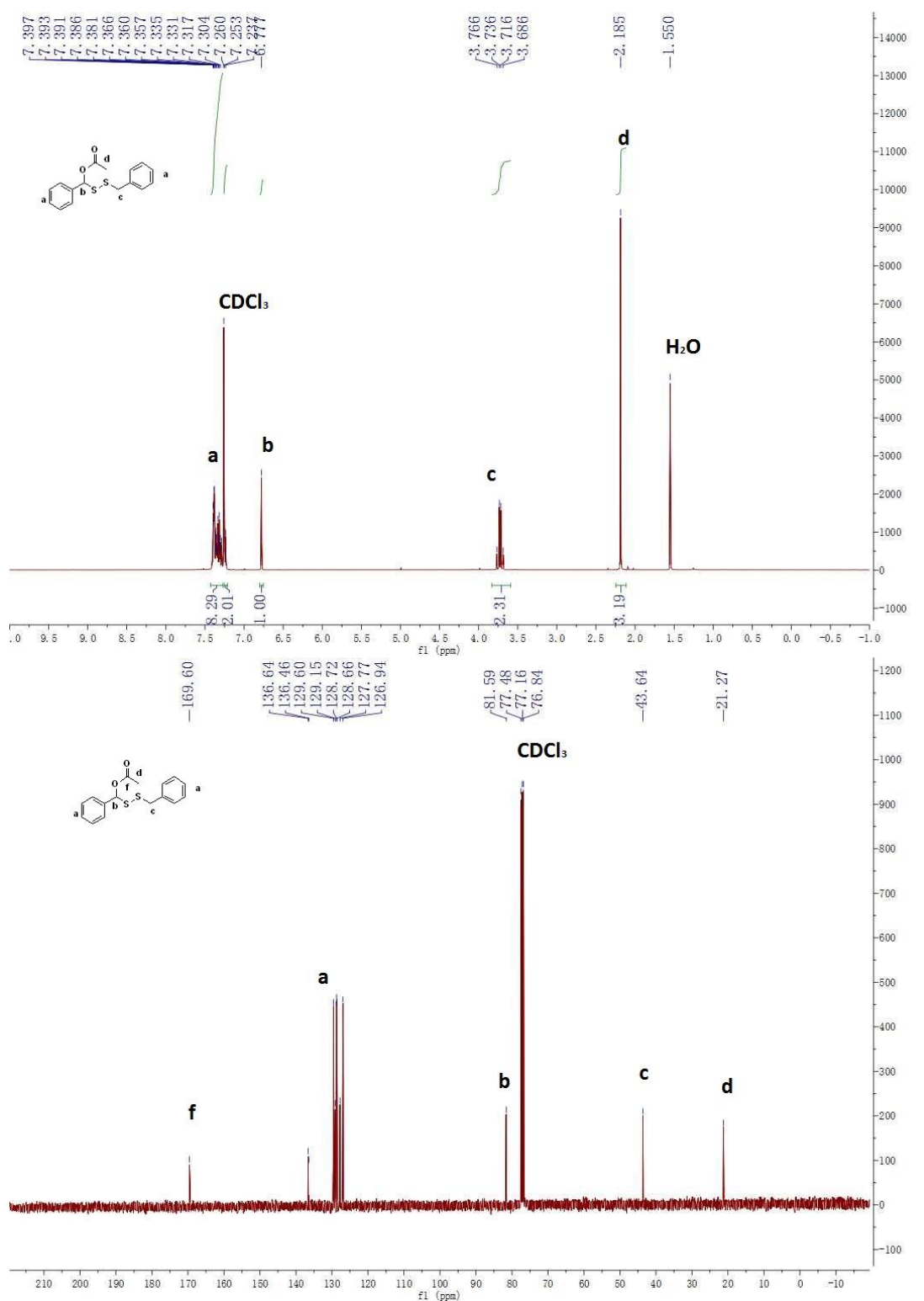


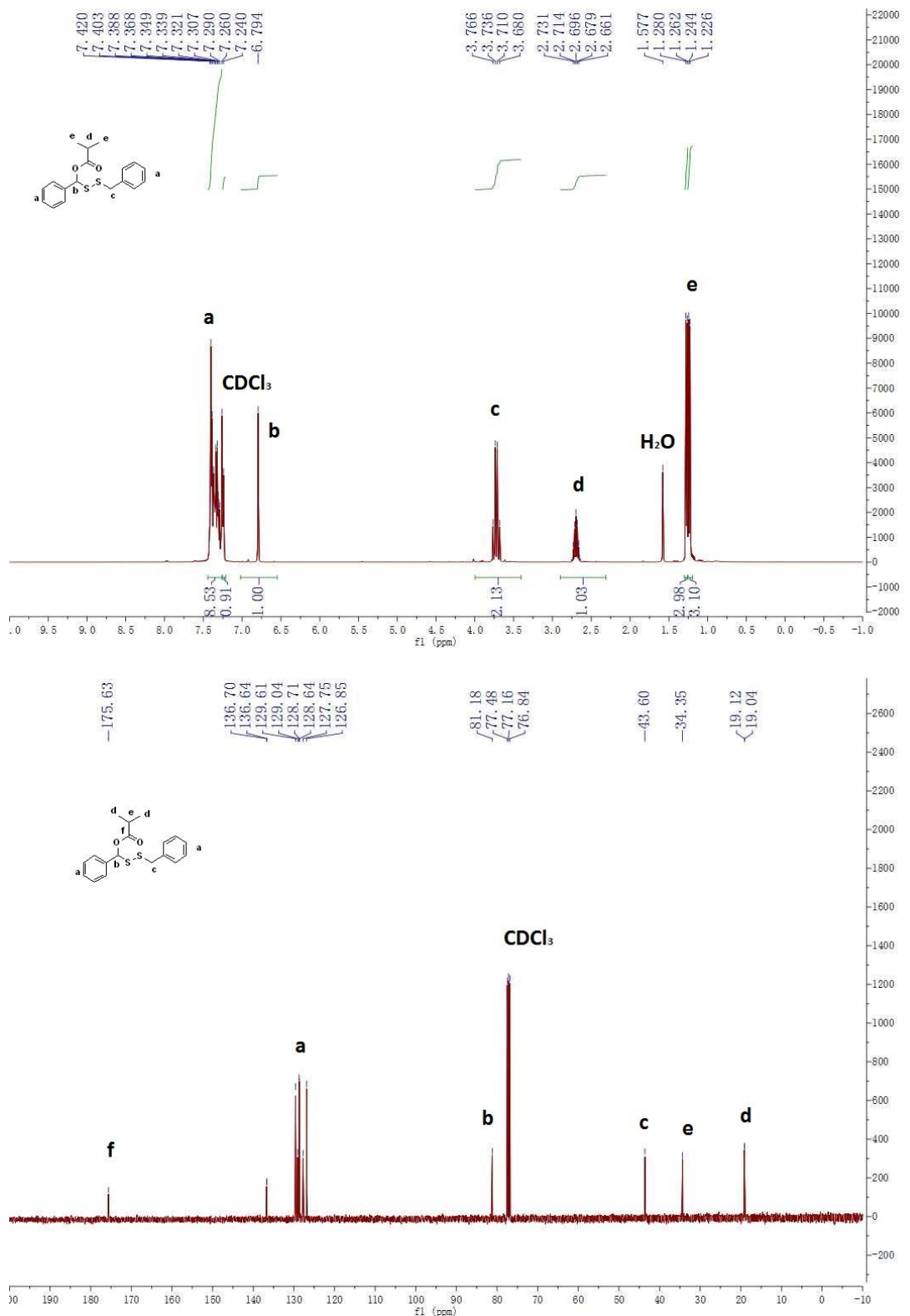
Appendix B. ^1H and ^{13}C Spectra of compounds in chapter 2

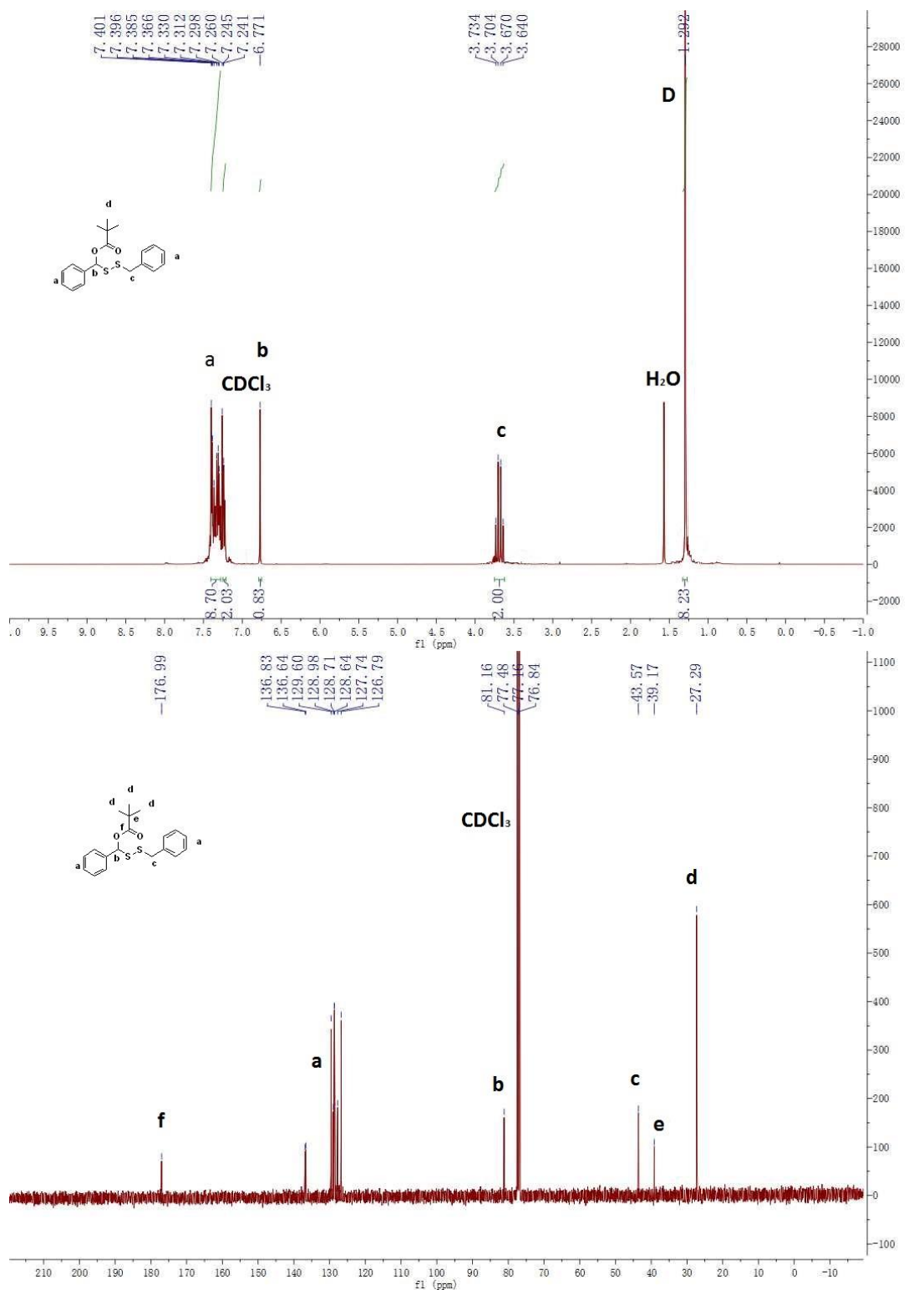


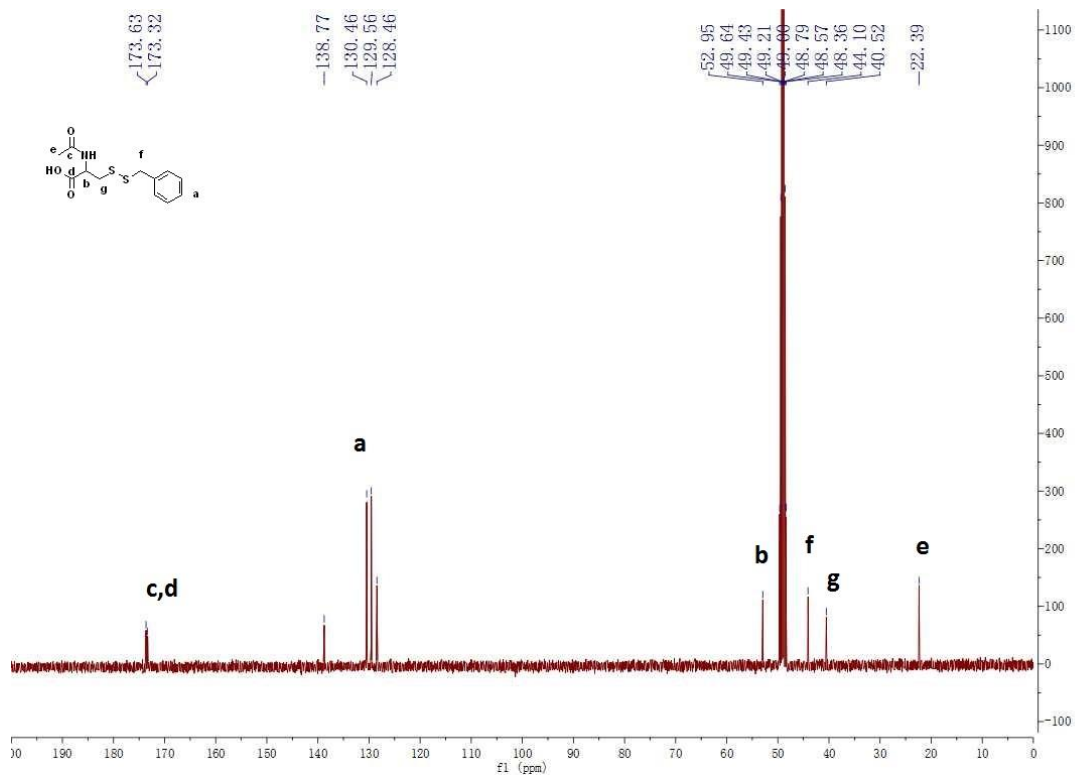
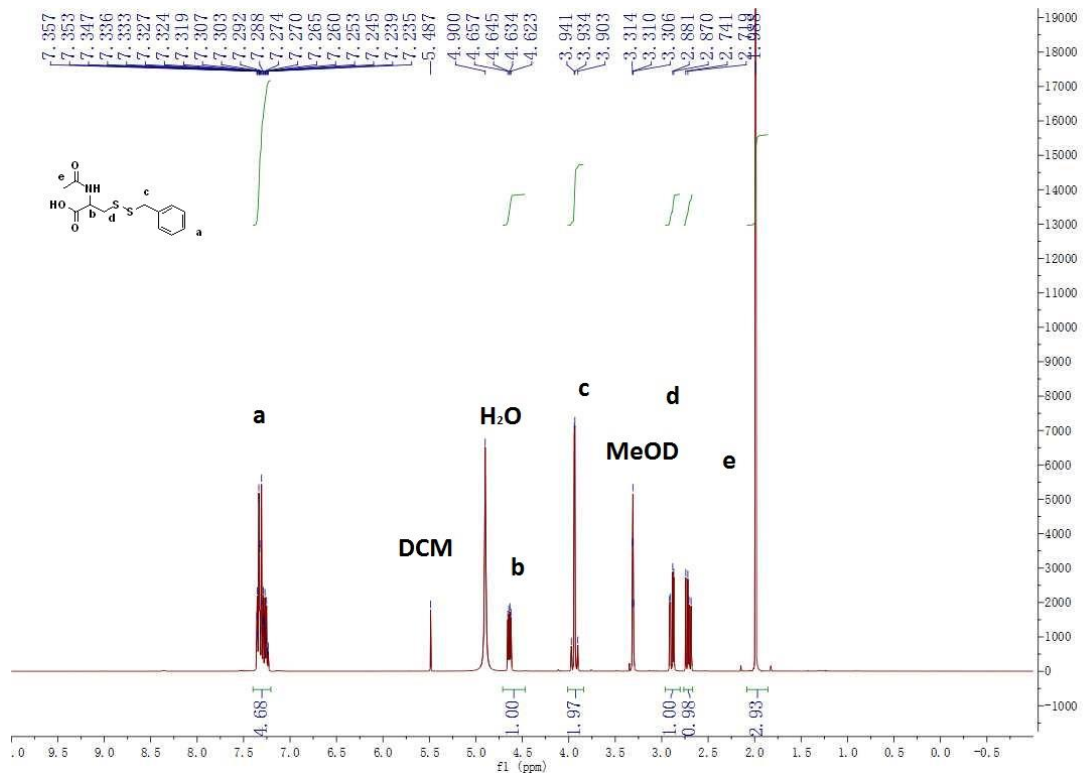


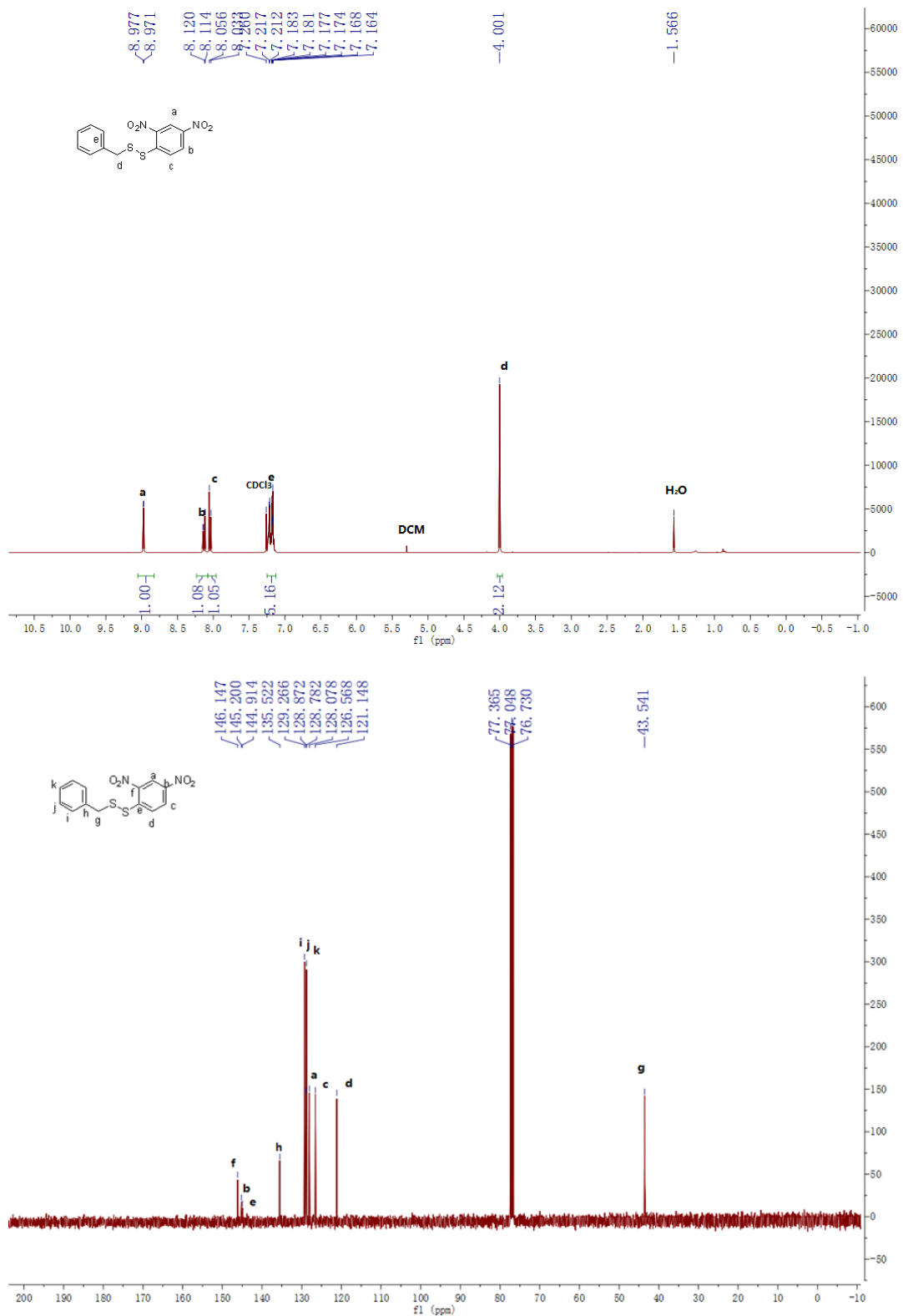


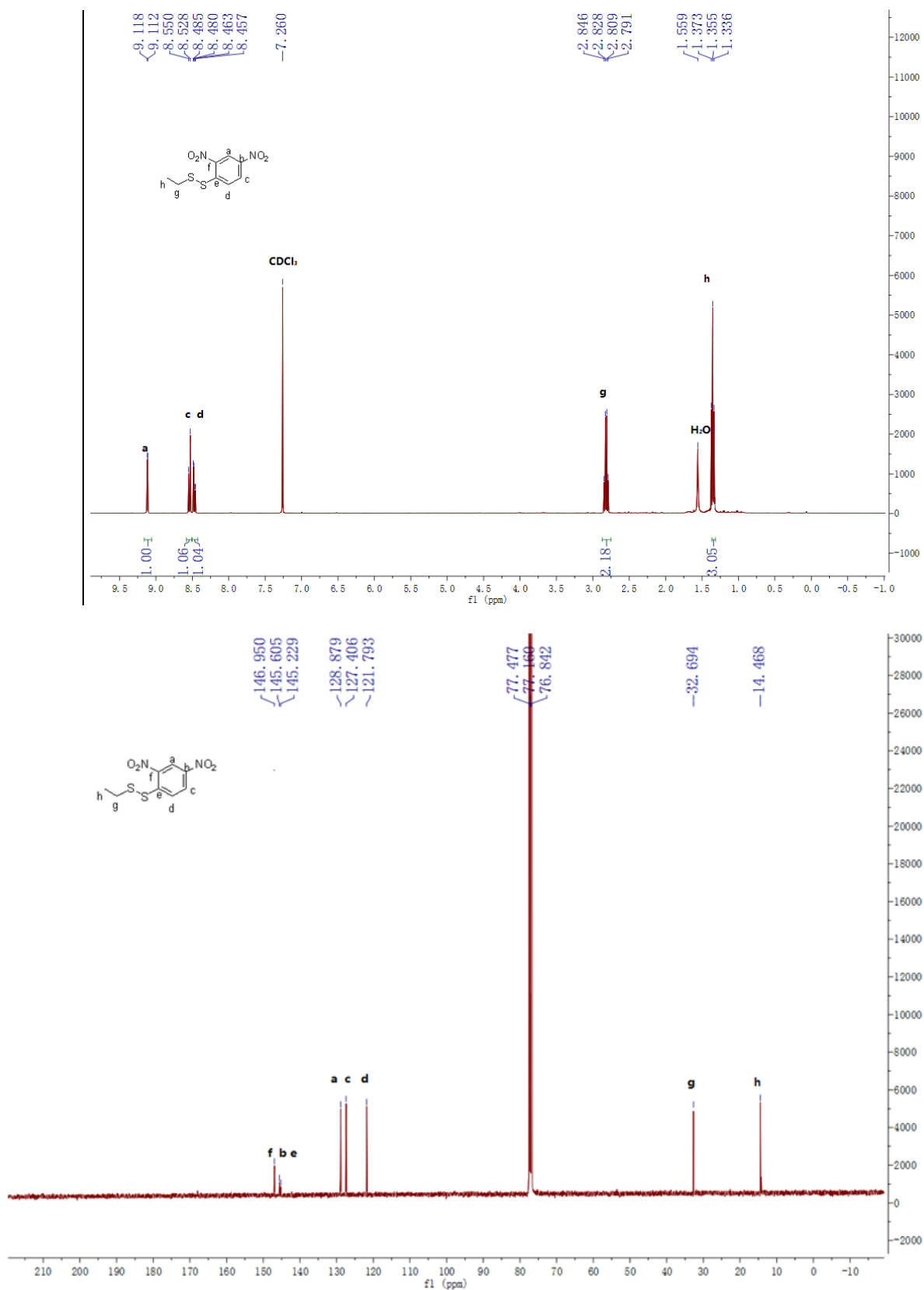




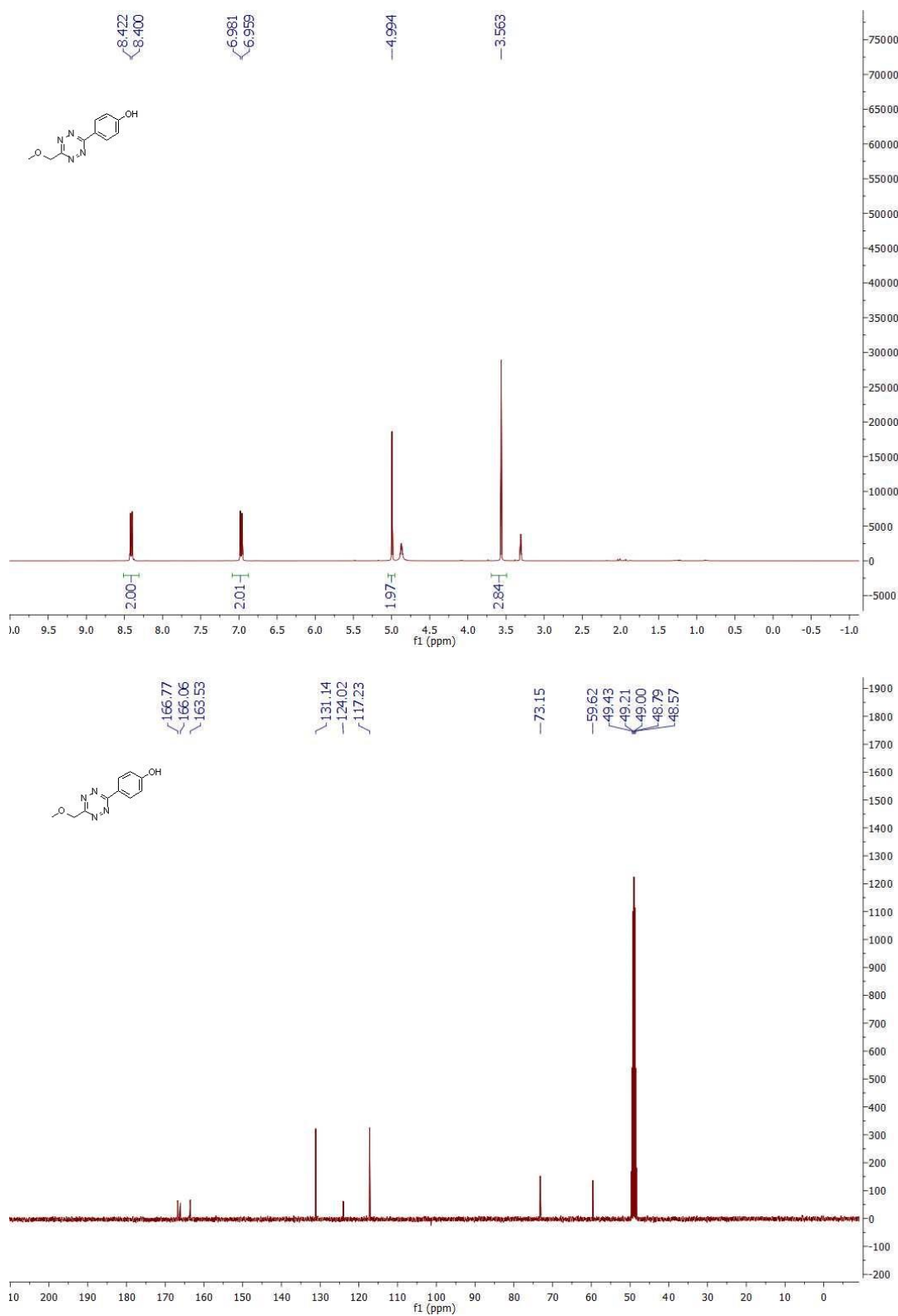


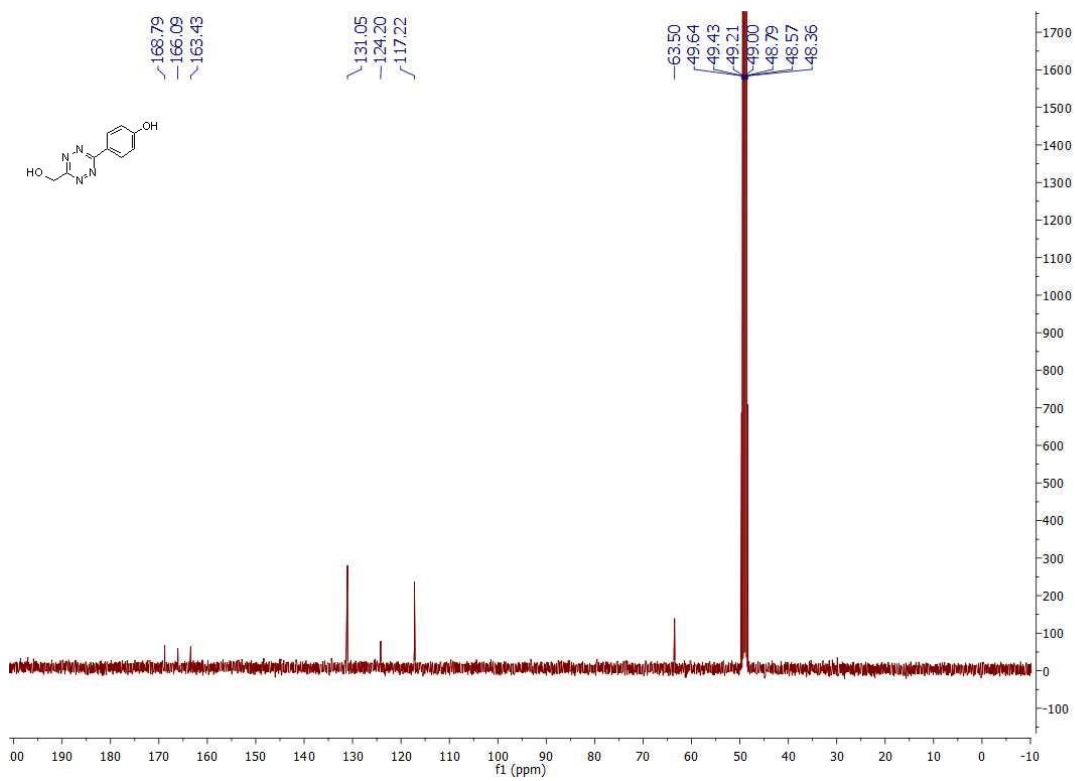
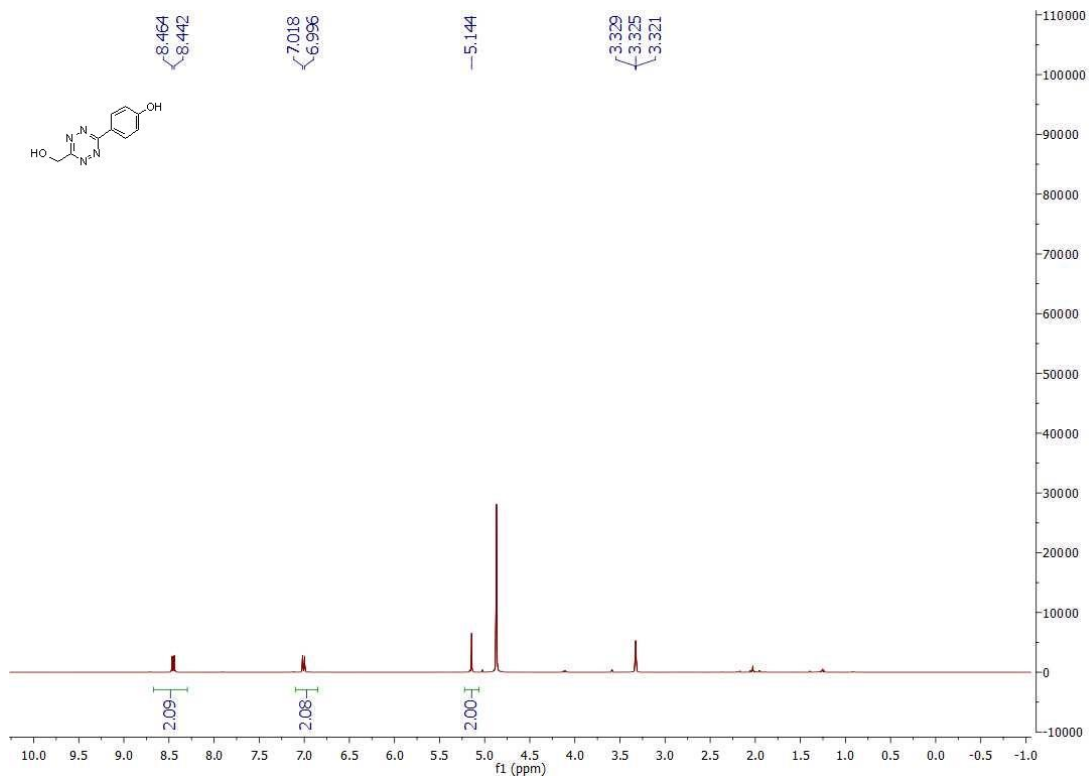


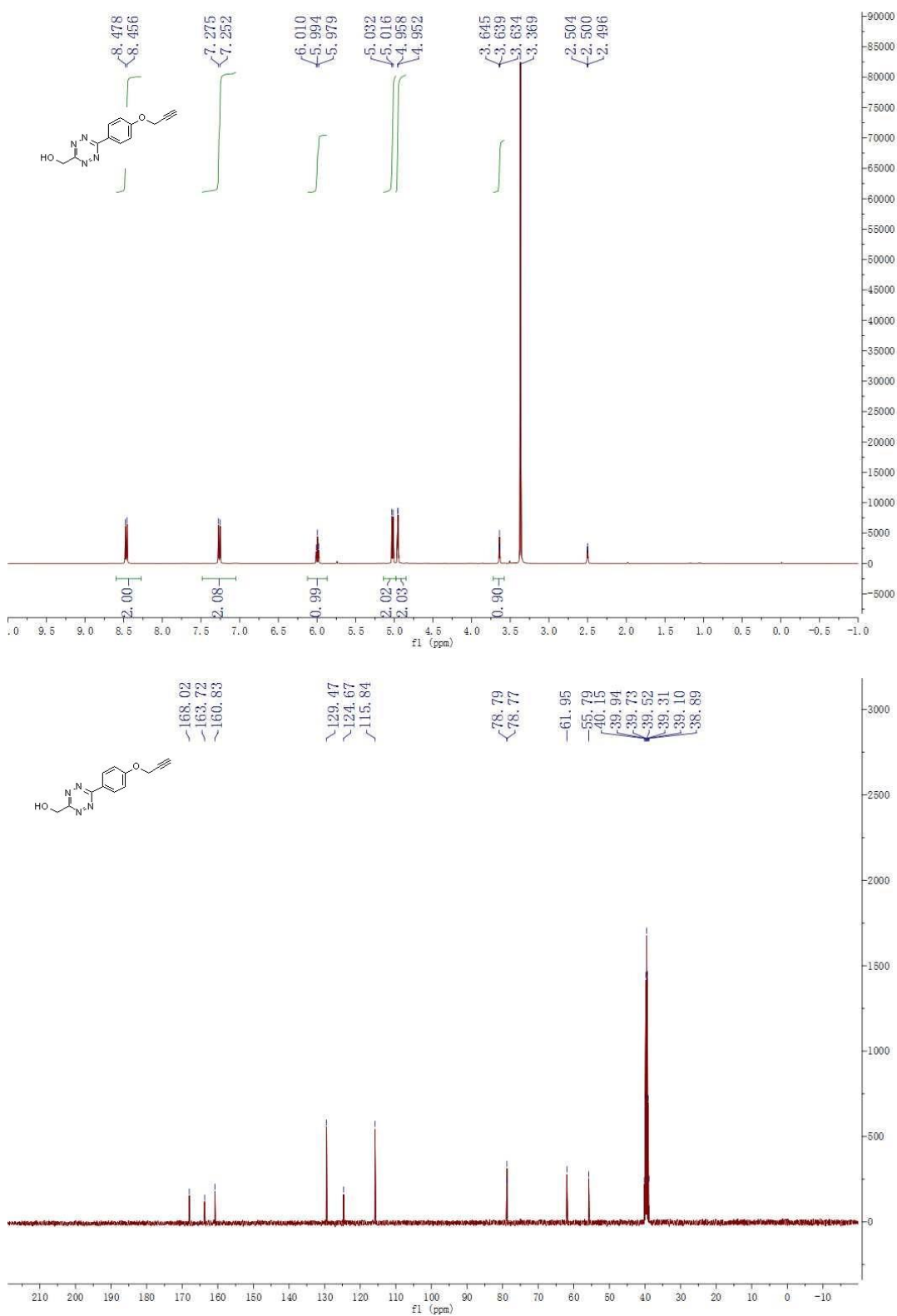


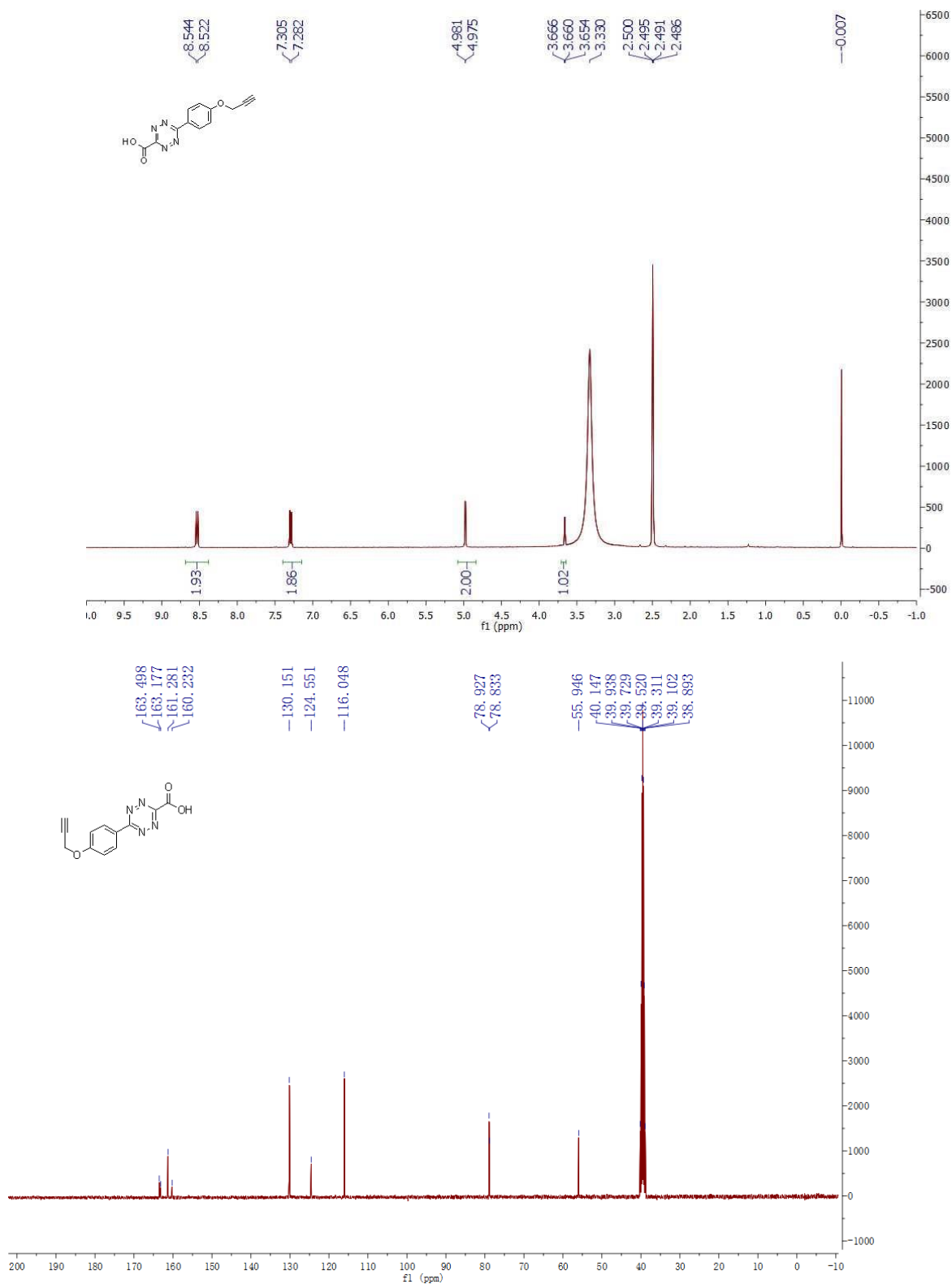


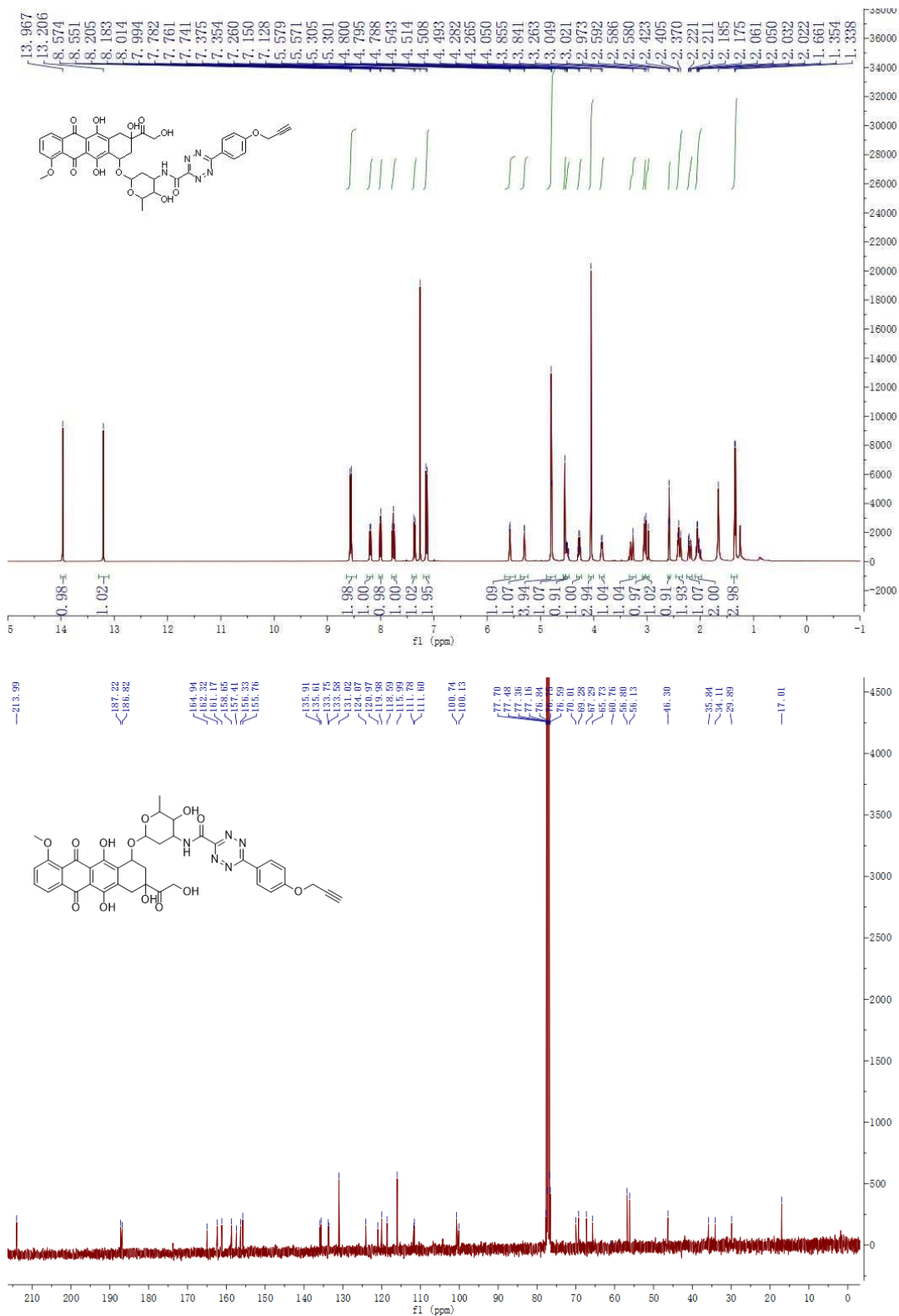
Appendix C. ^1H and ^{13}C Spectra of compounds in chapter 3

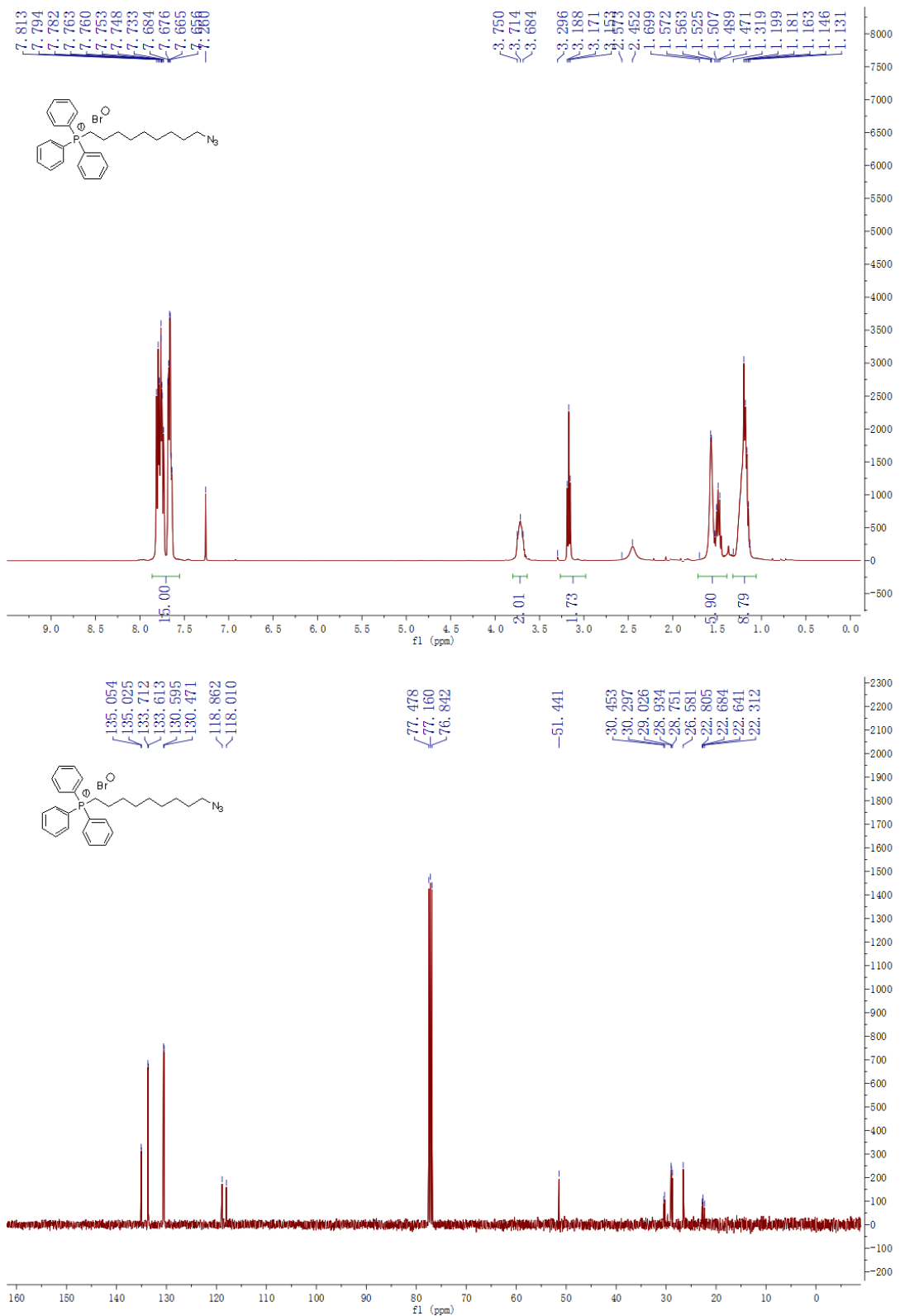


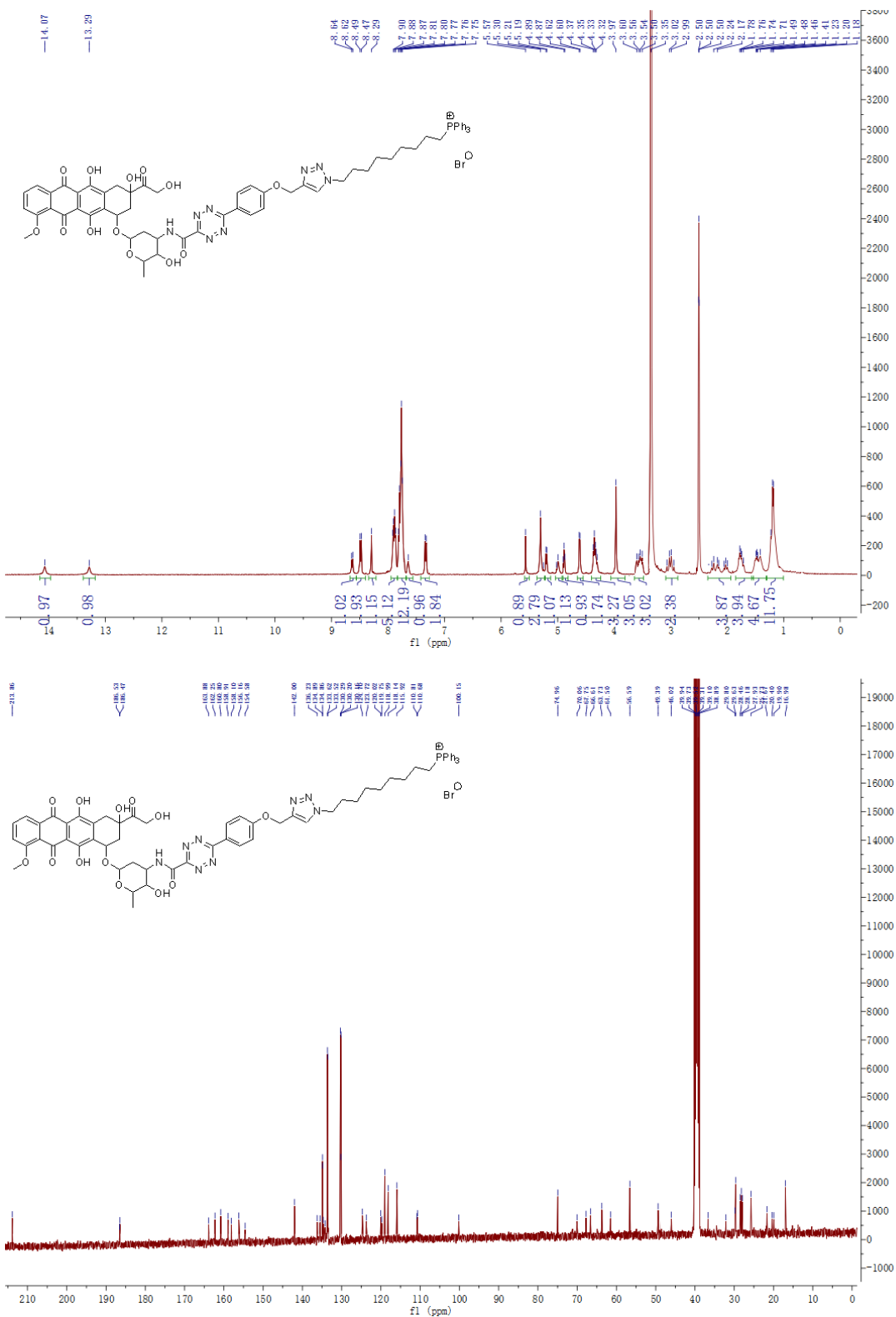


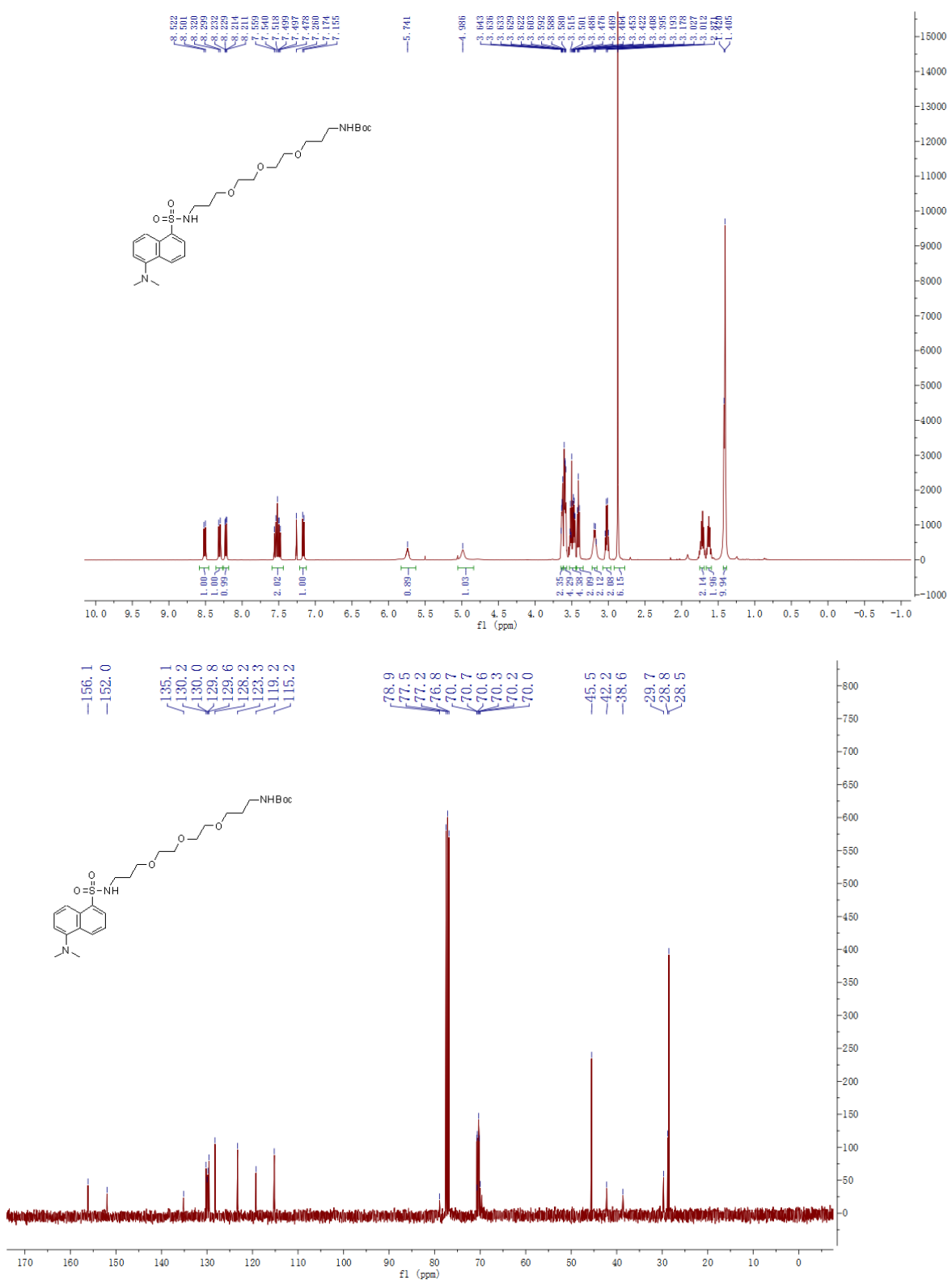


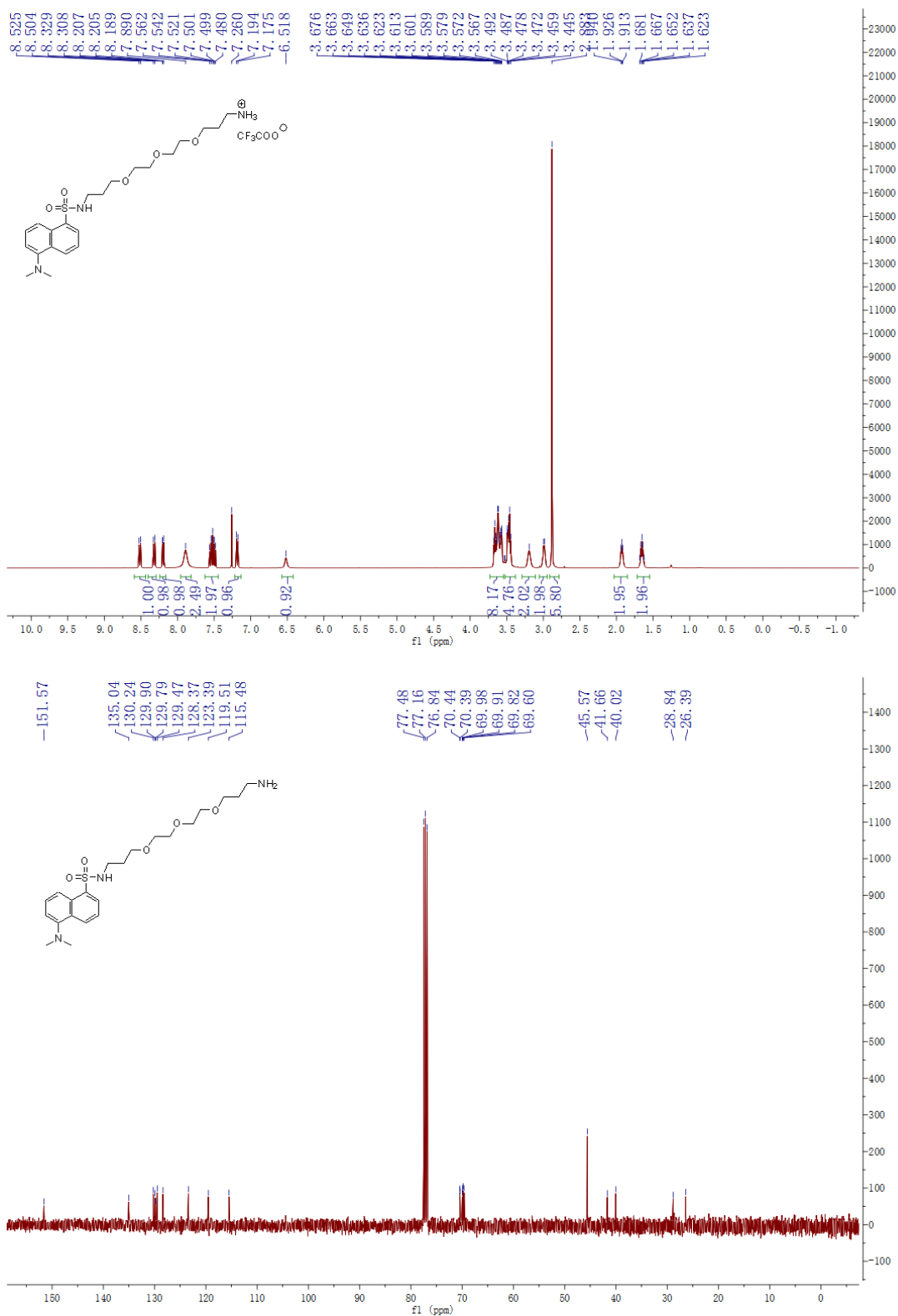


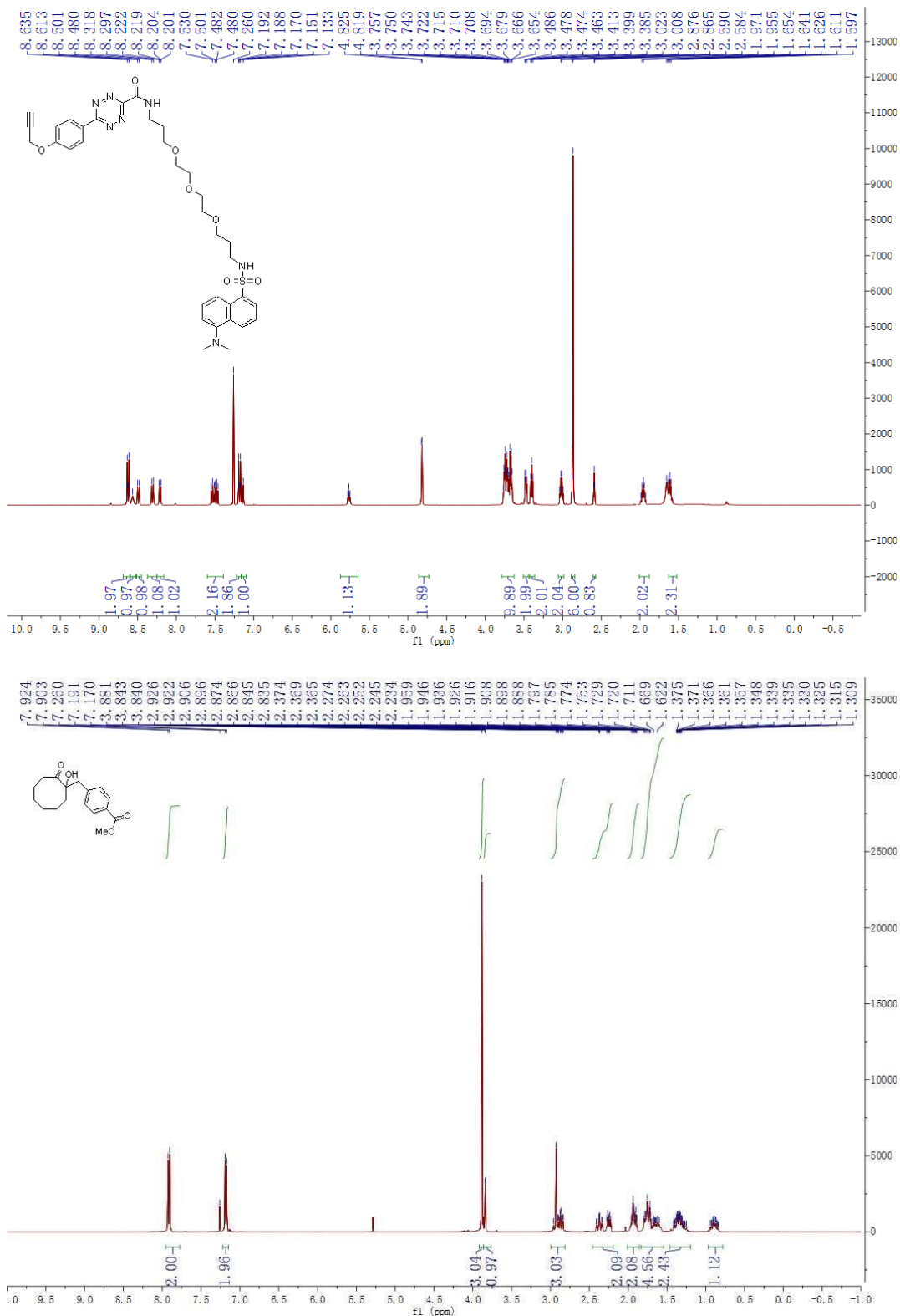


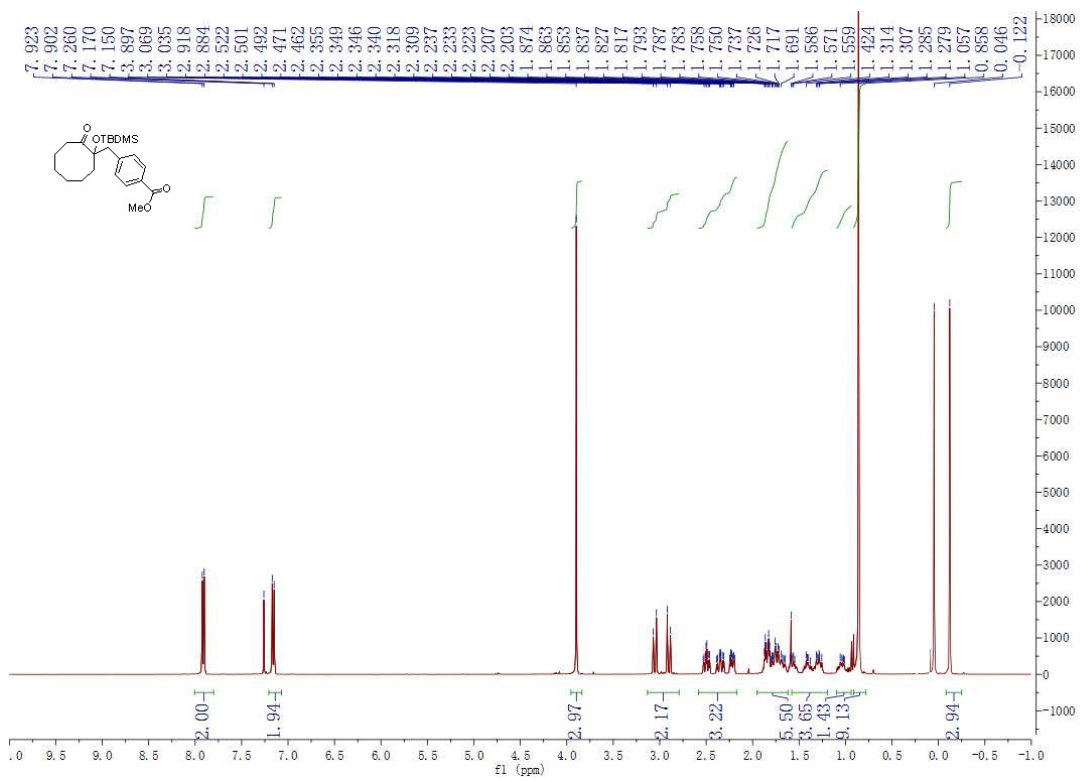
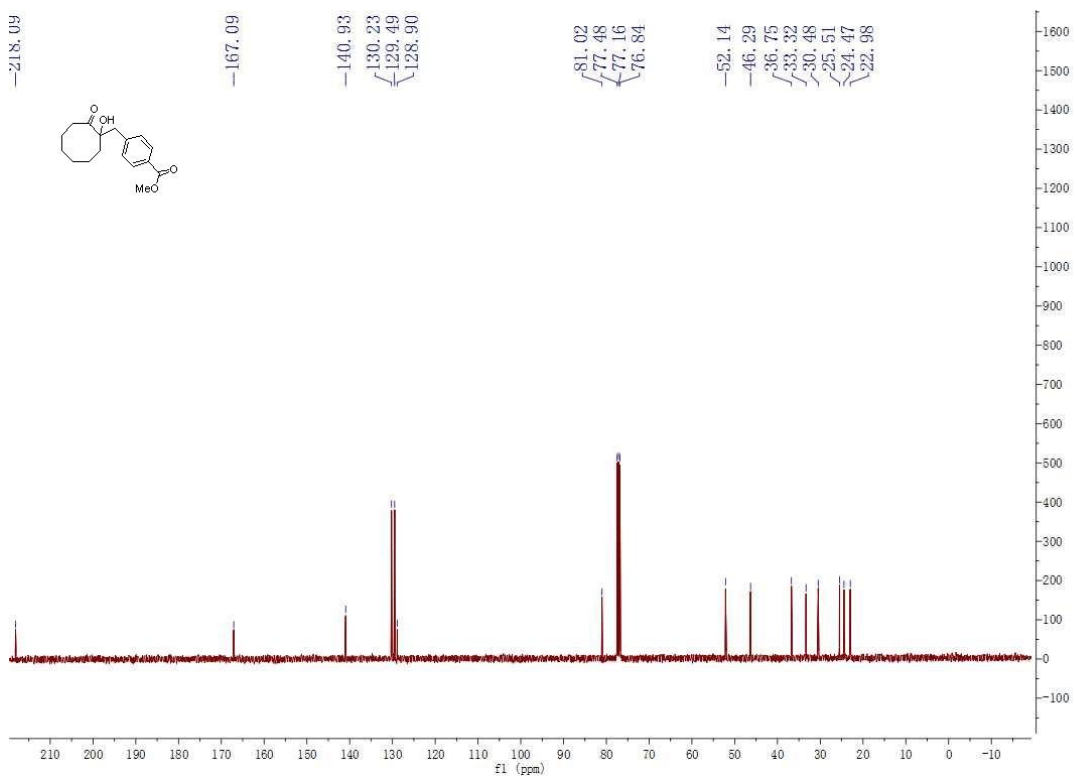


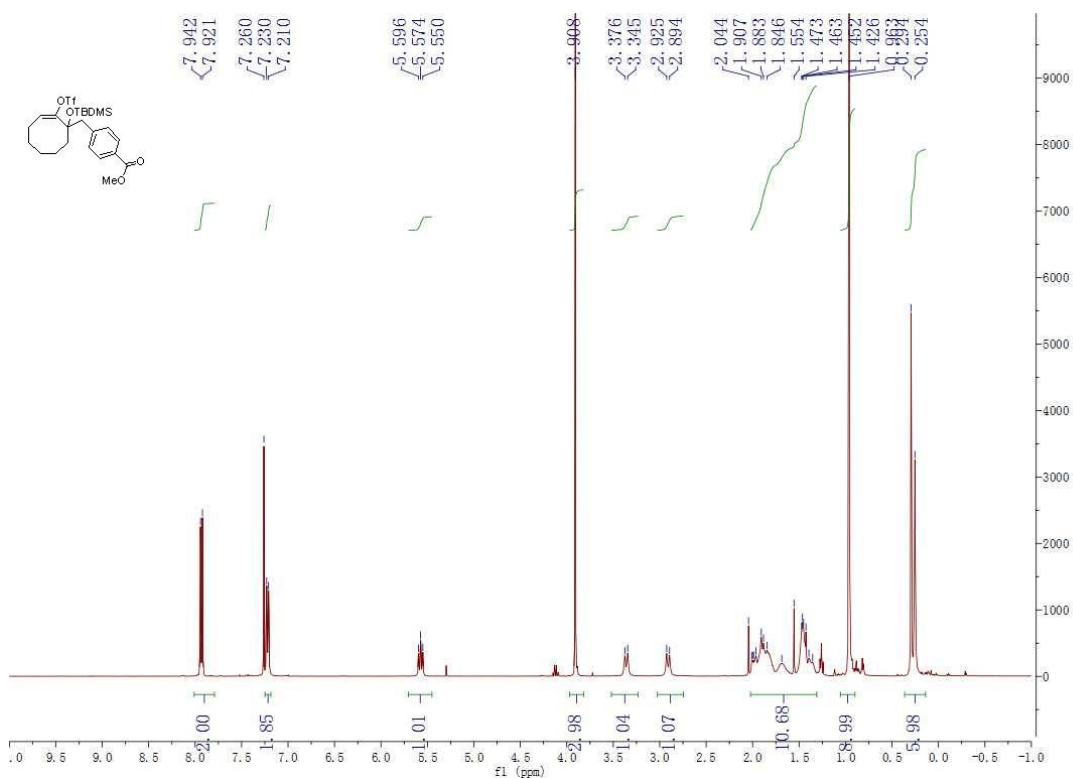
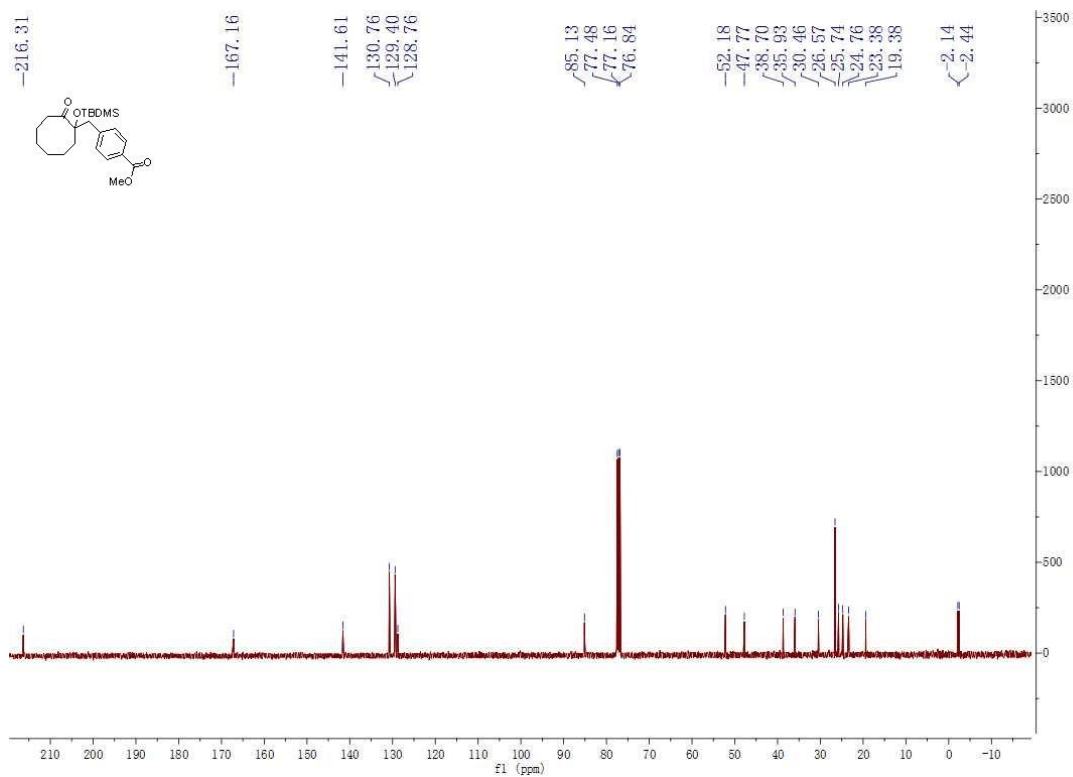


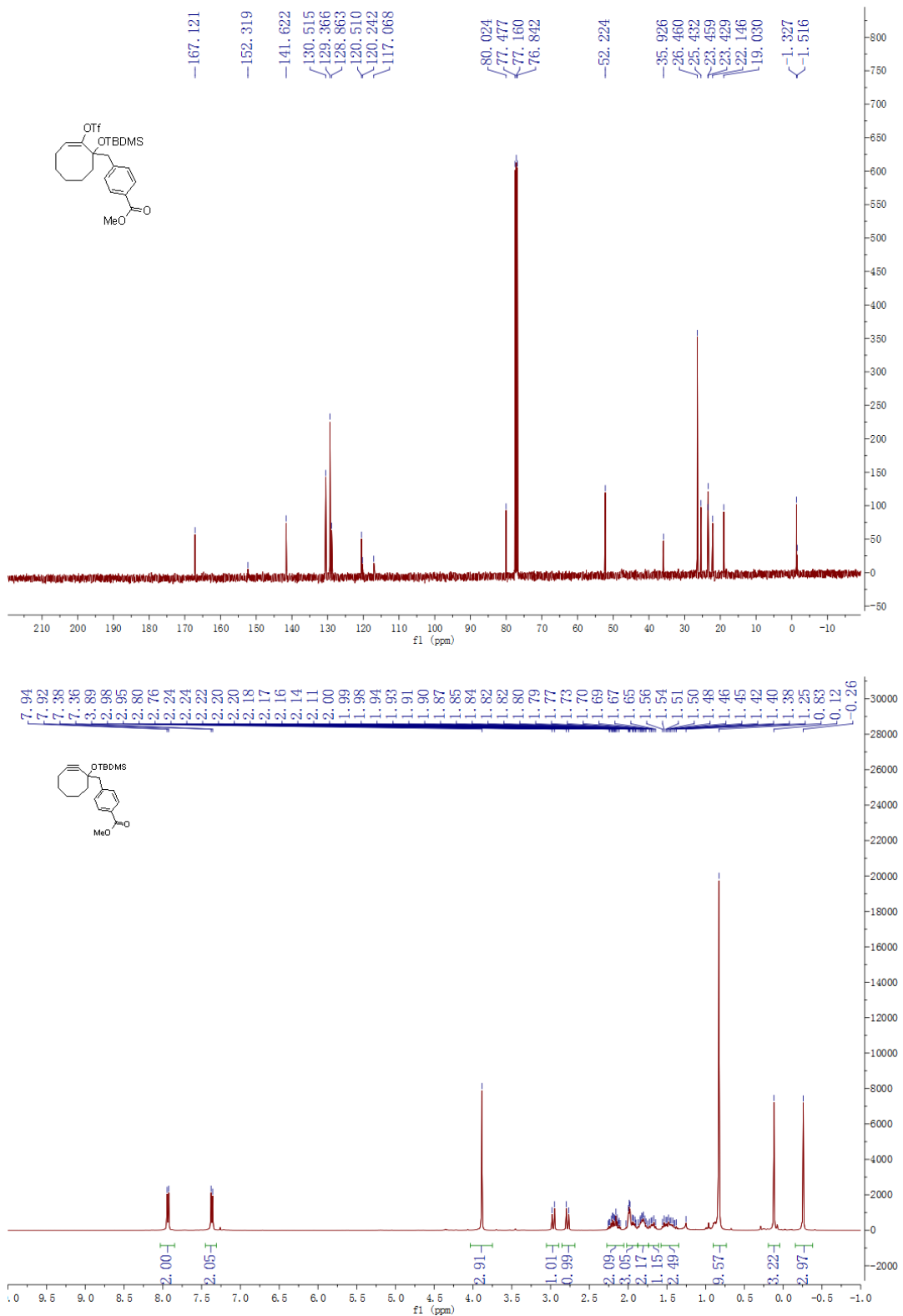


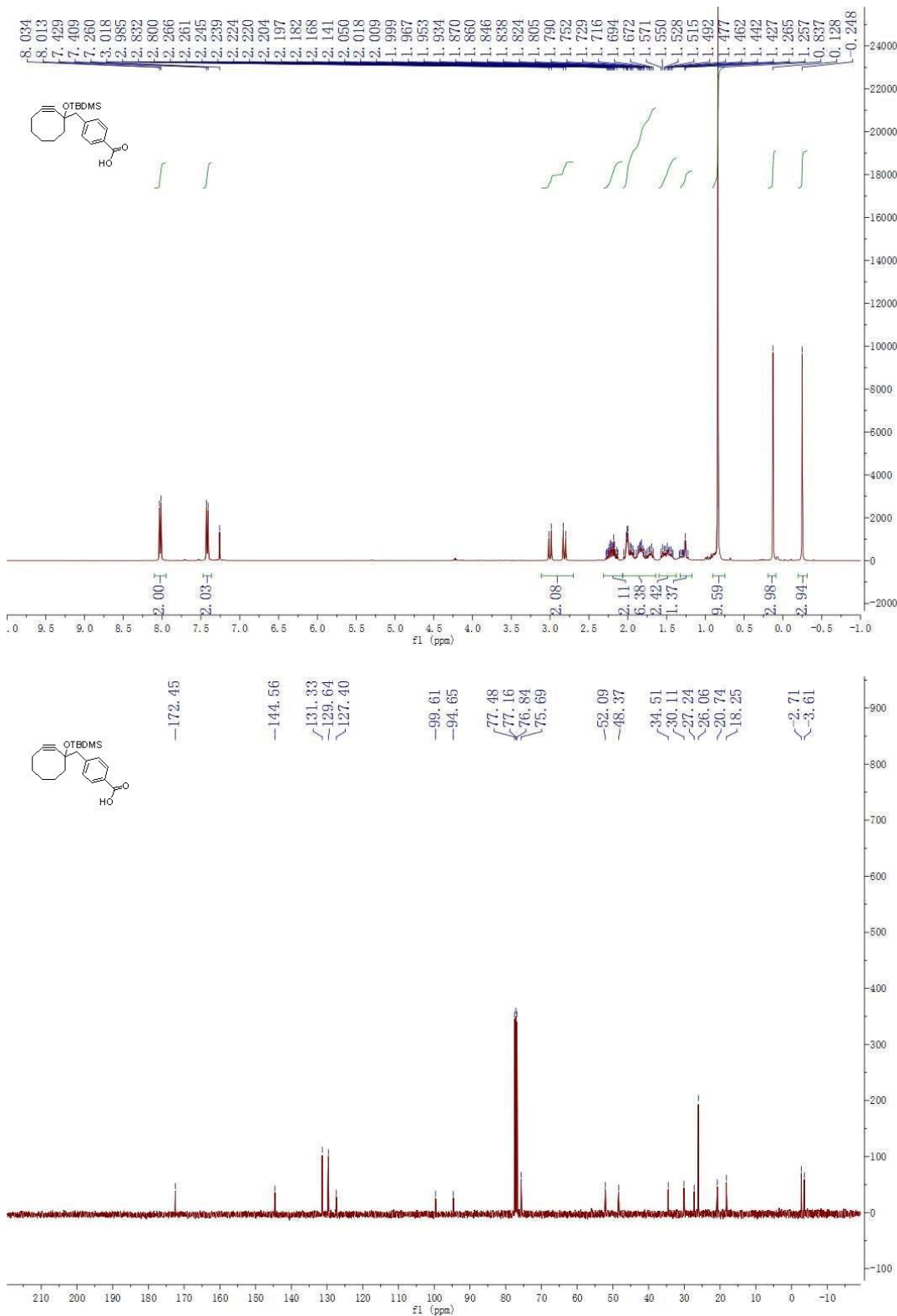


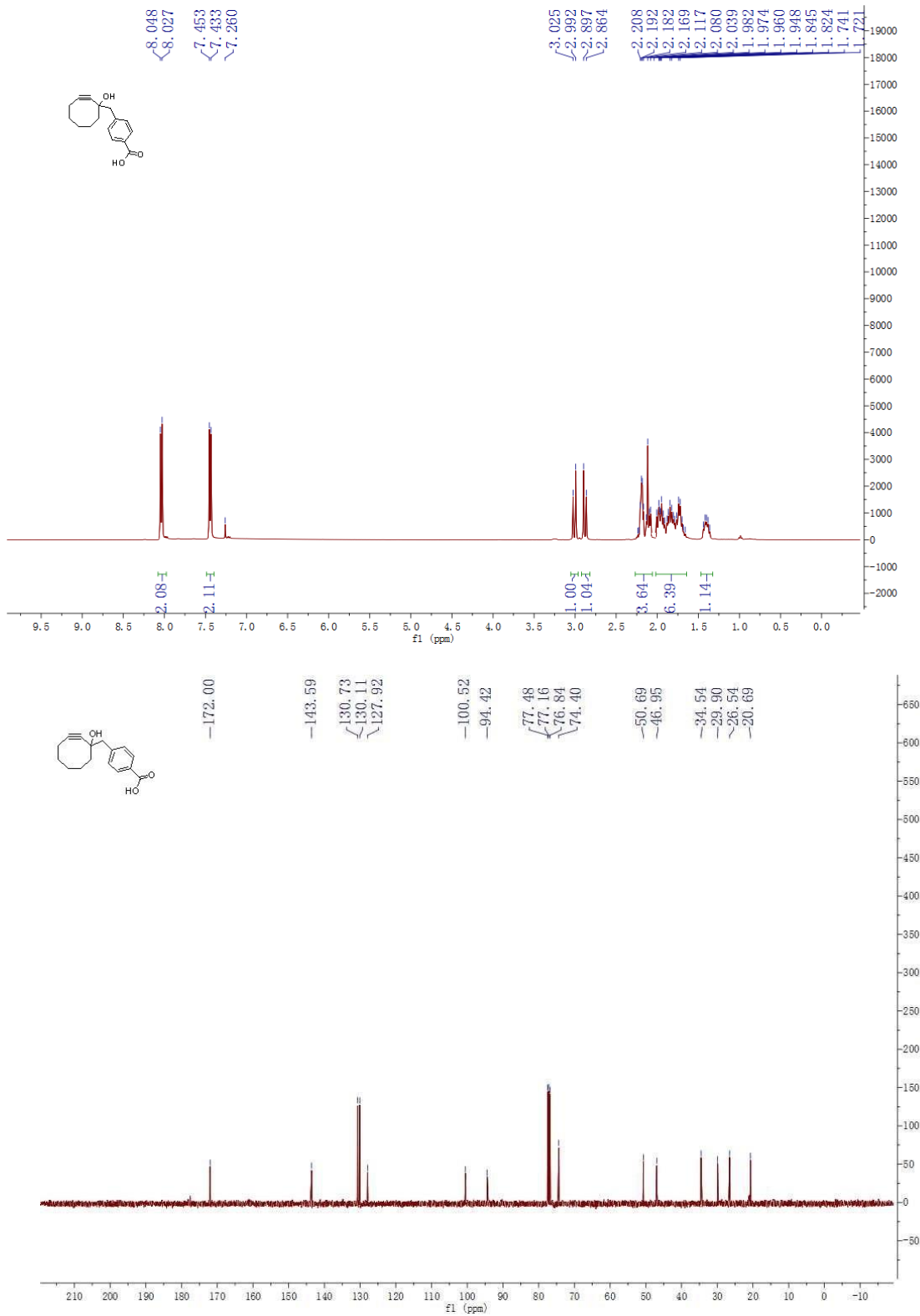


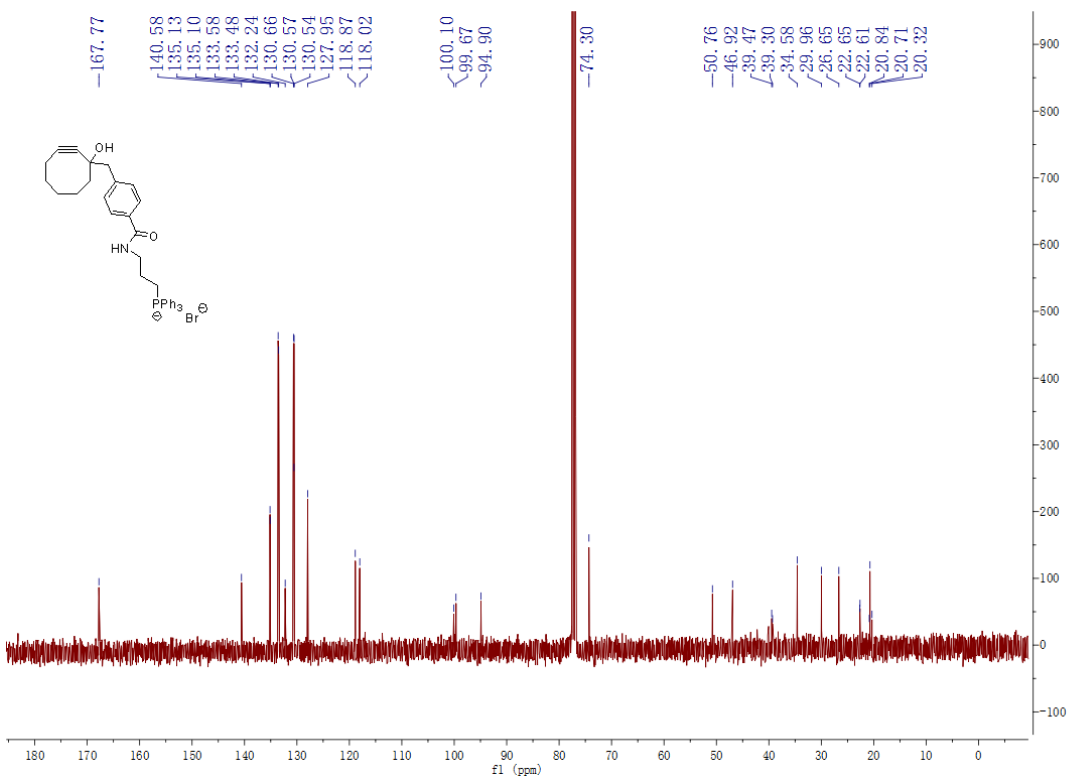
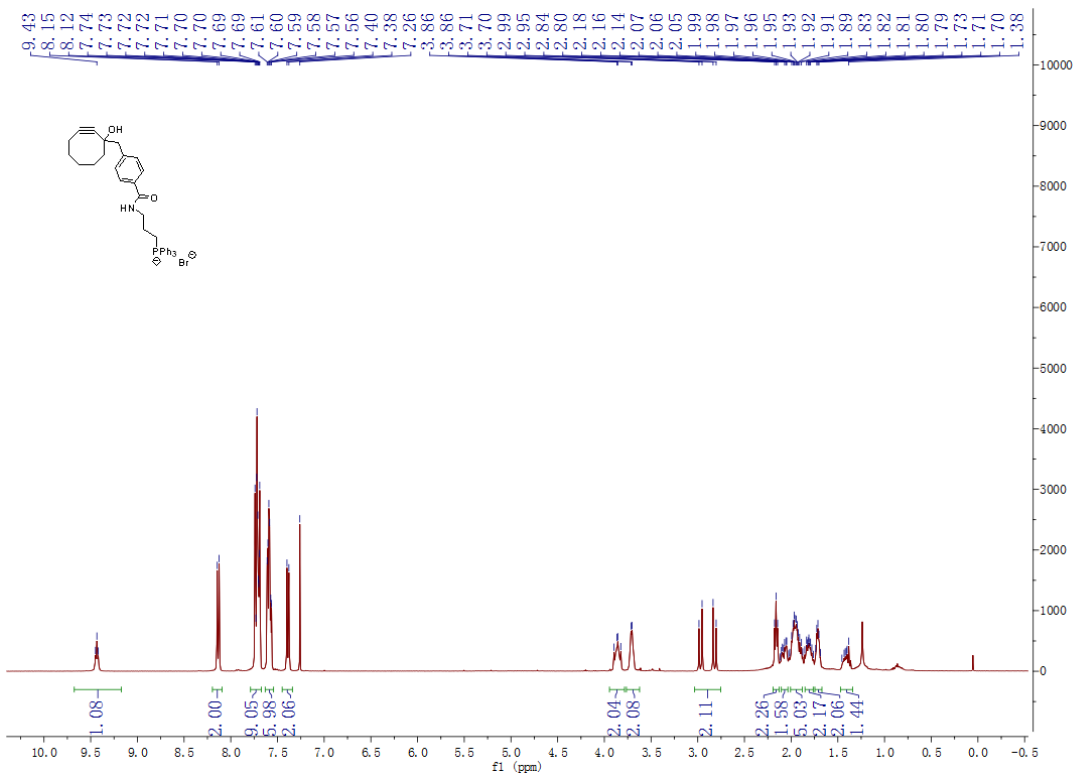


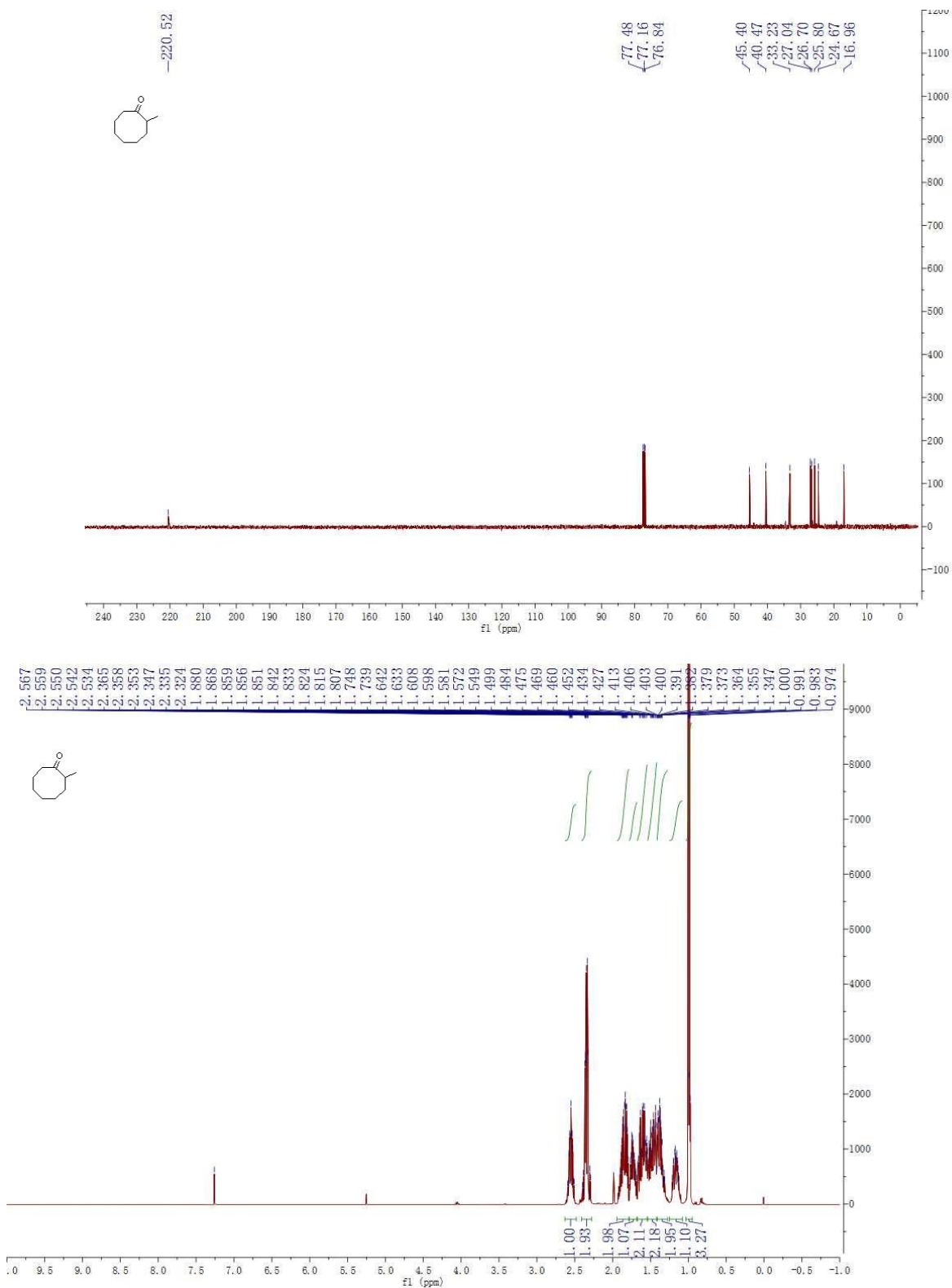


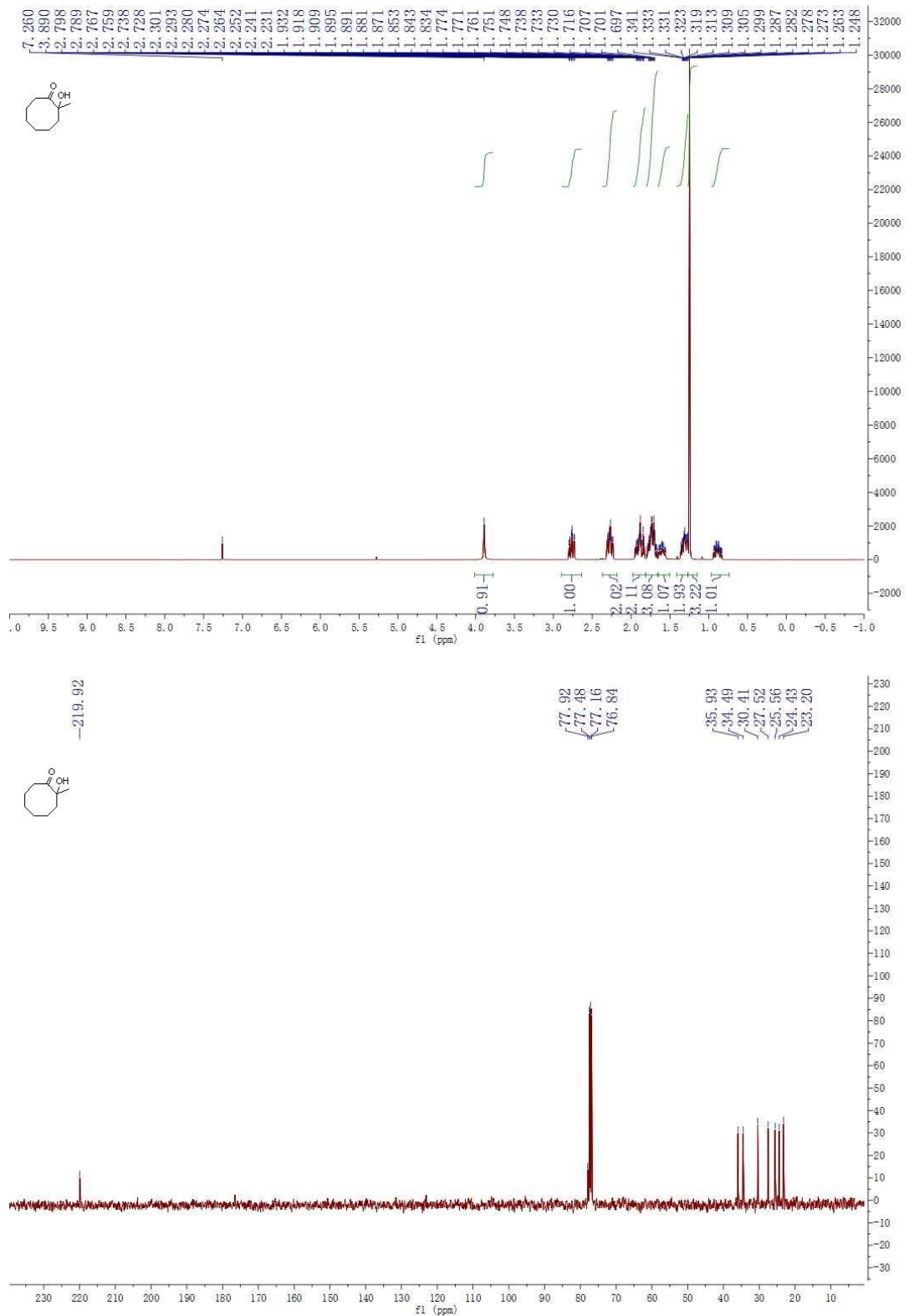


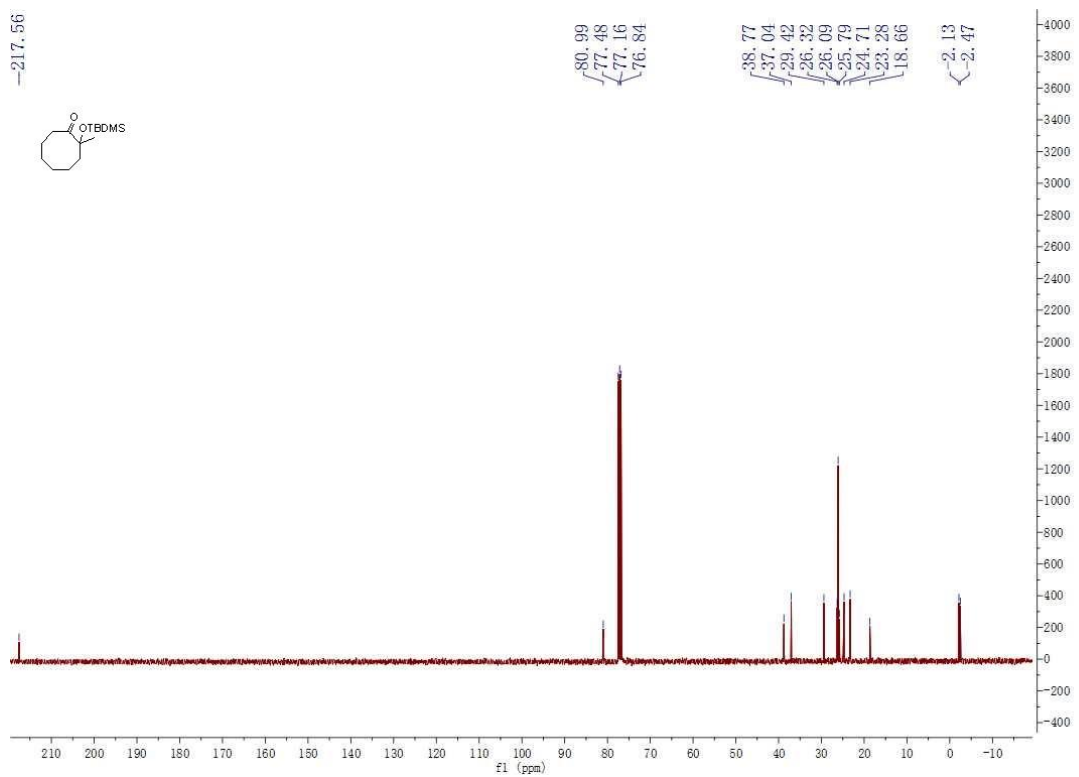
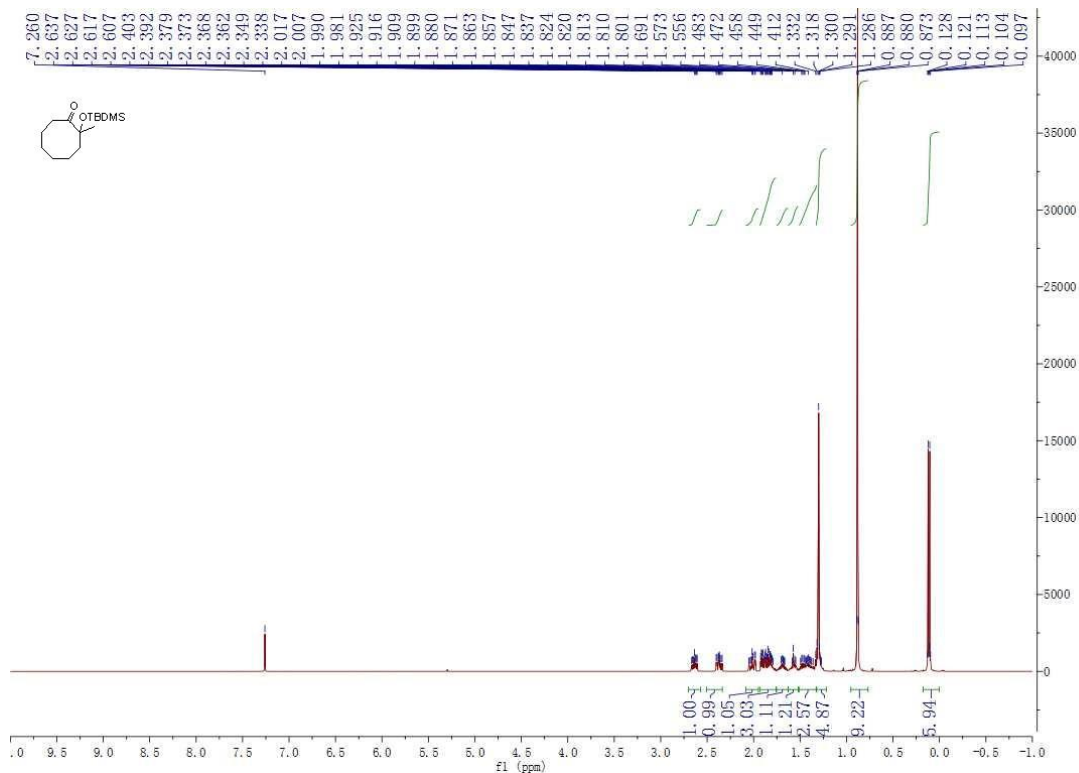


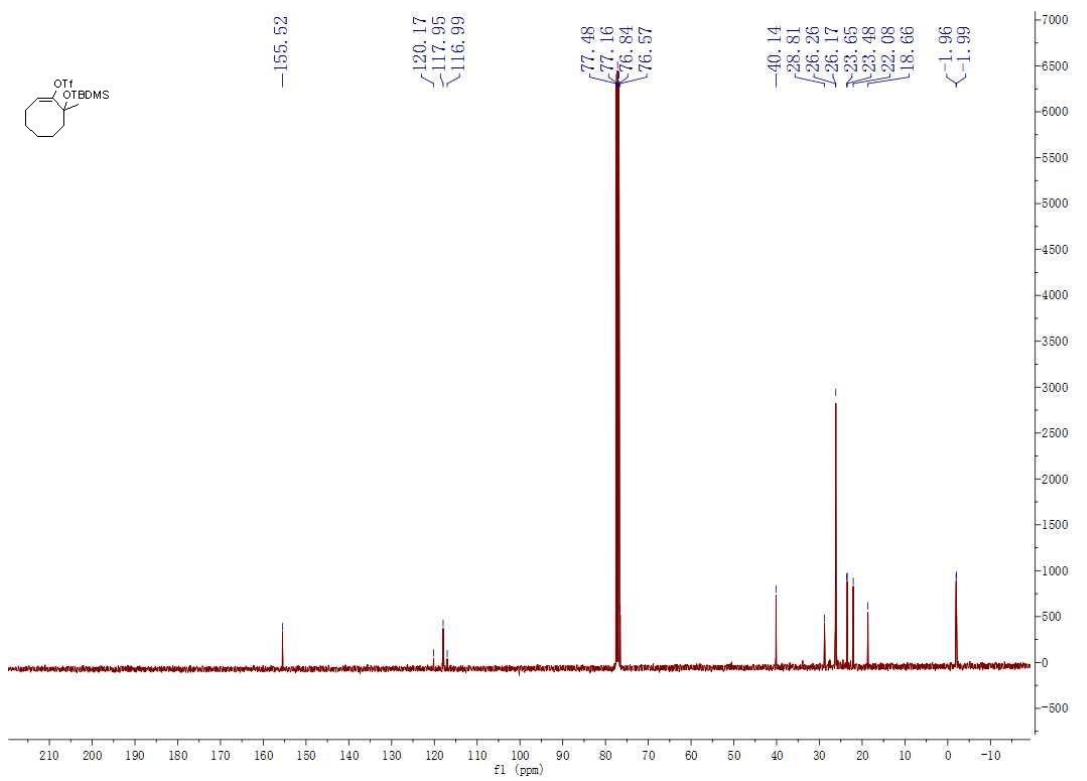
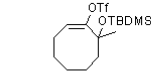
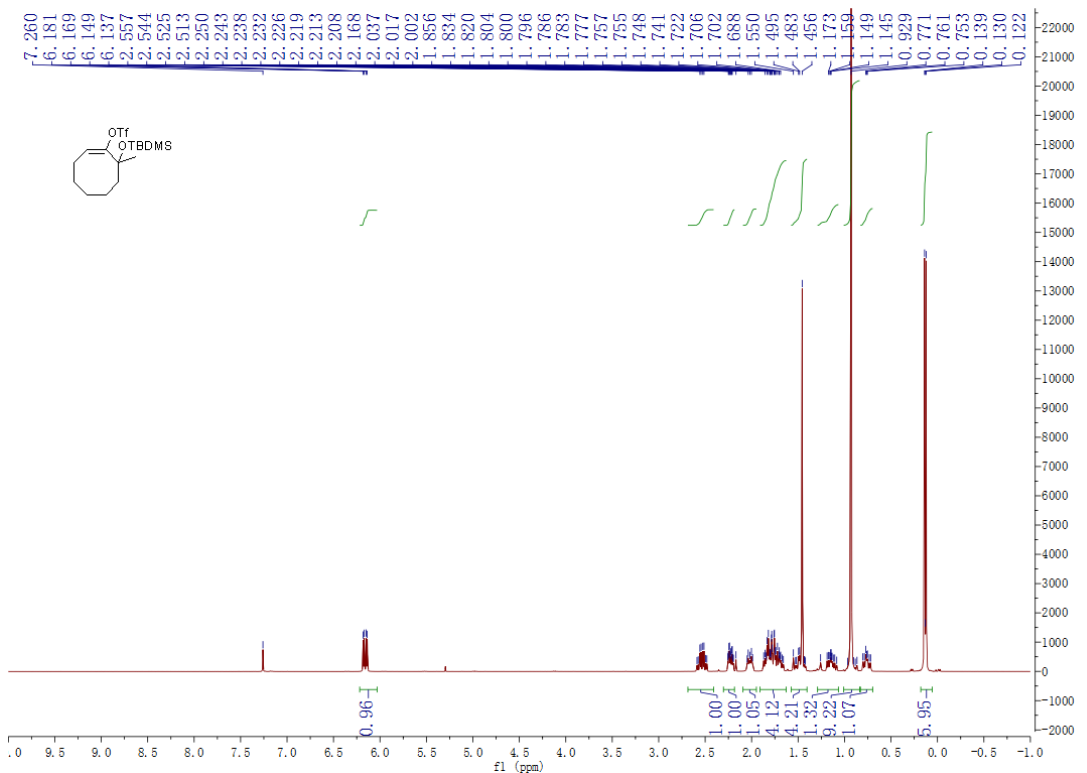


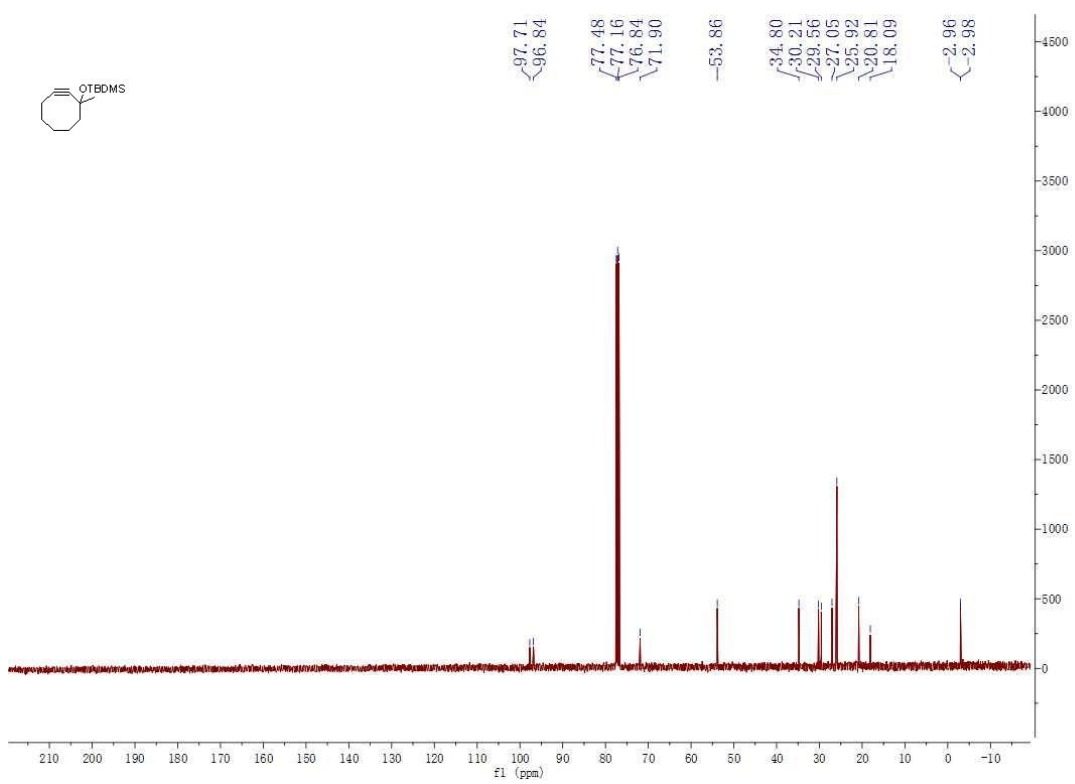
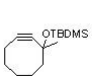
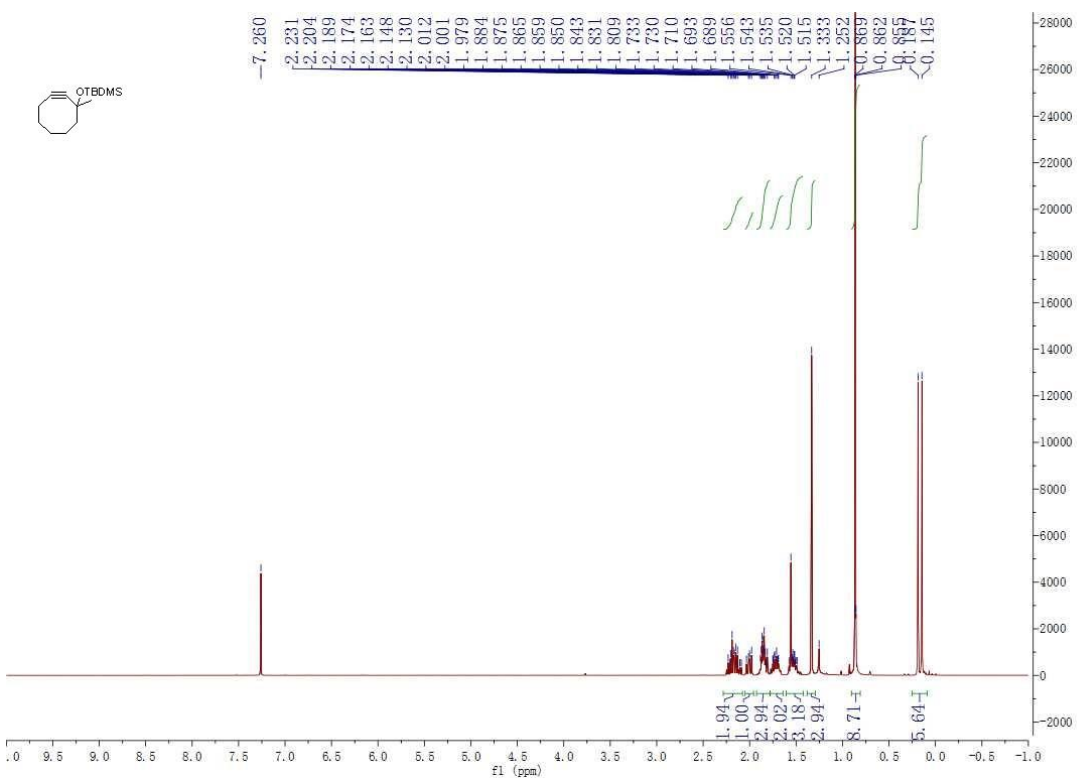


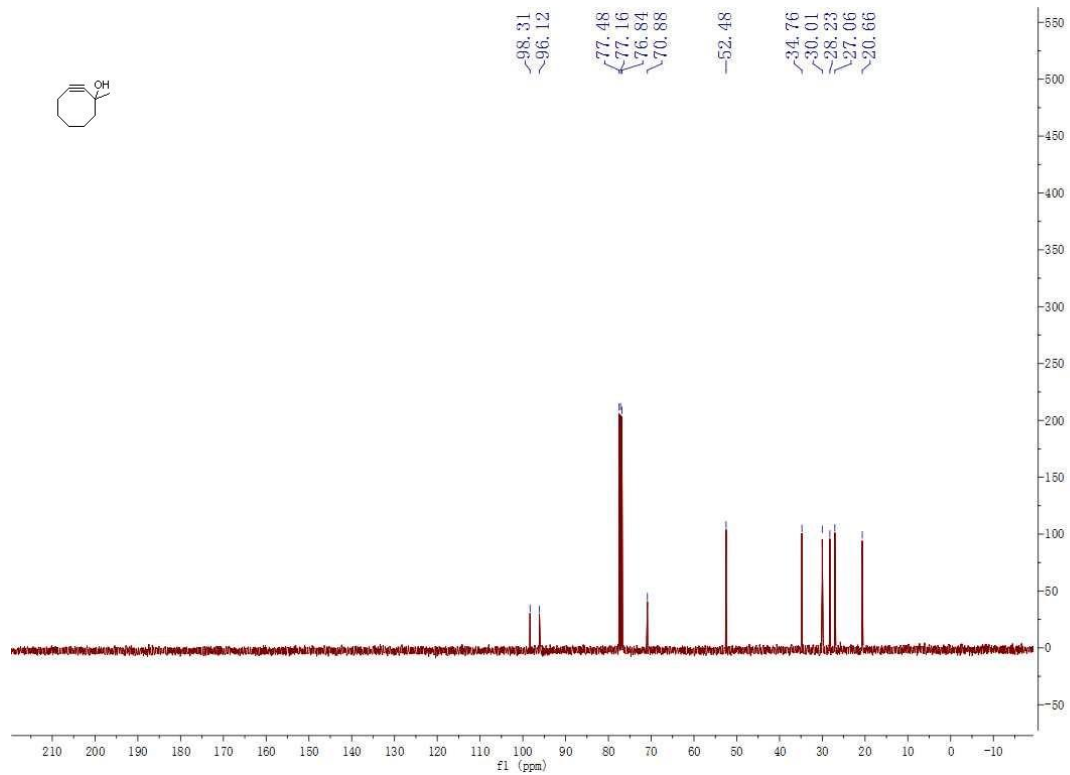
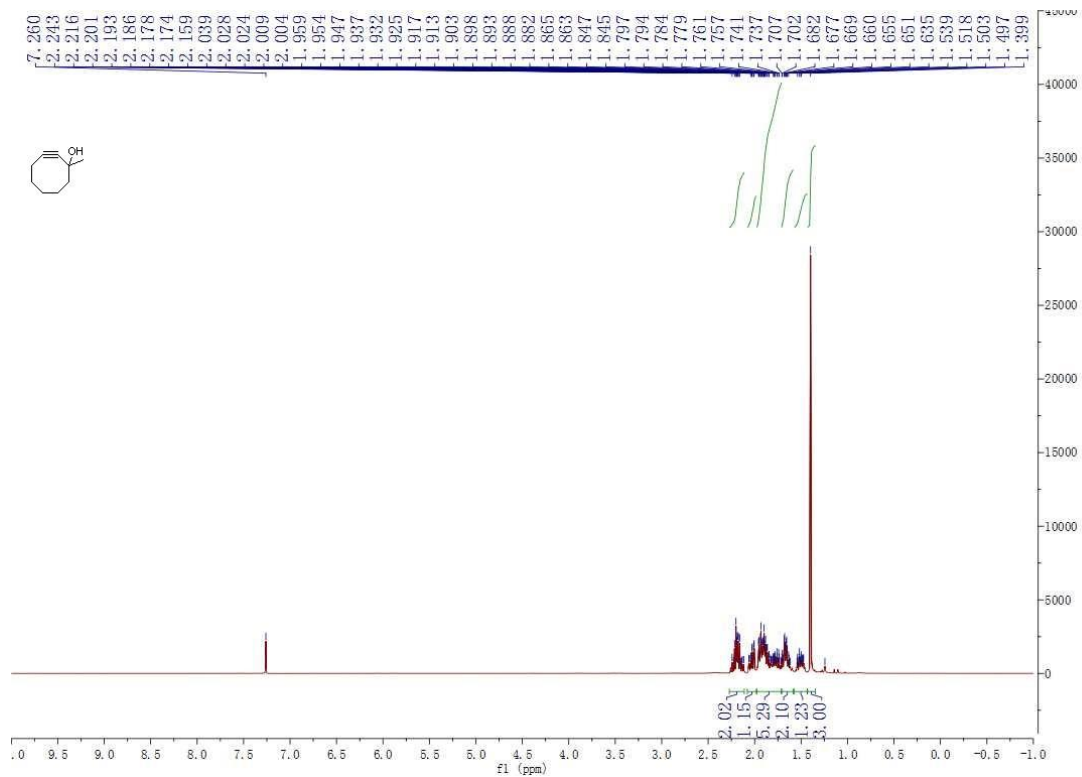




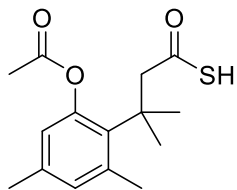




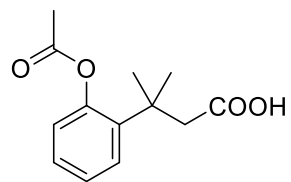
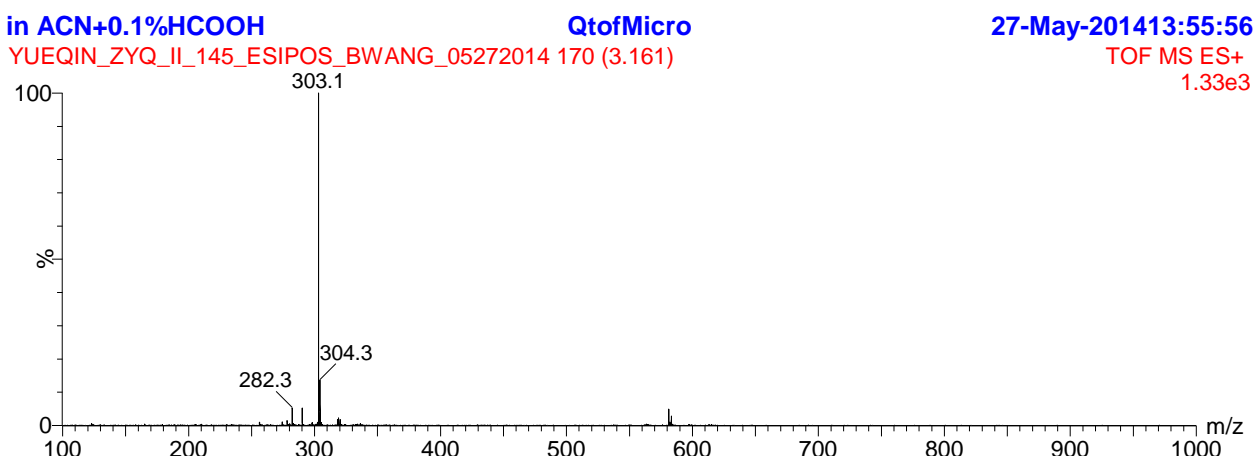




Appendix D. Mass spectrum of new compounds.

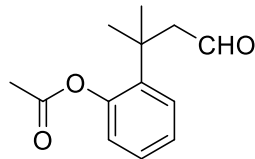
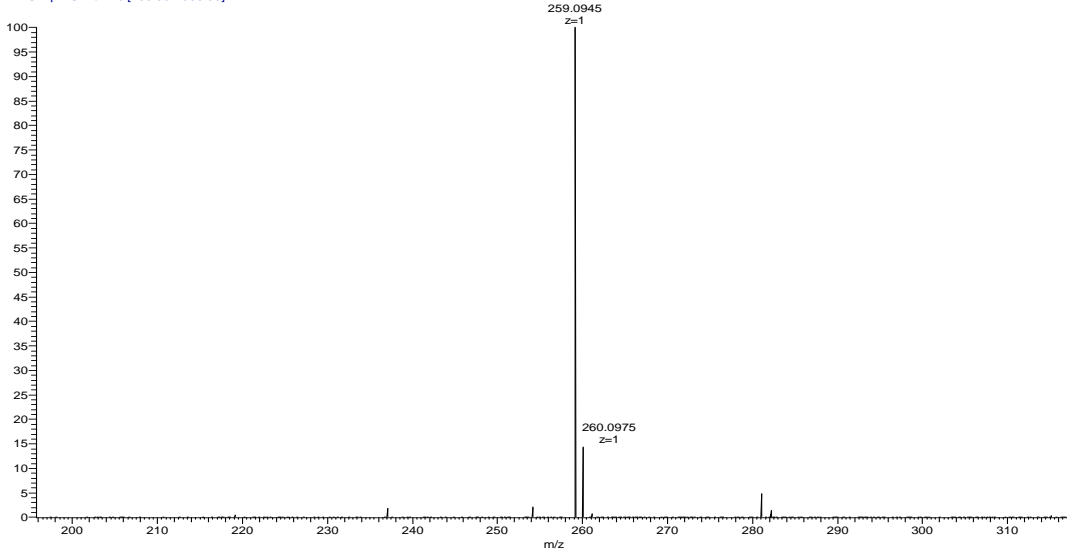


Chemical Formula: C₁₅H₂₀O₃S
Exact Mass: 280.1133



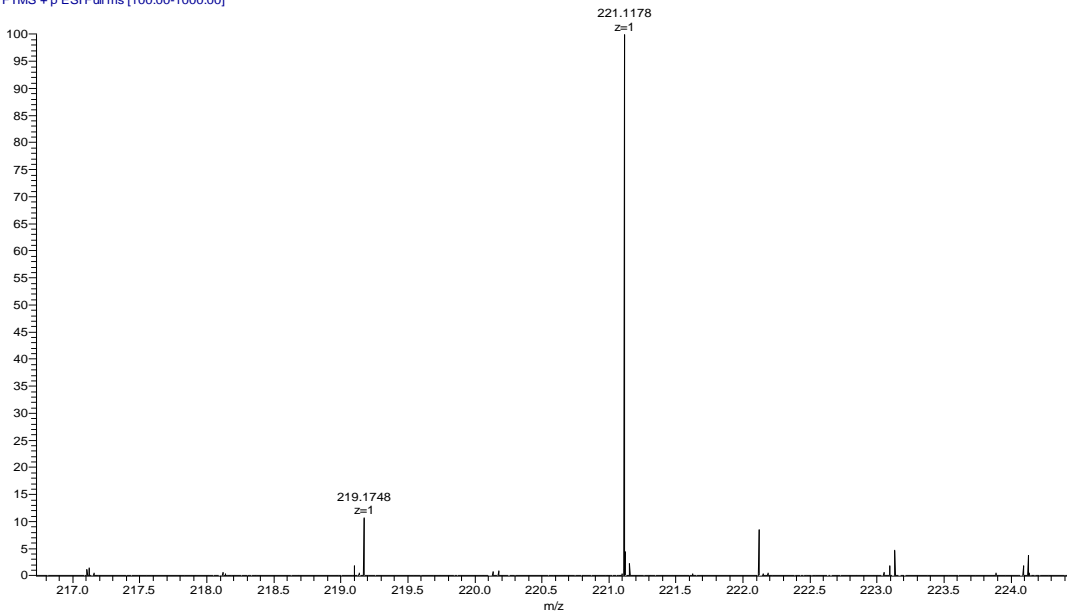
Chemical Formula: C₁₃H₁₆O₄
Exact Mass: 236.1049

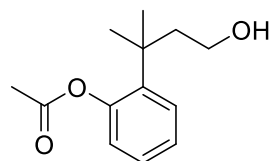
YBC_P67_ESIPOS_BWANG_12102014 #182-212 RT: 2.57-2.98 AV: 31 NL: 9.93E5
T: FTMS + p ESI Full ms [100.00-1000.00]



Chemical Formula: C₁₃H₁₆O₃
Exact Mass: 220.1099

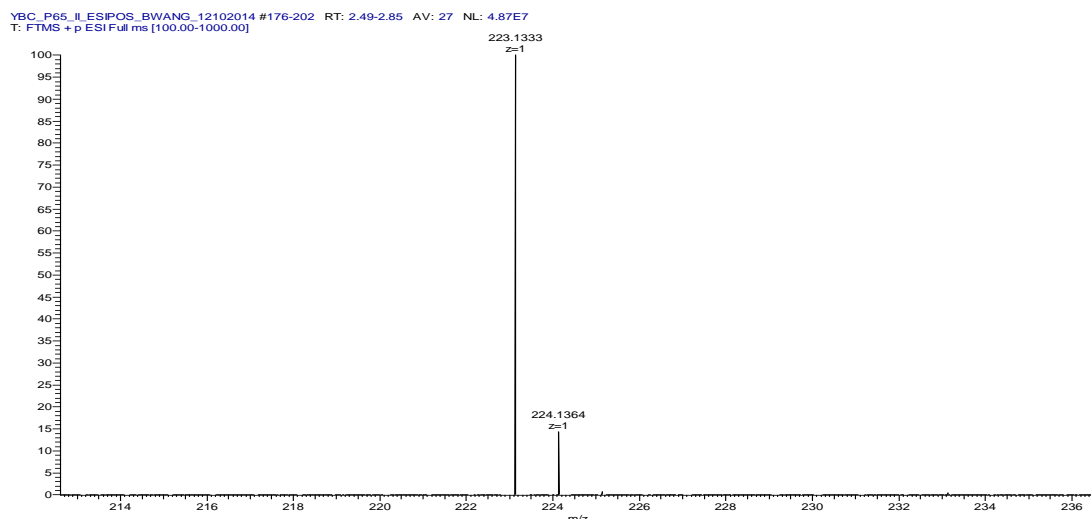
YBC_P66_ESIPOS_BWANG_12102014 #172-199 RT: 2.45-2.82 AV: 28 NL: 3.54E5
T: FTMS + p ESI Full ms [100.00-1000.00]

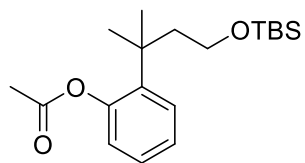




Chemical Formula: C₁₃H₁₈O₃

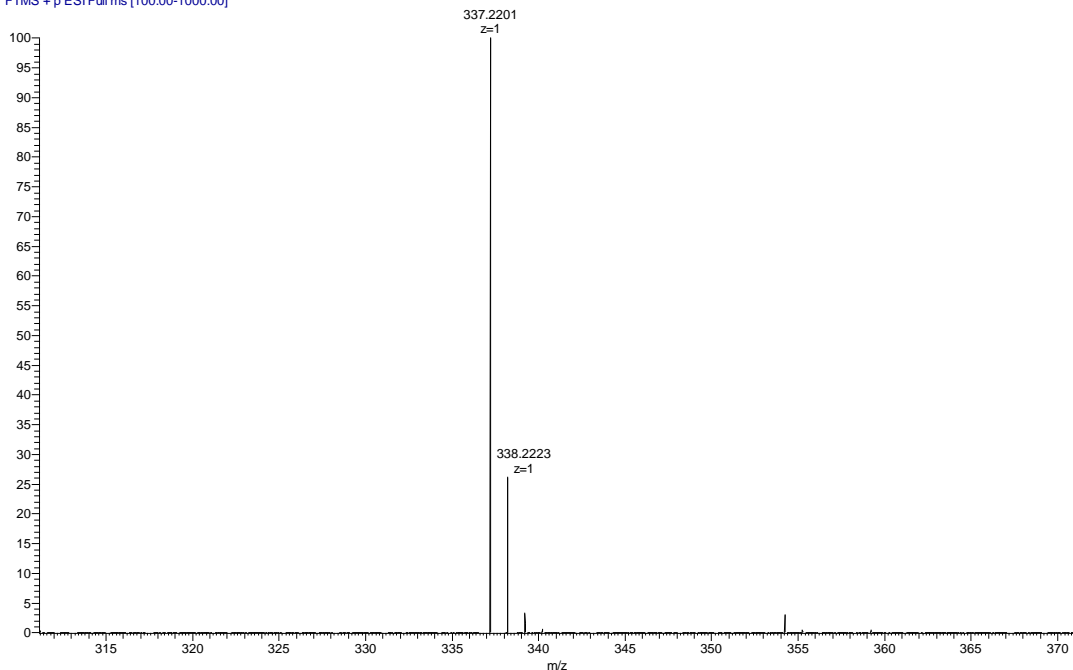
Exact Mass: 222.1256

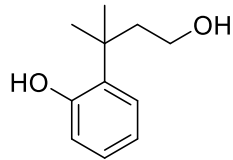




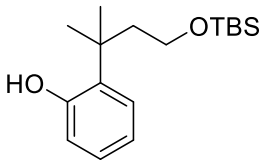
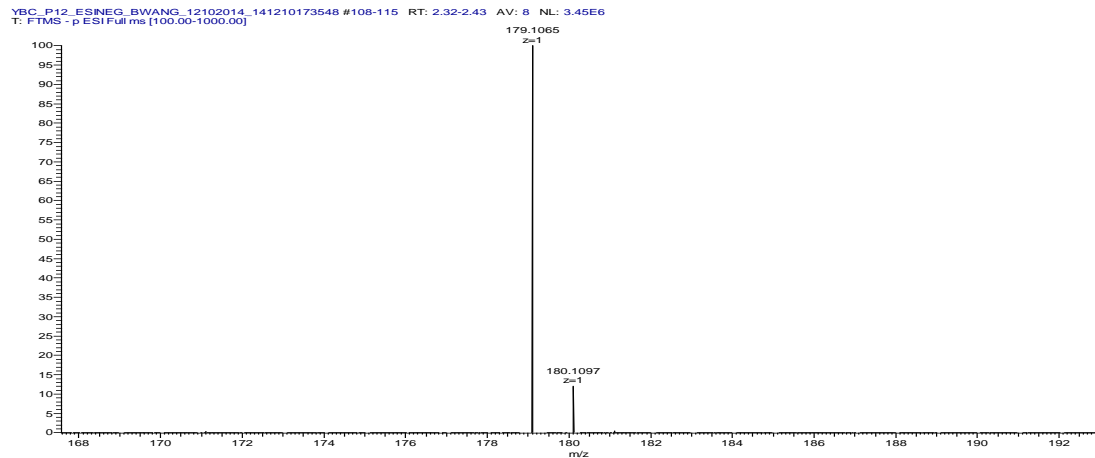
Chemical Formula: C₁₉H₃₂O₃Si
Exact Mass: 336.2121

YBC_P64_ESIPOS_BWANG_12102014 #171-188 RT: 2.43-2.66 AV: 18 NL: 7.65E7
T: FTMS + p ESI Full ms [100.00-1000.00]

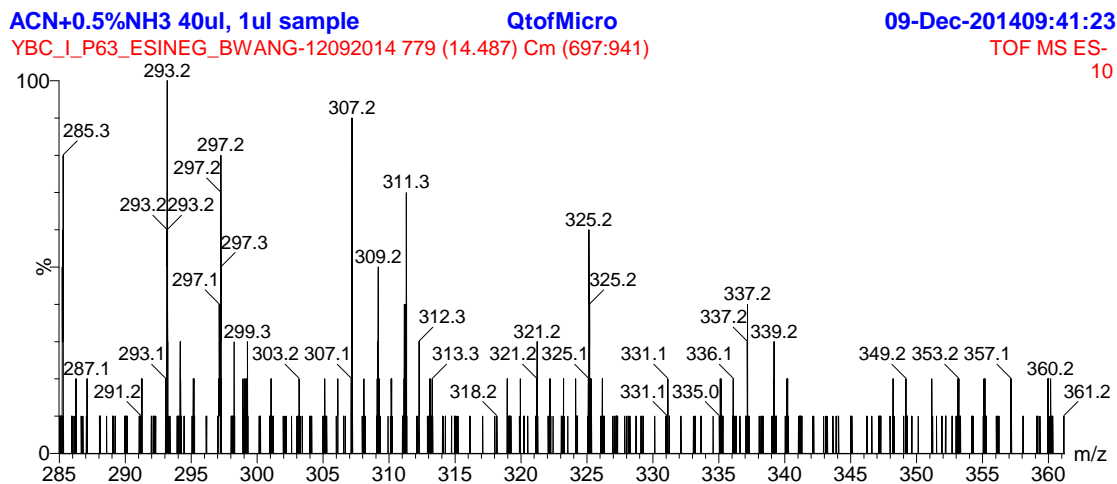


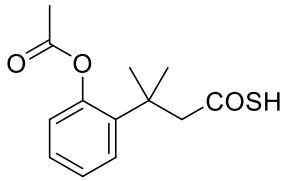


Chemical Formula: C₁₁H₁₆O₂
Exact Mass: 180.1150

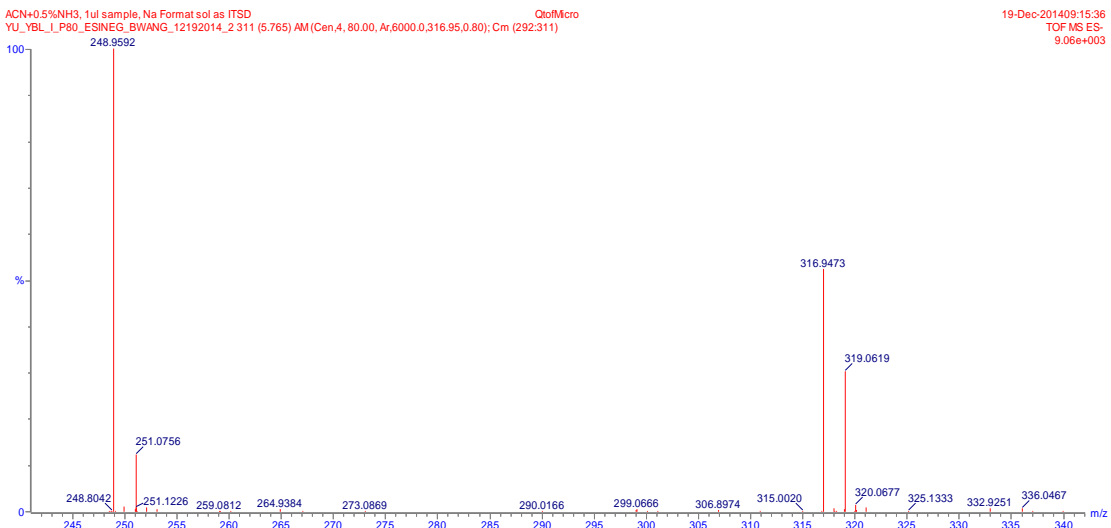


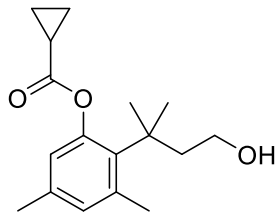
Chemical Formula: C₁₇H₃₀O₂Si
Exact Mass: 294.2015





Chemical Formula: C₁₃H₁₆O₃S
Exact Mass: 252.0820



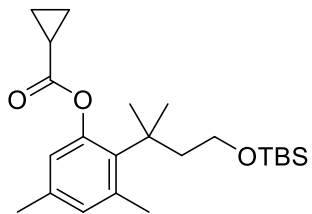
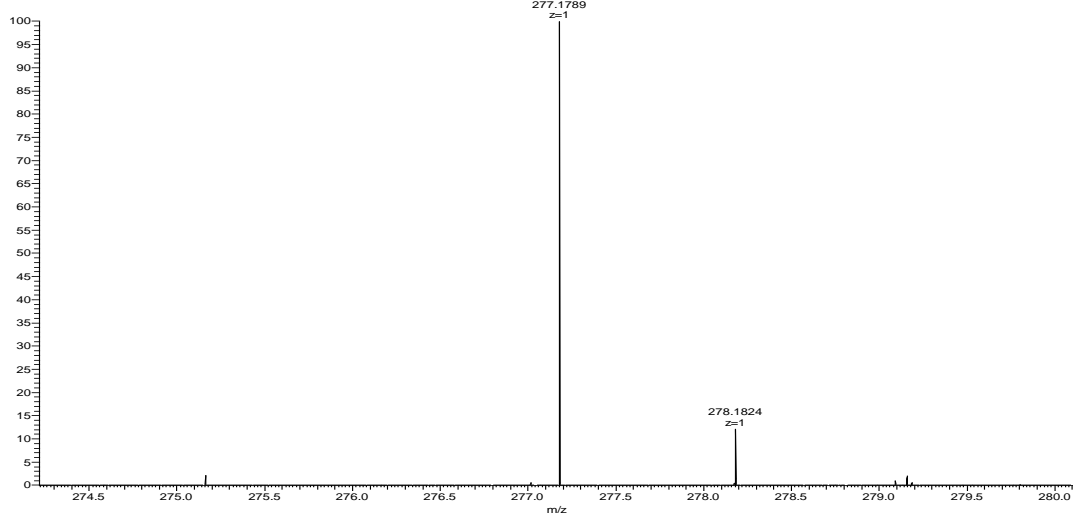


Chemical Formula: C₁₇H₂₄O₃

Exact Mass: 276.1725

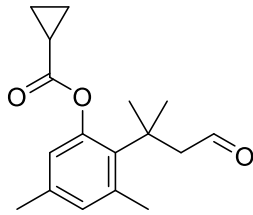
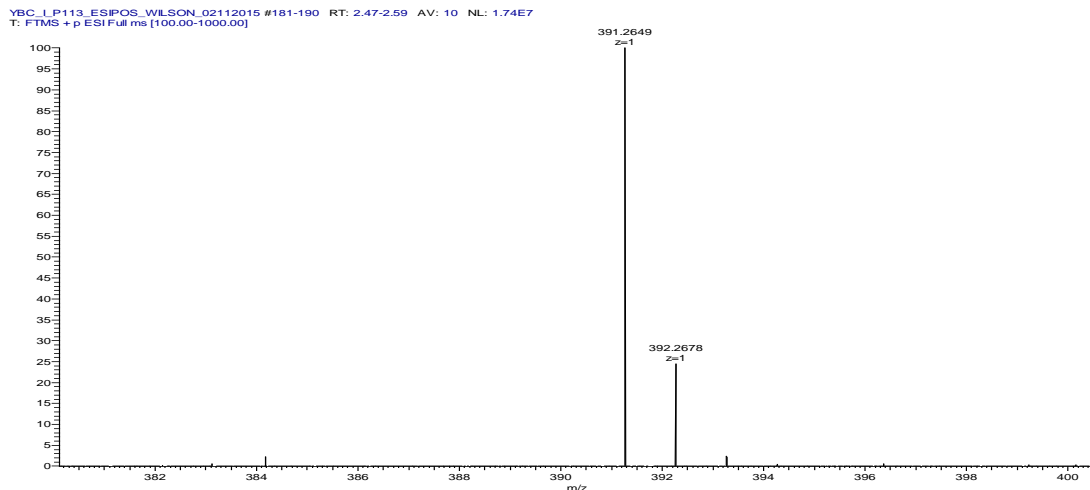
YBC_I_P115_ESIPOS_WILSON_02112015 #183-193 RT: 2.49-2.63 AV: 11 NL: 4.73E5

T: FTMS + p ESI Full ms [100.00-1000.00]



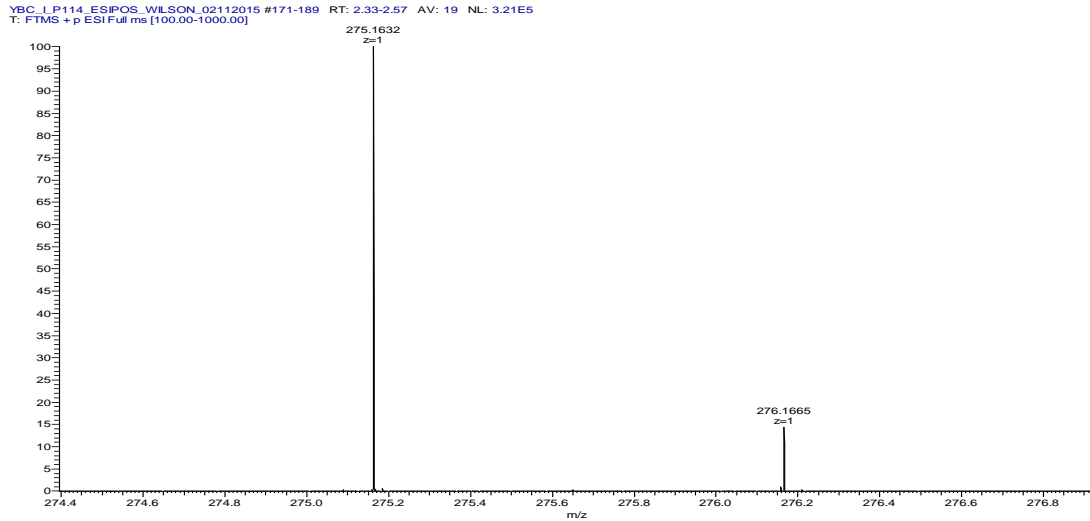
Chemical Formula: C₂₃H₃₈O₃Si

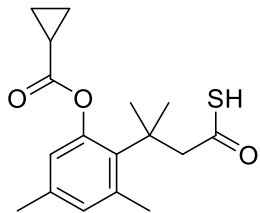
Exact Mass: 390.2590



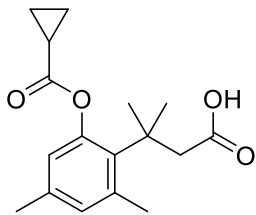
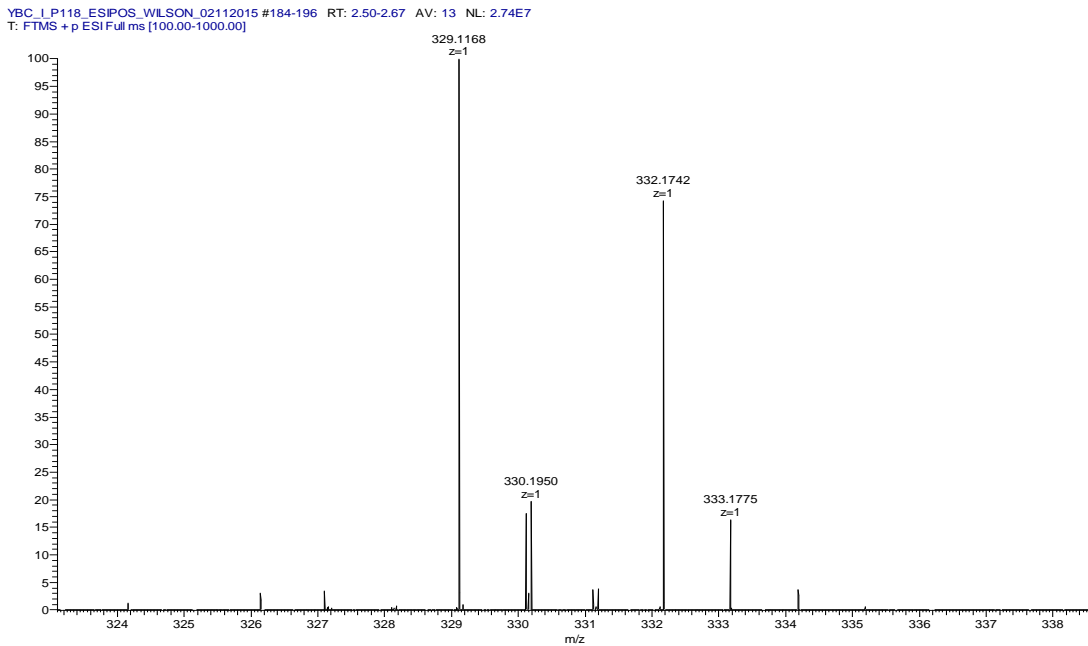
Chemical Formula: C₁₇H₂₂O₃

Exact Mass: 274.1569

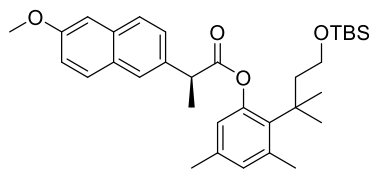
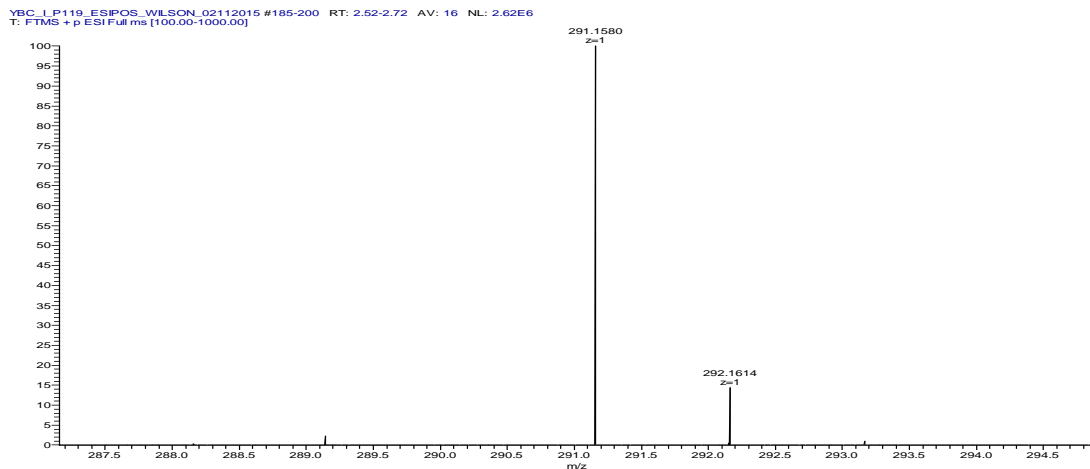




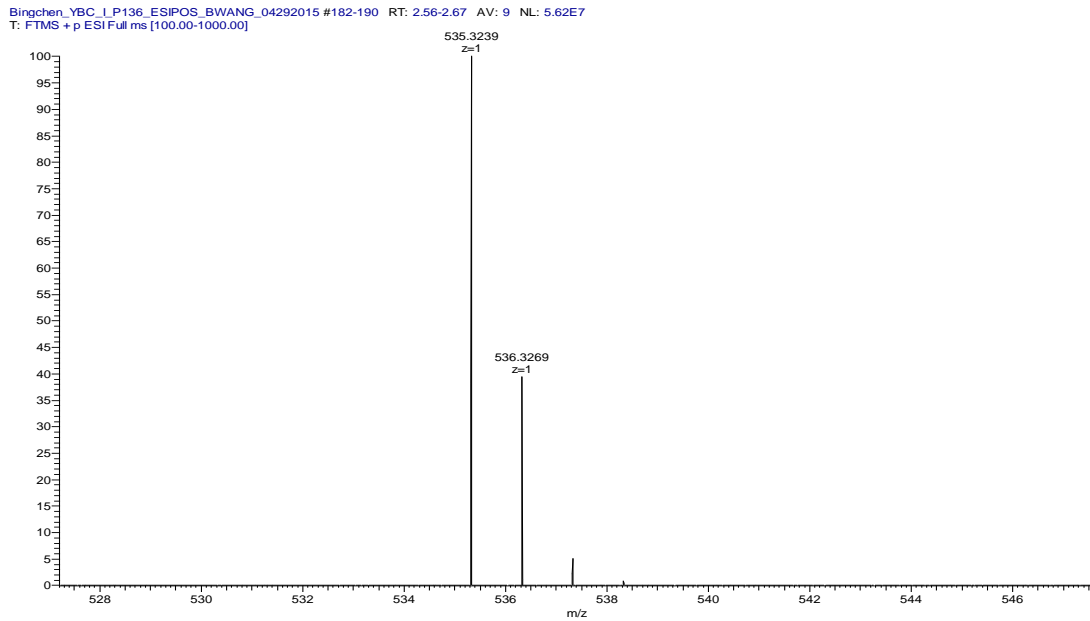
Chemical Formula: C₁₇H₂₂O₃S
Exact Mass: 306.1290

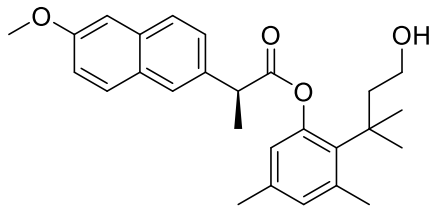


Chemical Formula: C₁₇H₂₂O₄
Exact Mass: 290.1518



Chemical Formula: $C_{33}H_{46}O_4Si$
Exact Mass: 534.3165

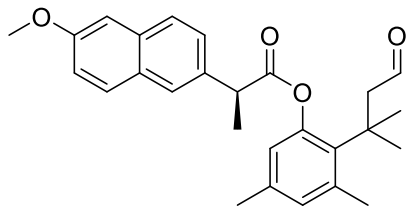
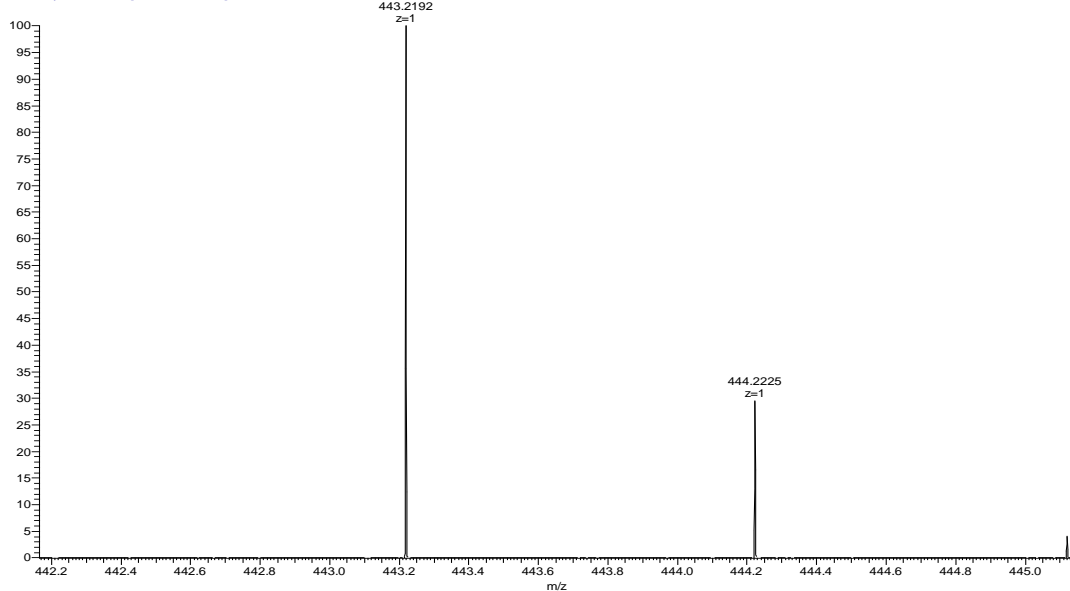




Chemical Formula: C₂₇H₃₂O₄

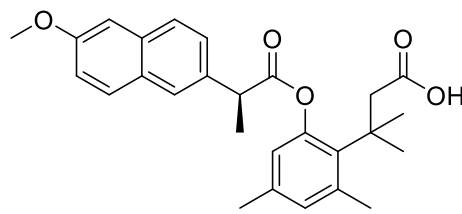
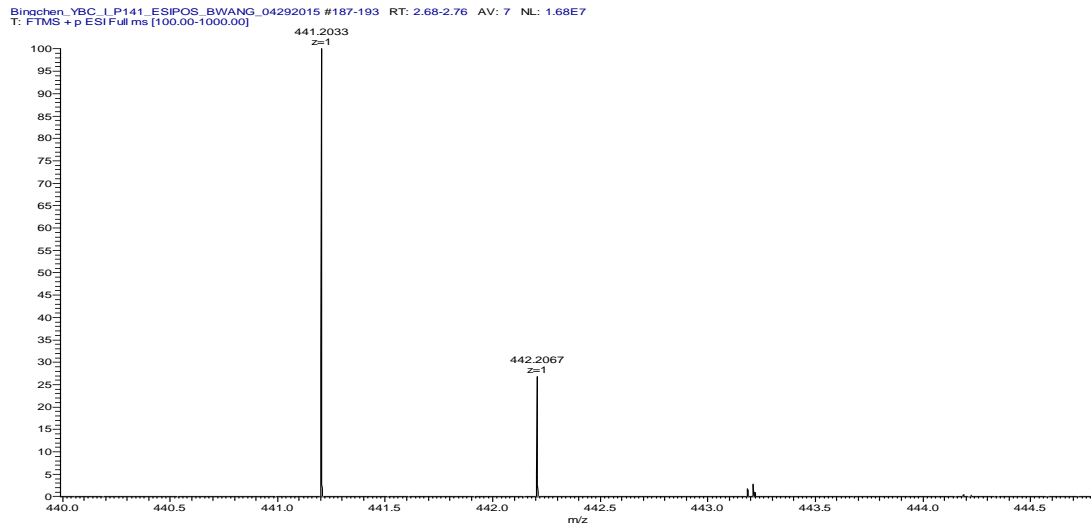
Exact Mass: 420.2301

Bingchen_YBC_L_P140_ESIPOS_BWANG_04292015 #187-199 RT: 2.66-2.82 AV: 13 NL: 1.60E7
T: FTMS + p ESI Full ms [100.00-1000.00]

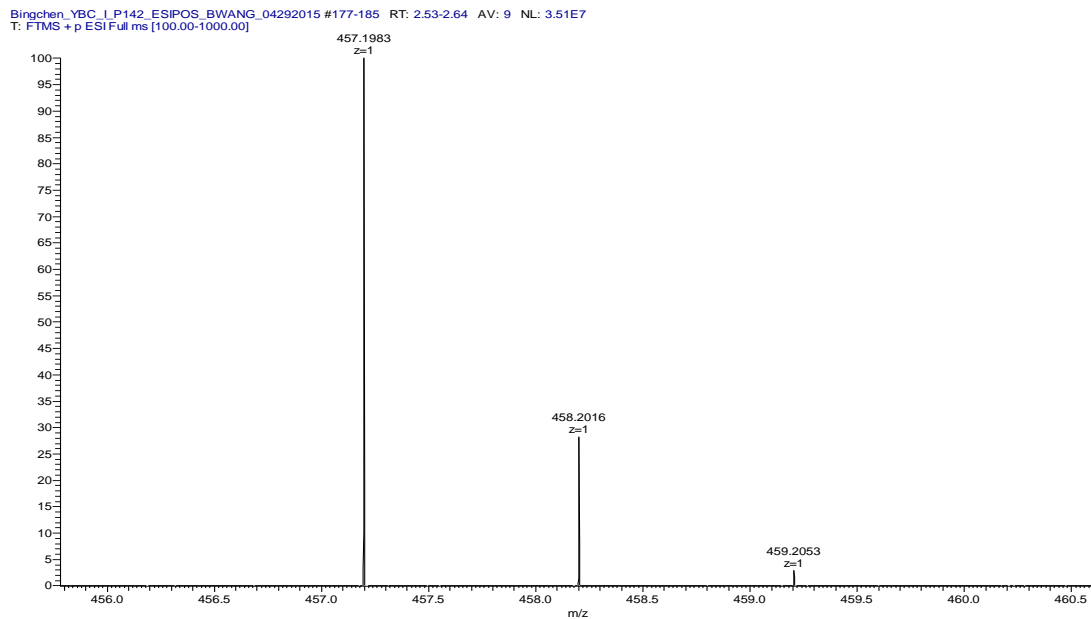


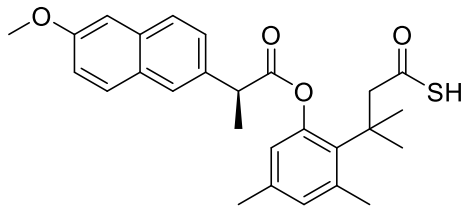
Chemical Formula: C₂₇H₃₀O₄

Exact Mass: 418.2144



Chemical Formula: C₂₇H₃₀O₅
Exact Mass: 434.2093

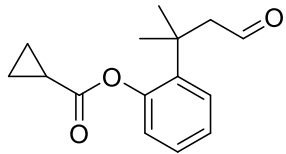
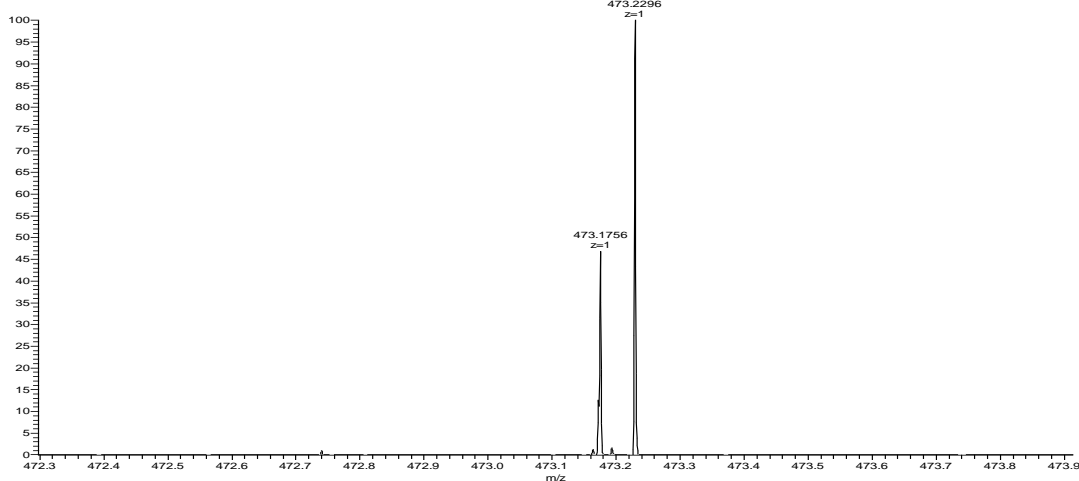




Chemical Formula: C₂₇H₃₀O₄S

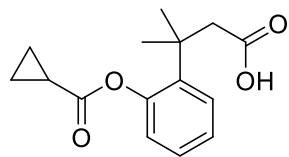
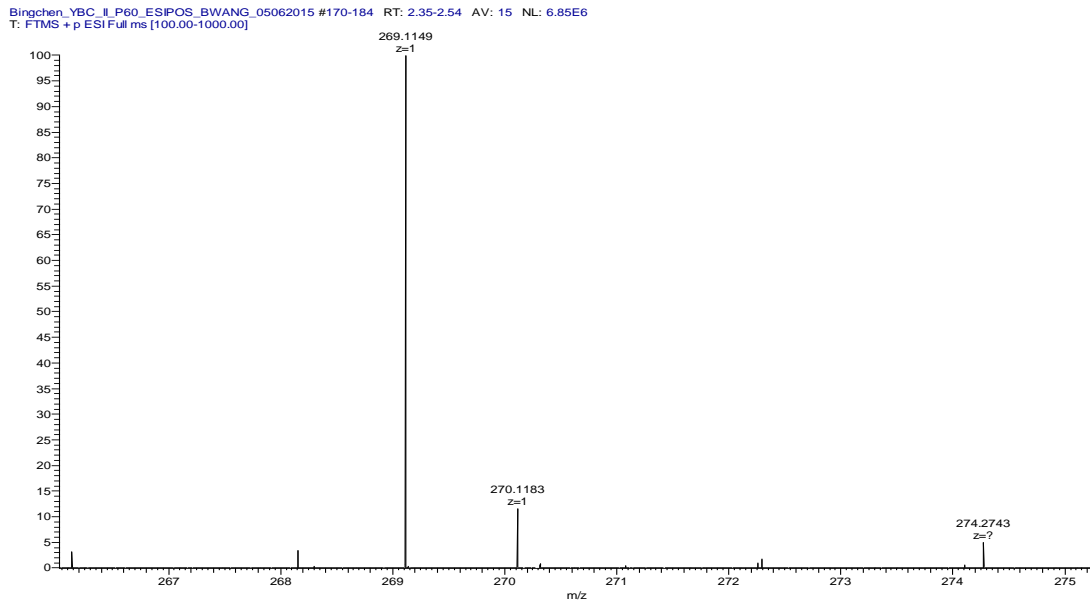
Exact Mass: 450.1865

Bingchen_YBC_L_P143_ESIPOS_BWANG_04292015 #180-193 RT: 2.57-2.75 AV: 14 NL: 4.13E6
T: FTMS + p ESI Full ms [100.00-1000.00]

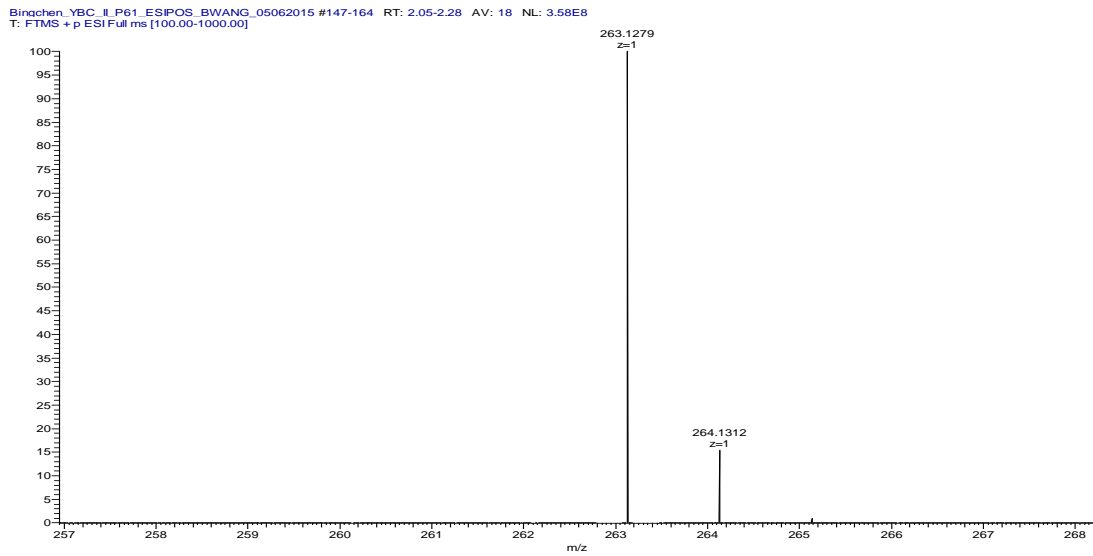


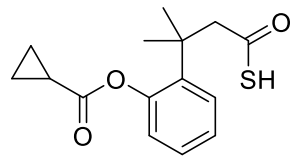
Chemical Formula: C₁₅H₁₈O₃

Exact Mass: 246.1256

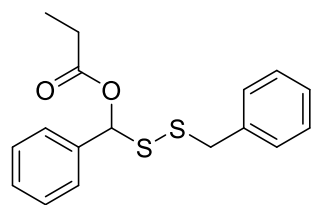
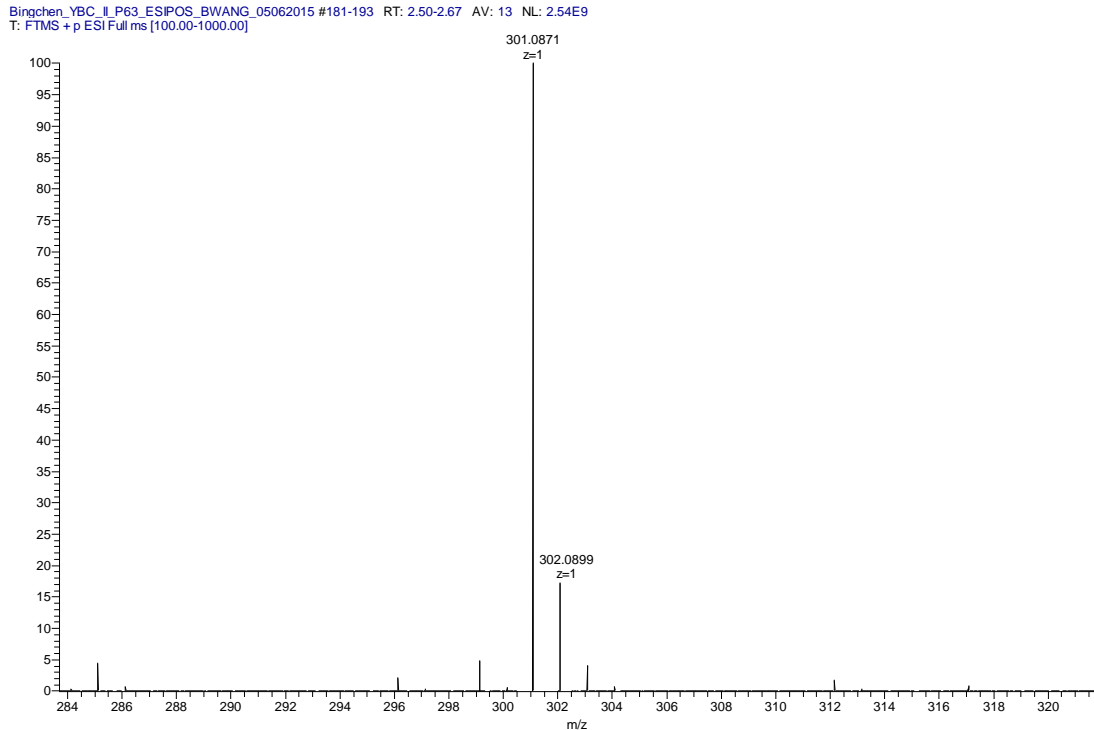


Chemical Formula: $C_{15}H_{18}O_4$
Exact Mass: 262.1205



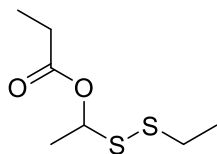
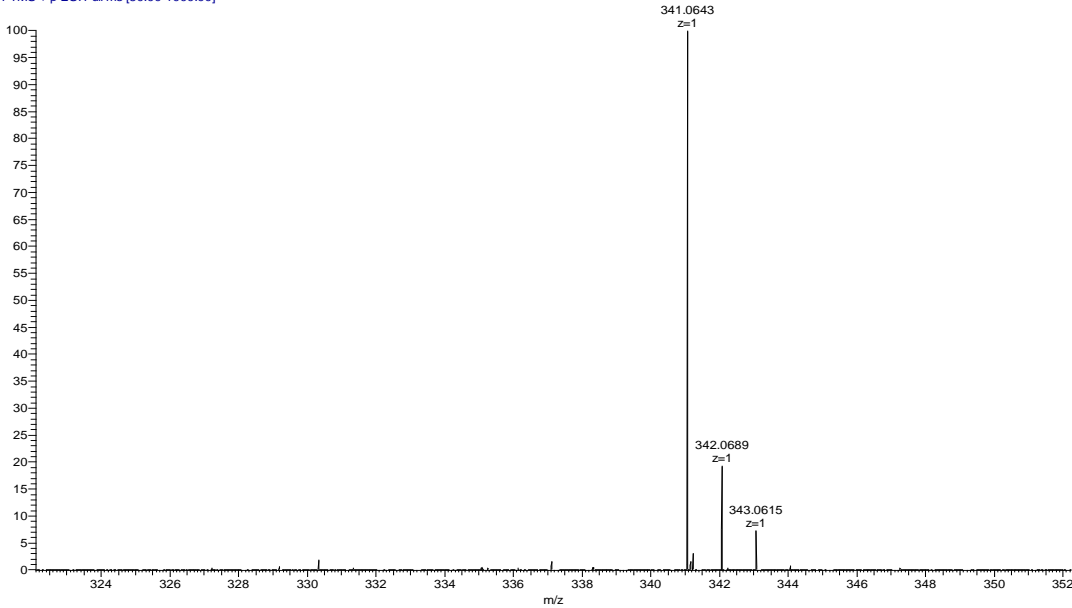


Chemical Formula: C₁₅H₁₈O₃S
Exact Mass: 278.0977

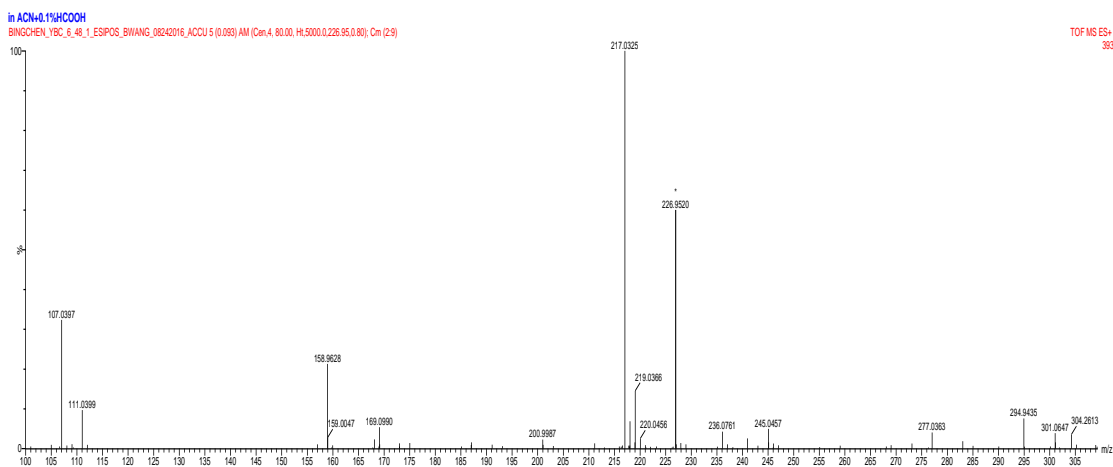


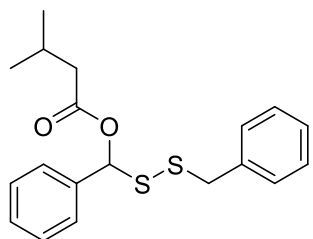
Chemical Formula: C₁₇H₁₈O₂S₂
Exact Mass: 318.0748

YU_6_P42_ESIPOS_BWang_10272016 #116-155 RT: 1.90-2.45 AV: 40 NL: 6.25E5
T: FTMS + p ESI Full ms [50.00-1000.00]

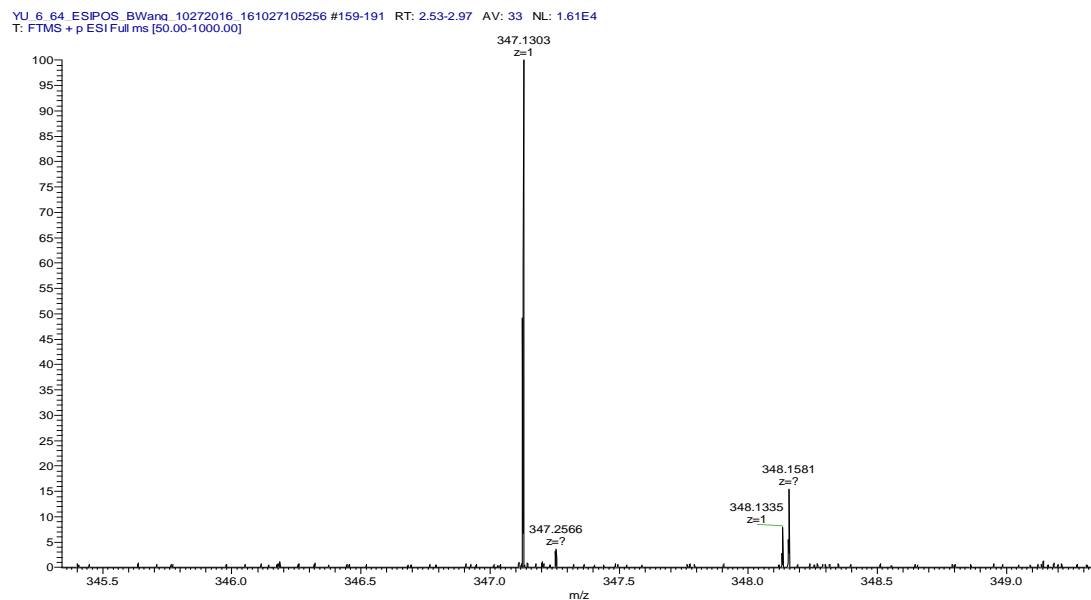


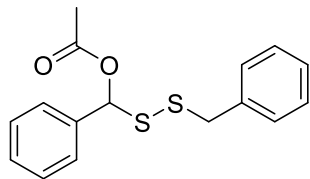
Chemical Formula: C₇H₁₄O₂S₂
Exact Mass: 194.0435





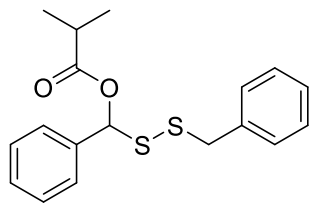
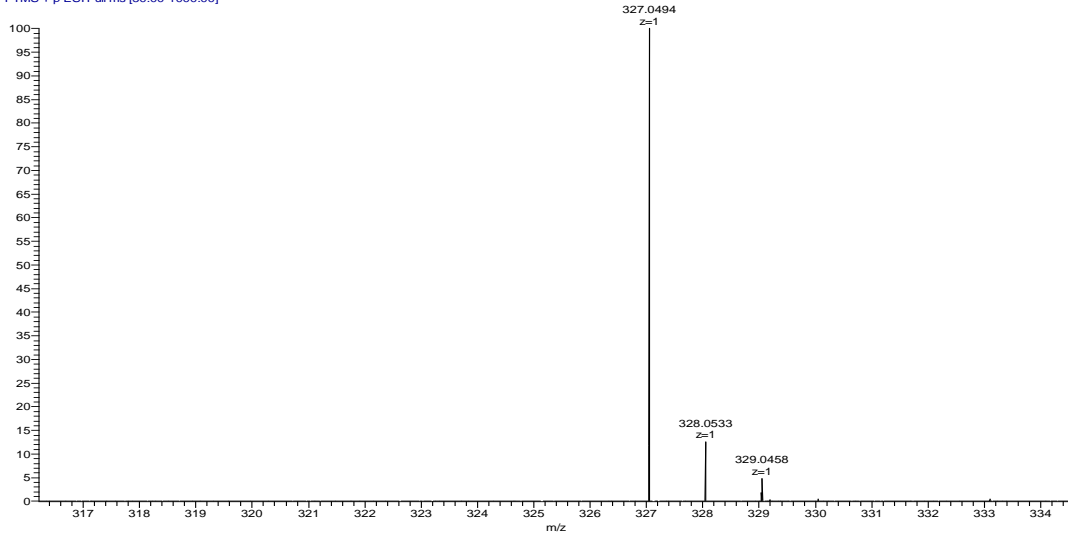
Chemical Formula: C₁₉H₂₂O₂S₂
Exact Mass: 346.1061



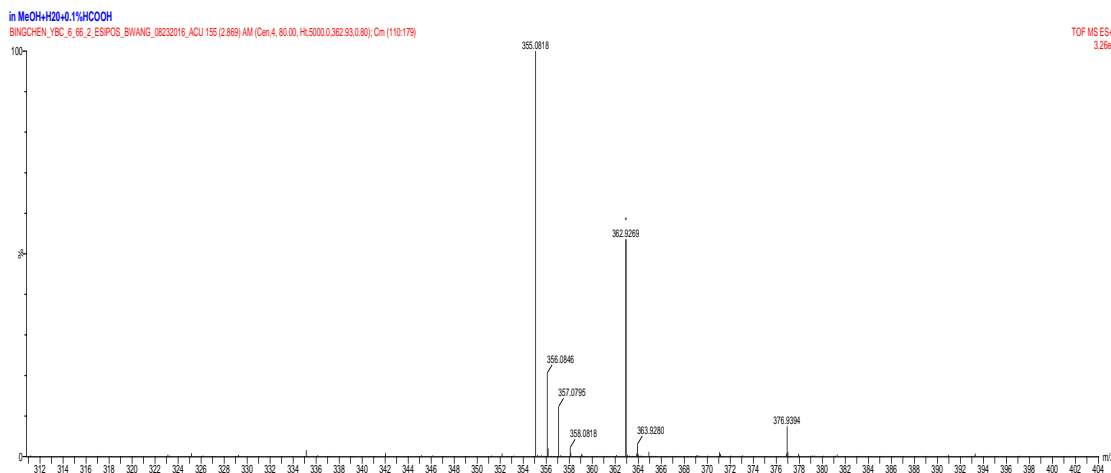


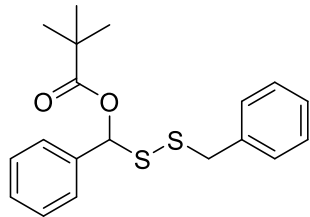
Chemical Formula: C₁₆H₁₆O₂S₂
Exact Mass: 304.0592

YU_6_52 ESIPOS_BWang_10272016 #171-184 RT: 2.72-2.91 AV: 14 NL: 8.79E5
T: FTMS + p ESIFull ms [50.00-1000.00]



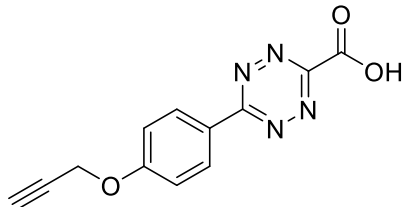
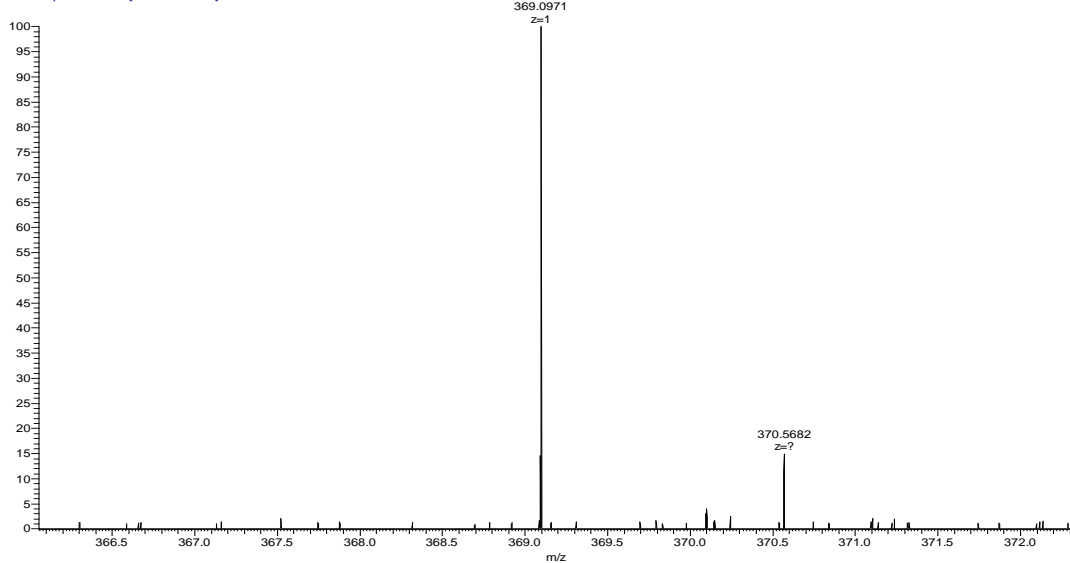
Chemical Formula: C₁₈H₂₀O₂S₂
Exact Mass: 332.0905





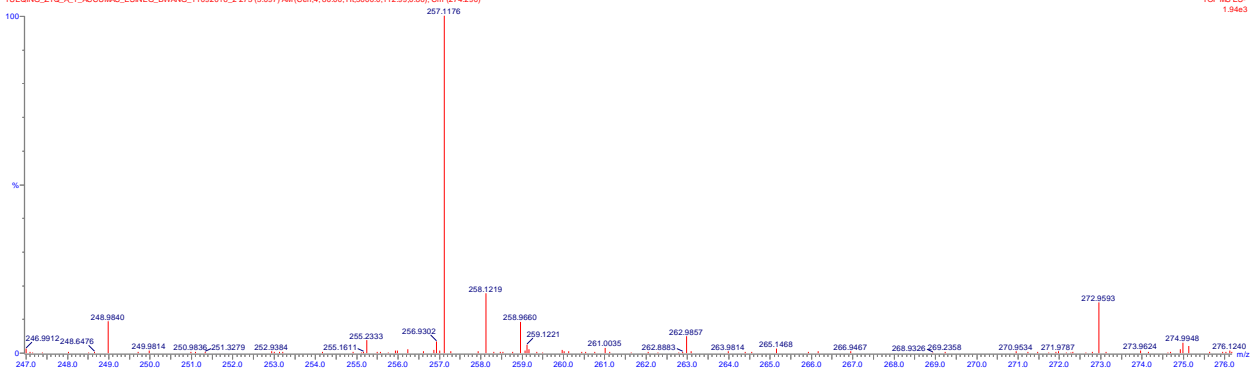
Chemical Formula: C₁₉H₂₂O₂S₂
Exact Mass: 346.1061

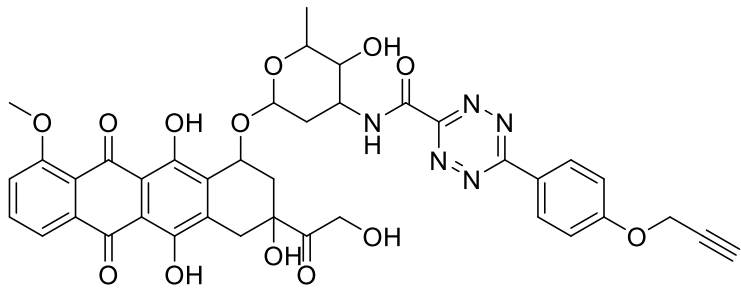
YU_7_26_ESIPOS_BWANG_11032016 #156-167 RT: 2.34-2.50 AV: 12 NL: 5.07E3
T: FTMS + p ESI Full ms [50.00-1000.00]



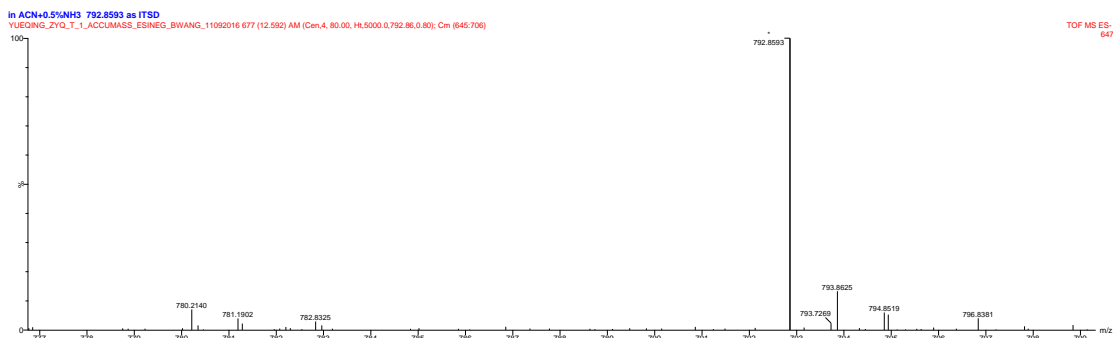
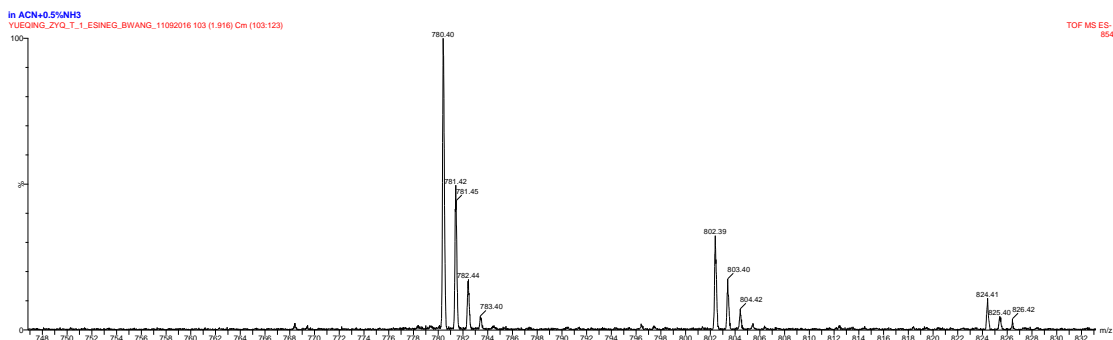
in ACN+0.5%NH3 792.8593 as ITSD
YUEQING_ZYQ_A_1_ACQUITY_ESINEG_BWANG_11092016_2_275 (5.097) AM (Cen,4,80.00,Hi5000.0,112.99,0.80); Cm (274.290)

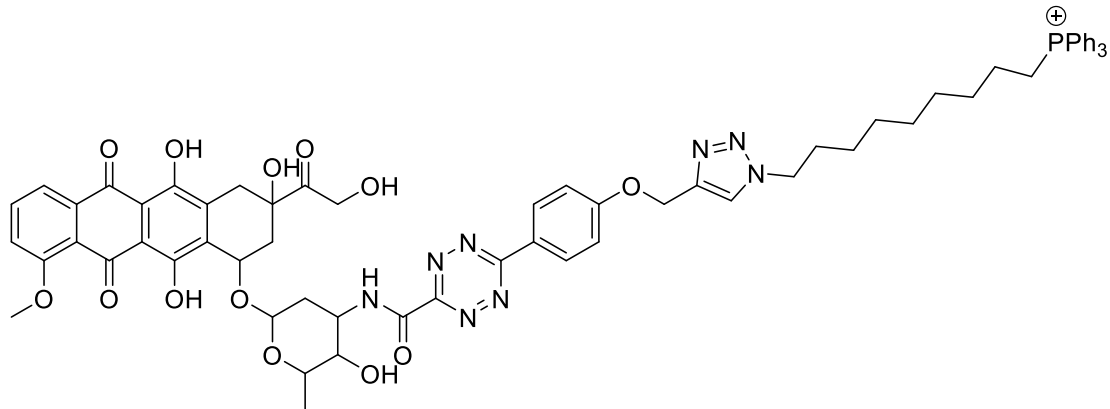
TOF MS ES-
1.94e3





Chemical Formula: C₃₉H₃₅N₅O₁₃
Exact Mass: 781.2231

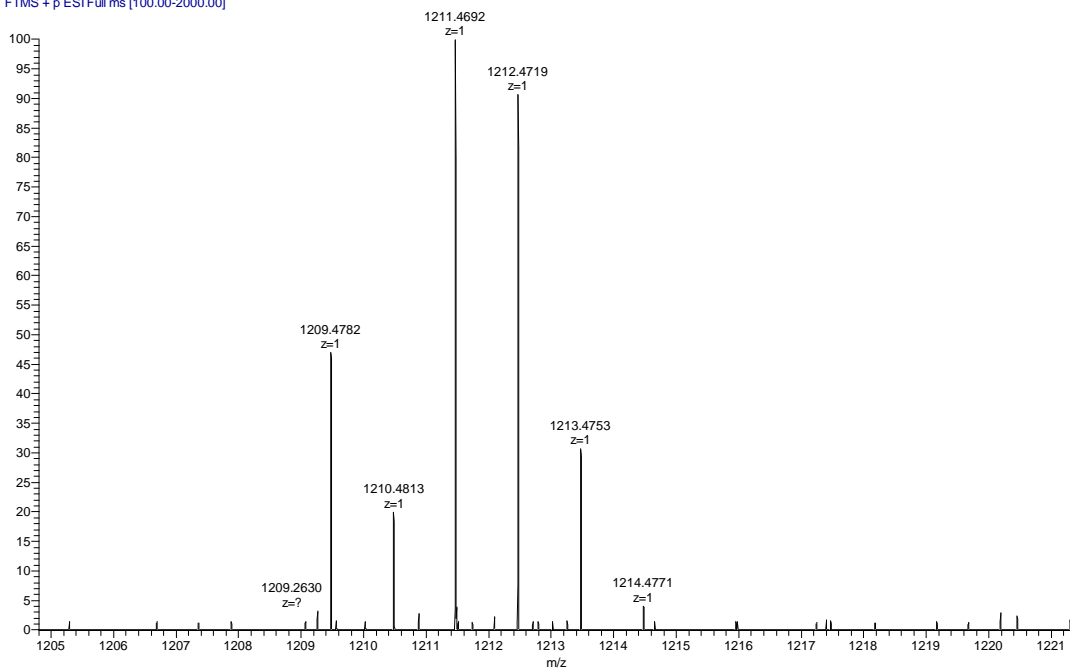


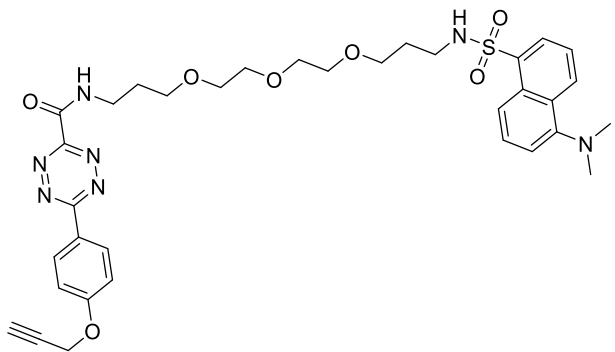


Chemical Formula: $\text{C}_{66}\text{H}_{68}\text{N}_8\text{O}_{13}\text{P}^+$

Exact Mass: 1211.4638

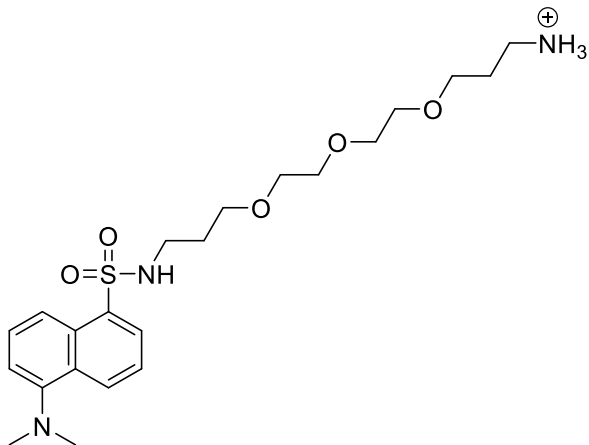
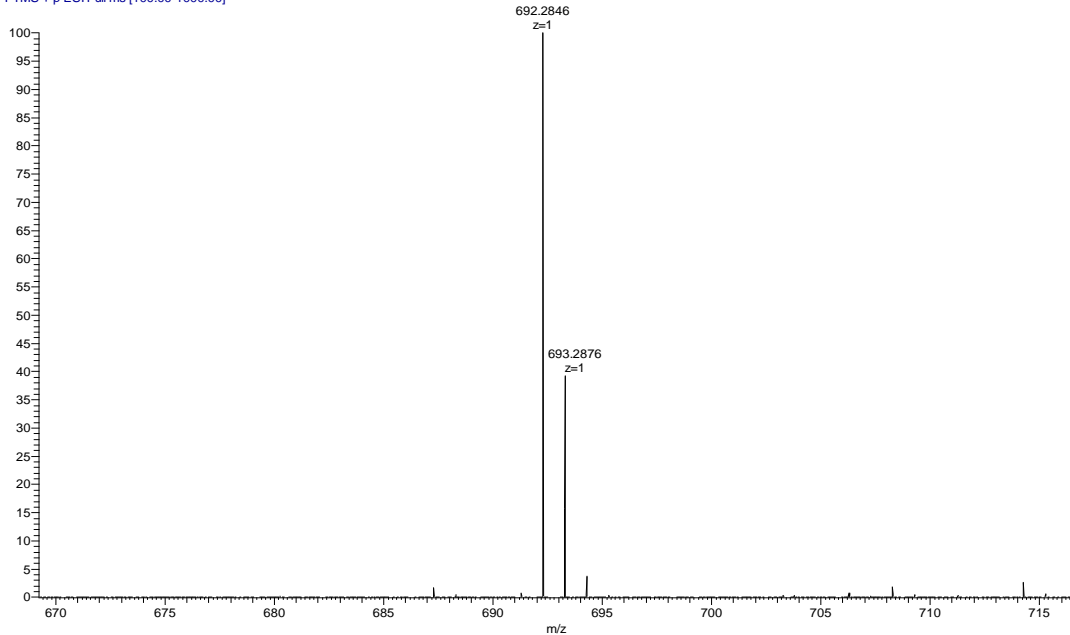
YU_7_22_ESIPOS_BWang_10272016_161027123156 #160-171 RT: 2.24-2.39 AV: 12 NL: 1.82E5
T: FTMS + p ESI Full ms [100.00-2000.00]

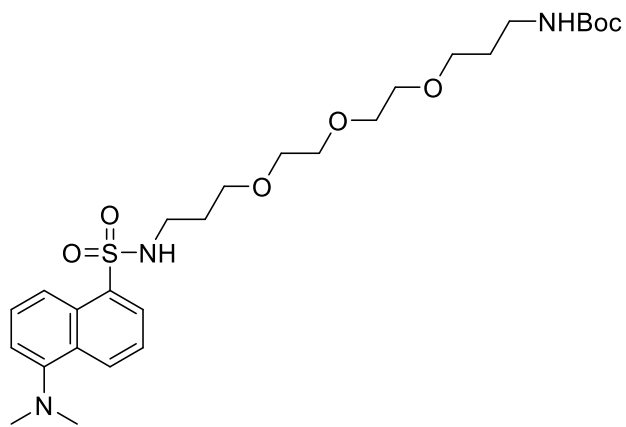
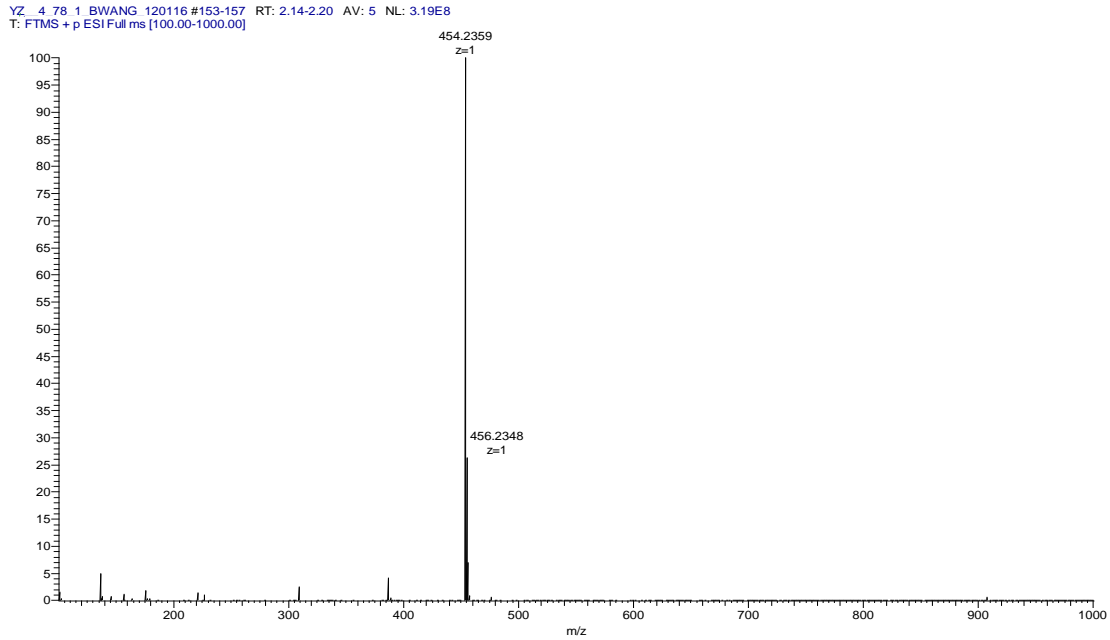




Chemical Formula: C₃₄H₄₁N₇O₇S
Exact Mass: 691.2788

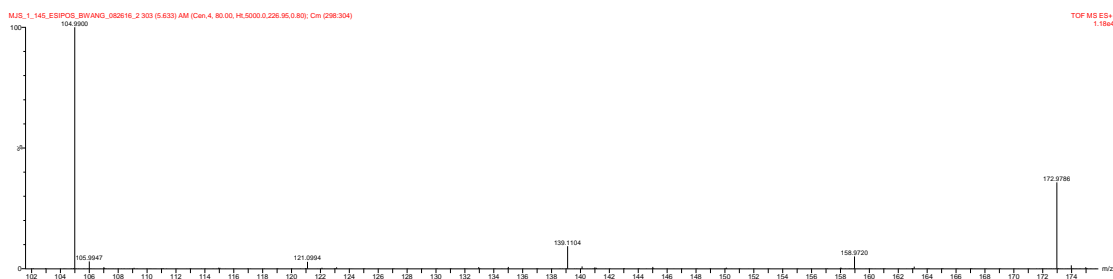
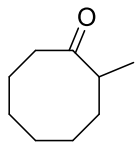
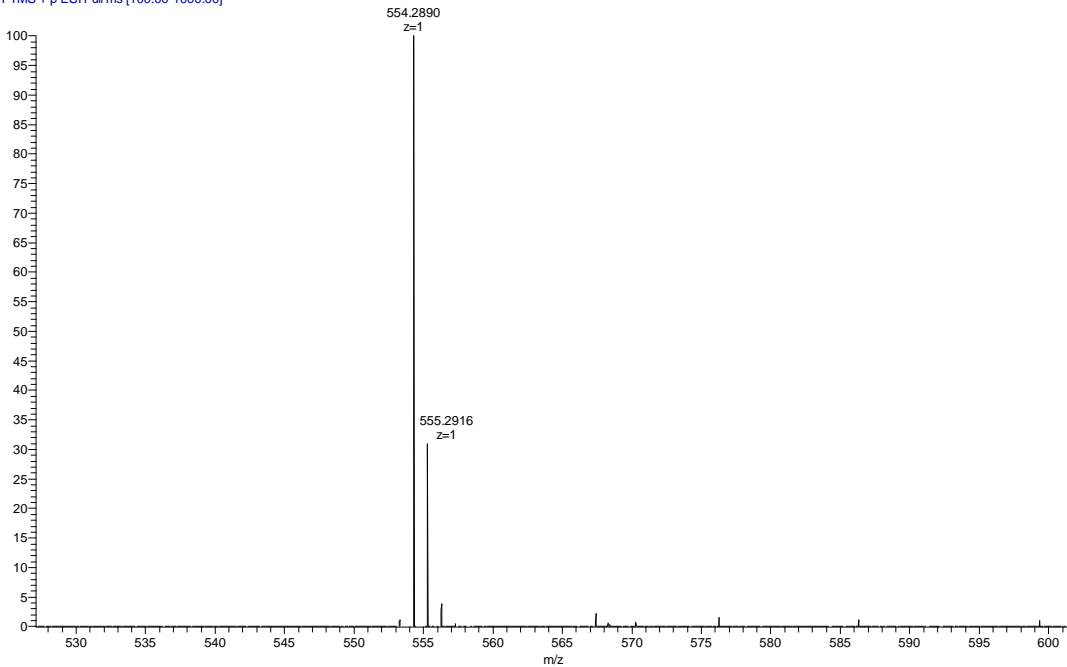
YZ_4_79_1_BWANG_120116 #111-150 RT: 1.57-2.13 AV: 40 NL: 2.52E6
T: FTMS + p ESI Full ms [100.00-1000.00]

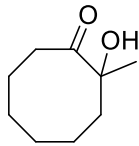




Chemical Formula: C₂₇H₄₃N₃O₇S
Exact Mass: 553.2822

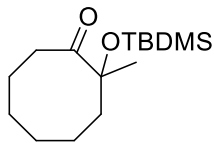
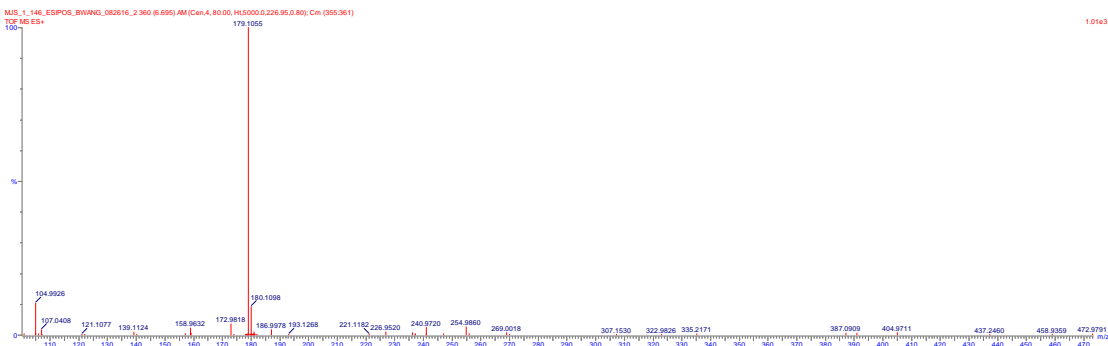
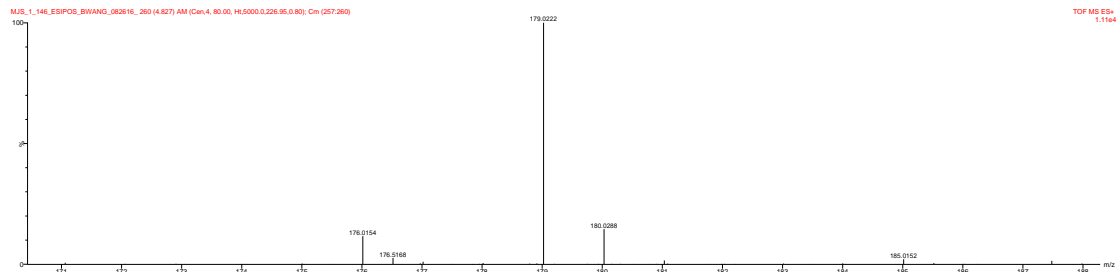
YZ_4_77_1_BWANG_120116 #143-152 RT: 1.99-2.11 AV: 10 NL: 7.22E7
T: FTMS + p ESI Full ms [100.00-1000.00]



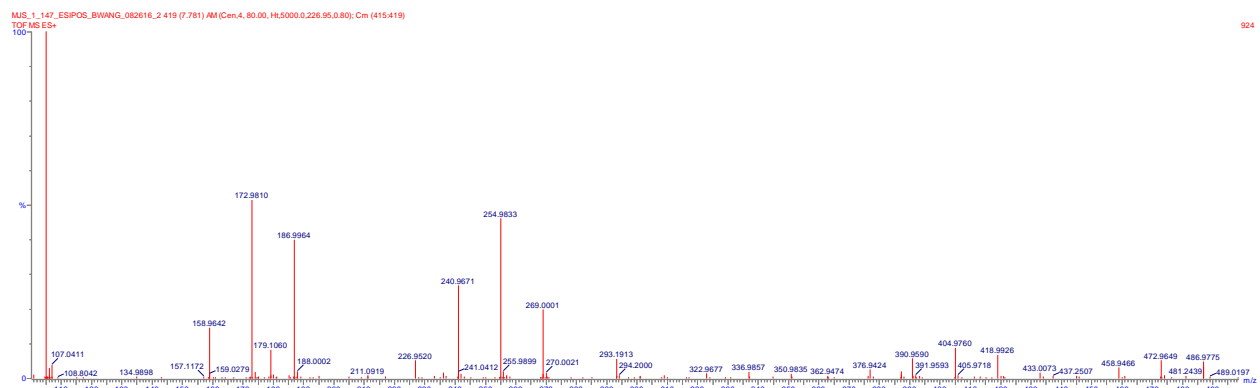


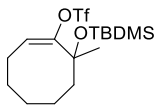
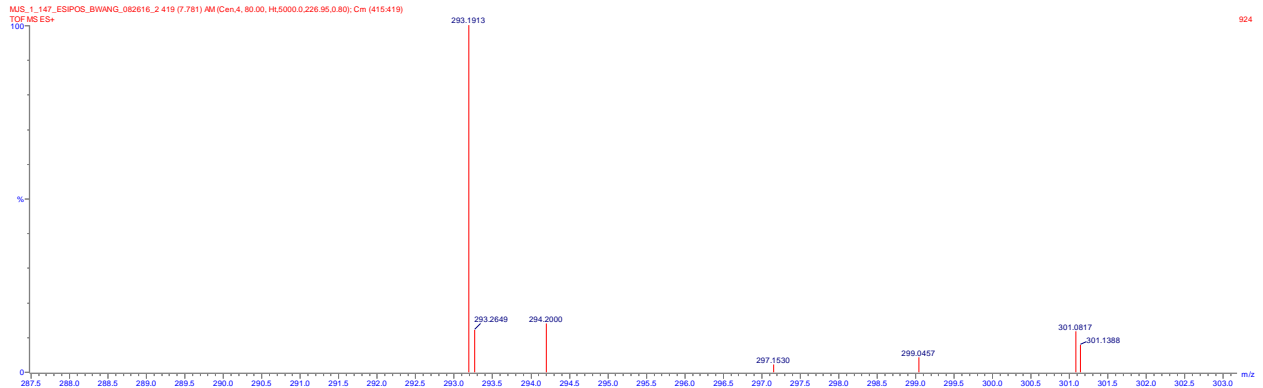
Chemical Formula: C₉H₁₆O₂

Exact Mass: 156.1150

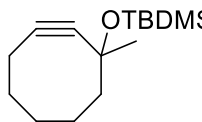
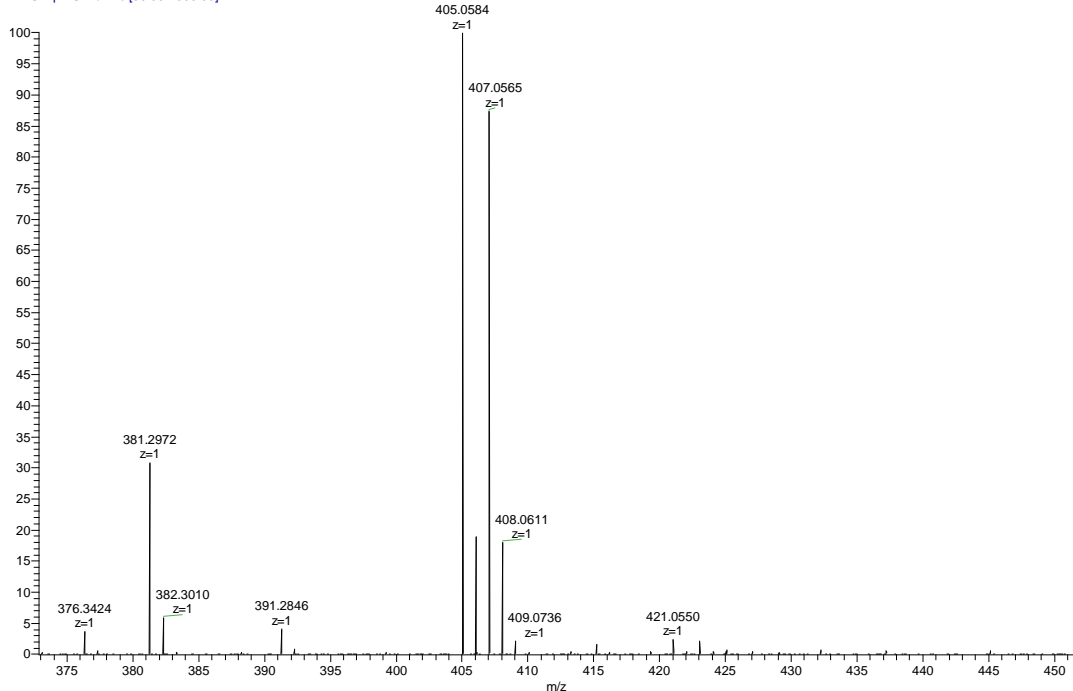


Exact Mass: 270.20

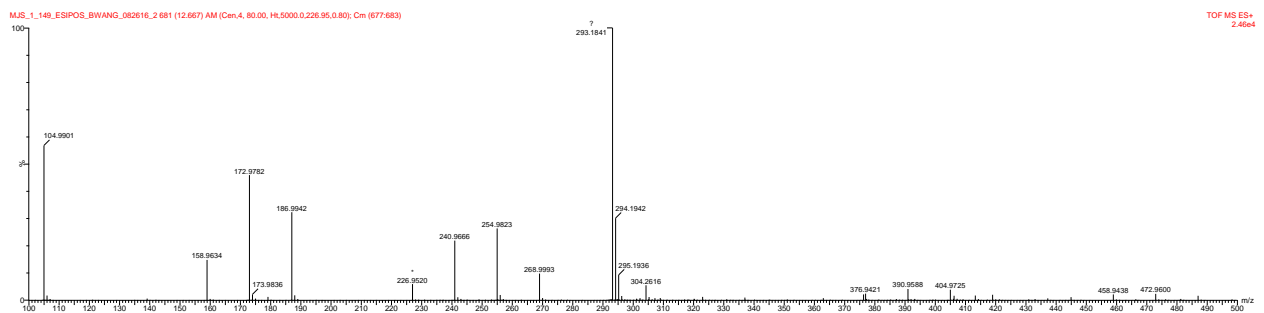
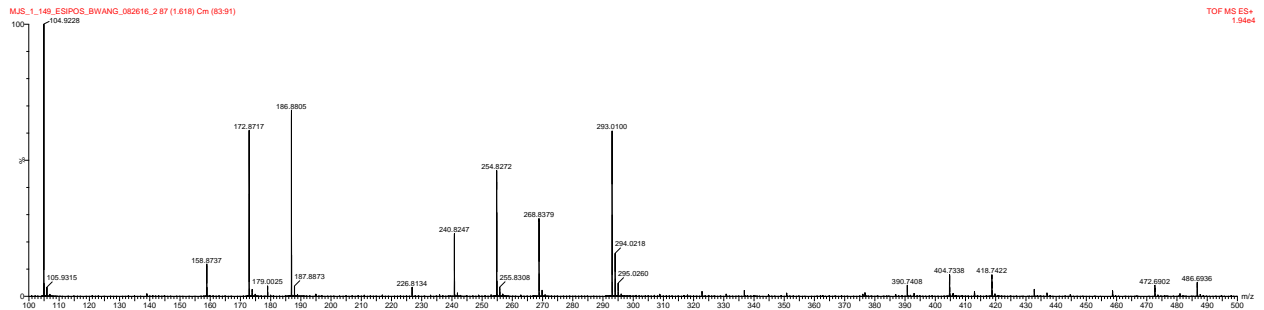


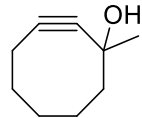


MIS_1_154_ESIPOS_BWang_09152016 #173-255 RT: 2.90-4.29 AV: 83 NL: 1.64E5
T: FTMS + p ESI Full ms [50.00-1000.00]



Exact Mass: 252.19

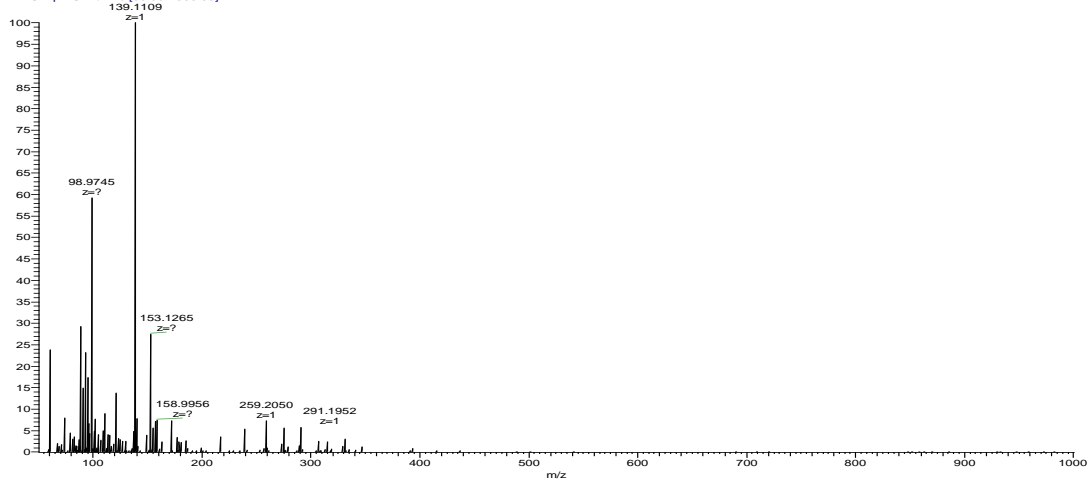




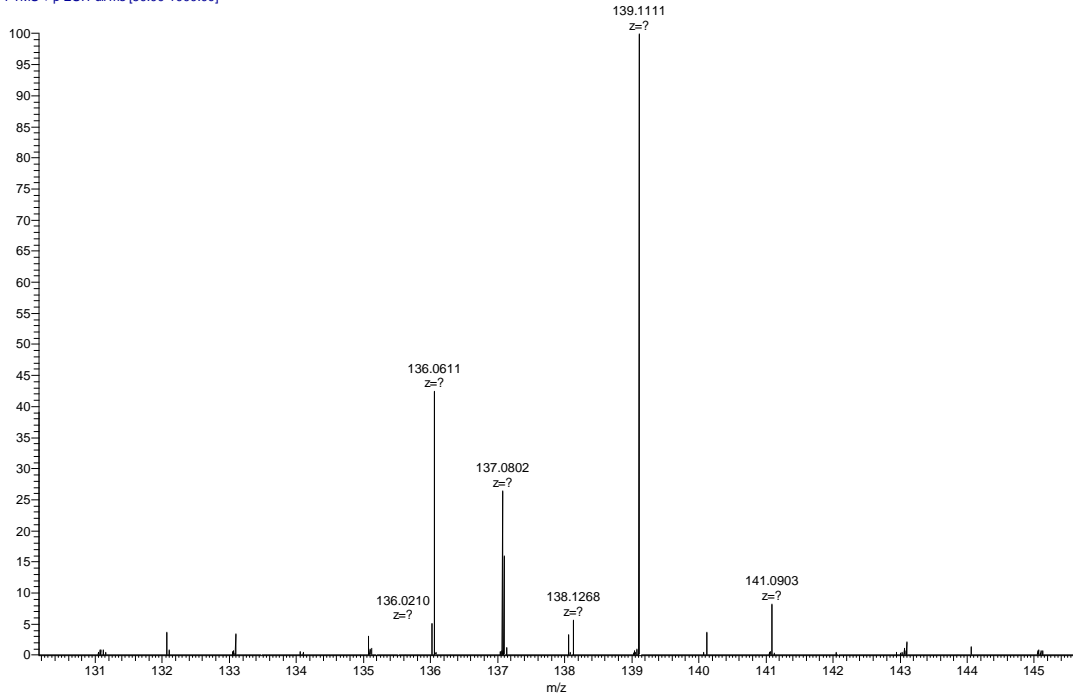
Chemical Formula: C₉H₁₄O

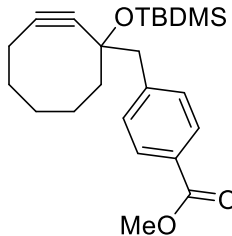
Exact Mass: 138.1045

MIS_1_155_ESIPOS_BWang_09152016 #127-166 RT: 2.13-2.79 AV: 40 NL: 6.12E5
T: FTMS + p ESI Full ms [50.00-1000.00]

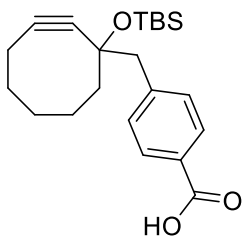
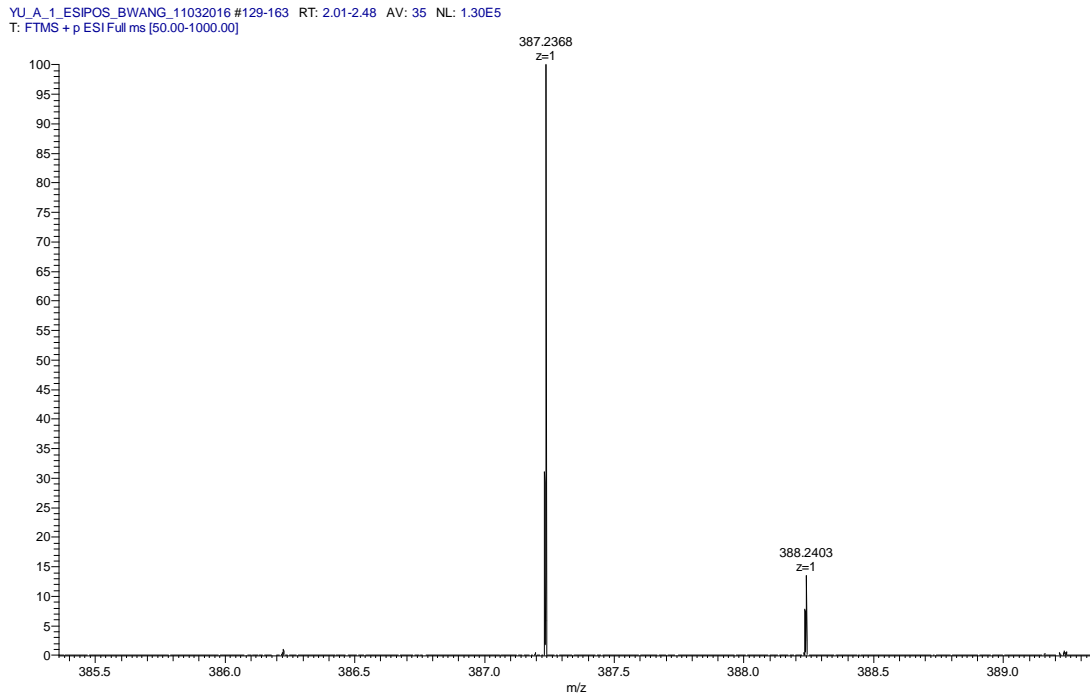


MIS_1_155_ESIPOS_BWang_09152016 #200 RT: 3.36 AV: 1 NL: 1.58E5
T: FTMS + p ESI Full ms [50.00-1000.00]

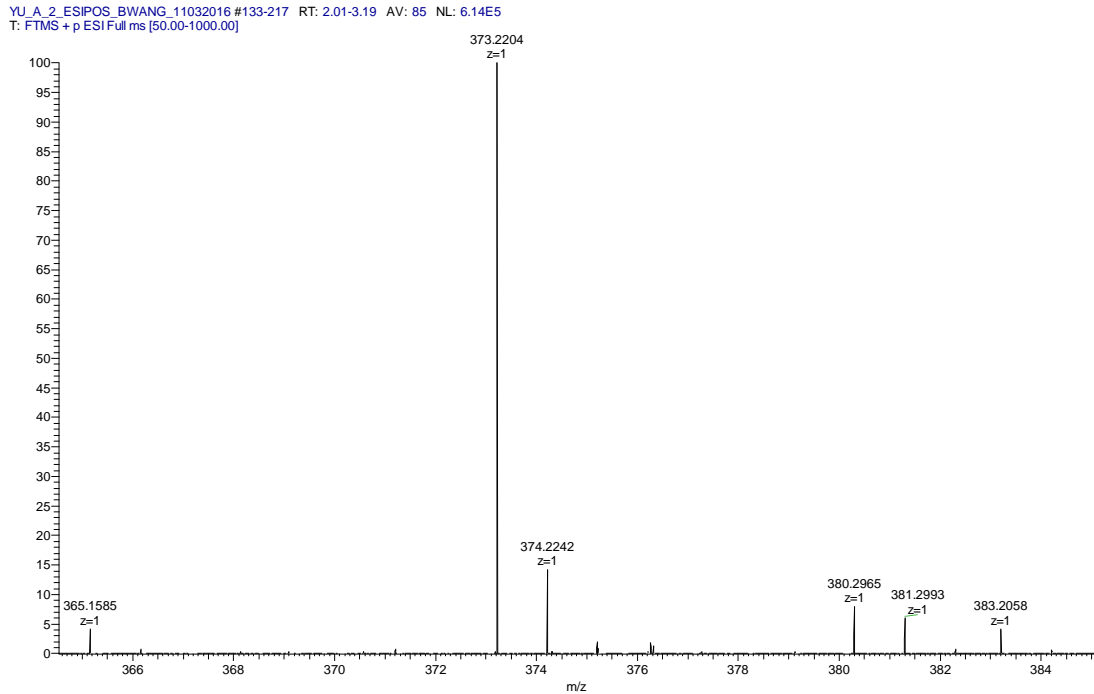


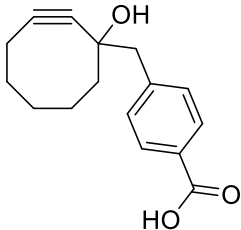


Chemical Formula: $\text{C}_{23}\text{H}_{34}\text{O}_3\text{Si}$
Exact Mass: 386.2277



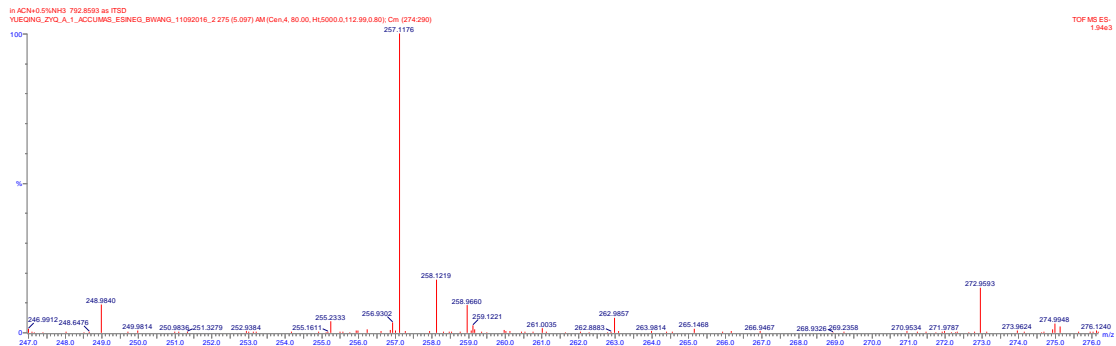
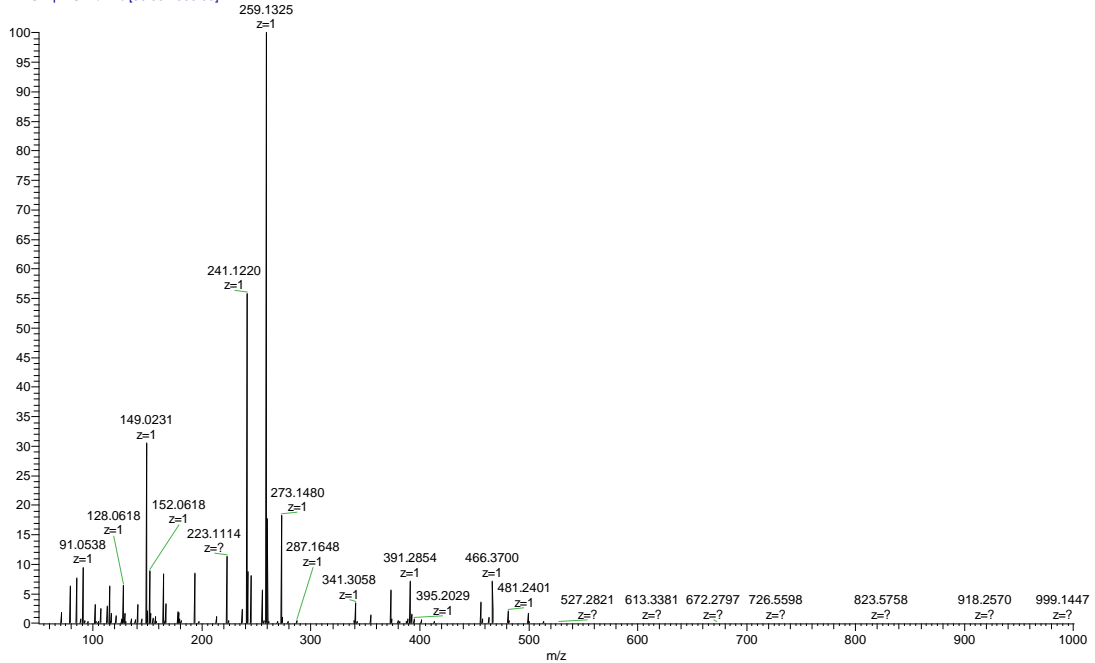
Chemical Formula: $\text{C}_{22}\text{H}_{32}\text{O}_3\text{Si}$
Exact Mass: 372.2121

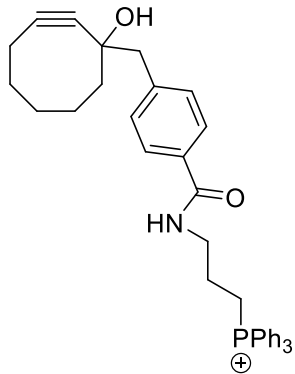




Chemical Formula: C₁₆H₁₈O₃
Exact Mass: 258.1256

YU_A_2_ESIPOS_BWANG_11032016 #133-217 RT: 2.01-3.19 AV: 85 NL: 1.10E7
T: FTMS + p ESI Full ms [50.00-1000.00]

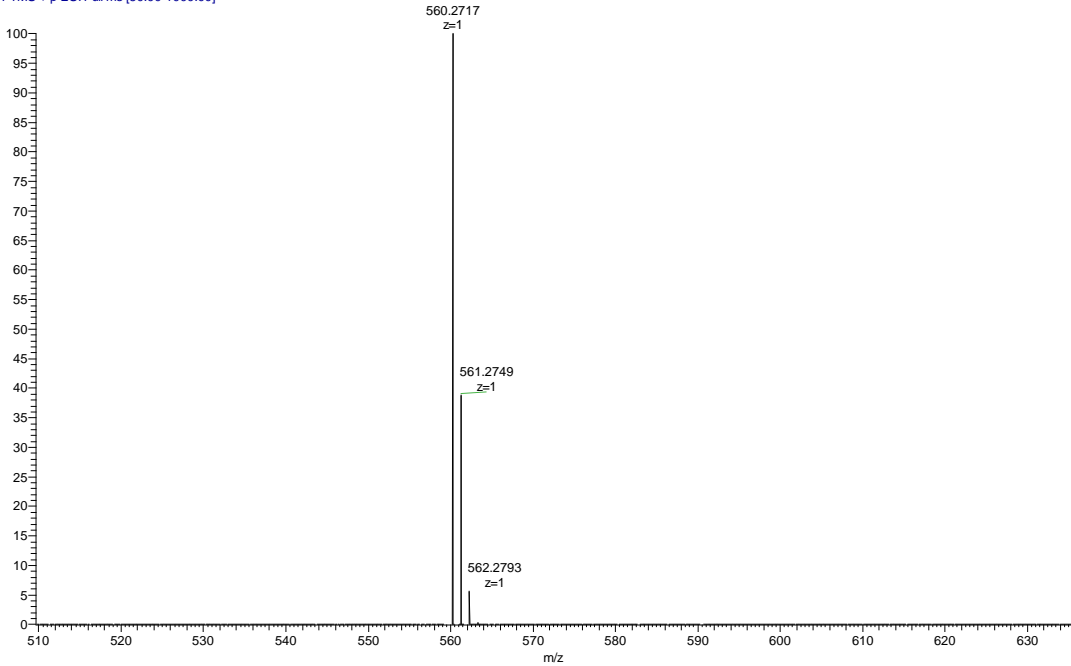




Chemical Formula: C₃₇H₃₉NO₂P⁺

Exact Mass: 560.2713

ZYQ_A_2_ESIPOS_BWANG_11102016 #139-148 RT: 2.14-2.26 AV: 10 NL: 9.53E6
T: FTMS + p ESI Full ms [50.00-1000.00]



Compound 109

